THE PHYSIOLOGY AND PHARMACOLOGY OF LEUCINE-RICH REPEAT GPCRS

EDITED BY: Brian J. Arey and James A. Dias

PUBLISHED IN: Frontiers in Endocrinology

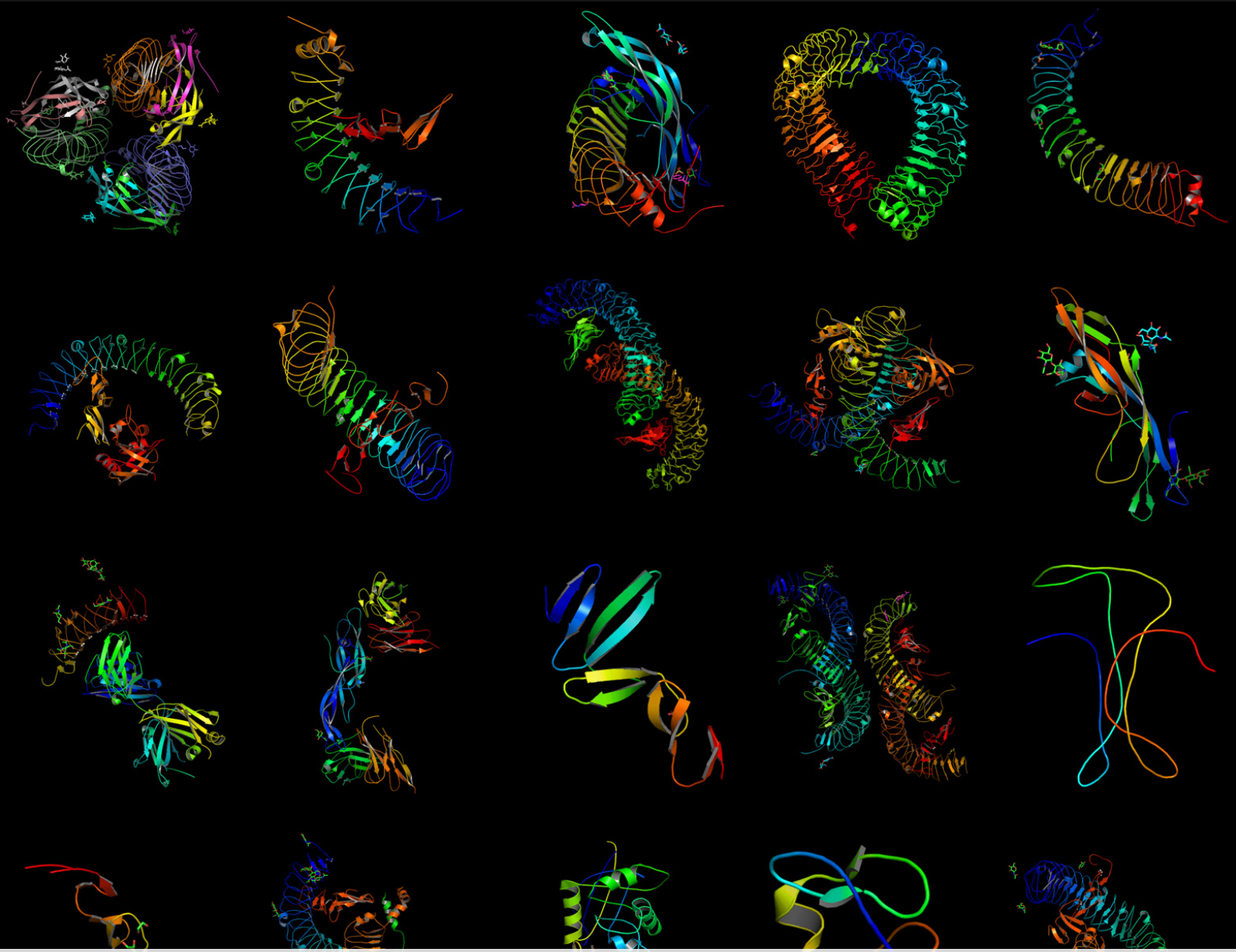

frontiers Research Topics

ISSN 1664-8714
ISBN 978-2-88919-958-7
DOI 10.3389/978-2-88919-958-7

About Frontiers

Frontiers is more than just an open-access publisher of scholarly articles: it is a pioneering approach to the world of academia, radically improving the way scholarly research is managed. The grand vision of Frontiers is a world where all people have an equal opportunity to seek, share and generate knowledge. Frontiers provides immediate and permanent online open access to all its publications, but this alone is not enough to realize our grand goals.

Frontiers Journal Series

The Frontiers Journal Series is a multi-tier and interdisciplinary set of open-access, online journals, promising a paradigm shift from the current review, selection and dissemination processes in academic publishing. All Frontiers journals are driven by researchers for researchers; therefore, they constitute a service to the scholarly community. At the same time, the Frontiers Journal Series operates on a revolutionary invention, the tiered publishing system, initially addressing specific communities of scholars, and gradually climbing up to broader public understanding, thus serving the interests of the lay society, too.

Dedication to quality

Each Frontiers article is a landmark of the highest quality, thanks to genuinely collaborative interactions between authors and review editors, who include some of the world's best academicians. Research must be certified by peers before entering a stream of knowledge that may eventually reach the public - and shape society; therefore, Frontiers only applies the most rigorous and unbiased reviews.
Frontiers revolutionizes research publishing by freely delivering the most outstanding research, evaluated with no bias from both the academic and social point of view.
By applying the most advanced information technologies, Frontiers is catapulting scholarly publishing into a new generation.

What are Frontiers Research Topics?

Frontiers Research Topics are very popular trademarks of the Frontiers Journals Series: they are collections of at least ten articles, all centered on a particular subject. With their unique mix of varied contributions from Original Research to Review Articles, Frontiers Research Topics unify the most influential researchers, the latest key findings and historical advances in a hot research area! Find out more on how to host your own Frontiers Research Topic or contribute to one as an author by contacting the Frontiers Editorial Office: **researchtopics@frontiersin.org**

THE PHYSIOLOGY AND PHARMACOLOGY OF LEUCINE-RICH REPEAT GPCRS

Topic Editors:
Brian J. Arey, Research and Development, Bristol-Myers Squibb Co., USA
James A. Dias, University at Albany, State University of New York, USA

G protein-coupled receptors (GPCRs) represent a large and physiologically important class of cell surface receptors. There are approximately 750 known GPCRs present in the human genome that can be subdivided into general classes based upon sequence homology within their transmembrane domains. Therapeutically, GPCRs represent a fertile source for the development of therapies as they are a significant percentage of our current pharmacopeia.

Among the three subclasses of GPCRs, the Class A (rhodopsin-like) receptors are by far the most prevalent and extensively studied. However, within the Class A receptors, sub-families of receptors can be distinguished based upon common sequence motifs within the transmembrane domains

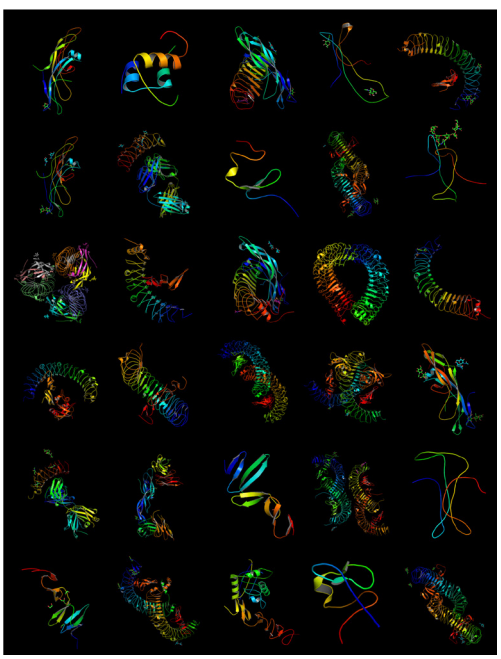

The cover image depicts the conformational structures of the receptors and associated ligands for the members of the Leucine-rich Repeat Family of G protein- coupled receptors. The image was graciously prepared by Dr. Xuliang Jiang, coauthor of the landmark paper describing the crystal structure of the human follicle stimulating hormone extracellular domain trimer in complex with its ligand human follicle stimulating hormone (4MQW). PDB files used to create the image are (listed left to right, top to bottom): 1HCN, 2H8B, 1XWD, 1E9J, 4KT1, 1HRP, 3G04, 2JM4, 4BSU. 1HD4, 4MQW, 4QXF, 4QXE, 4LI1, 4AY9, 4UFS, 4LI2, 4UFR, 4KNG, 1FL7, 2XWT, 1QFW, 4BSP, 4BSS, 1DZ7, 4BSO, 4BSR, 4CDK, 2M96, 4BST.

as well as extracellular and intracellular domains. One such family of Class A receptors is characterized by multiple leucine-rich repeats within their amino- terminal domains (the Leucine-rich Repeat family (LRR)). This family of GPCRs are best represented by the glycoprotein hormone receptors (LHR, FSHR and TSHR) which have been studied extensively but also includes receptors for the peptide hormone relaxin (RXFP1 and RXFP2 (RXFP2 also binds insulin-like peptide 3)) and three other receptors (LGR4, LGR5 and LGR6). LGR4-6 were, until recently, considered orphan receptors. However, emerging data have revealed that these proteins are the receptors for a family of growth factors called R-spondins.

Over the last 20 years much has been learned about LRR receptors, including the development of synthetic agonists and antagonists, new insights into signaling (including signaling bias) and the physiological role these receptors play in regulating the function of many tissues. This topic will focus on what is known concerning the regulation of these receptors, their signaling pathways, functional consequences of activation and pharmacology.

Citation: Arey, B. J., Dias, J. A., eds. (2016). The Physiology and Pharmacology of Leucine-rich Repeat GPCRs. Lausanne: Frontiers Media. doi: 10.3389/978-2-88919-958-7

Table of Contents

frontiers in Endocrinology

EDITORIAL
published: 17 June 2016
doi: 10.3389/fendo.2016.00056

Editorial: The Physiology and Pharmacology of Leucine-rich Repeat GPCRs

Brian J. Arey[1] and James A. Dias[2]*

[1] Research and Development Bristol-Myers Squibb Co., Princeton, NJ, USA, [2] University at Albany, State University of New York, Albany, NY, USA

Keywords: G protein-coupled receptors, leucine-rich repeat family of receptors, LGR, GPCRs, physiology and pharmacology

The Editorial on the Research Topic

The Physiology and Pharmacology of Leucine-rich Repeat GPCRs

G protein-coupled receptors represent a large family of proteins that act as receptors for many types of physiological ligands, including peptides, metabolites, and lipids. These receptors are important for understanding physiology since they contribute to the regulation of all major organ systems. Additionally, they are also a key focus for the development of therapeutics for the treatment of pathophysiology and are still recognized as the most druggable class of macromolecules today. GPCRs are classified into separate subfamilies (Classes A, B, and C) based on protein sequence homology in their transmembrane domains. Within the Class A family of GPCRs, these receptors can be further placed into sub-groups based on other structural features and similarities in function. In this Special Topic for Frontiers in Endocrinology: Molecular and Structural Endocrinology, we have focused on a subfamily of Class A GPCRs, the leucine-rich repeat family of receptors (LGR). The Physiology and Pharmacology of Leucine-rich Repeat GPCRs captures the continuum of structure to function, agonist to effector, and reproduction to metabolism that provides an overview of this important family of receptors.

The LGRs are characterized by the leucine-rich repeat structural motif (1) that provides the rigid structure of their large extracellular domains. The predicted heptahelical transmembrane domains and their sequence homology in this region with other receptors classify them as Class A GPCRs (2). Furthermore, there are currently three sub-groups of LGRs recognized. The Type A receptors have been extensively studied and are receptors for the pituitary and placental glycoprotein hormones. The endogenous ligands for the Type B (R-spondins) and C (relaxin) receptors have only recently been identified and rapid progress has been made that has advanced understanding of their structure and function. These receptors are important mediators in the regulation of diverse physiological process, such as reproduction, cardio-renal function, cell growth, and stem cell differentiation. Within this Special Topic, we seek to provide an understanding of this family of receptors while addressing both future opportunities and challenges that lay ahead.

Petrie et al. provide an overview of LGRs in terms of structure and organization that places this family of receptors within the larger context. This review provides in depth knowledge of the RXFP1 and RXFP2 receptors whose cognate ligands are two insulin- related peptides, H2 relaxin, and INSL3. Thus, this review while calling out the uniqueness of the Type C LGRs RXFP1 and RXFP2, also introduces us nicely to the three Types of LGRs based on the size of their leucine-rich repeat extracellular domains.

Continuing on this theme of structure and function, activation of the most well studied of the LGRs, the gonadotropin receptors, is reviewed. The structural basis of activation of the gonadotropin receptors in the absence of a full crystal structure remains an enigma. However, we do know that the large extracellular domains are the binding site of the large heterodimeric ligands for these receptors.

OPEN ACCESS

Edited and Reviewed by:
Pierre De Meyts,
De Meyts R&D Consulting, Belgium

****Correspondence:***
Brian J. Arey
brian.arey@bms.com

Specialty section:
This article was submitted to Molecular and Structural Endocrinology, a section of the journal Frontiers in Endocrinology

Received: *13 May 2016*
Accepted: *23 May 2016*
Published: *17 June 2016*

Citation:
Arey BJ and Dias JA (2016) Editorial: The Physiology and Pharmacology of Leucine-rich Repeat GPCRs. Front. Endocrinol. 7:56. doi: 10.3389/fendo.2016.00056

A remaining question is the potential role of the other parts of the receptor structure in determining function. Banerjee and Mahale provide evidence using site-directed mutagenesis that signaling of the LH receptor is dependent on specific residues of the extracellular loops. Furthermore, Grzesik et al. demonstrate that differences in signaling by the two physiological ligands of the LH receptor, are at least in part, mediated by the hinge region of the extracellular domain. While both receptors coexist in the same cell during folliculogenesis, it is unclear how their agonist-induced signals are parsed out. Further refining this thought, this paper addresses how one receptor can bind two nearly identical ligands and produce two different signaling profiles. It turns out that both hormone and extracellular loops coordinate to produce the breadth of nuance seen in signaling of these receptors. This seems a critical point if small molecules are to be developed which mimic some or all of these signaling patterns.

The physiological and therapeutic importance of the Type B and C receptors is discussed as well. The importance of RXFP1 in cancers is exemplified by Thanasupawat et al. in a review of new ligands for RXFP1 other than the canonical relaxin and INSL3; specifically C1q/TNF-related proteins and the role of RXFP1 as a brain cancer promoter. The theme is further explored with an in-depth look by Li et al. of the Type B LGR4 where we learn that this receptor that is critical for developmental signaling and tissue homeostasis has as its ligand, R-spondins. We learn that R-spondins are the sole secreted potentiators of Wnt signaling and stem cell maintenance and appreciate that the Type B LGRs do not signal via G-proteins but do interact with the FZD–LRP complex to stimulate unique signaling pathways.

The LGR receptor family has been the subject of drug development for decades. Focusing on improving the natural ligand for therapeutics based on these receptors, a perspective is provided by Szkudlinski on a journey toward the successful development of superagonists of the thyroid-stimulating hormone receptor, a Type A LGR. This review shines light on the potential of utilizing the naturally occurring ligands as a scaffold for engineering by structure-based drug design to develop "super biosimilars." This is contrasted with the development of small molecule agonists and antagonists that act at this same class of LGR Type A as described by Nataraja et al. Here, we learn that it is possible to bypass the complicated interactions of heterodimeric ligands and the large extracellular domains of the LGR Type A receptors, to effect activation or inhibition with molecules a fraction of the size of the natural ligands. Although this represents a clear step forward in our ability to develop small molecule agonists and antagonists to these receptors, it is not without its challenges. In what would seem to be a reasonable assumption that cAMP as readout would predict efficacy *in vivo*, this is shown to not necessarily be the case. In the end, primary cells and iterative testing reveal the true candidate.

This concept is further exemplified in the article by Huang et al. An overwhelming majority of the preclinical animal testing for relaxin treatment includes rodent models and, thus, the inability of small molecule agonists to activate the mouse receptor has hampered preclinical studies. In a search for animal models to study RXFP1 small molecule agonists as potential acute heart failure therapeutics, it was determined that non-human primate and porcine species could be used but the standard laboratory mouse model was unable to respond to the lead compound! These examples illustrate how development of small molecule therapeutics is fraught with potential pitfalls and how appropriate models are needed for screening and selection of leads.

Finally, in an era of optogenetics and real-time inquiry, the use of transgenic methods may yield some recourse. Narayan describes how, for the gonadotropin receptors, a combination of knockout and knock-in approaches can yield novel mouse models that either simulates human disease or tests whether genomic variants can explain disease. In this regard, the luteinizing hormone receptor has been very well studied using transgenic animals to better understand the effect of mutations causing constitutive activation as a model for Familial Male Precocious Puberty.

Advanced methods in cellular imaging are also available which will aid in the study of LGR signaling. Certainly in the area of the gonadotropin receptors, these methods have contributed to an understanding that, although the canonical cAMP pathway is operative in the gonadotropin receptors, additional pathways are likely at play. Thus, Ayoub et al. describes the use of bioluminescence resonance energy transfer (BRET) to study activation of gonadotropin receptors in living cells. Using this method, they confirm that these receptors exhibit biased agonism.

It has been nearly a century since Smith discovered the relationship between pituitary extracts and follicular development and 60 years since Hisaw discovered relaxin as a hormone that could cause a loosening of the pubic symphysis prior to parturition. These seminal findings have led to the identification of the importance of these peptides on the physiology of the reproductive system but have also ultimately revealed a more complex endocrine role of these hormones and the identification of a unique family of receptors. Research over the ensuing decades has revealed that the LGRs exert varied and comprehensive controls on processes that include but are certainly not limited to reproduction and point to their potential as therapeutic targets to treat disease.

AUTHOR CONTRIBUTIONS

BA and JD contributed equally to this manuscript.

Conflict of Interest Statement: The authors declare that the research was conducted in the absence of any commercial or financial relationships that could be construed as a potential conflict of interest.

REFERENCES

1. Kobe B, Deisenhofer J. Proteins with leucine-rich repeats. *Curr Opin Struct Biol* (1995) 5:409–16. doi:10.1016/0959-440X(95)80105-7
2. Shonberg J, Kling RC, Gmeiner P, Lober S. GPCR crystal structures: medicinal chemistry in the pocket. *Bioorg Med Chem* (2015) 23:3880–906. doi:10.1016/j.bmc.2014.12.034

frontiers in Endocrinology

REVIEW
published: 07 September 2015
doi: 10.3389/fendo.2015.00137

In a class of their own – RXFP1 and RXFP2 are unique members of the LGR family

Emma J. Petrie[1,2], *Samantha Lagaida*[1,2], *Ashish Sethi*[1,2], *Ross A. D. Bathgate*[1,3] *and Paul R. Gooley*[1,2]*

[1] Department of Biochemistry and Molecular Biology, University of Melbourne, Parkville, VIC, Australia, [2] Bio21 Molecular Science and Biotechnology Institute, University of Melbourne, Parkville, VIC, Australia, [3] Florey Institute of Neuroscience and Mental Health, University of Melbourne, Parkville, VIC, Australia

The leucine-rich repeat-containing G protein-coupled receptors (LGRs) family consists of three groups: types A, B, and C and all contain a large extracellular domain (ECD) made up of the structural motif – the leucine-rich repeat (LRR). In the LGRs, the ECD binds the hormone or ligand, usually through the LRRs, that ultimately results in activation and signaling. Structures are available for the ECD of type A and B LGRs, but not the type C LGRs. This review discusses the structural features of LRR proteins, and describes the known structures of the type A and B LGRs and predictions that can be made for the type C LGRs. The mechanism of activation of the LGRs is discussed with a focus on the role of the low-density lipoprotein class A (LDLa) module, a unique feature of the type C LGRs. While the LDLa module is essential for activation of the type C LGRs, the molecular mechanism for this process is unknown. Experimental data for the potential interactions of the type C LGR ligands with the LRR domain, the transmembrane domain, and the LDLa module are summarized.

Keywords: leucine-rich repeat-containing G protein-coupled receptors, LGR, RXFP1, RXFP2, GPCR

OPEN ACCESS

Edited by:
Brian J. Arey, Bristol-Myers Squibb, USA

Reviewed by:
Guillermo Romero, University of Pittsburgh, USA
Mikhail Karganov, Russian Academy of Medical Sciences, Russia

***Correspondence:**
Paul R. Gooley, Department of Biochemistry and Molecular Biology, Bio21 Molecular Science and Biotechnology Institute, University of Melbourne, 30 Flemington Road, Parkville, VIC 3010, Australia
prg@unimelb.edu.au

Specialty section:
This article was submitted to Molecular and Structural Endocrinology, a section of the journal Frontiers in Endocrinology

Received: *26 June 2015*
Accepted: *20 August 2015*
Published: *07 September 2015*

Citation:
Petrie EJ, Lagaida S, Sethi A, Bathgate RAD and Gooley PR (2015) In a class of their own – RXFP1 and RXFP2 are unique members of the LGR family. Front. Endocrinol. 6:137. doi: 10.3389/fendo.2015.00137

Introduction

The receptors for the peptide hormones H2 relaxin and insulin-like peptide-3 (INSL3) are unique members of the leucine-rich repeat-containing G protein-coupled receptors (LGRs) family (1). LGRs are class A G protein-coupled receptors (GPCRs) and are divided into three groups: types A, B, and C. Type A LGRs are receptors for the glycoprotein hormones follicle-stimulating hormone (FSH), luteinizing hormone (LH), and thyroid-stimulating hormone (TSH). Although the Type B LGRs were identified in 1998 (1, 2), LGR4-6 were only recently deorphanized as the R-spondin (Rspo) receptors (3, 4). These receptors have roles in stem cell differentiation and are associated with cancers affecting the gut. The identification of LGR7 in 2000 resulted in the formation of the third group, Type C (1). Soon after, LGR7 was joined by the receptor encoded by the *GREAT* gene (5), (LGR8), when the phenotype of the knockout mouse correlated with abnormal testicular descent noted in INSL3 knockout mice (6, 7). In 2002, LGR7 and LGR8 were deorphanized as H2 relaxin receptors (8). At this exciting time of GPCR deorphanization, the grouping of LGR7 [later defined as RXFP1 in Ref. (9)] and LGR8 (RXFP2) with the glycoprotein hormone receptors into the LGR family appeared to correlate with the known reproductive roles and tissue-specific expression of H2 relaxin and INSL3. H2 relaxin is a major circulating hormone produced by the corpus luteum and placenta with important roles in maintaining pregnancy and facilitating parturition [reviewed in Ref. (10)]. INSL3

is produced in testicular Leydig cells in males and follicular theca cells in the female ovary (11), and therefore, has central roles in fertility.

Almost 15 years since the initial identification of RXFP1, the landscape of H2 relaxin research is diverse and complex. H2 relaxin is considered a pleiotropic hormone with many functions, including central roles in collagen turnover (12, 13) wound healing (14), and roles in cardiovascular function (15) [further reviewed in Ref. (10)]. The key roles of relaxin in cardiovascular function lead to the use of the human form of relaxin, H2 relaxin, in clinical trials for the treatment of acute heart failure. With the success of these clinical trials (16–18), a clear understanding of the mechanism of how H2 relaxin binds and activates RXFP1 is highly desirable. Unfortunately, no structures of a Type C LGR are available. In this context, as structural understanding of other members of the LGR family grows, we review the structural knowledge of the LGR family, and examine what is known about ligand interactions at the extracellular domains (ECDs) of the Class C LGRs in comparison to the other members of this diverse family of GPCRs.

Leucine-Rich Repeat-Containing G-Protein Receptor

The LGR family is classified as "Type A" rhodopsin-like GPCRs based on the similarity of its transmembrane (TM) domain. They are unified into this family based on their large ECDs containing leucine-rich repeats (LRRs). The first LRR-containing protein to be identified was leucine-rich α2-glycoprotein (LRG) (19) but since then, LRR domains have been identified in various proteins including extracellular, intracellular, and TM proteins with a wide variety of functions, such as neural circuit formation [reviewed in Ref. (20)], inflammation [reviewed in Ref. (21)], immune response against pathogen (22, 23), and development and immunity in plants (24).

LGRs Classification

The LGR family is differentiated on the basis of the number of LRRs within the ECD, the length of the hinge region between the LRR domain and the TM domain and the presence of a low-density lipoprotein class A (LDLa) module (25, 26). Currently, there are three types of LGRs: type A, type B, and type C (**Table 1**). Mammalian type A LGRs include the follicle-stimulating hormone receptor (FSHr), thyroid-stimulating hormone receptor (TSHr), and luteinizing hormone receptor (LHr) [or lutropin/choriogonadotropic receptor (LCGr)] (27). Type A are characterized by 7–9 LRRs within the LRR domain and have a distinctively long hinge region, connecting the LRR to the TM domain, which is essential for receptor activation (26). The type B LGRs (LGR4–6) are the receptors for the Rspo family (R-spondin1–4) and have roles in development, including cell proliferation and differentiation, and oncogenesis (28). These LGRs, typically have 16–18 LRRs and so constitute a longer LRR domain than type A and type C LGRs (26). The hinge region of type B LGRs is "medium length" compared to that of type A. Type C members are distinct in that they have an N-terminal LDLa module, which is also known to be important for receptor activation (29). These latter receptors include the mammalian LGR7 and LGR8 (now known as RXFP1 and RXFP2, respectively) along with a snail LGR and LGR3 and LGR4 from *Drosophila* (30) and are grouped as C1 or C2 based on the number of LDLa modules in their ECD. Type C LGRs have a similar number of LRRs compared to type A LGRs, although they have a shorter hinge region connecting the LRR domain to the TM domain (26). There is no evidence to suggest that the hinge has the same role in modulating receptor activity as it does in type A LGRs. RXFP1 and RXFP2 are the only mammalian class C LGRs and contain a single LDLa module, while type C LGRs found in echinoderm and molluskan can contain up to 12 modules (26). Thus, the evolution of these receptors is difficult to determine and in the context of this

TABLE 1 | Ectodomains and ligands of the LGR family.

Name	Short annotated name	Ligand	No of LRRs	Residues per repeat	Ligand affinity[a]	PDB
Type A						
LGR1	FSHr	Follicle-stimulating hormone	9	21–25	0.03–3 nM[b]	1XWD, 4AY9, 4MQW
LGR2	LH/CGr	Lutropin or choriogonadotropic hormone	6	22–31	0.3–0.5 nM[c]	
LGR3	TSHr	Thyrotropin (thyroid-stimulating hormone)	7	20–31	0.25 nM[d]	3XWT,3GO4
Type B						
LGR4	LGR4	Rspondin1–4	17	20–25	56 nM[e]	4KT1, 4QXE, 4QXF
LGR5	LGR5	Rspondin1–4	17	21–26	3 nM[f]	4BSR, 4BSS, 4BST 4BSU, 4KNG
LGR6	LGR6	Rspondin1–4	17	21–25	0.5–7 nM[g]	
Type C						
LGR7	RXFP1	H2 relaxin	10	24–25	9.2–9.8[h]	2JM4 (LDLa module)
LGR8	RXFP2	INSL3, H2 relaxin	10	24	9.3–9.7, 8.5–9.0[h]	2M96 (LDLa module)

[a] *Reported K_d, unless noted.*
[b] *Simoni et al. (31).*
[c] *Ascoli et al. (32).*
[d] *Harfst et al. (33).*
[e] *Wang et al. (34).*
[f] *de Lau et al. (3).*
[g] *IC_{50} (35).*
[h] *pK_d or pK_i (36).*

review only the mammalian RXFP1 and RXFP2 receptors will be discussed.

Structural Features of LRR Domains

The LRR Domain

The first structure of a LRR-containing protein, ribonuclease inhibitor (RI), showed a horseshoe-shaped structure (37). This curved structure consists of a β-sheet on the concave side of the LRR and an array of α-helices on the convex side. A single LRR consists of a β-strand and α-helix connected with loops and therefore a sequence of LRRs forms alternating parallel β-strands and α-helices along the α/β fold (38). The β-strand is formed by a highly conserved motif, xLx, within a LRR, connected to adjacent parallel β-strands by hydrogen bonds to form the β-sheet on the concave side of the structure. Comparison of LRR domains show the presence of a repeated conserved hydrophobic-rich sequence motif, LxxLxLxxNxL, where the underlined residues form the β-strand, x is any amino acid and leucine may be substituted by valine, isoleucine or phenylalanine; and asparagine by cysteine, serine or threonine (38, 39).

The convex side of the LRR domain is comprised of more variable sequence and secondary structure including 3^{10} helices, polyproline II helices, β-turn or β-strand (39). In addition to the length, the nature of the sequence contributes to the curvature of the LRR domain. Two distinct sequences are observed on the convex side, LPxxL (LP motif) and IxxxAF (AF motif) (40). The prototype LRR protein comprising the LP motif is the platelet-receptor glycoprotein Ibα that has a steep curvature (41), whereas the prototype AF motif is the Nogo receptor which has a relatively flat curvature (42). The LRR domain is an exceptionally stable solenoid-like structure. The side chains of the leucine residues (or other aliphatic residues) are closely packed and oriented toward the interior of the domain to form a hydrophobic core in a similar fashion as observed in other globular proteins (39). The β-sheet along its concave side also contributes to the stability of the structure as each β-strand forms five hydrogen bonds to the adjacent β-strand. To further stabilize the structure, the conserved asparagine residues (on the concave side) form an asparagine ladder where the side chains stack on top of adjacent asparagine residues and form hydrogen bonds (39, 43). For LRR proteins with repeating AF motifs, the phenylalanines on the convex side form a phenylalanine spine that also adds to the stability of the LRR domain (42, 44). Commonly, a binding site is located in the concave surface of the LRR domain, however, the convex surface also can be utilized as site of ligand interaction (39).

The N- and C-Terminal Caps

Although the LRR domain is a stable solenoid structure, it would appear that capping structures are essential to maintain stability. In most cases, especially extracellular LRR and membrane-associated LRR proteins, there are cysteine-rich subdomains at the N- and C-terminal ends of the LRR domain, termed N-terminal (LRRNT) and C-terminal (LRRCT) capping motifs, respectively. Based on sequence analysis, LRRNT motifs have a consensus sequence of CPx(2-5)CxCx(6-19)Cx(6-8)Px(3)Px(5)LxL, where x indicates any residue (39, 45). The typical structure of LRRNT contains a β-strand antiparallel to the main LRR β-sheet, followed by 20 to 21 residues before entering a β-strand that is parallel to the LRR. As this strand is often not a canonical LRR, it is excluded from the description of the body of the LRR domain.

Based on phylogenetic analysis and the number of cysteine residues present, there are four types of LRRCT motifs, CF1–4 (45). CF1 is the most common capping structure containing four cysteines (CxCx(17–24)Cx(9–18)CxxP). CF2 has two cysteines, separated by 33 to 34 residues and is found in small proteoglycans, CF3 has three cysteines (CCx(14–27)C) found in GPCRs, and CF4 has two cysteines separated by 1 to 11 residues and is found in plant LRR proteins.

Structures of LGRs

Type A LGRs

The FSHr crystal structure is the best understood of the LGRs (46). The LRR domain consists of repeats of irregular length and conformation (**Figure 1A**). As expected the LRR domain contains an LRRNT with an antiparallel β-strand followed by the expected parallel β-strand of this cap. This is then followed by nine parallel β-strands of the LRR domain (**Table 1**), and additional two parallel β-strands in the C-terminal cysteine cap, which form a typical CF3 cap. Prior to the last parallel β-strand, there is an insertion of an α-helix and a long hairpin loop that contains a sulfated tyrosine, collectively referred to as the hinge region, and forms an integrated structure within the LRR domain (**Figure 1A**) (47). Consequently, the entire LRR domain consists of 12 parallel β-strands. On the convex side of the LRR domain, there are seven short β-strands separated into three β-sheets. Importantly, the intervening sequences of the convex side follow from the N-terminal end as: an LP motif, three AF motifs, one LP motif, two AF motifs, and then three LP motifs. Thus, there is an increasing curvature of the domain running from N- to C-terminus. Superimposing the structures of the FSHr and TSHr LRR domains shows similar structures despite different primary sequences and disulfide connectivity (40).

Upon binding to ligand, there is a significant change to the hinge structure of FSHr, otherwise the LRR domain is similar to that of the ligand free (47). The binding of FSH is described as a "handclasp" interaction, where 10 parallel β-strands of FSHr, including the parallel β-strand of the LRRNT, are in contact with the hormone mainly via electrostatic interaction (46). The interactions can be divided into two flat surfaces; one is where the C-terminal end of the α- and β-units of FSH interact with the parallel β-strand of the LRRNT and the first six LRRs and the other is where the second loops of the α- and β-units of FSH interact with the tips of the β-strands of LRR1–5 and the C-terminal ends of LRR7–9, respectively. The hairpin loop between the last two parallel β-strands presents an essential tyrosine residue, which becomes sulfated (sTyr). This sTyr makes an important contribution to ligand binding by inserting into a hydrophobic pocket in FSH. As it is clear that FSH can bind in the absence of this hinge region, this structure provides evidence of a "two-step" binding mechanism (47). Following FSH binding to FSHr, the sTyr binds to the hormone lifting the hairpin loop from an inhibitory state of the TM domain that results in activation of the receptor.

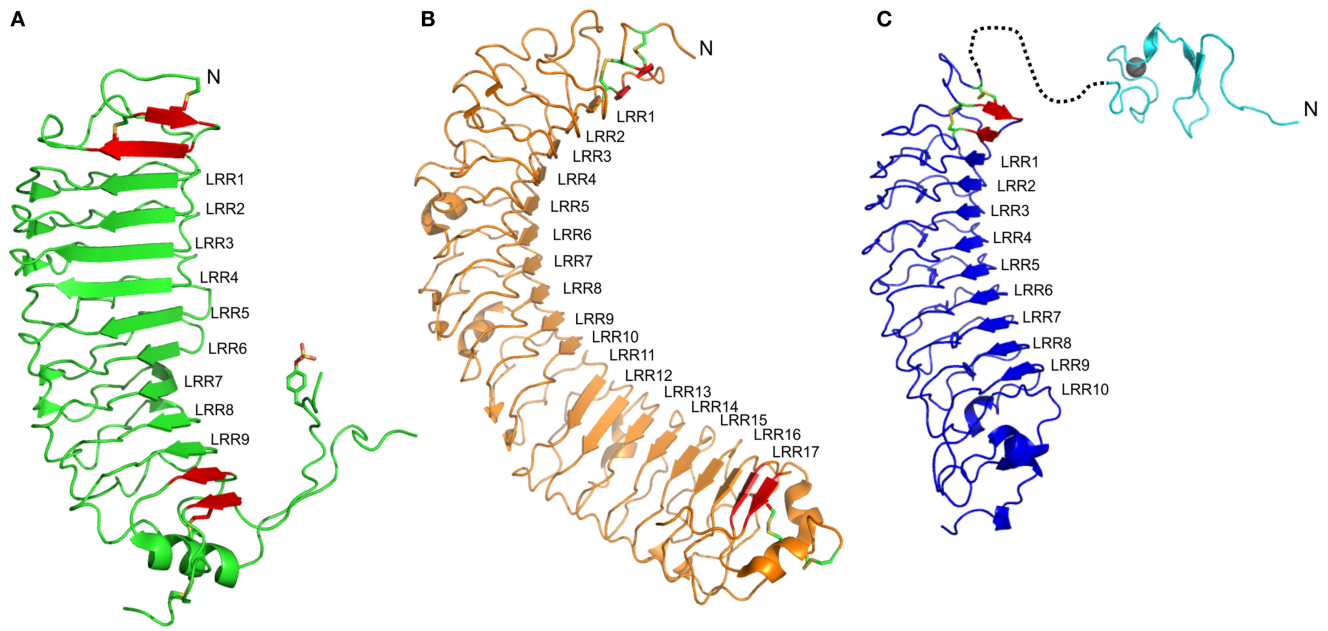

FIGURE 1 | Structures of ectodomains of members of the LGR family. **(A)** The type A member FSHr (PBD: 4AY9) shows nine LRRs. LRR1–6 show a shallow curvature while the dominance of LP motifs in the convex side of LRR7–9 results in a steep curvature. The ligand shows interactions to most of the LRRs, especially LRR1–5 and LRR7–9 **(B)** The type B member LGR4 (PDB: 4KT1). The concave side of the LRR protein is separated into two sheets, LRR1–10 and LRR11–17, due to the absence of the conserved Asn residues within the LRR motif of LRR11 and 12. The ligand binds to the first sheet, making contacts with residues in LRR1, LRR3–9. **(C)** A homology model of the ECD of the type C member RXFP1. The 10 LRRs are predicted to form a shallow curvature. The ligand, H2 relaxin, is expected to bind to LRR4–6 and LRR8. The structure of the N-terminal LDLa module (PDB: 2JM4) for this ECD is also shown, although the structure of the linker that joins to the LRR domain remains unknown. In each structure, additional β-strands (red), which are integral to the domain, are shown but these strands typically lack the xLx portion of the LRR motif, and usually include disulfide bonds characteristic of the N- and C-terminal capping motifs. At the N-terminal end of each LRR domain, an antiparallel β-strand followed by a β-strand parallel to the remainder of the LRR is observed. At the C-terminal end, significant differences for the three members are observed. For FSHr, a large hinge containing a functionally important sulfated Tyr residue is present; for LGR4, this hinge is absent, but a typical CF3 capping motif is present; for RXFP1, the C-terminal cap does not appear conserved, the hinge is short, and therefore, the structure of this region is difficult to predict.

The LRR domain and the ligand of FSHr and TSHr are similar, although the disulfide arrangement of the LRRNT differs (48). Nevertheless the mechanism is suggested to be the same for these receptors as TSHr has a structurally similar sTyr site (49, 50), which is essential for TSH binding and activation (51–53). Currently, there is limited knowledge about the activation mechanism of LHr. Although the sTyr site is present in the hinge region of LHr (54, 55), the mechanism of LHr differs from FSHr and TSHr as removal of the ectodomain does not result in constitutively active receptor (56).

Type B LGRs

The LRR domains in Type B LGRs are typically larger than those of Type A LGRs (**Table 1**). The crystal structures of both LGR4 and LGR5 comprise 17 typical LRR β-strands with an N-terminal antiparallel β-strand followed by another β-strand that is parallel to the LRR domain, and two additional parallel β-strands at the C-terminus (**Figure 1B**) (34, 57). On the convex side, the secondary structures are more variable with various lengths of loops, α-helices, and β-strands. In LGR4 and LGR5, the conserved asparagine residues in LRR11 and LRR12 are missing, resulting in two separate β-sheets, one from LRR1–10 and the other from LRR13–17 (**Figure 1B**) (34, 58–60). The intervening sequences on the convex side follow from the N-terminal end: in the first β-sheet, two AF, four LP, one AF, two LP, and one AF; and in the second β-sheet, three LP, two AF, and one LP motif. The large number of LP motifs result in a more curved surface than the type A receptors. These proteins have a typical LRRNT, whereas the LRRCT has a short four-residue intervening sequence within the otherwise CF3 cap.

Recently, Rspos were identified as the native ligands of type B LGRs (4, 61, 62). In LGR4, the ligand binds to the first LRR and LRR3–LRR9 (the first β-sheet) and the binding interface is smaller compared to FSH–FSHr (1860 compared to 2600 $Å^2$) (34, 60). The interface is mainly electrostatic within LRR4 and hydrophobic within LRR5–7. Similar to LGR4, the LGR5 binding interface consists of LRR3–9 with total surface area of 870 $Å^2$ (58). LGR5 binds to Rspo in a similar manner to LGR4, a mix of charged and hydrophobic clamping interactions. Based on these observations, the binding of Rspo is conserved across the type B LGRs and it is supported by the fact that there is lack of specificity between different Rspos and type B LGRs (3). In type B LGRs, there is no evidence that the hinge region or even the LRRCT is involved in ligand binding or activation. The LRRCT of LGR4 can be deleted or substituted with LRRCT motifs from other proteins without affecting activity or binding (63). Moreover, antibodies targeted to the LRRCT of LGR5 do not block Rspo activity (62). However, another antibody targeted specifically to

the hinge region has been shown to induce activity in the absence of Rspo (58).

While there are similarities in how type A and type B LGRs bind ligand, the signal pathways and receptor activation are different. Rspo signaling mediated by LGR4, LGR5, or LGR6 is through Wnt signaling and not the canonical GPCR pathways (3, 61, 63), which is in contrast to type A and type C LGRs. Multiple mechanisms have been proposed to explain how type B LGRs regulate Wnt signaling. The binding of Rspo to the ectodomains of LG4–6 recruits the E3 ligases (RNF4 and ZNRF3) to form a ternary complex that promotes clearance of the E3 ligase, thus a reduction in Wnt receptor ubiquitination and degradation, and consequently increased Wnt signaling (64). In addition, the Rspo–LGR4 recruits the scaffold protein IQ motif containing GTPase-activating protein 1 (IQGAP1) into the Wnt complex to potentiate signaling (65).

Type C LGRs

Presently, there are no structures of the LRR domains of type C LGRs. However, the structures of type A and type B LGRs, as well as those of other LRR domains, allow predictions to be made for this class of LGRs. Based on the primary sequence, the LRR domain is expected to have 10 LRR repeats (**Table 1**) with an N-terminal antiparallel β-strand and an additional parallel β-strand forming the N-terminal cap. Analysis of the LRRs from the type C LGRs, RXFP1 and RXFP2, suggests that the LRRs are more regular than the type A and type B LGRs. The intervening sequences on the convex side of RXFP1 following from the N-terminal end are predicted to be four AF, one LP, two AF, and one LP motif. Such an arrangement predicts a relatively flat surface and the predominance of the AF motif allows straight forward homology modeling of the LRR domain of RXFP1 based on the prototype AF motif Nogo receptor (42). A homology model built by Modeler (66), using the Nogo receptor (PDB: 1OZN) as a template with ~29% sequence identity, shows a spine of phenylalanine residues down the convex side, except at LRR5 where a leucine residue is aligned, and a ladder of asparagine residues of the LRR motif on the concave side of the model (**Figure 1C**). The conservation of the N-terminal cysteine residues predicts an LRRNT similar to type A and type B LGRs. However, there are only two cysteine residues in the C-terminal hinge of RXFP1, separated by eight residues, and therefore are CF4-like rather than the CF3 capping motif expected in LRR-containing GPCRs (45). Therefore modeling of this region against the Nogo receptor, or any other LRR protein, is highly speculative. The hinge region of RXFP1 and RXFP2 is relatively short (~30 residues compared to 72–123 residues in other LGRs) (1). Considering the shortness of the hinge region and the fact that the LDLa module at the N-terminus is key for receptor activation suggests that the hinge region in the RXFPs might not be involved in the binding and activation mechanism of these receptors.

The cognate ligands of RXFP1 and RXFP2 are H2 relaxin and INSL3, respectively. These peptides share structural similarity to insulin, where an A-chain and a B-chain are held together by two disulfide bonds (67, 68). Extensive studies of these two peptides conclude that the B-chain is essential for receptor binding [as reviewed in Ref. (10)]. The B-chain binding cassette of H2 relaxin is defined as RxxxRxxI/L, where x is any amino acid, and of INSL3 as HxxxRxxVR (68). Furthermore, a tryptophan residue located at the C-terminal of the B-chain is wrapped back around the structure of INSL3 and has been shown to be essential for binding and activation of its receptor, RXFP2 (69, 70). Binding to the LRR domains of RXFP1 and RXFP2 has been extensively studied by mutagenesis of both the receptors and H2 relaxin or INSL3. Previous modeling of the H2 relaxin–RXFP1 interaction has used RI as a template and subsequently, mutagenesis studies were performed to verify this model (71). The model of H2 relaxin–RXFP1 shows the conserved basic residues (Arg13 and Arg17) in the B-chain interact with acidic residues within the LRR6 and LRR8 of RXFP1, respectively. The other conserved hydrophobic residue (Ile20) within the B-chain is predicted to interact with a cluster of hydrophobic residues across LRR4-5. Hence, based on these data, it is proposed that H2 relaxin binds to the LRR domain at a 45^{o} angle across the face of LRR4–8. Scott et al. (72) also used the Nogo receptor as a template to model the INSL3–RXFP2 interaction, and given the expected structural similarity of RXFP1 and RXFP2 with the Nogo structure we present a model of RXFP1 (**Figure 1C**). The model of INSL3–RXFP2 concludes that the positively charged residues (Arg16 and Arg20) of INSL3 interact with negatively charged residues in LRR6 and 8 and the conserved hydrophobic residues in the B-chain of INSL3 (His12, Val19, and Trp27) with hydrophobic residues across LRR1–4. In this model, the B-chain of INSL3 requires a larger surface area than H2 relaxin and lies perpendicular to the LRRs.

The molecular details of how H2 relaxin and INSL3 bind and activate RXFP1 and RXFP2 are still ambiguous, despite extensive research. It is clear that a ligand-binding site is present in the LRR domain, but the relatively short LRRCT makes it unlikely to interact with the ligand in a type A LGR manner. While various receptor constructs show that neither the LDLa module nor the TM domain are required for high-affinity binding (29, 73), additional weak affinity binding sites for the ligand have been proposed for both RXFP1 and RXFP2 on the TM domain (73–75). Support for an interaction between the ligand and the TM domain includes experiments conducted on human relaxin 3 (H3 relaxin) (76), a homolog of H2 relaxin, and INSL3. H3 relaxin binds to both RXFP1 and RXFP3 (GPCR135). The latter lacks an ECD and so binding and activation is solely through the TM domain of RXFP3 (77). Taking advantage of the binding specificity of H3 relaxin for RXFP1 over RXFP2, ECD/TM domain chimeras of RXFP1/2 were constructed and tested for ligand binding and signaling (74). The chimera of the ECD of RXFP1 with the TM of RXFP2 binds H3 relaxin more weakly than to wild-type RXFP1, and signaling is reduced. On replacing the exoloop-2 of the TM domain in this construct with exoloop-2 of RXFP1, binding was similar to wild-type RXFP1 and signaling was fully restored, supporting an interaction by H3 relaxin with both the ECD and exoloop-2 of RXFP1. To further investigate the binding of H2 relaxin to the exoloops, exoloop-1 and exoloop-2 were engineered onto a soluble protein scaffold preserving the disulfide between exoloop-1 and -2 and therefore potentially creating a native-like structure of exoloop-2 (75). Using NMR spectroscopy and pull-down assays, specific interactions of H2 relaxin were observed to this scaffold, but not in a construct lacking the disulfide. These latter experiments show that the ligand binds to the exoloop-2, and also the importance of the integrity of the conformation of exoloop-2. Furthermore,

mutation of a phenylalanine residue (equivalent to Phe564) to alanine within exoloop-2 showed loss of binding to H2 relaxin, and when this mutation was tested in the full-length receptor signaling was lost. Collectively, these data indicate that for type C LGRs, in contrast to type A and possibly type B, the ligands have binding sites on both the ECD and TM domain, where the latter are also essential for activation.

H2 relaxin binds to both RXFP1 and RXFP2, whereas INSL3 only binds RXFP2. To investigate if important differences lie within the LRR domain or involve the TM domain, a series of RXFP1/2 chimeras were prepared (78). These included constructs that swapped the TM domains or consisted of only the ECDs attached to single TM helices: referred to as 7BP or ECD-1 for the protein containing the ECD of RXFP1, and 8BP or ECD-2 for RXFP2 (8, 78). To test the contribution of the LRRs within the ECDs to ligand specificity and activation, residues within the LRRs of the RXFP1 constructs were swapped with LRRs of RXFP2 in order to gain INSL3 binding. Notably, in contrast to RXFP1, 7BP (ECD-1) binds INSL3, albeit more weakly than 8BP or RXFP2 but suggests that a binding site for INSL3 already exists in RXFP1. A high-affinity binding site for INSL3 was engineered into 7BP with as little as swapping a single LRR (specifically LRR1), and this binding was indistinguishable to that for 8BP or RXFP2. However, when the mutations that produce a high-affinity binding of INSL3 in 7BP were tested in full-length RXFP1, no gain in the binding of INSL3 was observed. As additional binding sites for INSL3 and H2 relaxin are proposed to be present on the TM domain (73–75), the TM domain of RXFP2 was also replaced on the RXFP1 construct that included the putative high-affinity binding site for INSL3. However, again binding or activation by INSL3 was not recovered. These data suggest that while clearly the LRR domain of these receptors harbors a ligand-binding site, additional binding features remain to be elucidated. Indeed, issues of the juxtaposition of the LRR with respect to the TM domain may sterically hinder INSL3 binding (78).

There is additional evidence of distinct differences in the mode of peptide binding to the RXFP1 and RXFP2 ECDs and the impact on receptor activation. Studies on synthetic H2 relaxin and INSL3 peptides with A-chain truncations or substitutions show distinct differences in the ability of the peptides to bind and activate RXFP1 and RXFP2. H2 relaxin peptides with truncations of the A-chain (79) or A-chain substitutions with other relaxin family peptide A chains (80) show loss of binding affinity in both RXFP1 and RXFP2 with parallel decreases in activation whereas truncations or alterations in the A-chain of INSL3 do not affect the high-affinity binding to RXFP2 (81–83) but abolish activation. These observations highlight that differences in the mode of ligand binding to these receptors exist and these modes have not been fully elucidated. Additionally, they highlight that H2 relaxin binds to RXFP2 in a manner different from the INSL3 mode and similar to the mode it binds to RXFP1.

The LDLa Module of Type C LGRs

The presence of a unique N-terminal LDLa module distinguishes RXFP1 and RXFP2 from other LGRs, and indeed are the only GPCRs to contain this module (84). The LDLa module was first described as repeating units in the LDL receptor (85) and other related proteins (86) where they are involved in lipid metabolism. LDLa modules have since been described in a variety of proteins both as repeats and single domains in proteins with diverse functions, such as viral entry (87), breast cancer invasion and metastasis (88), and cell differentiation (89). LDLa modules are typically 4 kDa in size and have highly conserved structural features, including three disulfide bonds and an essential calcium ligation motif that contributes to maintaining overall fold and structure of the modules (85, 90, 91). The significance of the LDLa module in RXFP1 and RXFP2 was discovered during the characterization of splice variants of the receptors that lacked the LDLa modules (29). A naturally occurring splice variant of RXFP2 (LGR8-short) was identified and found to lack the LDLa module. While LGR8-short binds H2 relaxin and INSL3, no INSL3- or H2 relaxin-induced cAMP signaling was detected. This prompted the production of an engineered RXFP1 without the LDLa module (LGR7-short or RXFP1-short) and while it bound H2 relaxin equal to full-length RXFP1, no cAMP-induced signaling was detected (29). Recently, a panel of reporter genes was used to assess whether RXFP1 or RXFP2 without the LDLa module could signal through alternative GPCR signaling pathways other than those that signal through cAMP (92, 93). However, both RXFP1-short and RXFP2-short were unable to signal through any signaling pathway.

The structures of both the RXFP1 and RXFP2 LDLa modules have been solved using nuclear magnetic resonance (NMR) spectroscopy in an effort to understand the importance of specific residues (84, 93). While RXFP1 and RXFP2 have evolved to use the LDLa module for an essential role in signal activation, the molecular details are different between the two receptors. For example, chimeric RXPF2 (RXFP2–LB2), where the LDLa module is replaced with the second ligand-binding domain (LB2) of the low-density lipoprotein receptor (LDLr), showed some INSL3-induced cAMP activity (93), whereas a similar construct of RXFP1 (RXFP1–LB2) showed no significant H2 relaxin-induced cAMP activity (92). Adding back regions of the native RXFP2 LDLa sequence into RXFP2–LB2 did increase signaling of the module; however, this appeared to be due to reconstitution of the correct structure rather than specific side chain interactions. In comparison, in an attempt to rescue signaling in a RXFP1–LB2 chimera, the hydrophobic portions of the side chains of a cluster of residues (Leu7, Tyr9, and Lys17) were pinpointed to be essential, highlighting these residues may be involved in receptor activation (92). The capacity of these chimeric studies are insufficient to understand exactly the activation mechanism by the LDLa module, however, in a separate study using an engineered scaffold containing the extracellular loops of RXFP1, a weak interaction of the scaffold with the LDLa module was observed supporting the notion that it interacts with the TM domain for activation (75). Thus, in RXFP1 and RXFP2, the LDLa module is not involved in ligand binding, rather plays a crucial role in receptor activation by potentially interacting with the TM domain (29, 84, 92, 93). The LDLa module may therefore act as a tethered ligand that requires binding of H2 relaxin to mediate activation of the receptor; a mechanism which is distinct from the Type A LGRs two-step binding mechanism (47).

Joining the LDLa module to the LRR domain is a linker of variable length, 32 or 25 residues in human RXFP1 and RXFP2,

respectively. This linker has been considered a simple tether with the function of intramolecular localization of the LDLa module to the TM domain for efficient activation. Swapping the LDLa module of RXFP2 onto RXFP1 resulted in loss of signaling, suggesting that the LDLa modules cannot be swapped; although in this study a large portion of the linker of RXFP2 was also swapped (94). However, in a second study, the LDLa modules of RXFP1 and RXFP2 were swapped, taking care not to alter the linker length or sequence, and these showed ligand-mediated activation (95). In this latter work, swapping the LDLa module of RXFP2 onto RXFP1, thus preserving the linker, LRR, and TM domains of RXFP1, showed wild-type H2 relaxin-induced cAMP activation. Importantly, maximum activation could not be obtained, suggesting that the LDLa module of RXFP2 could not make essential interactions with the TM domain of RXFP1 for full activation. These observations are consistent with site-directed mutagenesis experiments of the LDLa module in full-length RXFP1 (84, 92). When both the LDLa module and TM domain of RXFP2 were swapped onto RXFP1, maximum activation was achieved suggesting that the LDLa module was now acting as a full agonist and the interactions between the LDLa module and TM domain were fully restored. Swapping the LDLa module of RXFP1 onto RXFP2, thus preserving the linker, LRR, and TM domains of RXFP2, showed similar potency for both ligands (95). This may reflect the fact that H2 relaxin is a ligand of both RXFP1 and RXFP2 and the RXFP2–INSL3 evolved more recently (96). Thus the RXFP1 LDLa module may be equally efficacious on both RXFP1 and RXFP2. These results are in contrast to the LDLa-linker deletion where activation was lost (94) and challenge the notion that the linker is only a tether. Furthermore, these data suggest that the linker may play a role in activation akin to the hinge of the type A receptors. Importantly, a natural splice variant of RXFP1 where the LDLa module and the following linker residues are expressed as a soluble protein can antagonize the activity of H2 relaxin at RXFP1 supporting a functional role of the linker (29). Further research into whether the linker interacts with H2 relaxin or the TM domain is required.

Conclusion

The LGR family has in common a LRR domain that serves as a ligand-binding site. From the point of view of mechanism, this is the only common feature of the three subtypes of receptors. At the extreme, the type B LGRs on binding ligand do not function through a canonical GPCR pathway by activation of either G-proteins or β-arrestin. When the ligand binds to type A LGRs, it undergoes a conformational change that enables an interaction between the ligand with the C-terminal hinge of the ECD, which is proposed to release the TM domain of the receptor from an inhibited state. Evidence presented for the type C LGRs, RXFP1 and RXFP2, shows that the true agonist of these receptors is the N-terminal LDLa module. Thus, it is hypothesized for these receptors that the binding of ligand results in a conformational change to the ECD to present the LDLa module to the TM domain for activation. Structures of the ECDs of type A and type B LGRs, free and in complex with ligand, suggest that conformational change of the LRR domain of the type C LGRs is unlikely. Given the size and structure of the ligands, H2 relaxin and INSL3, and the LDLa modules, it is difficult to envisage significant conformational changes to these molecules. Therefore, hypotheses of reorientation of the LDLa module or localization through modification of the structure of the linker that tethers the LDLa module to the LRR domain may be key to the activation process. Further research, including structure elucidation, is required to understand how the type C LGRs are activated.

Acknowledgments

This research was supported by National Health and Medical Research Council (NHMRC) of Australia project grants [628427] and [1043750] to RB and PG and the Victorian Government Operational Infrastructure Support Program. RB is a recipient of an NHMRC Research Fellowship. SL and AS are recipients of Melbourne International Research Scholarships.

References

1. Hsu SY, Kudo M, Chen T, Nakabayashi K, Bhalla A, Van Der Spek PJ, et al. The three subfamilies of leucine-rich repeat-containing G protein-coupled receptors (LGR): identification of LGR6 and LGR7 and the signaling mechanism for LGR7. *Mol Endocrinol* (2000) **14**:1257–71. doi:10.1210/mend.14.8.0510
2. Hsu SY, Liang S-G, Hsueh AJW. Characterization of two LGR genes homologous to gonadotropin and thyrotropin receptors with extracellular leucine-rich repeats and a G protein-coupled, seven-transmembrane region. *Mol Endocrinol* (1998) **12**:1830–45. doi:10.1210/mend.12.12.0211
3. de Lau W, Barker N, Low TY, Koo B-K, Li VSW, Teunissen H, et al. Lgr5 homologues associate with Wnt receptors and mediate R-spondin signalling. *Nature* (2011) **476**:293–7. doi:10.1038/nature10337
4. Glinka A, Dolde C, Kirsch N, Huang Y-L, Kazanskaya O, Ingelfinger D, et al. LGR4 and LGR5 are R-spondin receptors mediating Wnt/β-catenin and Wnt/PCP signalling. *EMBO Rep* (2011) **12**:1055–61. doi:10.1038/embor.2011.175
5. Overbeek PA, Gorlov IP, Sutherland RW, Houston JB, Harrison WR, Boettger-Tong HL, et al. A transgenic insertion causing cryptorchidism in mice. *Genesis* (2001) **30**:26–35. doi:10.1002/gene.1029
6. Nef S, Parada LF. Cryptorchidism in mice mutant for Insl3. *Nat Genet* (1999) **22**:295–9. doi:10.1038/10364
7. Zimmermann S, Steding G, Emmen JM, Brinkmann AO, Nayernia K, Holstein AF, et al. Targeted disruption of the Insl3 gene causes bilateral cryptorchidism. *Mol Endocrinol* (1999) **13**:681–91. doi:10.1210/mend.13.5.0272
8. Hsu SY, Nakabayashi K, Nishi S, Kumagai J, Kudo M, Sherwood OD, et al. Activation of orphan receptors by the hormone relaxin. *Science* (2002) **295**:671–4. doi:10.1126/science.1065654
9. Bathgate RA, Ivell R, Sanborn BM, Sherwood OD, Summers RJ. International union of pharmacology LVII: recommendations for the nomenclature of receptors for relaxin family peptides. *Pharmacol Rev* (2006) **58**:7–31. doi:10.1124/pr.58.1.9
10. Bathgate RA, Halls ML, van der Westhuizen ET, Callander GE, Kocan M, Summers RJ. Relaxin family peptides and their receptors. *Physiol Rev* (2013) **93**:405–80. doi:10.1152/physrev.00001.2012
11. Ivell R, Bathgate RA. Reproductive biology of the relaxin-like factor (RLF/INSL3). *Biol Reprod* (2002) **67**:699–705. doi:10.1095/biolreprod.102.005199
12. Unemori EN, Amento EP. Relaxin modulates synthesis and secretion of procollagenase and collagen by human dermal fibroblasts. *J Biol Chem* (1990) **265**:10681–5.
13. Unemori EN, Bouhana KS, Werb Z. Vectorial secretion of extracellular matrix proteins, matrix-degrading proteinases, and tissue inhibitor of metalloproteinases by endothelial cells. *J Biol Chem* (1990) **265**:445–51.

14. Casten GG, Boucek RJ. Use of relaxin in the treatment of scleroderma. *J Am Med Assoc* (1958) **166**:319–24. doi:10.1001/jama.1958.02990040005002
15. Conrad KP. Unveiling the vasodilatory actions and mechanisms of relaxin. *Hypertension* (2010) **56**:2–9. doi:10.1161/HYPERTENSIONAHA.109.133926
16. Metra M, Ponikowski P, Cotter G, Davison BA, Felker GM, Filippatos G, et al. Effects of serelaxin in subgroups of patients with acute heart failure: results from RELAX-AHF. *Eur Heart J* (2013) **34**:3128–36. doi:10.1093/eurheartj/eht371
17. Felker GM, Teerlink JR, Butler J, Hernandez AF, Miller AB, Cotter G, et al. Effect of serelaxin on mode of death in acute heart failure: results from the RELAX-AHF study. *J Am Coll Cardiol* (2014) **64**:1591–8. doi:10.1016/j.jacc.2014.05.071
18. Filippatos G, Teerlink JR, Farmakis D, Cotter G, Davison BA, Felker GM, et al. Serelaxin in acute heart failure patients with preserved left ventricular ejection fraction: results from the RELAX-AHF trial. *Eur Heart J* (2014) **35**:1041–50. doi:10.1093/eurheartj/eht497
19. Takahashi N, Takahashi Y, Putnam FW. Periodicity of leucine and tandem repetition of a 24-amino acid segment in the primary structure of leucine-rich alpha 2-glycoprotein of human serum. *Proc Natl Acad Sci U S A* (1985) **82**:1906–10. doi:10.1073/pnas.82.7.1906
20. de Wit J, Ghosh A. Control of neural circuit formation by leucine-rich repeat proteins. *Trends Neurosci* (2014) **37**:539–50. doi:10.1016/j.tins.2014.07.004
21. Westwell-Roper C, Nackiewicz D, Dan M, Ehses JA. Toll-like receptors and NLRP3 as central regulators of pancreatic islet inflammation in type 2 diabetes. *Immunol Cell Biol* (2014) **92**:314–23. doi:10.1038/icb.2014.4
22. Shin S, Brodsky IE. The inflammasome: learning from bacterial evasion strategies. *Semin Immunol* (2015) **27**:102–10. doi:10.1016/j.smim.2015.03.006
23. Williams M, Summers BJ, Baxter RHG. Biophysical analysis of anopheles gambiae leucine-rich repeat proteins APL1A1, APLB and APL1C and their interaction with LRIM1. *PLoS One* (2015) **10**(3):e0118911. doi:10.1371/journal.pone.0118911
24. McAndrew R, Pruitt RN, Kamita SG, Pereira JH, Majumdar D, Hammock BD, et al. Structure of the OsSERK2 leucine-rich repeat extracellular domain. *Acta Crystallogr D Biol Crystallogr* (2014) **70**:3080–6. doi:10.1107/S1399004714021178
25. Kajava AV, Vassart G, Wodak SJ. Modeling of the three-dimensional structure of proteins with the typical leucine-rich repeats. *Structure* (1995) **3**:867–77. doi:10.1016/S0969-2126(01)00222-2
26. Van Hiel MB, Vandersmissen HP, Van Loy T, Vanden Broeck J. An evolutionary comparison of leucine-rich repeat containing G protein-coupled receptors reveals a novel LGR subtype. *Peptides* (2012) **34**:193–200. doi:10.1016/j.peptides.2011.11.004
27. Pierce JG, Parsons TF. Glycoprotein hormones: structure and function. *Annu Rev Biochem* (1981) **50**:465–95. doi:10.1146/annurev.bi.50.070181.002341
28. Yoon JK, Lee JS. Cellular signaling and biological functions of R-spondins. *Cell Signal* (2012) **24**:369–77. doi:10.1016/j.cellsig.2011.09.023
29. Scott DJ, Layfield S, Yan Y, Sudo S, Hsueh AJW, Tregear GW, et al. Characterization of novel splice variants of LGR7 and LGR8 reveals that receptor signaling is mediated by their unique low density lipoprotein class A modules. *J Biol Chem* (2006) **281**:34942–54. doi:10.1074/jbc.M602728200
30. Van Loy T, Van Hiel MB, Vandersmissen HP, Poels J, Mendive F, Vassart G, et al. Evolutionary conservation of bursicon in the animal kingdom. *Gen Comp Endocrinol* (2007) **153**:59–63. doi:10.1016/j.ygcen.2006.12.004
31. Simoni M, Gromoll J, Nieschlag E. The follicle-stimulating hormone receptor: biochemistry, molecular biology, physiology, and pathophysiology. *Endocr Rev* (1997) **18**:739–73. doi:10.1210/er.18.6.739
32. Ascoli M, Fanelli F, Segaloff DL. The lutropin/choriogonadotropin receptor, a 2002 perspective. *Endocr Rev* (2002) **23**:141–74. doi:10.1210/edrv.23.2.0462
33. Harfst E, Johnstone AP, Gout I, Taylor AH, Waterfield MD, Nussey SS. The use of the amplifiable high-expression vector pEE14 to study the interactions of autoantibodies with recombinant human thyrotrophin receptor. *Mol Cell Endocrinol* (1992) **83**:117–23. doi:10.1016/0303-7207(92)90152-V
34. Wang D, Huang B, Zhang S, Yu X, Wu W, Wang X. Structural basis for R-spondin recognition by LGR4/5/6 receptors. *Genes Dev* (2013) **27**:1339–44. doi:10.1101/gad.219360.113
35. Gong X, Carmon KS, Lin Q, Thomas A, Yi J, Liu Q. LGR6 is a high affinity receptor of R-spondins and potentially functions as a tumor suppressor. *PLoS One* (2012) **7**(5):e37137. doi:10.1371/journal.pone.0037137
36. Halls ML, Bathgate RA, Sutton SW, Dschietzig TB, Summers RJ. International union of basic and clinical pharmacology. XCV. Recent advances in the understanding of the pharmacology and biological roles of relaxin family peptide receptors 1-4, the receptors for relaxin family peptides. *Pharmacol Rev* (2015) **67**:389–440. doi:10.1124/pr.114.009472
37. Kobe B, Deisenhofer J. Crystal structure of porcine ribonuclease inhibitor, a protein with leucine-rich repeats. *Nature* (1993) **366**:751–6. doi:10.1038/366751a0
38. Kobe B, Kajava AV. The leucine-rich repeat as a protein recognition motif. *Curr Opin Struct Biol* (2001) **11**:725–32. doi:10.1016/S0959-440X(01)00266-4
39. Bella J, Hindle KL, Mcewan PA, Lovell SC. The leucine-rich repeat structure. *Cell Mol Life Sci* (2008) **65**:2307–33. doi:10.1007/s00018-008-8019-0
40. Jiang X, Dias JA, He X. Structural biology of glycoprotein hormones and their receptors: insights to signaling. *Mol Cell Endocrinol* (2014) **382**:424–51. doi:10.1016/j.mce.2013.08.021
41. Huizinga EG, Tsuji S, Romijn RA, Schiphorst ME, De Groot PG, Sixma JJ, et al. Structures of glycoprotein Ibalpha and its complex with Von Willebrand factor A1 domain. *Science* (2002) **297**:1176–9. doi:10.1126/science.107355
42. He XL, Bazan JF, Mcdermott G, Park JB, Wang K, Tessier-Lavigne M, et al. Structure of the Nogo receptor ectodomain: a recognition module implicated in myelin inhibition. *Neuron* (2003) **38**:177–85. doi:10.1016/S0896-6273(03)00232-0
43. Kobe B, Deisenhofer J. Proteins with leucine-rich repeats. *Curr Opin Struct Biol* (1995) **5**:409–16. doi:10.1016/0959-440X(95)80105-7
44. Barton WA, Liu BP, Tzvetkova D, Jeffrey PD, Fournier AE, Sah D, et al. Structure and axon outgrowth inhibitor binding of the Nogo-66 receptor and related proteins. *EMBO J* (2003) **22**:3291–302. doi:10.1093/emboj/cdg325
45. Kajava AV. Structural diversity of leucine-rich repeat proteins. *J Mol Biol* (1998) **277**:519–27. doi:10.1006/jmbi.1998.1643
46. Fan QR, Hendrickson WA. Structure of human follicle-stimulating hormone in complex with its receptor. *Nature* (2005) **433**:269–77. doi:10.1038/nature03206
47. Jiang X, Liu H, Chen X, Chen P-H, Fischer D, Sriraman V, et al. Structure of follicle-stimulating hormone in complex with the entire ectodomain of its receptor. *Proc Natl Acad Sci U S A* (2012) **109**:12491–6. doi:10.1073/pnas.1206643109
48. Núñez Miguel R, Sanders J, Chirgadze DY, Blundell TL, Furmaniak J, Rees Smith B. FSH and TSH binding to their respective receptors: similarities, differences and implication for glycoprotein hormone specificity. *J Mol Endocrinol* (2008) **41**:145–64. doi:10.1677/JME-08-0040
49. Sanders J, Chirgadze DY, Sanders P, Baker S, Sullivan A, Bhardwaja A, et al. Crystal structure of the TSH receptor in complex with a thyroid-stimulating autoantibody. *Thyroid* (2007) **17**:395–410. doi:10.1089/thy.2007.0041
50. Sanders P, Young S, Sanders J, Kabelis K, Baker S, Sullivan A, et al. Crystal structure of the TSH receptor (TSHR) bound to a blocking-type TSHR autoantibody. *J Mol Endocrinol* (2011) **46**:81–99. doi:10.1530/JME-10-0127
51. Kosugi S, Ban T, Akamizu T, Kohn LD. Site-directed mutagenesis of a portion of the extracellular domain of the rat thyrotropin receptor important in autoimmune thyroid disease and nonhomologous with gonadotropin receptors. Relationship of functional and immunogenic domains. *J Biol Chem* (1991) **266**:19413–8.
52. Costagliola S, Panneels V, Bonomi M, Koch J, Many MC, Smits G, et al. Tyrosine sulfation is required for agonist recognition by glycoprotein hormone receptors. *EMBO J* (2002) **21**:504–13. doi:10.1093/emboj/21.4.504
53. Kleinau G, Neumann S, Grüters A, Krude H, Biebermann H. Novel insights on thyroid-stimulating hormone receptor signal transduction. *Endocr Rev* (2013) **34**:691–724. doi:10.1210/er.2012-1072
54. Bonomi M, Busnelli M, Persani L, Vassart G, Costagliola S. Structural differences in the hinge region of the glycoprotein hormone receptors: evidence from the sulfated tyrosine residues. *Mol Endocrinol* (2006) **20**:3351–63. doi:10.1210/me.2005-0521
55. Bruysters M, Verhoef-Post M, Themmen APN. Asp330 and Tyr331 in the C-terminal cysteine-rich region of the luteinizing hormone receptor are key residues in hormone-induced receptor activation. *J Biol Chem* (2008) **283**:25821–8. doi:10.1074/jbc.M804395200
56. Nurwakagari P, Breit A, Hess C, Salman-Livny H, Ben-Menahem D, Gudermann T. A conformational contribution of the luteinizing hormone–receptor ectodomain to receptor activation. *J Mol Endocrinol* (2007) **38**:259–75. doi:10.1677/jme.1.02160
57. Chen P-H, Chen X, Lin Z, Fang D, He X. The structural basis of R-spondin recognition by LGR5 and RNF43. *Genes Dev* (2013) **27**:1345–50. doi:10.1101/gad.219915.113
58. Peng WC, De Lau W, Forneris F, Granneman JCM, Huch M, Clevers H, et al. Structure of stem cell growth factor R-spondin 1 in complex with the

ectodomain of its receptor LGR5. *Cell Rep.* (2013) **3**:1885–92. doi:10.1016/j.celrep.2013.06.009
59. Xu K, Xu Y, Rajashankar KR, Robev D, Nikolov DB. Crystal structures of Lgr4 and its complex with R-spondin1. *Structure* (2013) **21**:1683–9. doi:10.1016/j.str.2013.07.001
60. Xu J-G, Huang C, Yang Z, Jin M, Fu P, Zhang N, et al. Crystal structure of LGR4-Rspo1: complex insights into the divergent mechanisms of ligand recognition by leucine-rich repeat G-protein-coupled receptrors (LGRs). *J Biol Chem* (2015) **290**:2455–65. doi:10.1074/jbc.M114.599134
61. Carmon KS, Gong X, Lin Q, Thomas A, Liu Q. R-spondins function as ligands of the orphan receptors LGR4 and LGR5 to regulate Wnt/β-catenin signaling. *Proc Natl Acad Sci U S A* (2011) **108**:11452–7. doi:10.1073/pnas.1106083108
62. Lau WD, Barker N, Low TY, Koo B-K, Li VSW, Teunissen H, et al. Lgr5 homologues associate with Wnt receptors and mediate R-spondin signalling. *Nature* (2011) **476**:293–7. doi:10.1038/nature10337
63. Ruffner H, Sprunger J, Charlat O, Leighton-Davies J, Grosshans B, Salathe A, et al. R-Spondin potentiates Wnt/β-catenin signaling through orphan receptors LGR4 and LGR5. *PLoS One* (2012) **7**(7):e40976. doi:10.1371/journal.pone.0040976
64. Hao H-X, Xie Y, Zhang Y, Charlat O, Oster E, Avello M, et al. ZNRF3 promotes Wnt receptor turnover in an R-spondin-sensitive manner. *Nature* (2012) **485**:195–200. doi:10.1038/nature11019
65. Carmon KS, Gong X, Yi J, Thomas A, Liu Q. RSPO–LGR4 functions via IQGAP1 to potentiate Wnt signaling. *Proc Natl Acad Sci U S A* (2014) **111**:E1221–9. doi:10.1073/pnas.1323106111
66. Sali A, Blundell TL. Comparative protein modelling by satisfaction of spatial restraints. *J Mol Biol* (1993) **234**:779–815. doi:10.1006/jmbi.1993.1626
67. Eigenbrot C, Randal M, Quan C, Burnier J, O'connell L, Rinderknecht E, et al. X-ray structure of human relaxin at 1.5 A. Comparison to insulin and implications for receptor binding determinants. *J Mol Biol* (1991) **221**:15–21. doi:10.1016/0022-2836(91)90796-9
68. Rosengren KJ, Zhang S, Lin F, Daly NL, Scott DJ, Hughes RA, et al. Solution structure and characterization of the LGR8 receptor binding surface of insulin-like peptide 3. *J Biol Chem* (2006) **281**:28287–95. doi:10.1074/jbc.M603829200
69. Büllesbach EE, Schwabe C. Synthetic cross-links arrest the C-terminal region of the relaxin-like factor in an active conformation. *Biochemistry* (2004) **43**:8021–8. doi:10.1021/bi049601j
70. Büllesbach EE, Schwabe C. LGR8 signal activation by the relaxin-like factor. *J Biol Chem* (2005) **280**:14586–90. doi:10.1074/jbc.M414443200
71. Büllesbach EE, Schwabe C. The trap-LIKE relaxin-binding site of the leucine-rich G-protein-coupled receptor 7. *J Biol Chem* (2005) **280**:14051–6. doi:10.1074/jbc.M500030200
72. Scott DJ, Wilkinson TN, Zhang S, Ferraro T, Wade JD, Tregear GW, et al. Defining the LGR8 residues involved in binding insulin-like peptide 3. *Mol Endocrinol* (2007) **21**:1699–712. doi:10.1210/me.2007-0097
73. Halls ML, Bond CP, Sudo S, Kumagai J, Ferraro T, Layfield S, et al. Multiple binding sites revealed by interaction of relaxin family peptides with native and chimeric relaxin family peptide receptors 1 and 2 (LGR7 and LGR8). *J Pharmacol Exp Ther* (2005) **313**:677–87. doi:10.1124/jpet.104.080655
74. Sudo S, Kumagai J, Nishi S, Layfield S, Ferraro T, Bathgate RA, et al. H3 relaxin is a specific ligand for LGR7 and activates the receptor by interacting with both the ectodomain and the exoloop 2. *J Biol Chem* (2003) **278**:7855–62. doi:10.1074/jbc.M212457200
75. Diepenhorst NA, Petrie EJ, Chen CZ, Wang A, Hossain MA, Bathgate RA, et al. Investigation of interactions at the extracellular loops of the relaxin family peptide receptor 1 (RXFP1). *J Biol Chem* (2014) **289**:34938–52. doi:10.1074/jbc.M114.600882
76. Bathgate RA, Samuel CS, Burazin TC, Layfield S, Claasz AA, Reytomas IG, et al. Human relaxin gene 3 (H3) and the equivalent mouse relaxin (M3) gene. Novel members of the relaxin peptide family. *J Biol Chem* (2002) **277**:1148–57. doi:10.1074/jbc.M107882200
77. Liu C, Eriste E, Sutton S, Chen J, Roland B, Kuei C, et al. Identification of relaxin-3/INSL7 as an endogenous ligand for the orphan G-protein-coupled receptor GPCR135. *J Biol Chem* (2003) **278**:50754–64. doi:10.1074/jbc.M308995200
78. Scott DJ, Rosengren KJ, Bathgate RA. The different ligand-binding modes of relaxin family peptide receptors RXFP1 and RXFP2. *Mol Endocrinol* (2012) **26**:1896–906. doi:10.1210/me.2012-1188
79. Hossain MA, Rosengren KJ, Haugaard-Jonsson LM, Zhang S, Layfield S, Ferraro T, et al. The A-chain of human relaxin family peptides has distinct roles in the binding and activation of the different relaxin family peptide receptors. *J Biol Chem* (2008) **283**:17287–97. doi:10.1074/jbc.M801911200
80. Hossain MA, Wade JD, Bathgate RA. Chimeric relaxin peptides highlight the role of the A-chain in the function of H2 relaxin. *Peptides* (2012) **35**:102–6. doi:10.1016/j.peptides.2012.02.021
81. Del Borgo MP, Hughes RA, Bathgate RA, Lin F, Kawamura K, Wade JD. Analogs of insulin-like peptide 3 (INSL3) B-chain are LGR8 antagonists in vitro and in vivo. *J Biol Chem* (2006) **281**:13068–74. doi:10.1074/jbc.M600472200
82. Shabanpoor F, Bathgate RA, Hossain MA, Giannakis E, Wade JD, Hughes RA. Design, synthesis and pharmacological evaluation of cyclic mimetics of the insulin-like peptide 3 (INSL3) B-chain. *J Pept Sci* (2007) **13**:113–20. doi:10.1002/psc.807
83. Shabanpoor F, Bathgate RD, Belgi A, Chan LJ, Nair VB, Wade JD, et al. Site-specific conjugation of a lanthanide chelator and its effects on the chemical synthesis and receptor binding affinity of human relaxin-2 hormone. *Biochem Biophys Res Commun* (2012) **420**:253–6. doi:10.1016/j.bbrc.2012.02.141
84. Hopkins EJ, Layfield S, Ferraro T, Bathgate RA, Gooley PR. The NMR solution structure of the relaxin (RXFP1) receptor lipoprotein receptor class A module and identification of key residues in the N-terminal region of the module that mediate receptor activation. *J Biol Chem* (2007) **282**:4172–84. doi:10.1074/jbc.M609526200
85. Yamamoto T, Davis CG, Brown MS, Schneider WJ, Casey ML, Goldstein JL, et al. The human LDL receptor: a cysteine-rich protein with multiple alu sequences in its mRNA. *Cell* (1984) **39**:27–38. doi:10.1016/0092-8674(84)90188-0
86. Südhof TC, Goldstein JL, Brown MS, Russell DW. The LDL receptor gene: a mosaic of exons shared with different proteins. *Science* (1985) **228**:815–22. doi:10.1126/science.2988123
87. Bates P, Young JA, Varmus HE. A receptor for subgroup A Rous sarcoma virus is related to the low density lipoprotein receptor. *Cell* (1993) **74**:1043–51. doi:10.1016/0092-8674(93)90726-7
88. Takeuchi T, Misaki A, Chen BK, Ohtsuki Y. H-cadherin expression in breast cancer. *Histopathology* (1999) **35**:87–8. doi:10.1046/j.1365-2559.1999.0728c.x
89. Demczuk S, Aledo R, Zucman J, Delattre O, Desmaze C, Dauphinot L, et al. Cloning of a balanced translocation breakpoint in the DiGeorge syndrome critical region and isolation of a novel potential adhesion receptor gene in its vicinity. *Hum Mol Genet* (1995) **4**:551–8. doi:10.1093/hmg/4.4.551
90. Brown MS, Herz J, Goldstein JL. LDL-receptor structure: calcium cages, acid baths and recycling receptors. *Nature* (1997) **388**:629–30. doi:10.1038/41672
91. Gent J, Braakman I. Low-density lipoprotein receptor structure and folding. *Cell Mol Life Sci* (2004) **61**:2461–70. doi:10.1007/s00018-004-4090-3
92. Kong RCK, Petrie EJ, Mohanty B, Ling J, Lee JCY, Gooley PR, et al. The relaxin receptor (RXFP1) utilizes hydrophobic moieties on a signaling surface of its N-terminal low density lipoprotein class A module to mediate receptor activation. *J Biol Chem* (2013) **288**:28138–51. doi:10.1074/jbc.M113.499640
93. Kong RC, Bathgate RA, Bruell S, Wade JD, Gooley PR, Petrie EJ. Mapping key regions of the RXFP2 low-density lipoprotein class-A module that are involved in signal activation. *Biochemistry* (2014) **53**:4537–48. doi:10.1021/bi500797d
94. Kern A, Agoulnik AI, Bryant-Greenwood GD. The low-density lipoprotein class A module of the relaxin receptor (leucine-rich repeat containing G-protein coupled receptor 7): its role in signaling and trafficking to the cell membrane. *Endocrinology* (2007) **148**:1181–94. doi:10.1210/en.2006-1086
95. Bruell S, Kong RC, Petrie EJ, Hoare B, Wade JD, Scott DJ, et al. Chimeric RXFP1 and RXFP2 receptors highlight the similar mechanism of activation utilizing their N-terminal low-density lipoprotein class A modules. *Front Endocrinol* (2013) **4**:171. doi:10.3389/fendo.2013.00171
96. Wilkinson TN, Bathgate RA. The evolution of the relaxin peptide family and their receptors. *Adv Exp Med Biol* (2007) **612**:1–13. doi:10.1007/978-0-387-74672-2_1

Conflict of Interest Statement: The authors declare that the research was conducted in the absence of any commercial or financial relationships that could be construed as a potential conflict of interest.

frontiers in Endocrinology

REVIEW
published: 17 July 2015
doi: 10.3389/fendo.2015.00110

Role of the extracellular and intracellular loops of follicle-stimulating hormone receptor in its function

Antara A. Banerjee[1] *and Smita D. Mahale*[1,2]*

[1] Division of Structural Biology, National Institute for Research in Reproductive Health, Indian Council of Medical Research, Mumbai, India, [2] ICMR Biomedical Informatics Centre, National Institute for Research in Reproductive Health, Indian Council of Medical Research, Mumbai, India

Follicle-stimulating hormone receptor (FSHR) is a leucine-rich repeat containing class A G-protein coupled receptor belonging to the subfamily of glycoprotein hormone receptors (GPHRs), which includes luteinizing hormone/choriogonadotropin receptor (LH/CGR) and thyroid-stimulating hormone receptor. Its cognate ligand, follicle-stimulating hormone binds to, and activates FSHR expressed on the surface of granulosa cells of the ovary, in females, and Sertoli cells of the testis, in males, to bring about folliculogenesis and spermatogenesis, respectively. FSHR contains a large extracellular domain (ECD) consisting of leucine-rich repeats at the N-terminal end and a hinge region at the C-terminus that connects the ECD to the membrane spanning transmembrane domain (TMD). The TMD consists of seven α-helices that are connected to each other by means of three extracellular loops (ELs) and three intracellular loops (ILs) and ends in a short-cytoplasmic tail. It is well established that the ECD is the primary hormone binding domain, whereas the TMD is the signal transducing domain. However, several studies on the ELs and ILs employing site directed mutagenesis, generation of chimeric receptors and *in vitro* characterization of naturally occurring mutations have proven their indispensable role in FSHR function. Their role in every phase of the life cycle of the receptor like post translational modifications, cell surface trafficking, hormone binding, activation of downstream signaling, receptor phosphorylation, hormone–receptor internalization, and recycling of hormone–receptor complex have been documented. Mutations in the loops causing dysregulation of these processes lead to pathophysiological conditions. In other GPHRs as well, the loops have been convincingly shown to contribute to various aspects of receptor function. This review article attempts to summarize the extensive contributions of FSHR loops and C-terminal tail to its function.

Keywords: C-tail, extracellular loops, FSH receptor, intracellular loops, receptor function

OPEN ACCESS

Edited by:
James A. Dias, University at Albany – State University of New York, USA

Reviewed by:
Alfredo Ulloa-Aguirre, Universidad Nacional Autónoma de México, Mexico
George Russell Bousfield, Wichita State University, USA

***Correspondence:**
Smita D. Mahale, Division of Structural Biology, ICMR Biomedical Informatics Centre, National Institute for Research in Reproductive Health, Indian Council of Medical Research, Jehangir Merwanji Street, Parel, Mumbai 400 012, India
smitamahale@hotmail.com

Specialty section:
This article was submitted to Molecular and Structural Endocrinology, a section of the journal Frontiers in Endocrinology

Received: *29 May 2015*
Accepted: *03 July 2015*
Published: *17 July 2015*

Citation:
Banerjee AA and Mahale SD (2015) Role of the extracellular and intracellular loops of follicle-stimulating hormone receptor in its function. Front. Endocrinol. 6:110. doi: 10.3389/fendo.2015.00110

Introduction

The ability of all organisms to receive external stimuli in the form of light, water, sound, hormones, odors, to name a few, is essential to bring about a necessary physiological response. This process is mediated through cell surface receptors, mainly the G-protein coupled receptors (GPCRs), which form the largest and most diverse class of receptors. GPCRs form a repertoire of about 800 receptors and are the largest set of drug targets in the market, thus signifying the importance of their study in

greater detail. The GPCR superfamily is composed of five major families as defined by phylogenetic analysis: glutamate, rhodopsin, adhesion, frizzled/taste2, and secretin, which constitute the GRAFS classification system (1). All GPCRs are characterized by a common structure consisting of a ligand binding extracellular domain (ECD) and a signal transducing transmembrane domain (TMD) consisting of seven alpha helices spanning the membrane. The helices are connected to each other by means of three extracellular loops (ELs) and three intracellular loops (ILs) and end in a cytoplasmic tail. The GRAFS system family members differ in the sizes of their ECDs, ranging from 60 to 80 residues for growth hormone releasing hormone and calcitonin receptors in Family S, to 280–580 residues for metabotropic, glutamate receptors in Family G. Rhodopsin Family R, receptor ECD sizes vary considerably, as this is the largest family and is subdivided into four groups designated as alpha, beta, gamma, and delta (2). The delta group consists of the glycoprotein hormone receptors (GPHRs), namely, the follicle-stimulating hormone receptor (FSHR), luteinizing hormone/choriogonadotropin receptor (LH/CGR), and thyroid-stimulating hormone receptor (TSHR). A hallmark of GPHRs is the presence of a large ECD of nearly 350–400 residues containing leucine-rich repeats (LRRs), which mediate ligand binding with high affinity and specificity (3). Several other receptors also harbor the horseshoe-shaped LRR structure, which facilitates high-affinity ligand binding, e.g., LGR 4–7 (4) and some members of the relaxin family peptide receptors, namely RXFP1 and RXFP2 (5). **Figure 1** is a diagrammatic representation of the GPCR families showing the delta group of Rhodopsin family containing leucine-rich repeat GPCRs.

The glycoprotein hormones include the gonadotropins, follicle-stimulating hormone (FSH), luteinizing hormone (LH), the placental hormone chorionic gonadotropin (CG), and the non-gonadotropin thyroid-stimulating hormone (TSH). They belong to the cystine-knot growth factor superfamily and share a common heterodimeric structure composed of two non-covalently associated α and β subunits (6). The α subunits are common for all the hormones, whereas the β subunits confer functional specificity. All the glycoprotein hormones bind to their cognate GPHRs to elicit specific biological effects. FSH binds to FSHR expressed on the granulosa cells of the ovary in females, to bring about follicular maturation (7) and on the Sertoli cells of the testis in males, where it maintains the Sertoli cell population and sperm production (8).

Although a lot of research has been focused on the ECD and TMD of FSHR, emerging evidence suggests the importance of the ELs and ILs of the receptor in its function. In spite of this, a compendium of available data on the role of the loops and especially the ELs of FSHR is lacking. Hence, in this review article, we have discussed the involvement of the loops in many FSHR functions like cell surface trafficking, hormone binding, signal transduction, internalization, and recycling of the hormone–receptor complex. A few relevant examples from studies on the loops of LH/CGR and TSHR have also been cited.

Life Cycle of FSH Receptor

The life cycle of the FSH receptor, like all other GPCRs, includes post translational modifications like glycosylation, palmitoylation, and also formation of higher order oligomers in the ER and Golgi networks, after which the mature receptor is trafficked to the cell surface (9). Abell et al. (10) have shown that deletion mutants of ELs of LH/CGR result in the mutant receptor being trapped intracellularly showing the importance of ELs in cell surface receptor trafficking. In the case of the FSHR, once the mature receptor is localized on the surface of target cells, FSH first binds to the high-affinity leucine-rich LRR domains of FSHR, which results in additional interactions at the hormone–receptor interface and formation of a sulfated Tyr pocket into which the FSHR sulfated Tyr^{335} is inserted, eventually resulting in receptor activation (11). This interaction of the ligand with the ECD and relay of the signal to the TMD is probably mediated by the ELs of the FSHR. Ji et al. (12) carried out an elegant study wherein FSHR mutants, which were either binding deficient or signaling deficient, were co-expressed. It was seen that FSHR ECD (of signaling deficient mutant which was capable of binding FSH) could transactivate non-binding FSHR mutants to bring about cAMP or IP production but not both. This hormone bound to the ECD probably contacts the ELs of the receptor to bring about its activation. In TSHR, co-operative signal amplification of constitutively activating mutations (CAMs) in ELs was shown by Kleinau et al. (13) by combining the CAMs and studying the effects *in vitro*. This proved that switching of the receptor from an inactive to an active conformation takes place by means of several contacts involving both the ECD and the ELs and this is the case for FSHR too. Binding of FSH to FSHR triggers several downstream signaling pathways other than the canonical cAMP/PKA pathway, such as the protein kinase B (PKB/Akt) and serum and glucocorticoid-induced kinase (Sgk) (14), p38 MAPK (15), ERK1/2 (MAPK3/1) (16), and IP3 production (17). The receptor is then uncoupled from the G-protein, the desensitized hormone–receptor complex becomes internalized, following which most of the complex is recycled back to the cell surface and a small fraction is routed to lysosomes for degradation (18). Reports from naturally occurring and induced mutations of residues in the ELs and ILs of FSHR provide evidence for the roles of each loop in various aspects of receptor function (**Figure 2**).

Extracellular Loop 1

Alanine scanning mutagenesis of the first five amino acids in extracellular loop 1 (EL1) of FSHR showed that a His^{407}Ala mutation decreased FSH binding affinity, whereas substitutions at Asp^{405}, Thr^{408}, and Lys^{409} abolished cAMP production (19). The revertant mutants showed FSH binding and cAMP production similar to WT indicating the importance of EL1 residues in FSH binding and signaling. Casas-González et al. (20) reported a novel activating FSHR mutation $N^{431}I$ in EL1 in a male who exhibited normal spermatogenesis but low-serum FSH levels. The mutation impaired the desensitization and internalization of the hormone–receptor complex due to its inability to recruit beta arrestin proteins, which mediate internalization, as well as affected the recycling of the complex, as studied by pulse chase assays. In case of TSHR, several activating mutations have been identified. One such mutation in the ECD that has been studied in detail is $S^{281}T/I/N$ (21). Ala substitution mutagenesis studies on the aromatic residues in the vicinity of S^{281}, proximal to TSHR

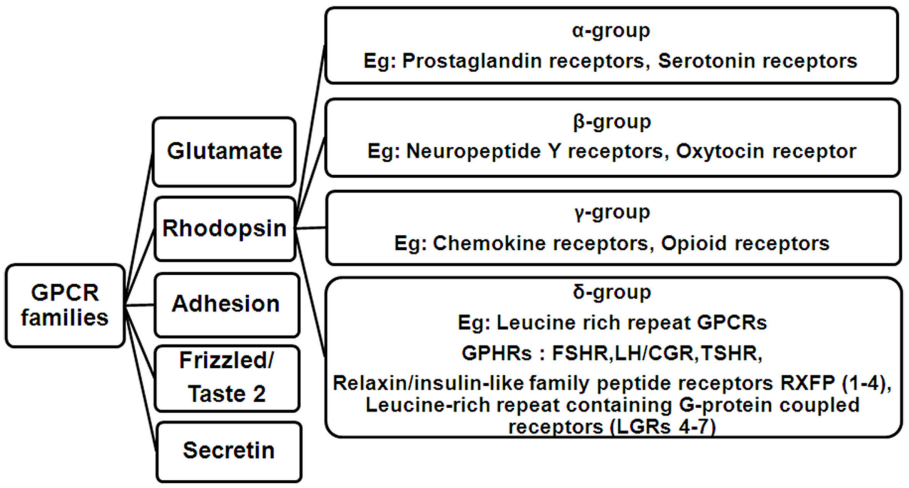

FIGURE 1 | Flowchart showing the classification of GPCR families. The rhodopsin family consists of four main groups designated as alpha (α), beta (β), gamma (γ), and delta (δ). Members of the delta group include the Leucine-rich repeat GPCRs comprising of the three glycoprotein hormone receptors (GPHRs: FSHR, LH/CGR, and TSHR), Relaxin/insulin-like family peptide receptors RXFP (1–4) and Leucine-rich repeat containing G-protein coupled receptors (LGRs 4–7).

EL1, revealed that mutation of Y^{481}in EL1 along with the surrounding aromatic residues was shown to affect receptor signaling. Antipeptide antibodies corresponding to EL1 region (residues 405–426) of FSHR could detect the receptor as determined by flow cytometry as well as inhibit FSH binding and cAMP production in a dose-dependant manner (22). Thus, FSHR EL1 residues are probable secondary hormone binding sites and important in FSH binding, cAMP signaling, internalization, and recycling of hormone–receptor complex.

Extracellular Loop 2

As in most other GPCRs, extracellular loop 2 (EL2) plays an indispensable role in FSHR function. Chimeric receptors of FSHR ECD/TMD and C-tail of the *Drosophila melanogaster* fly receptor LGR2 had high-basal cAMP levels suggesting constitutive activation of receptor due to removal of the constraint imposed by the interaction of exoloops with the ECD (23). In the case of the LHR, this constraint was imposed by EL2, and hence, it is possibly true for EL2 of the FSHR too. Meduri et al. (24) reported a novel homozygous mutation Pro^{519}Thr in a patient with primary amenorrhea. The mutation at this highly conserved Proline residue resulted in the inability of the mutant receptor to traffick to the cell surface and subsequently abolished FSH binding and cAMP production. Since the receptor was trapped intracellularly, follicular maturation was blocked, resulting in the clinical manifestation of premature ovarian failure. Functional characterization of a novel heterozygous mutation M^{512}I in a woman with spontaneous ovarian hyperstimulation syndrome (sOHSS): ovarian enlargement due to several luteinized cysts within the ovaries due to abnormally high levels of hCG in pregnancy (25) or sometimes due to high levels of TSH (26) revealed that the mutation impaired cAMP signaling and PI3K/AKT pathways (27). Recently, a novel mutation Val^{514}Ala was identified in a patient undergoing IVF who exhibited symptoms of iatrogenic ovarian hyperstimulation syndrome (aOHSS): excessive follicular recruitment and enlargement due to ovarian stimulation with exogenous FSH during ART (28). The mutation at this conserved Val residue conferred higher cell surface receptor expression, higher FSH binding, and attained saturation of cAMP production at low doses of FSH as compared to wild type receptor (29). Both the Pro^{519} and Val^{514} residues, mentioned here, are not only conserved across FSHR of all species but also across LHR and TSHR, indicating their importance. The significance of FSHR specific, that is, non-conserved residues of EL2 of FSHR was demonstrated by swapping six FSHR specific residues in EL2 with those from LH/CGR (30). The chimeric EL2M receptor had an impaired cAMP response as well as reduced internalization of the FSH–FSHR complex. Further, characterization of six individual substitution mutants of the FSHR specific residues of EL2 was performed and it was found that a L^{501}F mutant showed weak interaction with beta arrestins consistent with its low internalization, impaired FSH-induced cAMP response, as well as low levels of ERK phosphorylation (31). The I^{505}V substitution also affected receptor function to some extent. **Figure 3** shows the low levels of ERK phosphorylation in chimeric EL2M and the point mutants L^{501}F and I^{505}V as compared to WT FSHR as reported in Banerjee et al. (31). Molecular modeling studies revealed that the L^{501}F and I^{505}V substitutions in EL2 resulted in gain of interactions in the mutant receptors as compared to wild type receptor (**Figure 4**). Mutations in EL2 of LHR have also been reported to either enhance internalization and cAMP signaling (F^{515}A and T^{521}A) or impair internalization (S^{512}A and V^{519}A) and cAMP signaling (32) indicating the importance of ELs of GPHRs in agonist-induced internalization of the hormone–receptor complex. Thus, FSHR EL2 residues are essential for cell surface receptor trafficking, FSH binding, cAMP/ERK pathway/PI3K pathway, internalization of FSH–FSHR complex, and beta arrestin recruitment.

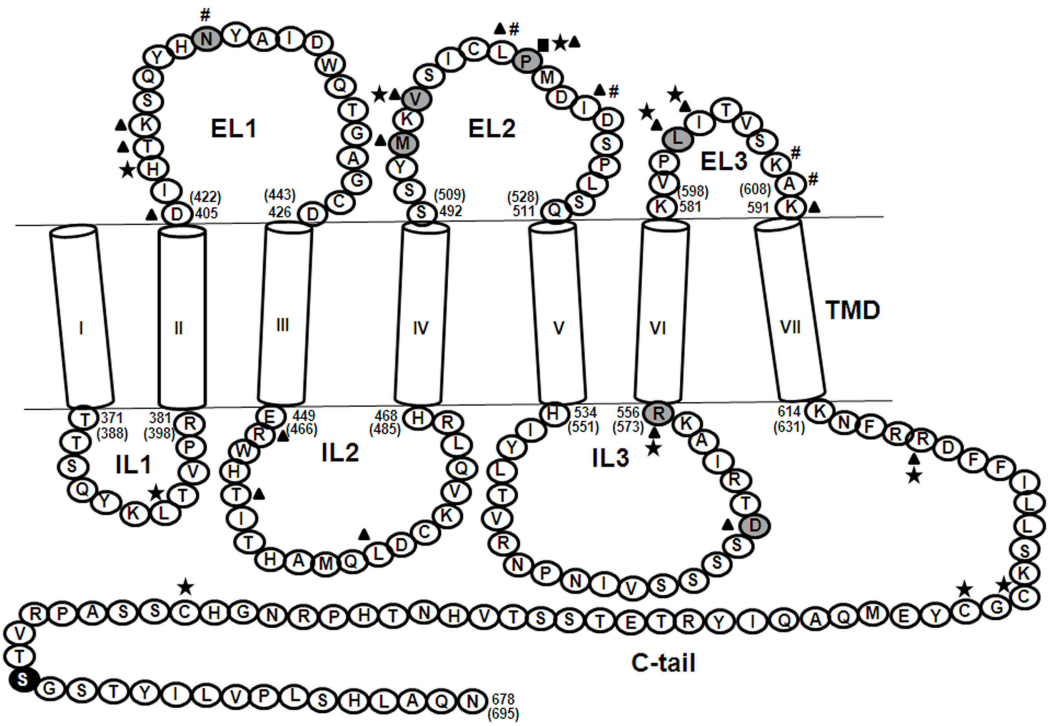

FIGURE 2 | Partial sequence of the human FSHR showing the TMD. The seven alpha helices, shown as cylinders designated, I–VII, are connected by means of three ELs and three ILs and ends in a short C-tail. Shaded residues (●) are naturally occurring mutations, (■) indicates residues crucial for cell surface receptor trafficking, (★) indicates residues important for FSH binding, (▲) indicates residues important for FSH-induced cAMP production, (#) indicates residues crucial for internalization of FSH-FSHR complex, and (●) indicates SNP. Explanation for each of these residues is provided in the text wherever applicable. The numbering system followed is according to that for the mature receptor without the 17 amino acid residue signal peptide. The numbers in parentheses correspond to the amino acid residue number including the signal peptide. The ECD comprising residues 1–349 is not shown.

Extracellular Loop 3

Extracellular loop 3 (EL3) is the shortest EL of FSHR consisting of only 11 amino acid residues compared to 22 for EL1 and 20 for EL2. *In vitro* characterization of a mutated FSH receptor in a compound heterozygous patient (Asp^{224}Val in ECD and Leu^{601}Val in EL3), with POF was carried out by Touraine et al. (33). Although the cell surface FSHR expression and FSH binding affinity of Leu^{601}Val mutant were similar to wild type receptor, this substitution impaired cAMP response, which might have led to a block in follicular maturation beyond the early antral stage. Contrary to this observation, Ryu et al. (34) and Sohn et al. (35) showed that substitution/deletion of Leu^{583} [same as Leu^{601} reported by Touraine et al. (33)] and Ile^{584}with a panel of amino acids enhanced FSH binding. However, substitutions at Leu^{583}, Ile^{584}, and Lys^{590} abolished cAMP, consistent with the study carried out by Touraine et al. (33), thus clearly indicating the importance of EL3 residues in cAMP signal transduction. Sohn et al. (35) also showed that substitution at Leu^{583}with the aromatic amino acids Phe or Tyr, improved the hormone binding and cAMP induction, but impaired inositol phosphate (IP) production. IP induction was also found to be abolished for Ile^{584} and Lys^{590} substitutions. Photoaffinity labeling studies revealed that interaction of FSH–FSHR takes place through contact of FSH beta with the N-terminal ECD, whereas the FSH alpha subunit is oriented toward EL3, indicating the important role of this loop in hormone–receptor interaction (36). Along with EL1, antipeptide antibodies corresponding to EL3 (FSHR residues 581–591) were also found to be surface accessible and capable of inhibiting hormone–receptor interaction as determined by radioreceptor assay and cAMP assay (22). This information along with the data obtained by the study conducted by Sohn et al. (36) indicate that the ELs of FSHR probably serve as secondary hormone binding sites by means of their interaction with the alpha subunit of FSH. In the TSHR, Claus et al. (37) showed that a hydrophobic cluster in the center of EL3 is essential for cAMP signaling as seen by the loss of signal generation after mutation of residues 652–656, comprising the cluster. Another interesting observation with respect to the role of EL3 in receptor function was obtained by generation of FSHR/LH-CGR chimeric receptors, as mentioned earlier (30). Substitution of the three FSHR specific residues in EL3 of FSHR with the corresponding residues in LH/CGR resulted in the chimeric EL3M receptor exhibiting higher internalization of FSH–FSHR complex without any change in the affinity for hormone binding. The cAMP signaling response, however, was comparable to that of wild type receptor. Pulse chase experiments revealed that recycling of the chimeric EL3M receptor was affected. Thus, FSHR EL3 residues seem to be essential for FSH–FSHR

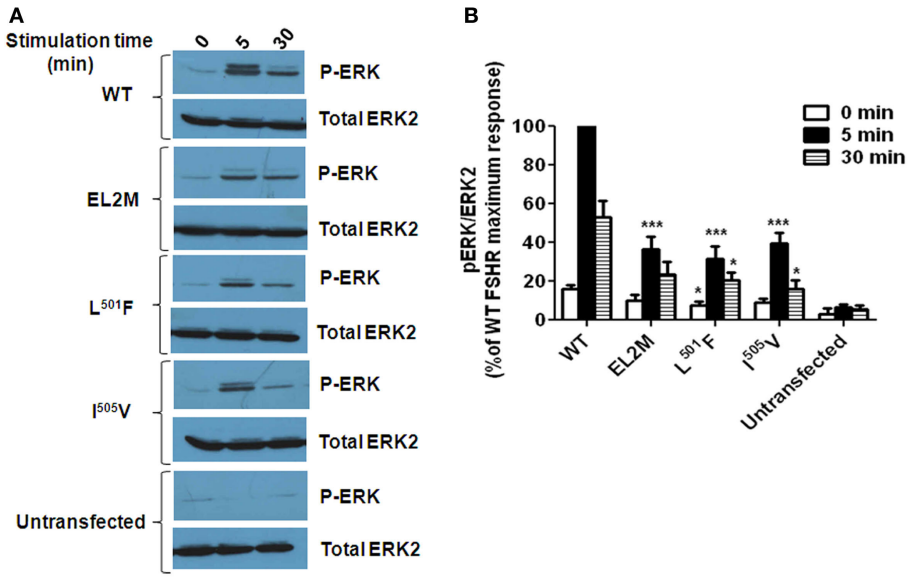

FIGURE 3 | FSH-induced ERK phosphorylation in wild type (WT) FSHR, chimeric EL2M FSHR, and the point mutants $L^{501}F$ and $I^{505}V$ (31). **(A)** Representative western blot showing the levels of phospho ERK (P-ERK) and total ERK2 in cell lysates from HEK293 cells transiently expressing the FSHR constructs and stimulated without or with 100 ng FSH for 5 or 30 min. Untransfected cells served as a negative control. **(B)** Densitometric analysis showing the ratio of phosphorylated ERK: total ERK2. The maximum response obtained by WT FSHR at 5 min post stimulation with 100 ng FSH was considered to be 100% and the % response obtained for the mutants at 0, 5, and 30 min post FSH induction (100 ng) was determined by comparing it with the maximum response and plotted. The value of $*P < 0.05$ and $***P < 0.001$ with respect to WT FSHR was considered to be statistically significant.

interaction, FSH binding, FSH-induced cAMP and IP production and internalization, and recycling of FSH–FSHR complex.

Intracellular Loop 1

Phosphorylation of FSH receptor post ligand stimulation was reported by Quintana et al. (17). Phosphorylation is mediated by G-protein-related kinases (GRKs), mainly GRK2 and GRK6, in the case of FSHR (38). The phosphorylated receptor then recruits adaptor proteins called beta arrestins, which help in mediating the internalization of the hormone–receptor complexes via clathrin coated pits (39). Generation of a mutant rFSHR-1L where the S/T residues in intracellular loop 1 (IL1) of rat FSHR were mutated ($T^{369}I$, $S^{371}I$, $T^{376}N$ of IL1) greatly affected the phosphorylation of the receptor even though FSH binding affinity was unaffected and basal cAMP response of mutant receptor was higher (constitutively active) (40). This study showed that phosphorylation of IL1 of FSHR is required both for uncoupling of receptor in response to FSH stimulation and its internalization. Further, abolishing the phosphorylation sites at IL1 was shown to affect beta arrestin-2 recruitment, hence receptor internalization (41). Nechamen et al. (42) have also shown interaction of the APPL1 (adaptor protein containing PH domain, PTB domain, and leucine zipper motif) with hFSHR IL1 and that it links the FSH-stimulated receptor to the PI3K/Akt pathway essential for survival of the dominant follicle. Alanine scanning mutagenesis of IL-1 residues demonstrated that $L^{377}A$ and $F^{382}A$ mutants showed low-FSH binding, whereas $K^{376}A$ showed FSH binding and cAMP production similar to wild type FSHR (43). However, the $K^{376}A$ mutation in FSHR inhibited its interaction with the adaptor protein APPL1 and abrogation of this interaction blocked FSHR-mediated inositol 1, 4, 5-trisphosphate (IP3) induction and FSH-induced calcium signaling. Thus, FSHR IL1 residues seem to be crucial for FSH binding, FSH-induced PI3K pathway, interaction with APPL1 protein to bring about IP3 production, receptor phosphorylation, and interaction with beta arrestins to mediate internalization.

Intracellular Loop 2

A yeast-based interaction trap assay identified the interaction of intracellular loop 2 (IL2) of FSHR with 14-3-3 tau protein, which is important for ER localization of membrane proteins (44). Scanning alanine mutagenesis of the IL2 residues ^{447}TLE^{449} and ^{450}RWH^{452} resulted in loss of this interaction with 14-3-3 tau protein thus identifying the residues crucial for this interaction (45). Despite normal FSH binding, the $H^{452}A$ mutant showed low levels of internalization and no cAMP production indicating the importance of IL2 residues. IL2 of FSHR bears the highly conserved class A GPCR ERW motif, which is crucial for receptor activation (46). Timossi et al. (47) generated minigene constructs of three ILs of human FSHR and found the IL2 to be essential for Gs coupling and cAMP production. Minigene encoding free IL-2 as well as minigene IL2 mutants $R^{467}A$ and $R^{467}K$ and co-expression of full length WT with minigene mutant $L^{477}A$ lowered FSH stimulated but not basal cAMP levels. Further full length IL2 mutants were made and it was found that FSH binding to these mutants was moderately affected in the constitutively active mutants $L^{477}A/D/P$ and to a lesser extent in $L^{477}K/R$ mutants. Full length FSHR IL2 mutants

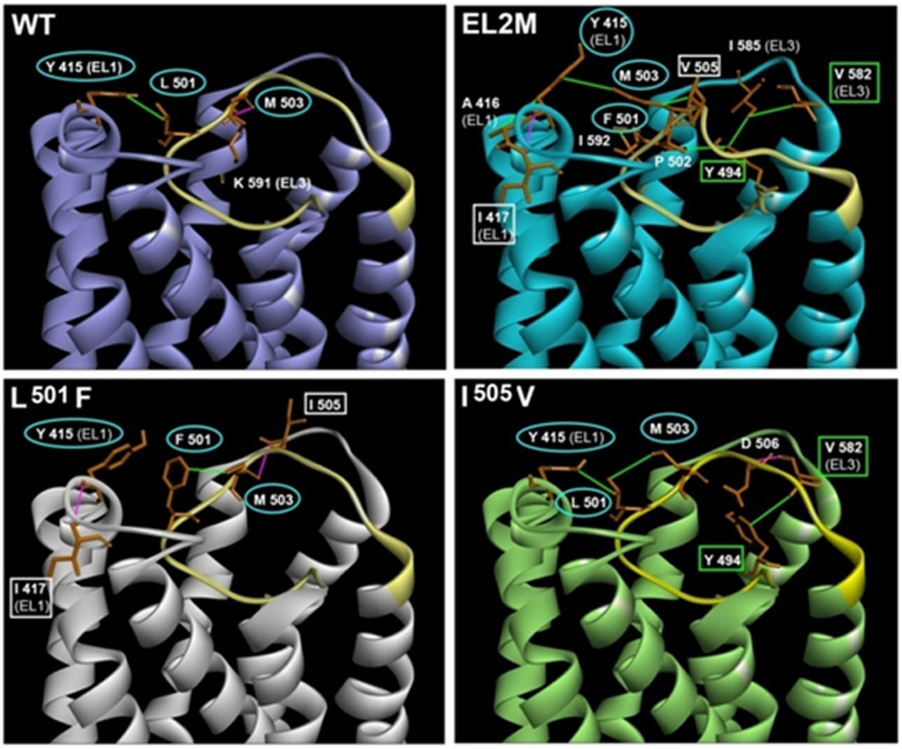

FIGURE 4 | Structural models of the TMD and ELs of WT FSHR, chimeric EL2M FSHR, and the point mutants $L^{501}F$ and $I^{505}V$ (31). The acquired interactions in chimeric EL2M FSHR and point mutants $L^{501}F$ and $I^{505}V$ with the adjacent residues in EL1 and EL3, which are absent in WT FSHR is depicted. EL2 region in all the models is shown in yellow. The residues involved in interaction in all the four models are circled in cyan (Y^{415}, L^{501}/F^{501}, and M^{503}). Residues showing similar interaction in chimeric EL2M and $L^{501}F$ mutant are shown in white square boxes (I^{417} and I^{505}/V^{505}). Residues showing similar interaction in chimeric EL2M and $I^{505}V$ are shown in green square boxes (Y^{494} and V^{582}). Hydrogen bonds and hydrophobic interactions are depicted in pink and green lines. The models were built using Discovery Studio 3.5 and minimized using Schrodinger 2013 OPLS 2005 force field with default parameters, as described in Banerjee et al. (31).

$R^{467}A/H$, $T^{470}A$ abolished FSH-induced cAMP production without altering basal levels, $L^{477}A/D/P$ mutations led to elevated basal cAMP levels, $L^{477}K/R$ mutants showed less FSH-induced cAMP production. The FSHR-2L mutant, in which the two threonine of IL2 were subjected to alanine substitution ($Thr^{451}Ala$, $Thr^{453}Val$), and a rFSHR-(2L + 3L) mutant, in which the two threonines in the second IL along with the seven Ser/Thr residues in the intracellular loop 3 (IL3) were substituted with alanine residues ($Thr^{451}Ala$, $Thr^{453}Val$, $Thr^{536}Ala$, $Thr^{541}Ala$, $Ser^{544}Ala$, $Ser^{545}Ala$, $Ser^{546}Ala$, $Ser^{547}Ala$, $Thr^{549}Ala$), were deficient in phosphorylation, bound FSH with comparable affinity to WT but showed low levels of FSH-induced cAMP production (inactivating mutations) (48). Further, in this study, it was shown that rFSHR-$D^{389}N$ and rFSHR-$Y^{530}F$ (D and Y are highly conserved residues across GPCRs), two inactivating mutations possessing intact phosphorylation sites showed impairment in phosphorylation. Overexpression with GRK-2 was shown to rescue phosphorylation of both the mutants but internalization of only $D^{389}N$ mutant, whereas overexpression of arrestin-3 (β-arrestin 2) could rescue internalization of both mutants providing the first evidence of the role of beta arrestins in FSH-mediated receptor internalization post receptor phosphorylation with GRKs. In LHR too, mutagenesis studies revealed several residues in IL2, like Lys^{455} and His^{460}, to be essential for ligand binding and $Glu^{441}$and His^{460} to be important for cAMP response (49). Thus, FSHR IL2 residues are especially important for cAMP production and also for receptor phosphorylation.

Intracellular Loop 3

A synthetic peptide corresponding to residues 533–555 of IL3 of the rat FSHR was shown to inhibit cAMP production and estradiol synthesis in cultured Sertoli cells from immature rat testes (50). Along with IL1, mutations in IL3 residues also were shown to affect receptor phosphorylation; however, the effect was not as pronounced as in IL1 mutation. The rFSHR-3L mutant, in which the Ser/Thr residues in IL3 were mutated to alanine ($Thr^{536}Ala$, $Thr^{541}Ala$, $Ser^{544}Ala$, $Ser^{545}Ala$, $Ser^{546}Ala$, $Ser^{547}Ala$, $Thr^{549}Ala$ of IL3)and a rFSHR-(3L + CT) mutant, in which the Ser/Thr residues in both IL3 and C-tail were mutated to alanine ($Thr^{536}Ala$, $Thr^{541}Ala$, $Ser^{544}Ala$, $Ser^{545}Ala$, $Ser^{546}Ala$, $Ser^{547}Ala$, $Thr^{549}Ala$, $Ser^{624}Ala$), showed unaltered FSH binding, whereas rFSHR-3L was found to be a constitutively active mutant, as it exhibited high-basal cAMP response (40). The mutant receptors affected the phosphorylation of FSHR to some extent, as well as its uncoupling from adenylyl cyclase enzyme without affecting its internalization. Using chimeric FSHR and LHR receptors, the

interaction of threonine residues in IL3 with beta arrestin proteins, and hence, internalization of these gonadotropin receptors was shown by Bhaskaran et al. (51). GPCRs harbor a BBXXB motif (where B represents a basic amino acid whereas any amino acid can be presented at "X") in the intracellular domains, which is an essential determinant of receptor activation. FSHR contains a reverse BXXBB situated at the juxtamembrane region of IL3and C tail, which was subjected to Ala substitution mutagenesis (52). All the IL3 mutant receptors BXXAB, AXXBB, and BXXBA showed FSH binding similar to WT, but binding was affected in the same three mutants of C-tail. However, cAMP production was abolished in AXXBB and BXXBA mutants but was normal in BXXAB mutant of IL3. In the case of the C-tail, cAMP production of all three mutants was affected. Thus, it appears that the BXXBB motif at the IL3 of the hFSHR is essential for Gαs coupling and cAMP production, whereas the same motif in the C-tail is more important for membrane expression as the mutation resulted in an immature form of the receptor, which was unable to bind the hormone. An interesting study by Cohen et al. (53) identified IL3 to be a site of FSHR ubiquitination by a yeast two-hybrid screen. However, mutating the only Lys residue available for ubiquitination ($K^{555}R$) did not disrupt FSHR–ubiquitin interaction indicating that other determinations of receptor ubiquitination exist. The importance of this loop is further emphasized by the presence of naturally occurring mutations in the loop that affect receptor function. Beau et al. (54) reported that a woman with secondary amenorrhea and high-serum FSH levels was found to harbor two FSHR mutations: $Ile^{160}Thr$ (ECD) and $Arg^{573}Cys$ (IL3). The mutation in the ECD affected cell surface receptor expression, whereas the IL3 mutation impaired cAMP signaling. A constitutively active mutation $D^{567}G$ was identified by Gromoll et al. (55) in a hypophysectomized man. Later in 2003, Smits et al. (56) reported a mutation at the same position in FSHR IL3 in a woman with spontaneous OHSS. The $D^{567}N$ substitution in this case conferred high-basal cAMP response as well as loss of functional specificity as the mutant receptor showed a dose-dependent increase in cAMP production upon hCG or TSH stimulation. The importance of this residue is further corroborated by the fact that it lies in a protein kinase CK2 consensus site and brings about phosphorylation of adaptor proteins like beta arrestins, which mediate receptor internalization (57) via their interaction with FSHR (58). Kluetzman et al. (59) showed that both the naturally occurring $D^{550}G$ (same as $D^{567}G$) mutation and the alanine substituted mutation $D^{550}A$ showed accumulation of FSH in mutant receptors in intracellular stores due to decreased degradation after internalization as evidenced by radioreceptor assay as well as visualization by confocal microscopy. Thus, FSHR IL3 residues seem to be important for receptor phosphorylation, cAMP response as well as ubiquitination.

C-Terminal Tail

As in all other GPCRs, the carboxy-terminal tail bears the highly conserved $F(X)_6LL$motif (where X can be any residue, and L is leucine or isoleucine), which is important for trafficking of the mature receptor from ER to the cell surface (60). This motif is located between 616 and 624 residues in the mature FSH receptor (9). Another important post translational modification in GPHRs is palmitoylation of the cysteine residues and this is crucial for receptor endocytosis and other post endocytic events (61). Two conserved cysteine residues (at positions 629 and 655) and one non-conserved Cys residue (at position 627) are present in the C-tail of human FSHR, which are potential sites for S-acylation with palmitic acid, were investigated by Uribe et al. (62). Low-FSH binding in $C^{629}A$, double mutants $C^{627/629}A$ and $C^{629/655}A$, and the triple $C^{627/629/655}A$ receptor mutants without change in FSH binding affinity was observed due to low-cell surface FSHR expression of mutants, whereas low internalization for FSH–FSHR complex of $Cys^{655}A/S/T$ mutants was seen. $C^{629}A$, $C^{655}A/S/T$, the double mutant $C^{627/629}A$, and the triple mutant $C^{627/629/655}A$ showed low-cAMP production. The triple mutant $C^{627/629/655}A$ did not show palmitoylation indicating the importance of all the three residues for palmitoylation. Single-alanine substitutions of residues in the IL3 of TSHR also revealed that the residues were crucial for G-protein activation (63). Truncation mutants of the C-terminal tail (removal of the last eight residues) of hFSHR and rFSHR decreased the amount of internalized ^{125}I-hFSH (18). Confocal microscopy analysis showed that in contrast to the internalized WT receptors, which localized only to endosomes, the internalized truncated receptors localized to both endosomes and lysosomes. This study showed that most of the FSH–FHSR complex gets recycled back to the cell surface and truncation of eight residues from the C-tail reroute a substantial portion of the internalized FSH–FSHR complex to a degradation pathway. Ala substitution of the Ser/Thr cluster $T^{638}A$, $T^{640}A$, $S^{641}A$, $S^{642}A$, $T^{644}A$ in the C-tail of rFSHR showed similar FSH binding affinity to mutant receptor as compared to WT but impaired internalization of FSH–FSHR complex (64). Loss of the Ser/Thr cluster in the mutant FSHR resulted in enhanced cAMP production due to its inability to get desensitized, impaired phosphorylation, β-arrestin recruitment, and hence, impaired internalization of FSH–FSHR substantiated the importance of the C-tail in FSHR function. Thomas et al. (65) reported that FSHR forms oligomers in a constitutive manner before coming to the cell surface and discovered during the course of this study that the C-terminal epitope tags undergo proteolytic processing, so such C-terminal tagged receptors could not be exploited to study receptor oligomerization. To overcome this shortcoming, Mazurkiewicz et al. (66) generated chimeras of FSHR and extreme C-tail fluorescent fusion proteins: FSHR-LHRcT-YFP/FSHR-LHRcT-mCherry pairs possessing amino acid residues 1–611 of the hFSHR and residues 604–674 of the rLHR. Fluorescence correlation spectroscopy and photon counting histogram studies with these chimeric FRET pairs demonstrated the presence of freely diffusing FSHR homodimers on the surface of live cells. FRET experiments also demonstrated that the hFSHR-rLHR-cT chimera formed hetero-dimers/hetero-oligomers with LHR and this possibly occurred during granulosa cell differentiation. Zariñán et al. (67) had reported that co-transfection of WT FSHR with mutants $R^{556}A$ (IL3) or $R^{618}A$ (C-tail) showed dose-dependent inhibition in FSH binding and cAMP production with increasing amounts of mutant DNA and subsequently rescue of function by co-transfection with WT fragments of TMD 5, 6, or 7 and/or C-tail suggesting oligomerization of FSHR. The crucial role played by the C-tail in receptor function is reinforced by the existence of a SNP $p.Asn^{680}Ser$ (rs6166), which has been studied extensively in various ethnic groups across the world and is

believed to serve as a marker to predict ovarian response in women undergoing assisted reproductive technology programs (68–74). Thus, the C-tail of FSHR plays an indispensable role in palmitoylation, cell surface receptor trafficking, receptor phosphorylation, interaction with beta arrestin proteins, and hence, internalization of FSH–FSHR complex.

Conclusion and Future Directions

Genetic alterations in GPCRs, resulting in loss or gain of function, lead to several pathological conditions and are being studied by several groups to develop drugs targeted at the receptor to rescue its function (75, 76). Knowledge of combination of SNPs in FSH beta and FSHR is essential for determining patient risk/treatment outcome and for designing treatment in cases of infertility (77). Also, *in vitro* studies on several naturally occurring mutations [reviewed by Desai et al. (78)] and studies on both FSH beta and FSHR knockout mice (79) indicate the pivotal role of this hormone–receptor interaction, failure of which leads to reproductive dysfunctions. Owing to the large size of the receptor, its interaction with FSH takes place at several discrete regions on the ECD and this hormone–receptor ECD complex possibly makes contacts with the ELs and the signal is then relayed downstream through the TMD. Other than mutations in the ECD and TMD, which may result in intracellular retention of the receptor, its inability to bind FSH or bring about signal transduction, several such mutations in the loops display similar characteristics and this necessitates their study in greater detail. Therefore, in order to develop drugs targeted to rescue the function of the receptor, a thorough understanding of the epitopes crucial for FSH–FSHR interaction is a must. In recent times, several small molecule FSHR agonists, which can be orally administered like Org 214444-0 (80), FSHR allosteric modulators like Compound 5 (81) have been developed, which can be administered to patients for ovulation induction. Pharmacoperones (pharmacological chaperones that assist in folding and routing of mutant receptors to the cell surface) like Org 41841 have been shown to rescue the function of the $A^{189}V$ FSHR mutant, which was trapped intracellularly and hence exhibited low-cell surface FSHR expression (82). As these molecules hold great therapeutic potential, the understanding of the biochemical mechanism of their interaction with the receptor and identification of sites of interaction with the receptor is imperative. Along with the ECD and TMD, detailed analysis of the residues in the ELs and ILs is therefore of utmost importance given their versatile roles in FSH–FSHR interaction.

Acknowledgments

The research work carried out and mentioned in this article from authors laboratory was supported by Grants received from the Indian Council of Medical Research (NIRRH/IR/263/05-2015 and BIC/12(10)/2013) and Department of Science and Technology (SR/SO/HS-0053/2009), Government of India. The award of Junior Research Scholarship to Ms. AB by the Lady Tata Memorial Trust, India, is gratefully acknowledged. We wish to acknowledge Ms. B. Sur Roy for the *in silico* studies. We also wish to acknowledge the help provided by Dr. S. Mukherjee, in-charge of DNA sequencing facility and the technical expertise of Mr. C. Saravanan and Ms. N. Joshi for DNA sequencing. We also thank Dr. N. Balasinor, in-charge of Confocal Facility and Ms. S. Sonawane and Ms. R. Gaonkar for all the assistance provided.

References

1. Fredriksson R, Lagerström MC, Lundin LG, Schiöth HB. The G-protein-coupled receptors in the human genome form five main families. Phylogenetic analysis, paralogongroups, and fingerprints. *Mol Pharmacol* (2003) **6**:1256–72. doi:10.1124/mol.63.6.1256
2. Karnik SS, Gogonea C, Patil S, Saad Y, Takezako T. Activation of G-protein-coupled receptors: a common molecular mechanism. *Trends Endocrinol Metab* (2003) **14**:431–7. doi:10.1016/j.tem.2003.09.007
3. Vassart G, Pardo L, Costagliola S. A molecular dissection of the glycoprotein hormone receptors. *Trends Biochem Sci* (2004) **29**:119–26. doi:10.1016/j.tibs.2004.01.006
4. Hsu SY, Kudo M, Chen T, Nakabayashi K, Bhalla A, van der Spek PJ, et al. The three subfamilies of leucine-rich repeat-containing G protein-coupled receptors (LGR): identification of LGR6 and LGR7 and the signaling mechanism for LGR7. *Mol Endocrinol* (2000) **14**:1257–71. doi:10.1210/mend.14.8.0510
5. Bathgate RA, Halls ML, van der Westhuizen ET, Callander GE, Kocan M, Summers RJ. Relaxin family peptides and their receptors. *Physiol Rev* (2013) **93**:405–80. doi:10.1152/physrev.00001.2012
6. Pierce JG, Parsons TF. Glycoprotein hormones: structure and function. *Annu Rev Biochem* (1981) **50**:465–95. doi:10.1146/annurev.bi.50.070181.002341
7. Robker RL, Richards JS. Hormonal control of the cell cycle in ovarian cells: proliferation versus differentiation. *Biol Reprod* (1998) **59**:476–82. doi:10.1095/biolreprod59.3.476
8. Foulkes NS, Schlotter F, Pevet P, Sassone-Corsi P. Pituitary hormone FSH directs the CREM functional switch during spermatogenesis. *Nature* (1993) **362**:264–7. doi:10.1038/362264a0
9. Ulloa-Aguirre A, Conn PM. Targeting of G protein-coupled receptors to the plasma membrane in health and disease. *Front Biosci (Landmark Ed)* (2009) **14**:973–94. doi:10.2741/3290
10. Abell A, Liu X, Segaloff DL. Deletions of portions of the extracellular loops of the lutropin/choriogonadotropin receptor decrease the binding affinity for ovine luteinizing hormone, but not human choriogonadotropin, by preventing the formation of mature cell surface receptor. *J Biol Chem* (1996) **271**:4518–27. doi:10.1074/jbc.271.8.4518
11. Jiang X, Liu H, Chen X, Chen PH, Fischer D, Sriraman V, et al. Structure of follicle-stimulating hormone in complex with the entire ectodomain of its receptor. *Proc Natl Acad Sci U S A* (2012) **109**:12491–6. doi:10.1073/pnas.1206643109
12. Ji I, Lee C, Jeoung M, Koo Y, Sievert GA, Ji TH. Trans-activation of mutant follicle-stimulating hormone receptors selectively generates only one of two hormone signals. *Mol Endocrinol* (2004) **18**:968–78. doi:10.1210/me.2003-0443
13. Kleinau G, Jaeschke H, Mueller S, Raaka BM, Neumann S, Paschke R, et al. Evidence for cooperative signal triggering at the extracellular loops of the TSH receptor. *FASEB J* (2008) **22**:2798–808. doi:10.1096/fj.07-104711
14. Gonzalez-Robayna IJ, Falender AE, Ochsner S, Firestone GL, Richards JS. FSH stimulates phosphorylation and activation of protein kinase B (PKB/Akt) and serum and glucocorticoid-induced kinase (Sgk): evidence for A kinase-independent signaling in granulosa cells. *Mol Endocrinol* (2000) **14**:1283–300. doi:10.1210/mend.14.8.0500
15. Maizels ET, Cottom J, Jones JCR, Hunzicker-Dunn M. Follicle stimulating hormone (FSH) activates the p38 mitogen-activated protein kinase pathway, inducing small heat shock protein phosphorylation and cell rounding in immature rat ovarian granulosa cells. *Endocrinology* (1998) **139**:3353–6. doi:10.1210/endo.139.7.6188
16. Cottom J, Salvador LM, Maizels ET, Reierstad S, Park Y, Carr DW, et al. Follicle stimulating hormone activates extracellular signal-regulated kinase but not extracellular signal-regulated kinase kinase through a 100-kDa phosphotyrosine phosphatase. *J Biol Chem* (2003) **278**:7167–79. doi:10.1074/jbc.M203901200
17. Quintana J, Hipkin RW, Sanchez- Yague J, Ascoli M. Follitropin (FSH) and a phorbol ester stimulate the phosphorylation of the FSH receptor in intact cells. *J Biol Chem* (1994) **269**:8772–9. doi:10.1210/jbc.Fedrrv.2.5.0409

18. Krishnamurthy H, Kishi H, Shi M, Galet C, Bhaskaran RS, Hirakawa T, et al. Postendocytotic trafficking of the follicle-stimulating hormone (FSH)-FSH receptor complex. *Mol Endocrinol* (2003) **17**:2162–76. doi:10.1210/me.2003-0118
19. Ji I, Ji TH. Differential roles of exoloop 1 of the human follicle-stimulating hormone receptor in hormone binding and receptor activation. *J Biol Chem* (1995) **270**:15970–3. doi:10.1074/jbc.270.27.15970
20. Casas-González P, Scaglia HE, Pérez-Solís MA, Durand G, Scaglia J, Zariñán T, et al. Normal testicular function without detectable follicle-stimulating hormone. A novel mutation in the follicle-stimulating hormone receptor gene leading to apparent constitutive activity and impaired agonist-induced desensitization and internalization. *Mol Cell Endocrinol* (2012) **364**:71–82. doi:10.1016/j.mce.2012.08.011
21. Jaeschke H, Neumann S, Kleinau G, Mueller S, Claus M, Krause G, et al. An aromatic environment in the vicinity of serine 281 is a structural requirement for thyrotropin receptor function. *Endocrinology* (2006) **147**:1753–60. doi:10.1210/en.2005-1138
22. Dupakuntla M, Mahale SD. Accessibility of the extracellular loops of follicle stimulating hormone receptor and their role in hormone-receptor interaction. *Mol Cell Endocrinol* (2010) **315**:131–7. doi:10.1016/j.mce.2009.10.002
23. Nishi S, Nakabayashi K, Kobilka B, Hsueh AJ. The ectodomain of the luteinizing hormone receptor interacts with exoloop 2 to constrain the transmembrane region: studies using chimeric human and fly receptors. *J Biol Chem* (2002) **277**:3958–64. doi:10.1074/jbc.M109617200
24. Meduri G, Touraine P, Beau I, Lahuna O, Desroches A, Vacher-Lavenu MC, et al. Delayed puberty and primary amenorrhea associated with a novel mutation of the human follicle-stimulating hormone receptor: clinical, histological, and molecular studies. *J Clin Endocrinol Metab* (2003) **88**:3491–8. doi:10.1210/jc.2003-030217
25. Ludwig M, Gembruch U, Bauer O, Diedrich K. Ovarian hyperstimulation syndrome (OHSS) in a spontaneous pregnancy with fetal and placental triploidy: information about the general pathophysiology of OHSS. *Hum Reprod* (1998) **13**:2082–7. doi:10.1093/humrep/13.8.2082
26. Nappi RG, Di Nero E, D'Aries AP, Nappi L. Natural pregnancy in hypothyroid woman complicated by spontaneous ovarian hyperstimulation syndrome. *Am J Obstet Gynecol* (1998) **178**:610–1. doi:10.1016/S0002-9378(98)70448-X
27. Uchida S, Uchida H, Maruyama T, Kajitani T, Oda H, Miyazaki K, et al. Molecular analysis of a mutated FSH receptor detected in a patient with spontaneous ovarian hyper stimulation syndrome. *PLoS One* (2013) **8**:e75478. doi:10.1371/journal.pone.0075478
28. Delbaere A, Smits G, Olatunbosun O, Pierson R, Vassart G, Costagliola S. New insights into the pathophysiology of ovarian hyperstimulation syndrome. What makes the difference between spontaneous and iatrogenic syndrome? *Hum Reprod* (2004) **19**:486–9. doi:10.1093/humrep/deh124
29. Desai SS, Achrekar SK, Sahasrabuddhe KA, Meharji PK, Desai SK, Mangoli VS, et al. Functional characterization of two naturally occurring mutations (val(514)ala and ala(575)val) in follicle-stimulating hormone receptor. *J Clin Endocrinol Metab* (2015) **100**:E638–45. doi:10.1210/jc.2014-3662
30. Dupakuntla M, Pathak B, Roy BS, Mahale SD. Extracellular loop 2 in the FSH receptor is crucial for ligand mediated receptor activation. *Mol Cell Endocrinol* (2012) **362**:60–8. doi:10.1016/j.mce.2012.05.008
31. Banerjee AA, Dupakuntla M, Pathak BR, Mahale S. FSH receptor specific residues L501 and I505 in extracellular loop 2 are essential for its function. *J Mol Endocrinol* (2015) **54**:193–204. doi:10.1530/JME-14-0275
32. Li S, Liu X, Min L, Ascoli M. Mutations of the second extracellular loop of the human lutropin receptor emphasize the importance of receptor activation and de-emphasize the importance of receptor phosphorylation in agonist-induced internalization. *J Biol Chem* (2001) **276**:7968–73. doi:10.1074/jbc.M010482200
33. Touraine P, Beau I, Gougeon A, Meduri G, Desroches A, Pichard C, et al. New natural inactivating mutations of the follicle-stimulating hormone receptor: correlations between receptor function and phenotype. *Mol Endocrinol* (1999) **13**:1844–54. doi:10.1210/mend.13.11.0370
34. Ryu K, Gilchrist RL, Tung CS, Ji I, Ji TH. High affinity hormone binding to the extracellular N-terminal exodomain of the follicle-stimulating hormone receptor is critically modulated by exoloop 3. *J Biol Chem* (1998) **273**:28953–8. doi:10.1074/jbc.273.44.28953
35. Sohn J, Ryu K, Sievert G, Jeoung M, Ji I, Ji TH. Follicle-stimulating hormone interacts with exoloop 3 of the receptor. *J Biol Chem* (2002) **277**:50165–75. doi:10.1074/jbc.M207646200
36. Sohn J, Youn H, Jeoung M, Koo Y, Yi C, Ji I, et al. Orientation of follicle-stimulating hormone (FSH) subunits complexed with the fsh receptor. *J Biol Chem* (2003) **278**:47868–76. doi:10.1074/jbc.M307751200
37. Claus M, Jaeschke H, Kleinau G, Neumann S, Krause G, Paschke R. A hydrophobic cluster in the center of the third extracellular loop is important for thyrotropin receptor signaling. *Endocrinology* (2005) **146**:5197–203. doi:10.1210/en.2005-0713
38. Lazari MF, Liu X, Nakamura K, Benovic JL, Ascoli M. Role of G protein-coupled receptor kinases on the agonist-induced phosphorylation and internalization of the follitropinreceptor. *Mol Endocrinol* (1999) **13**:866–78. doi:10.1210/mend.13.6.0289
39. Lefkowitz RJ. G protein-coupled receptors. III. New roles for receptor kinases and β-arrestins in receptor signaling and desensitization. *J Biol Chem* (1998) **273**:18677–80. doi:10.1074/jbc.273.30.18677
40. Nakamura K, Hipkin RW, Ascoli M. The agonist-induced phosphorylation of the rat follitropin receptor maps to the first and third intracellular loops. *Mol Endocrinol* (1998) **12**:580–91. doi:10.1210/mend.12.4.0087
41. Krishnamurthy H, Galet C, Ascoli M. The association of arrestin-3 with the follitropin receptor depends on receptor activation and phosphorylation. *Mol Cell Endocrinol* (2003) **204**:127–40. doi:10.1016/S0303-7207(03)00088-1
42. Nechamen CA, Thomas RM, Cohen BD, Acevedo G, Poulikakos PI, Testa JR, et al. Human follicle-stimulating hormone (FSH) receptor interacts with the adaptor protein APPL1 in HEK 293 cells: potential involvement of the PI3K pathway in FSH signaling. *Biol Reprod* (2004) **71**:629–36. doi:10.1095/biolreprod.103.025833
43. Thomas RM, Nechamen CA, Mazurkiewicz JE, Ulloa-Aguirre A, Dias JA. The adapter protein APPL1 links FSH receptor to inositol 1,4,5-trisphosphate production and is implicated in intracellular Ca(2+) mobilization. *Endocrinology* (2011) **152**:1691–701. doi:10.1210/en.2010-1353
44. Cohen BD, Nechamen CA, Dias JA. Human follitropin receptor (FSHR) interacts with the adapter protein 14-3-3tau. *Mol Cell Endocrinol* (2004) **220**:1–7. doi:10.1016/j.mce.2004.04.012
45. Dias JA, Mahale SD, Nechamen CA, Davydenko O, Thomas RM, Ulloa-Aguirre A. Emerging roles for the FSH receptor adapter protein APPL1 and overlap of a putative 14-3-3τ interaction domain with a canonical G-protein interaction site. *Mol Cell Endocrinol* (2010) **329**:17–25. doi:10.1016/j.mce.2010.05.009
46. Gershengorn MC, Osman R. Minireview: insights into G protein-coupled receptor function using molecular models. *Endocrinology* (2001) **142**:2–10. doi:10.1210/endo.142.1.7919
47. Timossi C, Maldonado D, Vizcaíno A, Lindau-Shepard B, Conn PM, Ulloa-Aguirre A. Structural determinants in the second intracellular loop of the human follicle-stimulating hormone receptor are involved in G(s) protein activation. *Mol Cell Endocrinol* (2002) **189**:157–68. doi:10.1016/S0303-7207(01)00720-1
48. Nakamura K, Krupnick JG, Benovic JL, Ascoli M. Signaling and phosphorylation-impaired mutants of the rat follitropin receptor reveal an activation- and phosphorylation-independent but arrestin dependent pathway for internalization. *J Biol Chem* (1998) **273**:24346–54. doi:10.1074/jbc.273.38.24346
49. Fernandez LM, Puett D. Evidence for an important functional role of intracellular loop II of the lutropin receptor. *Mol Cell Endocrinol* (1997) **128**:161–9. doi:10.1016/S0303-7207(97)04035-5
50. Grasso P, Leng N, Reichert LE Jr. A synthetic peptide corresponding to the third cytoplasmic loop (residues 533 to 555) of the testicular follicle-stimulating hormone receptor affects signal transduction in rat testis membranes and in intact cultured rat Sertoli cells. *Mol Cell Endocrinol* (1995) **110**:35–41. doi:10.1016/0303-7207(95)91392-T
51. Bhaskaran RS, Min L, Krishnamurthy H, Ascoli M. Studies with chimeras of the gonadotropin receptors reveal the importance of third intracellular loop threonines on the formation of the receptor/nonvisual arrestin complex. *Biochemistry* (2003) **42**:13950–9. doi:10.1021/bi034907w
52. Timossi C, Ortiz-Elizondo C, Pineda DB, Dias JA, Conn PM, Ulloa-Aguirre A. Functional significance of the BBXXB motif reversed present in the cytoplasmic domains of the human follicle-stimulating hormone receptor. *Mol Cell Endocrinol* (2004) **223**:17–26. doi:10.1016/j.mce.2004.06.004
53. Cohen BD, Bariteau JT, Magenis LM, Dias JA. Regulation of follitropin receptor cell surface residency by the ubiquitin-proteasome pathway. *Endocrinology* (2003) **144**:4393–402. doi:10.1210/en.2002-0063
54. Beau I, Touraine P, Meduri G, Gougeon A, Desroches A, Matuchansky C, et al. A novel phenotype related to partial loss of function mutations of the follicle stimulating hormone receptor. *J Clin Invest* (1998) **102**:1352–9. doi:10.1172/JCI3795
55. Gromoll J, Simoni M, Nieschlag E. An activating mutation of the follicle-stimulating hormone receptor autonomously sustains spermatogenesis in a hypophysectomized man. *J Clin Endocrinol Metab* (1996) **81**:1367–70. doi:10.1210/jcem.81.4.8636335

56. Smits G, Olatunbosun O, Delbaere A, Pierson R, Vassart G, Costagliola S. Ovarian hyperstimulation syndrome due to a mutation in the follicle-stimulating hormone receptor. *N Engl J Med* (2003) **349**:760–6. doi:10.1056/NEJMoa030064
57. Lin FT, Chen W, Shenoy S, Cong M, Exum ST, Lefkowitz RJ. Phosphorylation of beta-arrestin2 regulates its function in internalization of beta(2)-adrenergic receptors. *Biochemistry* (2002) **41**:10692–9. doi:10.1021/bi025705n
58. Dias JA, Nechamen CA, Atari R. Identifying protein interactions in gonadotropin action. *Endocrine* (2005) **26**:241–7. doi:10.1385/ENDO:26:3:241
59. Kluetzman KS, Thomas RM, Nechamen CA, Dias JA. Decreased degradation of internalized follicle-stimulating hormone caused by mutation of aspartic acid 6.30(550) in a protein kinase-CK2 consensus sequence in the third intracellular loop of human follicle-stimulating hormone receptor. *Biol Reprod* (2011) **84**:1154–63. doi:10.1095/biolreprod.110.087965
60. Duvernay MT, Zhou F, Wu G. A conserved motif for the transport of G protein-coupled receptors from the endoplasmic reticulum to the cell surface. *J Biol Chem* (2004) **279**:30741–50. doi:10.1074/jbc.M313881200
61. Menon KM, Clouser CL, Nair AK. Gonadotropin receptors: role of post-translational modifications and post-transcriptional regulation. *Endocrine* (2005) **26**:249–57. doi:10.1385/ENDO:26:3:249
62. Uribe A, Zariñán T, Pérez-Solis MA, Gutiérrez-Sagal R, Jardón-Valadez E, Piñeiro A, et al. Functional and structural roles of conserved cysteine residues in the carboxyl-terminal domain of the follicle-stimulating hormone receptor in human embryonic kidney 293 cells. *Biol Reprod* (2008) **78**:869–82. doi:10.1095/biolreprod.107.063925
63. Claus M, Neumann S, Kleinau G, Krause G, Paschke R. Structural determinants for G-protein activation and specificity in the third intracellular loop of the thyroid-stimulating hormone receptor. *J Mol Med (Berl)* (2006) **84**:943–54. doi:10.1007/s00109-006-0087-8
64. Kara E, Crépieux P, Gauthier C, Martinat N, Piketty V, Guillou F, et al. A phosphorylation cluster of five serine and threonine residues in the C-terminus of the follicle-stimulating hormone receptor is important for desensitization but not for beta-arrestin-mediated ERK activation. *Mol Endocrinol* (2006) **20**:3014–26. doi:10.1210/me.2006-0098
65. Thomas RM, Nechamen CA, Mazurkiewicz JE, Muda M, Palmer S, Dias JA. Follice-stimulating hormone receptor forms oligomers and shows evidence of carboxyl-terminal proteolytic processing. *Endocrinology* (2007) **148**:987–95. doi:10.1210/en.2006-1672
66. Mazurkiewicz JE, Herrick-Davis K, Barroso M, Ulloa-Aguirre A, Lindau-Shepard B, Thomas RM, et al. Single molecule analyses of fully functional fluorescent protein tagged follitropin receptor reveals homodimerization and specific heterodimerization with lutropin receptor. *Biol Reprod* (2015) **92**:100. doi:10.1095/biolreprod.114.125781
67. Zariñán T, Perez-Solís MA, Maya-Núñez G, Casas-González P, Conn PM, Dias JA, et al. Dominant negative effects of human follicle-stimulating hormone receptor expression-deficient mutants on wild-type receptor cell surface expression. Rescue of oligomerization-dependent defective receptor expression by using cognate decoys. *Mol Cell Endocrinol* (2010) **321**:112–22. doi:10.1016/j.mce.2010.02.027
68. Perez-Mayorga M, Gromoll J, Behre HM, Gassner C, Nieschlag E, Simoni M. Ovarian response to follicle-stimulating hormone (FSH) stimulation depends on the FSH receptor genotype. *J Clin Endocrinol Metab* (2000) **85**:3365–9. doi:10.1210/jcem.85.9.6789
69. Behre HM, Greb RR, Mempel A, Sonntag B, Kiesel L, Kaltwasser P. Significance of a common single nucleotide polymorphism in exon 10 of the follicle-stimulating hormone (FSH) receptor gene for the ovarian response to FSH: a pharmacogenetic approach to controlled ovarian hyperstimulation. *Pharmacogenet Genomics* (2005) **15**:451–6. doi:10.1097/01.fpc.0000167330.92786.5e
70. Jun JK, Yoon JS, Ku SY, Choi YM, Hwang KR, Park SY, et al. Follicle-stimulating hormone receptor gene polymorphism and ovarian responses to controlled ovarian hyperstimulation for IVF-ET. *J Hum Genet* (2006) **51**:665–70. doi:10.1007/s10038-006-0005-5
71. Loutradis D, Patsoula E, Minas V, Koussidis GA, Antsaklis A, Michalas S, et al. FSH receptor gene polymorphisms have a role for different ovarian response to stimulation in patients entering IVF/ICSI-ET programs. *J Assist Reprod Genet* (2006) **23**:177–84. doi:10.1007/s10815-005-9015-z
72. Wunsch A, Sonntag B, Simoni M. Polymorphism of the FSH receptor and ovarian response to FSH. *Ann Endocrinol (Paris)* (2007) **68**:160–6. doi:10.1016/j.ando.2007.04.006
73. Boudjenah R, Molina-Gomes D, Torre A, Bergere M, Bailly M, Boitrelle F, et al. Genetic polymorphisms influence the ovarian response to rFSH stimulation inpatients undergoing in vitro fertilization programs with ICSI. *PLoS One* (2012) **7**:e38700. doi:10.1371/journal.pone.0038700
74. Desai SS, Achrekar SK, Paranjape SR, Desai SK, Mangoli VS, Mahale SD. Association of allelic combinations of FSHR gene polymorphisms with ovarian response. *Reprod Biomed Online* (2013) **27**:400–6. doi:10.1016/j.rbmo.2013.07.007
75. Thompson MD, Hendy GN, Percy ME, Bichet DG, Cole DE. G protein-coupled receptor mutations and human genetic disease. *Methods Mol Biol* (2014) **1175**:153–87. doi:10.1007/978-1-4939-0956-8_8
76. Thompson MD, Cole DE, Capra V, Siminovitch KA, Rovati GE, Burnham WM, et al. Pharmacogenetics of the G protein-coupled receptors. *Methods Mol Biol* (2014) **1175**:189–242. doi:10.1007/978-1-4939-0956-8_9
77. Simoni M, Casarini L. Mechanisms in endocrinology: genetics of FSH action: a 2014-and-beyond view. *Eur J Endocrinol* (2014) **170**:R91–107. doi:10.1530/EJE-13-0624
78. Desai SS, Roy BS, Mahale SD. Mutations and polymorphisms in FSH receptor: functional implications in human reproduction. *Reproduction* (2013) **146**:R235–48. doi:10.1530/REP-13-0351
79. Siegel ET, Kim HG, Nishimoto HK, Layman LC. The molecular basis of impaired follicle-stimulating hormone action: evidence from human mutations and mouse models. *Reprod Sci* (2013) **20**:211–33. doi:10.1177/1933719112461184
80. Van Koppen CJ, Verbost PM, van de Lagemaat R, Karstens WJ, Loozen HJ, van Achterberg TA. Signaling of an allosteric, nanomolar potent, low molecular weight agonist for the follicle-stimulating hormone receptor. *Biochem Pharmacol* (2013) **85**:1162–70. doi:10.1016/j.bcp.2013.02.001
81. Sriraman V, Denis D, de Matos D, Yu H, Palmer S, Nataraja S. Investigation of a thiazolidinone derivative as an allosteric modulator of follicle stimulating hormone receptor: evidence for its ability to support follicular development and ovulation. *Biochem Pharmacol* (2014) **89**:266–75. doi:10.1016/j.bcp.2014.02.023
82. Janovick JA, Maya-Núñez G, Ulloa-Aguirre A, Huhtaniemi IT, Dias JA, Verbost P, et al. Increased plasma membrane expression of human follicle-stimulating hormone receptor by a small molecule thienopyr(im)idine. *Mol Cell Endocrinol* (2009) **298**:84–8. doi:10.1016/j.mce.2008.09.015

Conflict of Interest Statement: The authors declare that the research was conducted in the absence of any commercial or financial relationships that could be construed as a potential conflict of interest.

frontiers in Endocrinology

ORIGINAL RESEARCH
published: 22 September 2015
doi: 10.3389/fendo.2015.00140

Differences in signal activation by LH and hCG are mediated by the LH/CG receptor's extracellular hinge region

*Paul Grzesik[1], Annika Kreuchwig[1], Claudia Rutz[1], Jens Furkert[1], Burkhard Wiesner[1], Ralf Schuelein[1], Gunnar Kleinau[2], Joerg Gromoll[3] and Gerd Krause[1]**

[1] *Leibniz Institut für Molekulare Pharmakologie (FMP), Berlin, Germany,* [2] *Institute of Experimental Paediatric Endocrinology, Charité-Universitätsmedizin Berlin, Berlin, Germany,* [3] *Centre of Reproductive Medicine and Andrology, University Hospital Münster, Munich, Germany*

OPEN ACCESS

Edited by:
Brian J. Arey, Bristol-Myers Squibb Co, USA

Reviewed by:
Leigh Stoddart, University of Nottingham, UK
Guillermo Romero, University of Pittsburgh, USA

***Correspondence:**
Gerd Krause, Leibniz Institut für Molekulare Pharmakologie (FMP), Robert-Rössle-Strasse 10, Berlin 13125, Germany
gkrause@fmp-berlin.de

Specialty section:
This article was submitted to Molecular and Structural Endocrinology, a section of the journal Frontiers in Endocrinology

Received: *26 May 2015*
Accepted: *24 August 2015*
Published: *22 September 2015*

Citation:
Grzesik P, Kreuchwig A, Rutz C, Furkert J, Wiesner B, Schuelein R, Kleinau G, Gromoll J and Krause G (2015) Differences in signal activation by LH and hCG are mediated by the LH/CG receptor's extracellular hinge region. Front. Endocrinol. 6:140. doi: 10.3389/fendo.2015.00140

The human lutropin (hLH)/choriogonadotropin (hCG) receptor (LHCGR) can be activated by binding two slightly different gonadotropic glycoprotein hormones, choriogonadotropin (CG) – secreted by the placenta, and lutropin (LH) – produced by the pituitary. They induce different signaling profiles at the LHCGR. This cannot be explained by binding to the receptor's leucine-rich-repeat domain (LRRD), as this binding is similar for the two hormones. We therefore speculate that there are previously unknown differences in the hormone/receptor interaction at the extracellular hinge region, which might help to understand functional differences between the two hormones. We have therefore performed a detailed study of the binding and action of LH and CG at the LHCGR hinge region. We focused on a primate-specific additional exon in the hinge region, which is located between LRRD and the serpentine domain. The segment of the hinge region encoded by exon10 was previously reported to be only relevant to hLH signaling, as the exon10-deletion receptor exhibits decreased hLH signaling, but unchanged hCG signaling. We designed an advanced homology model of the hormone/LHCGR complex, followed by experimental characterization of relevant fragments in the hinge region. In addition, we examined predictions of a helical exon10-encoded conformation by block-wise polyalanine (helix supporting) mutations. These helix preserving modifications showed no effect on hormone-induced signaling. However, introduction of a structure-disturbing double-proline mutant LHCGR-Q303P/E305P within the exon10-helix has, in contrast to exon10-deletion, no impact on hLH, but only on hCG signaling. This opposite effect on signaling by hLH and hCG can be explained by distinct sites of hormone interaction in the hinge region. In conclusion, our analysis provides details of the differences between hLH- and hCG-induced signaling that are mainly determined in the L2-beta loop of the hormones and in the hinge region of the receptor.

Keywords: lutropin receptor, GPCR activation, lutropin, choriogonadotropin, glycoprotein hormone receptors

Introduction

The G protein-coupled receptors (GPCR) comprise a large superfamily of signal-mediating membrane bound proteins. The human lutropin (hLH)/choriogonadotropin (hCG) receptor (LHCGR) is evolutionary linked with the follitropin receptor (FSHR) and the thyrotropin receptor (TSHR). These three receptors belong to the group of glycoprotein-hormone receptors (GPHR), a subfamily of the rhodopsin-like GPCR (1). The structural topology of the GPHR is characterized by a large N-terminal extracellular region, which can be subdivided into the leucine-rich-repeat domain (LRRD) and the hinge region. The LRRD is responsible for the initial interaction with its corresponding hormone; the hinge region (LHCGR: L285-E354), harbors a second hormone binding site. It acts as a structural and functional link with the transmembrane region and thus assumes a key role in signal initiation and transduction (2). The transmembrane spanning region consists of seven transmembrane helices (TMH), connected by intra-cellular loops (ICLs) and extracellular loops (ECLs) and a cytoplasmic tail (**Figure 1**). Conformational changes in the TMH region during the activation lead to interaction and release of the intracellular signaling proteins (3).

In mammals, especially in primates, LHCGR has an essential role during male sexual differentiation and fertility. This is mainly mediated by the receptor-mediated signal transduction stimulating androgen biosynthesis, either in female theca or male Leydig cells. Lack of androgen biosynthesis due to impaired or inactivated LHCGR results in severe disturbances in male sexual differentiation (Leydig cell hypoplasia) or primary amenorrhea (4). An additional glycoprotein, choriogonadotropin (CG), is specific to primates. This is produced by the trophoblasts during pregnancy and is required for androgen production in male fetuses. Thus, in human and (most) primates, we have a unique two hormone/one receptors system consisting of LH/CG and its cognate receptor the LHCGR. The two hormones are evolutionary homologs, with LH being produced by the pituitary and CG secreted by the placenta/trophoblasts (4).

Both hormones are heterodimeric glycoproteins that consist of a common α-subunit but differ in a non-covalently associated specific β-subunit. These differences lead to the activation of different signaling pathways and finally to distinct physiological responses (5). Moreover, differences in G-protein activation of Gs and Gq (6) and in trans-activation and cis-activation have been reported for hCG and hLH (7), which suggest that the hinge region does not only participate in signal initiation, but also plays a key role in the differentiation of signal transduction at the level of receptor activation. Functional studies have focused on this issue and have uncovered sensitive sections within the hinge region that are responsible for LH- and CG-mediated function (8, 9).

The concept that the hinge region within the ectodomain of the GPHR may have a key role in their activation was initially developed decades ago for TSHR, FSHR (10, 11), and also for the LHCGR (12). Subsequent work on numerous mutations and studies on chimeric receptors [TSHR (13–16), on FSHR (17) and on LHCGR (17–20)] have identified several key residues in the respective hinge regions that are essential in conveying the activation signal. Although the sequence differs most between the GPHRs in the hinge region, these studies on chimeric receptors showed that the hinge region of TSHR can be replaced by that

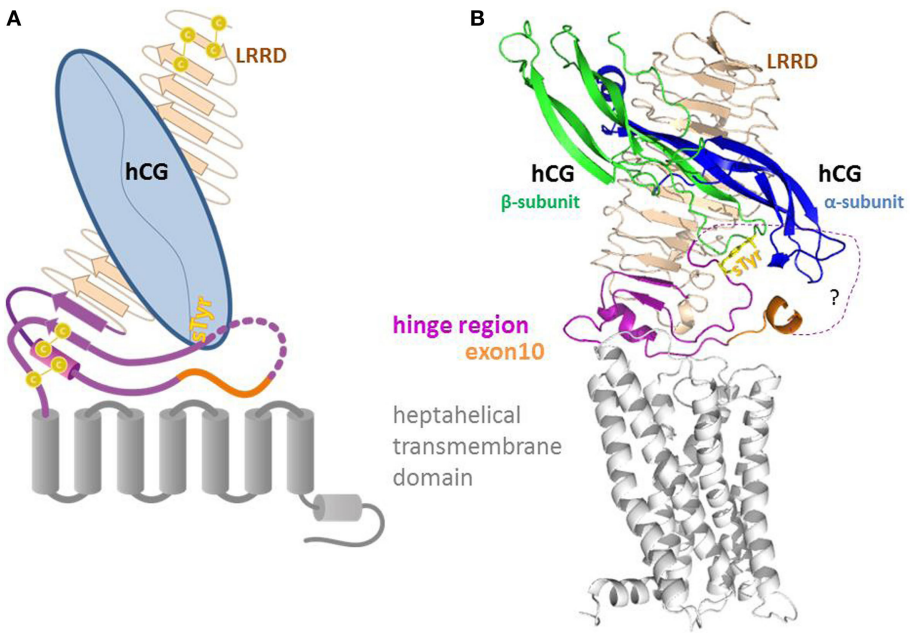

FIGURE 1 | Sketch (A) and homology model (B) of the full length LHCG-receptor with heterodimeric hormone (α and β subunit) bound to the extracellular leucine-rich-repeat domain (LRRD) and the hinge region. The hinge region that harbors exon10 and the second hormone binding site (sTyr) provides a structural and functional link between the LRRD and the heptahelical transmembrane domain.

of FSHR (21) and LHCGR (10) while maintaining function to a certain extent, which indicates both a common topology, but also specificity, e.g., in the case of FSHR (22).

In this context, the naturally occurring deletion in LHCGR of the complete exon10-encoded segment (LHCGR-delExon10), corresponding to 27 amino acids (**Figure 2A**) within the hinge region of the hLHCGR, could be directly linked to a case of *type 2 Leydig cell hypoplasia* in which the natural hLH-, but not hCG-induced function was disturbed (8, 9). The resulting dysfunction in sexual puberty could be overcome by medication with hCG, but the observed functional differences in the exon10-deletion mutant have not yet been fully explained at the molecular level.

Further investigation on this receptor region uncovered a signaling-sensitive motif in close proximity to the exon10-region. A tyrosine rich-motif, located downstream of the exon10-region (**Figure 2A**), was proved to be crucial for hormone-induced receptor function. *In vitro* studies on the LHCGR showed that the sulfated tyrosine 331 (sTyr331) is essential for hLH triggering during receptor activation, but less sensitive toward hCG function (23). However, the complex structure–function relationship of the LHCGR and its hormones, in which LH and CG induce different signaling pathways upon receptor activation, is still unclear.

We postulated that specific structural determinants for the activation process lead to the differences in signaling. We aimed to shed light on the structure–function relationship of the LHCGR hinge region toward its hormones and gain in depth structural insights, by generating homology models of the interaction between the LHCGR hinge region with bound hLH and hCG hormones. In combination with functional data from mutagenesis studies within the exon10-region, our studies led us

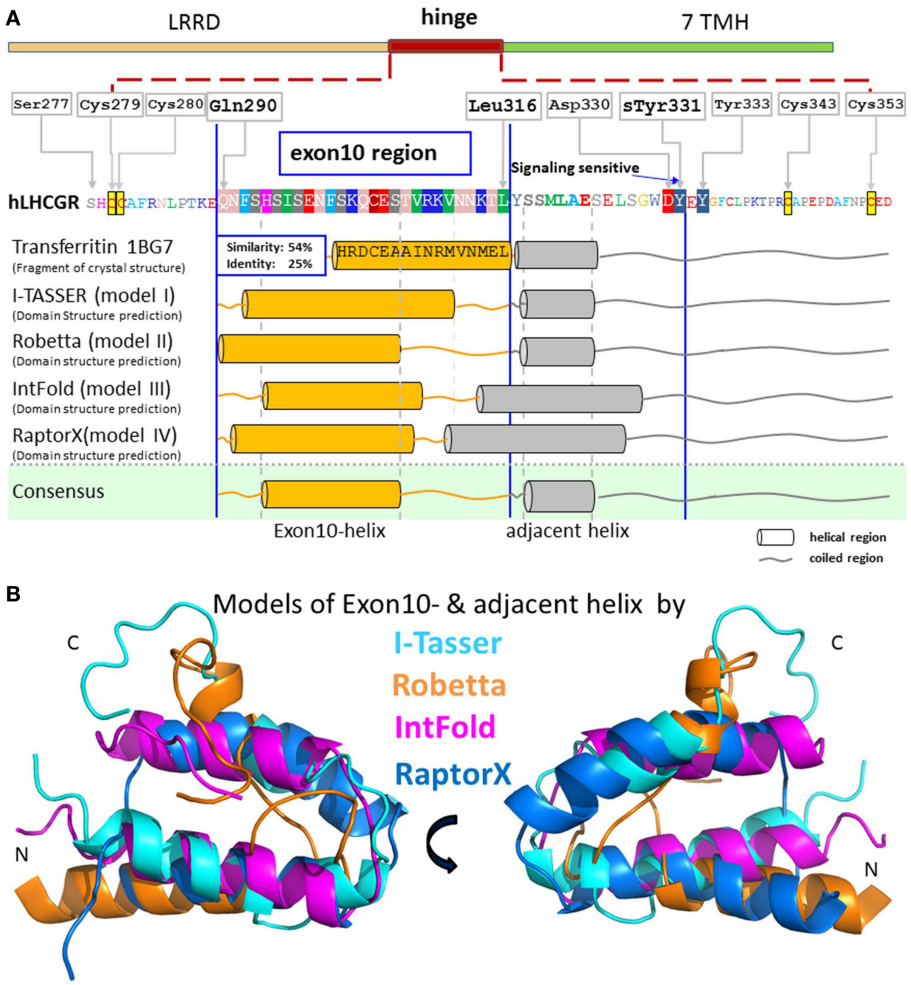

FIGURE 2 | Predicted structural segments for the middle part of the extracellular hinge region of LHCGR. For exon10, and the following residues, there is great sequence similarity to the crystal structural fragment of transferritin, which contains a helix. Four different methods I-TASSER [Cyan in **(B)**] (30, 31), Robetta [orange in **(B)**] (32), IntFold [magenta in **(B)**] (33), and RaptorX [blue in **(B)**] (34) predicted a common tertiary structure of the middle hinge region resulting in two helix segments, one for the exon10-region [orange cylinders in **(A)**] and for the following residues [gray cylinders in **(A)**]. Due to the consistent helix predictions by different methods and with the existing helix structure in homologous fragments, it is likely that this sequence contains a high propensity for an exon10-helix and an adjacent helix. The hormone binding sensitive sulfation site sTyr331 is located in an accessible coiled region.

to propose a molecular interaction model which is able to explain the complex situation in this hormone/receptor system during activation.

Materials and Methods

Experimental Setup

Construction of Vectors and Site-Directed Mutagenesis

The expression vector pEGFP-N1 (clontech) containing the fluorescent protein GFP as a C-terminal fusion partner was prepared for ligation by restriction with the restriction enzymes *Kpn*I and *Bam*HI. Amplicons of human receptor constructs wild-type LHCGR, hLHCGR-delExon10, and alanine-block constructs LHCGR-Ala1–6 were synthesized by standard PCR and overlapping extension-PCR, respectively, digested with corresponding restriction enzymes and sub-cloned into the backbone of vector pEGFP-N1. Site-directed mutagenesis of the LHCGR-wild type was performed by using the QuikChange Site-Directed Mutagenesis Kit (Stratagene), resulting in the proline mutants LHCGR-Q303P/E308P and LHCGR-M320P. The entire coding region of each LHCGR construct was sequenced. Recombinant expression vectors were propagated using the DH5α *E. coli* strain.

Cell Culture and Transfection

LHCGR constructs were expressed as GFP fusion proteins in HEK 293 cells (DSMZ), by growing in Dulbecco's modified Eagle's medium (DMEM) supplemented with 10% fetal calf serum (Biochrom) at 37°C in a humidified 5% CO_2 incubator. HEK293 cells were seeded in 24-well plates and transfected with 0.8 μg DNA/7.5 × 10^4 cells. After 24 h of culture, one portion of the cells was prepared for FACS measurements, while the second portion was stimulated with the hormones hLH or hCG and prepared for the cAMP accumulation assay. For qualitative determination of cell surface expression, transfected cells were seeded in 24-well plates with 12 mm glass cover slips (pretreated with 100 μg/ml poly-L-lysine) and prepared in 12 mm diameter dishes for scanning microscopy. Transfection with PEI was carried out according to the supplier's recommendations 24 h after seeding the cells.

Determination of Overall Receptor Expression Levels by FACS

The overall expression levels of the GFP-tagged LHCGR constructs in singly transfected HEK 293 cells were quantified with a FACS flow cytometer (FACSCalibur; Becton-Dickinson). All steps were performed at 4°C. Twenty-four hours after seeding in 24-well plates, cells were harvested by the use of 1 mM EDTA in PBS. After detachment, cells were centrifuged at 300 g for 3 min, and the supernatant was discarded. Cells were washed three times in FACS buffer (PBS containing 0.5% BSA), centrifuged (300 g for 3 min), and incubated for 5 min on ice. 7-Aminoactinomycin D (7-AAD) (Becton–Dickinson) was added to exclude damaged cells from analysis. The fluorescence of at least 10,000 cells per tube was assayed (FL1, 505–540 nm band pass filter). Expression of single expressed receptor constructs was determined from the mean fluorescence intensity. The overall receptor expression is presented as percentages of the corresponding singly expressed constructs compared with wild-type LHCGR, which is set as reference at 100%.

Confocal LSM: Localization and Quantification of the Receptor Constructs at the Plasma Membrane

Transiently transfected HEK 293 cells (1.5 × 10^5) expressing the receptors were grown on 30 mm glass cover slips (pretreated with 100 μg/ml poly-L-lysine) in 35 mm dishes. After 24 h of culture, cover slips were transferred into a self-made chamber (details on request) and covered with 1ml DPBS(+)(+).

For colocalization studies, the GFP-tagged receptor constructs were visualized using the laser confocal scanning microscope LSM510 (Carl Zeiss Microscopy GmbH, Jena, Germany) with a 100×/1.3 oil objective. The GFP-tagged constructs were detected in one channel (argon laser λ_{exc} = 488 nm, 495–545 nm band pass filter). Plasma membrane staining was performed with trypan blue, as previously described (24). The red fluorescence of trypan blue was recorded on a second channel (HeNe laser λ_{exc} = 543 nm, 560 nm long pass) and the overlay with the GFP-signals was computed. The spectral ranges were split using an MBS 488/543. Images were analyzed using AIM software (release 3.2, Carl Zeiss Microscopy GmbH, Jena, Germany). Images were imported into PHOTOSHOP software (Adobe Systems), and contrast was adjusted to approximate the original image.

Quantification of the fluorescence intensity of the GFP-tagged constructs in the plasma membrane was carried out using the same microscope system. In this case, only one channel (green fluorescence, see above) was used. Images with frame sizes of 512 × 512 pixels were generated and the ratio of receptor expression at the plasma membrane to that in intracellular membranes was calculated by measuring the fluorescence signal intensities of GFP in the selected regions of interest. The membrane/intracellular ratio was calculated for each single cell after subtracting the background. At least 28 cells per construct were analyzed (**Table 1**).

Determination of Intracellular cAMP Accumulation by Radioimmunoassay

After transient transfection of HEK 293 cells, the functional properties of each LHCGR construct were tested by measuring the accumulated cAMP after stimulation with hLH and hCG in independent experiments performed in triplicate. HEK 293 cells were seeded in 24-well plates, cultured for 24 h, and stimulated for 1 h at 37°C with stimulation buffer (DMEM supplemented with 10 mM Hepes, 0.5% BSA, 0.25 mM 3-isobutyl-1-methylxanthine) alone, or with stimulation buffer containing increasing concentrations of hLH (14 000 IU/mg; Sigma-Aldrich) or hCG (5000 IU/mg; Merck 4Biosciences). The experimental procedure of the cAMP radioimmunoassay (RIA) was performed as previously described (25, 26).

Homology Models of LHCGR LRRD-Hinge Region With Bound Hormones LH and hCG

Structural homology models for the extracellular domains of LHCGR were built on the basis of the available FSHR crystal structures (27). The procedure for the homologous hTSHR

TABLE 1 | Expression of EC_{50} values and cAMP-max values from cAMP accumulation (A) and cell surface expression (B) of each LHCGR construct.

	A. cAMP accumulation						B. cell surface expression			
Constructs	**LH stimulation**			**CG stimulation**						
Name	**EC50 (IU/ml) (CI 95%)**	**Significance $p < 0.05$**	**cAMPmax % Wild type**	**EC50 [IU/ml] (CI 95%)**	**Significance $p < 0.05$**	**cAMPmax % Wild type**	**Overall expression % LHCGR-wild type**	**ratio Mem/Intr**	**SD**	***N***
LHCGR-wild type	0.13 (0.08–0.18)		100	0.15 (0.03–0.27)		100	100	2.2	0.4	31
LHCGR-Ala1	0.25 (0.04–1.03)	–	87 ± 11	0.13 (0.04–0.37)	-	94 ± 11	89 ± 08	2.3	0.8	31
LHCGR-Ala2	0.28 (0.01–0.60)	–	83 ± 12	0.04 (0.01–0.09)	-	88 ± 12	104 ± 10	2.2	0.6	30
LHCGR-Ala3	0.11 (0.05–0.19)	–	106 ± 10	0.05 (0.05–0.10)	-	88 ± 16	105 ± 12	2.1	0.6	29
LHCGR-Ala4	0.13 (0.07–0.20)	–	101 ± 08	0.06 (0.04–0.10)	-	86 ± 16	104 ± 12	2.2	0.5	30
LHCGR-Ala5	0.13 (0.07–0.27)	–	106 ± 11	0.08 (0.02–0.31)	-	102 ± 10	94 ± 02	2.2	0.4	31
LHCGR-Ala6	0.19 (0.13–0.38)	–	104 ± 07	0.13 (0.07–0.24)	-	98 ± 08	98 ± 03	2.2	0.6	30
LHCGR-M320P	0.28 (0.18–0.43)	–	98 ± 12	0.23 (0.13–0.41)	-	99 ± 04	99 ± 04	2.2	0.6	28
LHCGR-Q303P/ E305P	0.24 (0.04–0.89)	–	101 ± 10	0.85 (0.71–1.01)	***	98 ± 08	93 ± 03	2.2	0.6	30
LHCGR-delExon10	0.51 (0.13–0.89)	**	97 ± 08	0.18 (0.02–0.62)	–	102 ± 10	89 ± 08	2.2	0.4	31

*(A) EC_{50} and cAMP-max values were calculated from concentration-response curves (6 till 11 concentration values as duplicates or triplicates) of each construct and represent the mean (confidence interval CI 95%) from a representative experiment of at least two independent experiments. Within each single experimental run, the significance of the variance between the EC_{50} values and between the cAMP-max values of each LHCGR construct and LHCGR-wild type was tested in an ANOVA significance test. Significance is expressed as (–)-no significance, *significance ($p < 0.05$), **high significance ($p < 0.005$), ***very high significance ($p < 0.001$). (B) Relative cell surface receptor expression was calculated by combining FACS and membrane quantification data of single transfected cells. Calculated values are expressed as percentages of the corresponding singly expressed constructs tagged with GFP (FL1). Experiments were independently repeated at least three times, and data are shown ± SD. N, number of enumerated cells for membrane quantification.*

modeling has been already described in detail (28). Disulfide bridges between cysteines of cysteine boxes Cb-2 and Cb-3 were built as suggested by the FSHR crystal structure. The sulfated sTyr335 of hFSHR was already known to be mandatory for hormone binding and signaling and interacts tightly with amino acids of the hormone subunits between the L2-beta loop and the L1-alpha loop (27). Both interaction models, hLHCGR/hLH and hLHCGR/hCG, were built (**Figure 3**). For the complex with bound hCG, hFSH in the template structure of the hFSH–hFSHR complex was substituted with the crystal structure of hCG [PDB-code: 1HRP, Ref. (29)]. In the hLH model, the alpha and beta-subunit of this hormone structure were used as template. Except for sequence ^{70}PPLPQ^{74} that is different in the L2 loop of the beta-subunit, the corresponding fragment of another template 3TUV from PDB was used. On the basis of the N- and C-terminal fragments of the L2-beta loop of the crystal structures of CG (1QFW, 1HRP) and by overlapping superimposition with the elongated conformation of the ^{70}PPLPQ^{74} fragment, the homology model of L2-beta loop was changed for hLH. Initially, side chains of the homology models were subjected to conjugate gradient minimizations [until they converged at a termination gradient of 0.05 kcal/(mol*Å)]. The AMBER F99 force field was used. Finally, the models were minimized without constraints. Structural modifications and homology modeling procedures were performed with Sybyl X2.0 (Certara, Inc., St. Louis, MI, USA).

Structure Predictions of Exon10

To build a three-dimensional model of the exon10-region as a part of the hinge region of LHCGR, we applied four different *in silico* web accessible methods for structure prediction:

We selected I-TASSER (30, 31), a *de novo* fold recognition method, the Robetta (32) protein structure and analysis server, IntFold2 (33), an integrated protein structure prediction pipeline based on fragment assembly and fold recognition, and finally RaptorX (34), which excels at modeling without using a large set of sequence homologs.

These differing prediction methods were chosen since they are the most successful modeling procedures in the "template free" category of the CASP7 experiment (35). All four methods build the initial protein models from short fragments of known structures with similar sequences. The predicted structures were visualized in Pymol (PyMOL, version 1.7.4 Schrödinger, LLC) (**Figure 2B**).

Statistical Analysis

For statistical analysis, PRISM Version 3.00 (GraphPad Software) was used. Concentration–response curves of the cAMP accumulation data were obtained by utilizing a four-parameter logit-log model. Statistical significance was determined with one-way ANOVA (with Dunnett's multiple comparison test as a *post hoc* test) or unpaired *t*-tests (with the Welch correction for cases with significant variance differences). We analyzed the key parameters of the whole dose–response curves (EC_{50} and maximal activity) within each experimental run (see legend of **Table 1**) considering the kind of parameter distribution (logarithmic normal distribution or Gaussian distribution).

Results

First, we modeled the hormone receptor interactions, with consideration of (i) the differences between hLH and hCG and (ii) the potential structural conditions of the exon10-region of LHCGR. Second, we employed site-directed mutagenesis of exon10 in LHCGR to study the structure–function relationships of interaction of each hormone.

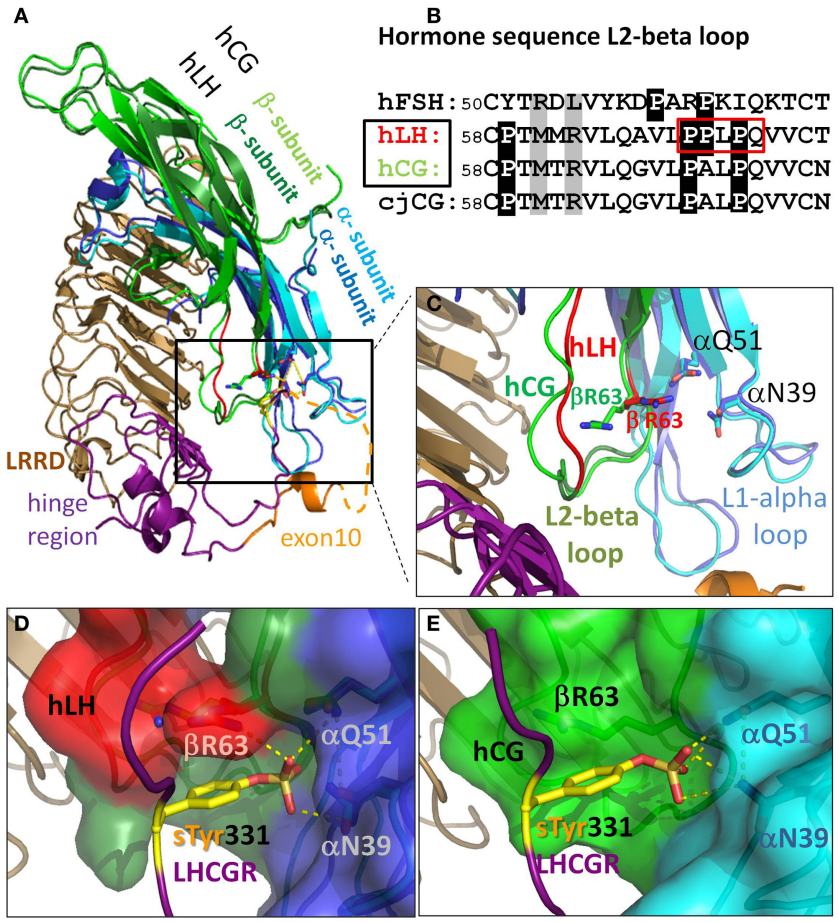

FIGURE 3 | There are differences in the L2-beta loop for hLH and hCG. This gives rise to tighter binding for hLH than for hCG at sTyr331, the second binding site at LHCGR. **(A)** Homology model details of superimposed hormones hLH and hCG extracellularly bound to LRRD and hinge region of LHCGR based on the crystal structure of FSH/FSHR [4AY9, Ref. (9)]. **(B)** Sequence differences in L2-beta loop of these glycoprotein hormones (cjCG: New world monkey *Callithrix jacchus*). Gray: positions representing interacting elements of the sTyr moiety of the LHCGR hinge region. White on black background: differences in prolines between FSH and hLH, hCG, and even between hLH (red boxed) and hCG. **(C)** hLH was modeled based on the hCG structure (PDB: 1HRP, light green). Close up view: the L1-alpha loop is similar for hLH (dark blue) and hCG (cyan). The differing conformations of the L2-beta loop for hLH is based on a fragment in the crystal structure of Insulysin (3TUV) with identical sequence PPLPQ. The resulting backbone conformation of hLH (red) clearly differs from that in hCG structure (light green). The additional proline in hLH (see red box in B) restricts the conformational degree of freedom of βR63 (red) located in the N-terminal flank of the L2-beta loop. **(D)** Detailed view for hLH. The resulting binding cavity for sTyr331 formed by the L1-alpha loop (dark blue surface) and L2-beta loop (red surface) is more surrounded in hLH, and is flanked by the βR63 (red) and thus provides an additional H-bond donor for the interaction with the sTyr331 (yellow) of LHCGR compared to **(E)** detailed view for hCG (light green), where βR63 does not interact with sTyr331 and the binding pocket is much wider.

Structural Differences Derived From the Homology Models of the Complexes Between hCG/hLHCGR and hLH/hLHCGR With Focus on the sTyr Binding Site

The binding mode of glycoprotein hormones (GPHs) at GPHRs was in principle determined by the crystal structures of the ectodomain of FSHR with bound FSH (9).

This structural complex confirmed previous assumptions of a primary (high affinity) and a secondary (low affinity) hormone binding site. The high affinity binding site at the LRRD has already been described in detail (36), but the structure of the low affinity site around the sulfated tyrosine (sTyr) (37) has not yet been described for the LHCGR. This point is of specific importance, as it has already been shown experimentally that there must be differences between the receptor/hormone interactions at this site at LHCGR (20). We therefore first analyzed the differences in our designed homology models between the LHCGR/LH and LHCGR/CG complexes in comparison to the FSHR/FSH structure (9).

The GPHs are heterodimers composed of a common alpha-subunit and a variant beta-subunit. The binding site for the common sTyr motif of the GPHR's hinge region (2) is formed by loops L1-alpha and L2-beta (**Figure 3**). The L1-alpha loop residues αN39 and αQ51 of the common alpha-subunit are thus matching parts of the receptors' sTyr moiety that interact with all GPHs. However, in the L2-beta loop of the beta-subunit, there are a few but significant sequence differences between the GPHs. We therefore focus on the structural differences in the L2-beta loop in the different GPHs (**Figure 3B**), especially hLH and hCG, as well as their interactions with the

respective receptor. The N- and C-terminal flanks of the L2-beta loop exhibit some differences among the GPHs. The N-terminal flank of this loop provides interactions with negatively charged residue(s) of the respective receptor's hinge region preceding the sTyr and with sTyr itself. For the different hormones, this is done by different residues in the relevant L2-beta loop. In FSH, the positively charged residue R53 and the hydrophobic residue L55 (**Figure 3B**) are the counterparts for the interaction with sTyr 335 (via water molecules) of the FSHR crystal structure (PDB: 4AY9, not shown).

Instead of an arginine (R53 in FSH) and leucine (L55 in FSH), the sequence of hLH and hCG exhibit at the corresponding positions: the hydrophobic M61 and the positively charged R63 at the N-terminal flank of the L2beta loop (**Figure 3B**). Thus, this opposite order of side chain properties lead to different spatial arrangements when hLH and hCG interact with sTyr331 of LHCGR, compared when FSH interacts with sTyr335 of FSHR.

Finally, these diverse molecular properties and interactions indicate that there are differences between FSHR and hLHCGR at this particular hormone/receptor interface.

In addition, the C-terminal flanking sequence of the L2beta loop differs between hLH and hCG with respect to specific and important prolines (**Figure 3B**). In contrast to hCG, hLH possesses two consecutive prolines (P70, P71). In order to model the different L2beta loop of hLH, a search for a structural template for the hLH motif ^{70}PPLPQ revealed a fragment in the crystal structure of insulysin (3TUV) with an identical sequence. This structural fragment was inserted into the L2beta loop of the hLH interaction model (red in **Figures 3B–D**) instead of the ^{70}PALPQ sequence (green in **Figures 3C,E** of the hCG structure). In this homologous conformation, the side chain of the second proline P71 of hLH is oriented oppositely to A71 of hCG located in the corresponding position. The resulting L2-beta loop backbone conformation of our hLH interaction model (red in **Figures 3C,D**) clearly differs from that in the crystal structures of hCG (green in **Figures 3C,E**). It is noticeable that this additional proline in our hLH interaction model is placed in a very similar orientation to the corresponding P63 in hFSH/FSHR crystal structure. However, due to the two consecutive prolines P70-P71 in hLH (**Figure 3B**), this proline restricts the conformational degree of freedom of βR63 located in the N-terminal flank of the hLH L2-beta loop, instead of the L37 in hFSH (**Figure 3B**). As a consequence, the side chain of βR63 (red stick in **Figure 3C**, red surface in **Figure 3D**) is oriented toward the L1-alpha loop. This in turn results in hLH being in a more bordered binding cavity flanked by the βR63 and thus providing additional H-bond donors for the interaction with the sTyr331 (**Figure 3D**). This scenario is different in the analogous hCG interaction model, which lacks the second proline. Therefore βR63 (green in **Figure 3C**, green surface in **Figure 3E**) is not forced to orient toward L1-beta loop and does not participate in the interaction with sTyr331 (**Figure 3E**). In turn, hCG provides fewer H-bond donors than hLH for the interaction with sTyr331, the second hormone binding site of hLHCGR.

Homology Models Predict a Helical Structure for the Exon10-Encoded Hinge Region of the LHCGR

Sequence-based secondary structure predictions suggest a helical secondary structure for the exon10-encoded region. An initial search for a structural template for the exon10-region of LHCGR by sequence similarity revealed a fragment of transferritin's crystal structure (PDB entry 1BG7) with 54% sequence similarity to the exon10-encoded amio acid sequence. This structure showed an alpha-helical conformation (**Figure 2A**). For the residues next to the exon10-region, an additional helical structure of transferritin could be assigned.

Four different methods [I-TASSER (30, 31), Robetta (32), IntFOLD2 (33), and RAPTORX (34)] were applied for prediction of the tertiary structure of the exon10-region. All four methods agreed in predicting two helix segments for the exon10-region as well as for the following residues (**Figures 2A,B**).

Although not identical in every particular position, the four resulting models (**Figure 2B**) share at least similar topologies for the exon10-region and the following structural parts. Comparison of the applied approaches show that helix predictions by different methods match with existing helix structures in homologous fragments. Therefore, it is likely that helical entities might exist within exon10 and within the directly following part of the hinge region of LHCGR prior to the sTyr moiety. Comparison of exon10 sequences of LHCGR among mammalian species revealed a sequence similarity/IDENDITY pattern "QNfsfSIfeNFSkQCEST.Rkpnnel," indicating that the identical residues (upper case) are matching with the conserved common region of the predicted helix.

The IntFold2 fragment matches the experimental data best. The initial homologous interaction model for the extracellular domain of LHCGR with bound hormones lacked the sequence in the middle of the hinge region, as this segment was unresolved in the crystal structure of FSH/FSHR (dashed orange line in **Figure 3A**). Thus, we inserted our predicted fragment for this missing part and generated an hLH/hLHCGR interaction model of the extracellular domain containing a complete hinge region for the first time. This resulted in an LHCGR/hLH interaction model, where – apart from the sTyr331 interaction with the binding pocket between alpha and beta-subunits of hLH (insert **Figure 4**) – the predicted exon10-helix and adjacent helix of LHCGR interact with the alpha-subunit of the hormone (zoomed in box, **Figure 4**).

Description of LHCGR Variants for Transient Single Expression and Functional Characterization

To reveal the structure–function properties of the exon10-encoded part of the LHCGR hinge region, an alanine-block scan was performed. Since polyalanine constructs are prone to form helix structures and helix formation was predicted, the 27 exon10 amino acids (Q290-L316) were systematically substituted by five (LHCGR-Ala1–LHCGR-Ala3) and six (LHCGR-Ala4 and LHCGR-ALa5) alanines in a row. The predicted adjacent helix (construct LHCGR-Ala6) contains an alanine-block substitution of the amino acids 318–324 (**Figure 5A**). This region has been described as signaling sensitive (23). Since alanine blocks are capable of mimicking a helical structure (38), we introduced proline mutations which might disturb potential helical portions, such as the double proline mutant at the position Q303P/E305P. Additionally, in the wild-type LHCGR, position M320 was mutated to proline.

The Occurrence of a Helical Structure Within Exon10 is Supported by Results of Mutagenesis Studies

FACS measurements revealed receptor expression of the LHCGR-alanine-block constructs and the LHCGR-proline mutants, which was comparable to that of wild type (**Table 1**). The membrane/intracellular ratio of expression of all the constructs was likewise similar to that of the wild type (**Table 1**). Analysis of confocal LSM (**Figure 5B**) confirmed plasma membrane expression of all LHCGR constructs.

The signaling properties of LHCGR-alanine-block mutants and proline mutants were then tested by cAMP accumulation assay. The EC_{50} and cAMP-max values were estimated from dose–response curves of hLH and hCG stimulation. All of the LHCGR-alanine-block mutants 1–6 (**Figure 5**) show stable cAMP-max values and also wild-type-like concentration-response curves with similar EC_{50} values for hLH and hCG stimulation (**Table 1**).

The LHCGR-delExon10 construct shows wild-type-like properties by stimulation with hCG [EC50 0.18 (0.02–0.62) IU/ml, **Table 1**; **Figure 6A**], however, a substantially right shifted concentration-response curve (**Figure 6B**) was observed for stimulation with hLH [EC_{50} 0.51 (0.13–0.89) IU/ml, **Table 1**]. This result indicates reduced receptor function with hLH and confirms previous observations (8, 9).

However, surprisingly the double proline LHCGR mutant Q303P/E305P substituted into exon10 gave exactly the opposite response to the deletion construct. The LHCGR-delExon10 construct, lacking exon 10 entirely, affects hLH but not hCG-induced function. By contrast, the LH-induced function is not affected by LHCGR-Q303P/E305P [EC50 0.24 (0.04–0.89) IU/ml]. However,

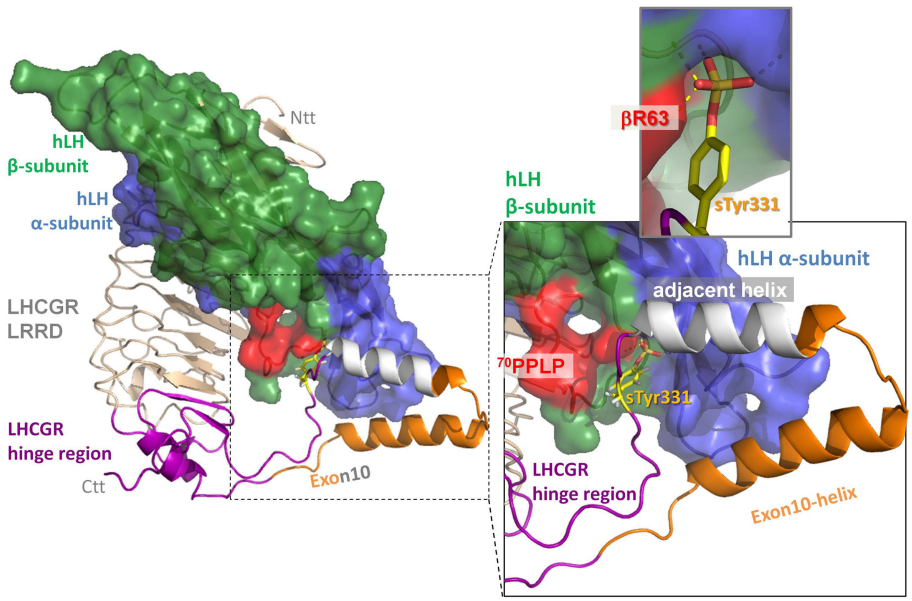

FIGURE 4 | Extension of the hinge region in the homology model of the ectodomain of LHCGR with hLH bound to both the leucine-rich-repeat domain (LRRD) (wheat) and to this extension of the hinge region (lilac). The two predicted helices within the middle of hinge region, the exon10-helix (orange) and the adjacent helix (gray), interact with the alpha-subunit of hLH. The following sulfation group of sTyr331 (yellow) binds in a binding pocket between the alpha-subunit (blue) and beta-subunit (green) of hLH. The specific conformation of the hLH beta-subunit in the L2-beta loop caused by ^{70}PPLP (colored in red) that differs from hCG (see also fig 2 colored in green) performs more productive H-bond interactions (insert upper right panel) than hCG.

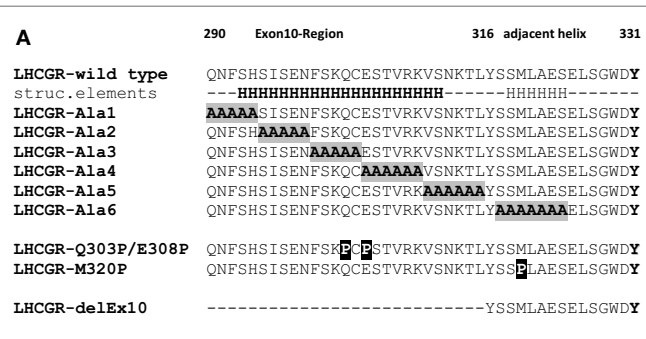

FIGURE 5 | Continued

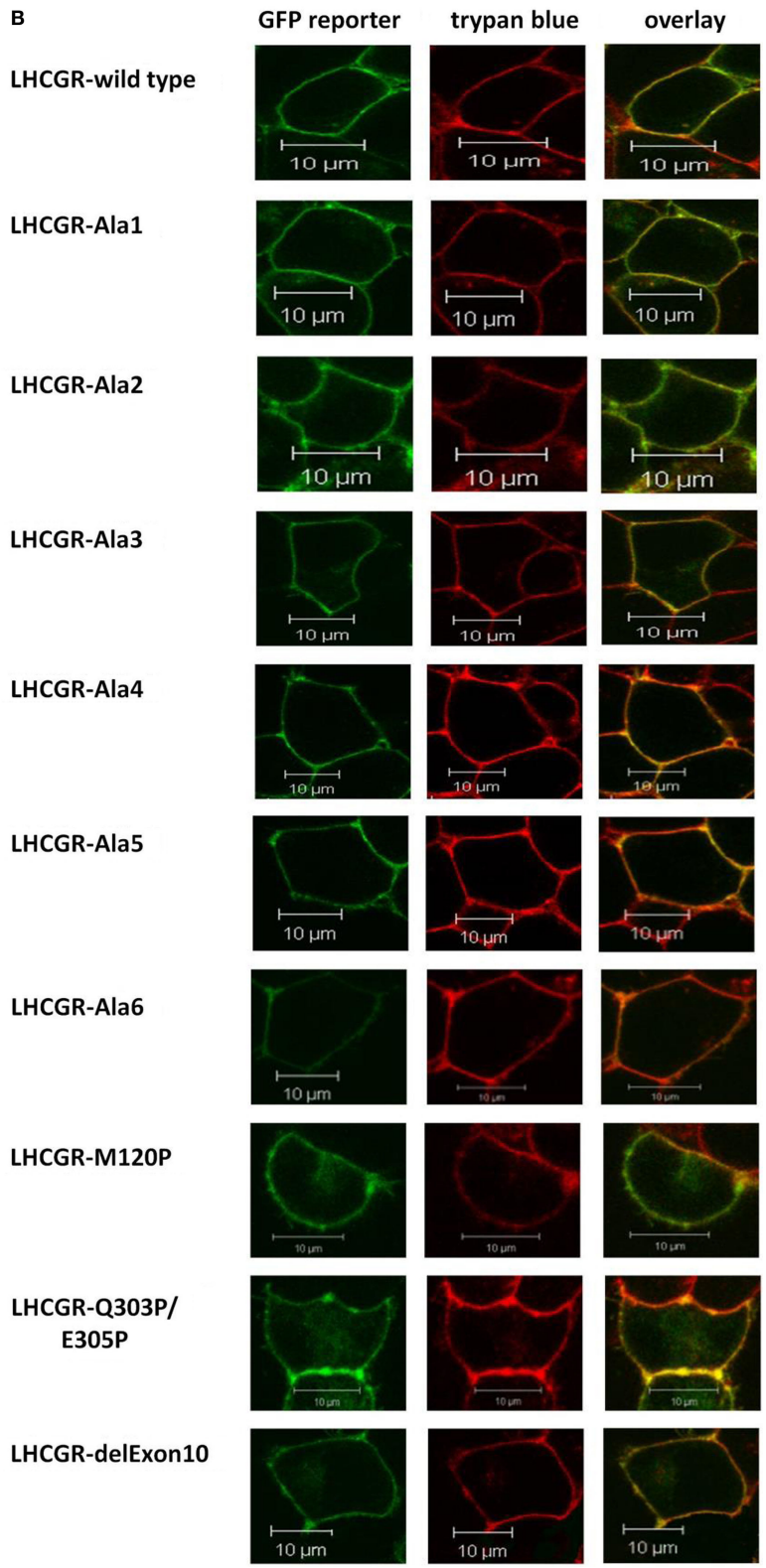

FIGURE 5 | Mutations introduced in the middle of the LGCGR hinge region. **(A)** Sequence of LHCGR constructs of helix supporting block-wise polyalanine and directed helix-disturbing proline mutations within the exon10-helix and adjacent helix. **(B)** Localization of the GFP fluorescence signals of the LHCGR constructs in transiently transfected HEK 293 cells by confocal LSM. The GFP-signals of the fusions (left panel, green) and the Trypan blue signals of the membranes of the same cells (central panels, red) were computer-overlayed (right panels, yellow). GFP fluorescence is detectable only for transfected cells, whereas all cells show cell surface trypan blue fluorescence. All constructs are expressed on the plasma membrane surface.

the potency of hCG at this helix-disturbing construct is reduced, as is indicated by a right-shifted concentration-response curve with an increased EC_{50} value [EC_{50} 0.85 (0.71–1.01) IU/ml, **Table 1**; **Figure 6A**]. It is striking that the single proline LHCGR mutant M320P shows no significant difference in comparison to the wild-type LHCGR for hLH and hCG stimulation (**Table 1**).

Discussion

The intramolecular activation mechanism at the extracellular side of LHCGR remains to be illuminated. Inspired by the crystal structure of the ectodomain of the FSHR/FSH complex (27), we recently described the specific hormone-hinge region interaction using a homology model of the TSH and TSHR complex (28). In this context, we have utilized the crystal structure of the FSHR/FSH complex as a template to study structure–function relationships of hormone/receptor interactions for LHCGR, with focus on the hinge region.

Thus, we initially built the first LHCGR model especially for the middle segment of the hinge region, not only since this section of 34 residues (I296-Y330) is not resolved in the FSHR structure (27), but also because molecular details of the interactions between the respective hormone and the receptor's hinge region evidently differ in this part of the LHCGR. The resulting LHCGR models share coincident spatial locations for LRRD and a pair of two cysteines from cysteine box 2 (Cb-2) and 3 (Cb-3) which form cysteine bridges between Cys279–Cys343 and Cys280–Cys353 (**Figures 1** and **8**). This is consistent with the reported spatial proximity of Cb-2 and Cb-3, due to the disulfide bridges for LHCGR (23) and also for TSHR (39).

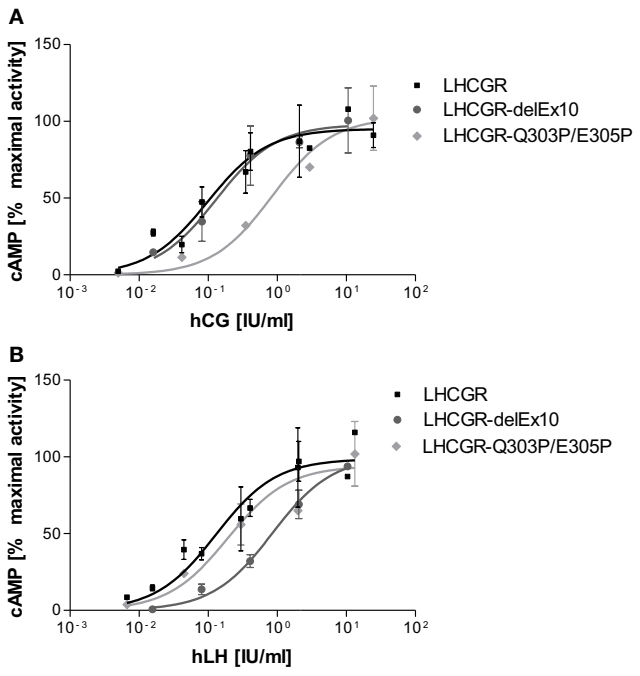

FIGURE 6 | Concentration-response curves differ for LH and hCG at LHCGR-wt and LHCGR-delExon10. It is shown that the mean of experimental values of two independent runs normalized on maximal activity. **(A)** Stimulation with hCG shows for the LHCGR-delExon10 construct (dark) LHCGR-wild-type (black) like properties; the helix-disturbing double proline LHCGR mutant Q303P/E305P substituted into exon10 (light) shows a right-shifted concentration-response curve. **(B)** By contrast, stimulation with hLH, shows a substantial right shift for the LHCGR-delExon10 construct (dark), whilst the function of the double proline LHCGR mutant Q303P/E305P is nearly unaffected (light).

The hLH Binding Site at a Sulfated Tyrosine is Different From That of hCG

Apart from hormone binding to the LRRD, the sTyr331 of the hinge region is crucial for the second hormone binding site in LHCGR. According to the crystal structure of the FSHR/FSH (27), the sulfated group of sTyr interacts with a binding cavity formed by the loops L1-alpha and L2-beta in the hormone.

In our bound hLH model, a sequence difference between hLH and hCG in the L2-beta loop, with a proline P71 in hLH, instead of an alanine in hCG, causes a different backbone conformation in the L2-beta loop, from that in hCG. Therefore, the orientation of βR63 in bound hLH in our LHCGR–hLH interaction model has a much greater tendency to interact with the oxygen atom in the sulfated group of sTyr331 in the hinge region of LHCGR than with bound hCG (**Figure 3**). Moreover, in our models for the sTyr binding pocket, βR63 of hLH functions as an additional interaction partner for sTyr331 (βR63: red in **Figure 3D**) that is not present in hCG (βR63: green in **Figure 3E**). This is in good agreement with previous experimental data (20), in which the LHCGR mutation of Tyr331 to Ala leads to a greater decrease in potency for hLH, by more than 2300-fold relative to CG. Therefore, our LHCGR interaction models differ between LH and CG and provide a plausible explanation as to why hLH binds more tightly to the sTyr binding site of LHCGR hinge region than does hCG. Other discrepancies between hLH and hCG have been described previously (40).

Moreover, it is also very likely that hCG binds slightly differently than hLH to the LRRD of LHCGR, due to the additional C-terminal tail of the hCG beta-subunit. In that case, the loops L1-alpha and L2-beta, and thus also the sTyr binding pocket of bound hCG, might be placed closer to the hinge region and cause less or different movement of the hinge region prior to helix determined by exon10 and in comparison to bound hLH.

In a broader context and with reference to the *in vivo* situation, it might be interesting to note, that in the aforementioned patient who suffered from a homozygous exon 10 deletion, LH signaling is severely hampered, while hCG action is seemingly normal (9). This observation corroborates our functional studies in this manuscript. Moreover, studies by others on the LHCG-receptor have revealed that, in New world primates, LHCGR naturally lacks exon 10, due to an aberrant splicing event. As a consequence thereof, the interacting hormone system has dramatically changed, with completely inactivated LH expression and activated CG system in the pituitary. This only can be explained by a selective interaction of the LHCGR lacking exon 10 with CG, but not LH (4).

The LHCGR Exon 10 Determined Region and Adjacent Parts are Probably in Helical Structure-Conformations

For homology modeling of the middle hinge region, including exon 10, for LHCGR, we selected four different servers, namely

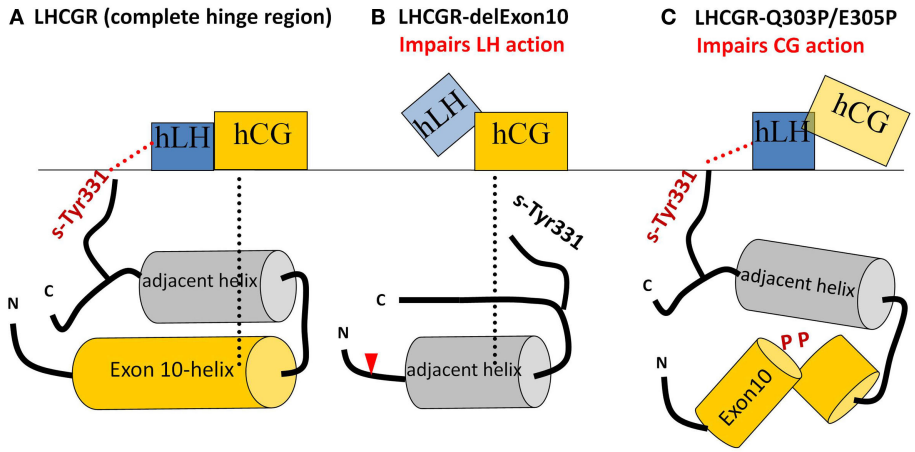

FIGURE 7 | Sketches of the different hLH and hCG interactions with the middle section of the hinge region with various LHCGR constructs. **(A)** LHCGR-wt: exon10-helix shifts the sulfated sTyr331 into an appropriate spatial position necessary to interact with hLH, while, for hCG, exon10-helix acts as a structural interface. **(B)** LHCGR-delExon10: deletion of exon 10 leads to displacement of the remaining residues beyond the cutting point (red triangle). Subsequently sTyr331 abrogates the interaction with hLH, However, the adjacent helix moves into the position previously occupied by the exon 10-helix and thus provides a structural interface for activation by hCG; **(C)** LHCGR-Q303P/E308P double proline mutation within exon10 disturbs the helical structure of exon10-helix and interferes with the hCG-induced hinge movement and signaling. However, in this case, the retained length of the middle hinge region allows the appropriate adjustment of sTyr331 for proper hLH interaction and signaling.

IntFold2, RaptorX, I-TASSER, and Robetta, because in competition they have proven to be successful methods in predicting fold and tertiary structures of medium sized proteins or domains (35). As regards their prediction of secondary structural elements, all four different approaches coincidently suggest the topology of two helical structural entities in exon10 and in the region following shortly after. As regards the tertiary structure predictions, the two helices of the four models overlap, but are not exactly identical (**Figure 2B**).

We analyzed this critically by incorporating all four predicted structures into the hinge region and selected the IntFOLD2 prediction that best fit the available data (**Figure 4**). We regarded these cautiously as rough estimates, since the regions – especially before exon 10 and after sTyr – might be conformationally flexible. This has already been suggested for the corresponding region in the TSHR, where in the hormone-unbound state the region prior to sTyr might come close to the agonistic unit proximal to Cys-box 2 and 3 located at the pivotal helix of the hinge (28) (see **Figure 8**). Complementary charge distributions on the C-terminal end of the LRRD and on the sTyr moiety have been discussed for TSHR/FSHR chimeras (22). This supported the view that negative charges of the Asp-sTyr-Glu motif might interact with particular positive charges located in the LHCGR at LRRD repeat 10 (R247) and on the pivotal helix of Cb-3 (e.g., R283) and on beta strand-12 (K339, R342; see residues, mutations and models also at our GPHR information resource: www.SSFA-GPHR.de (41)).

This hypothesis is consistent with the results reported for an activating antibody 13B1 of the hinge region of LHCGR (42), which interacts via a discontinuous sequence epitope comprising the N-terminal end of the exon10-region (Cb-2: 291–298), at Cb-3 with the signaling-sensitive tyrosine region (30–33), and two further residues (37, 39). It seems feasible that these three discontinuous sequence regions will be assembled close together as a fully accessible patch on the surface of the hinge region. Since this is the case in three of the four models of the exon 10 fragments (Figure S1 in Supplementary Material), it suggests that the hinge region model of LHCGR matches most of the known experimental data and might be considered in the future for further refinement by experimental validations.

Helix Supporting and Disturbing Mutations Confirm Suggested Structural Elements

Since polyalanines are thought to form helical structure [54] and to test whether particular amino acids and/or the helical character of exon10 are responsible for full activation of LHCGR by hLH, we introduced block-wise polyalanine mutants in the exon10-region and into the predicted adjacent helical-region (**Figure 5**). Each alanine-block construct showed wild-type behavior in terms of signaling properties, characterized by cAMPmax and EC_{50} values (**Table 1**).

Importantly, the presented polyalanine scan also revealed that there is no specific influence of a particular amino acid and side-chain in the studied region, but supports the predicted two potential helical portions, one in exon10 and a second in the proximate following region (**Figure 2**).

To validate the conclusion that there are two structural elements, we next substituted, in contrast to helix supporting mutations, prolines into the predicted helical portions of exon10 (Q303P, E305P) and into the adjacent helix (M320P), in order to disturb potential helical structures. The substituted prolines in exon10 gave completely opposite results for hLH- and hCG-induced function than had been found for deletion of exon 10 in LHCGR. While in the construct, which lacks exon 10, only hLH signaling is affected, the construct with two prolines introduced into exon10-helix showed a significant negative effect on signaling only for hCG.

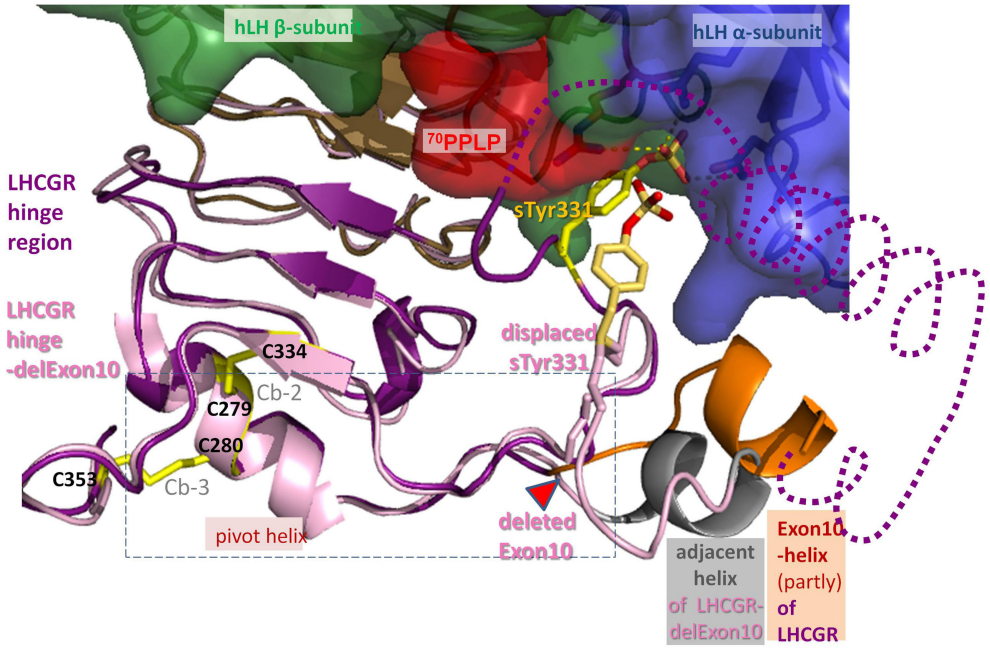

FIGURE 8 | Differences between hLH bound homology models of LHCGR hinge region and LHCGR hinge-delExon10. For LHCGR, the sulfated sTyr (yellow) of the hinge region (lilac) fits deep into the binding pocket of bound hLH between alpha- (surface blue) and beta-subunit (green, red adapted conformation for ^{70}PPLP). For clarity, exon10-helix (orange) of LHCGR is cut open and the adjacent helix is omitted (dotted line). By contrast, the deletion in LHCGR-delExon10 (pale pink) causes displacement of the residues in the middle of the hinge region after the deletion position (red triangle). Subsequently sTyr331 is displaced and thus the interaction of the sulfation group with the hLH binding pocket is impaired. However, the deletion of 27 residues in LHCGR-delEx10 (contains exon10-helix) causes the polypeptide chain to contract, so that the adjacent helix (gray) is arranged in the same place as the exon10-helix (orange). Upon hormone binding, the signal is conveyed via the hinge region (lilac) through a hormone-induced movement of the pivot helix, the disulfide linked agonistic unit and the area prior to the exon10-helix, both of which are probably embedded (dashed box) in between the loops of the transmembrane domain of LHCGR.

These data suggest that the exon10-region serves for the two hormones in a different manner. For hLH-induced receptor activation, the exon10-helix is necessary as a non-specific *spacer-element* to adjust the sulfated Tyr331 into an appropriate location and orientation for a compatible H-Bond interaction with hLH. For hCG-induced activation, the exon10 determined helix acts as a structural interface within the hinge region (**Figure 7A**). Deletion of exon 10 causes shortening of the middle hinge loop, which subsequently leads to spatial delocalization of the downstream regions. The sequence forming the adjacent helix comes into the position of the previous exon10-helix (**Figures 7B** and **8**). This might explain why hCG can induce signaling, probably because the displaced adjacent helix adopts the structural function of exon10-helix.

The delocalization also leads to displacement of the sulfate group of sTyr331, which is then unable to form H-bond interactions with hLH (**Figures 7B** and **8**). This explains why the LHCGR-del Exon10 construct affects hLH signaling much more strongly, since sulfated Tyr331 is not absolutely essential for hCG-induced function, in contrast to the case with hLH. In the case of the double proline mutation within exon10, the helical structure of exon10-helix is disturbed (**Figure 7C**); this interferes with the correct interaction of the hinge region with hCG and in consequence cAMP signaling is impaired. However, the length of the loop in the middle of the hinge region is retained, which still allows appropriate adjustment of sulfated Tyr331 for proper hLH interaction.

From these data, we conclude that LHCGR activation in the hinge region by hLH mainly depends on the distance from a specific amino acid (hormone in relation to sTyr331), while LHCGR function with hCG is closely related to an interaction with a structural element within the hinge region.

To summarize, by studying the activation mechanism of LHCGR using a naturally occurring pathogenic LHCGR-variant with reduced hLH function, we were able to pinpoint a sequence difference in the beta2 loop of hLH and hCG and assign two different structural features in the exon 10 determined region that are together probably responsible for the different modes of action of the hormones hLH and hCG within the receptor activation process. The exon10 part acts, on the one hand, as a non-specific spacer element that adjusts the sensitive residue sTyr331 to the appropriate position for triggering the hormone hLH. On the other hand, it functions as a structural interface for hCG-induced function. This implies that the two hormones interact differently with the hinge region. We conclude from previous work (27, 28) and our study here that the flexible part of the hinge region allows movement of the middle hinge region. In the hormone-free state, the hinge is arrested, probably by interactions between pivot helix (Cb-2 linked Cb-3) and sTyr vicinity, since both areas comprise positions of activating mutations in

TSHR (28). This is also supported by complementary charge interactions (22) occurring in all three types of GPHRs. Thus, the pivot helix and the section prior to exon 10 helix of the hinge region represent a convergent center for signaling and are spatially embedded in between the ECLs of the serpentine domain (**Figures 1B** and **8**). We conclude from our data that the two homologous hormones hLH and hCG trigger different conformational changes at the LHCGR convergent center and via the hinge region probably thereby also induce the previously reported different signaling pathways (5, 6). These details advance the understanding of trigger points where hLHCGR conveys and differentiates the activation signal and prospectively this may be helpful in developing biased agonists or antagonists addressing signaling pathways selectively.

Acknowledgments

This study was in part supported by the German Research Foundation (GR 1547/9-1 by JG. KR1273/2-1 by GKr).

Supplementary Material

The Supplementary Material for this article can be found online at http://journal.frontiersin.org/article/10.3389/fendo.2015.00140

References

1. Ascoli M, Fanelli F, Segaloff DL. The lutropin/choriogonadotropin receptor, a 2002 perspective. *Endocr Rev* (2002) **23**:141–74. doi:10.1210/edrv.23.2.0462
2. Jiang X, Dias JA, He X. Structural biology of glycoprotein hormones and their receptors: insights to signaling. *Mol Cell Endocrinol* (2014) **382**:424–51. doi:10.1016/j.mce.2013.08.021
3. Kleinau G, Krause G. Thyrotropin and homologous glycoprotein hormone receptors: structural and functional aspects of extracellular signaling mechanisms. *Endocr Rev* (2009) **30**:133–51. doi:10.1210/er.2008-0044
4. Troppmann B, Kleinau G, Krause G, Gromoll J. Structural and functional plasticity of the luteinizing hormone/choriogonadotrophin receptor. *Hum Reprod Update* (2013) **19**(5):583–602. doi:10.1093/humupd/dmt023
5. Casarini L, Lispi M, Longobardi S, Milosa F, La Marca A, Tagliasacchi D, et al. LH and hCG action on the same receptor results in quantitatively and qualitatively different intracellular signalling. *PLoS One* (2012) **7**:e46682. doi:10.1371/journal.pone.0046682
6. Jonas KC, Fanelli F, Huhtaniemi IT, Hanyaloglu AC. Single molecule analysis of functionally asymmetric G protein-coupled receptor (GPCR) oligomers reveals diverse spatial and structural assemblies. *J Biol Chem* (2015) **290**:3875–92. doi:10.1074/jbc.M114.622498
7. Grzesik P, Teichmann A, Furkert J, Rutz C, Wiesner B, Kleinau G, et al. Differences between lutropin-mediated and choriogonadotropin-mediated receptor activation. *FEBS J* (2014) **281**:1479–92. doi:10.1111/febs.12718
8. Gromoll J, Eiholzer U, Nieschlag E, Simoni M. Male hypogonadism caused by homozygous deletion of exon 10 of the luteinizing hormone (LH) receptor: differential action of human chorionic gonadotropin and LH. *J Clin Endocrinol Metab* (2000) **85**:2281–6. doi:10.1210/jcem.85.6.6636
9. Mueller T, Gromoll J, Simoni M, Muller T. Absence of exon 10 of the human luteinizing hormone (LH) receptor impairs LH, but not human chorionic gonadotropin action. *J Clin Endocrinol Metab* (2003) **88**:2242–9. doi:10.1210/jc.2002-021946
10. Nagayama Y, Wadsworth HL, Chazenbalk GD, Russo D, Seto P, Rapoport B. Thyrotropin-luteinizing hormone/chorionic gonadotropin receptor extracellular domain chimeras as probes for thyrotropin receptor function. *Proc Natl Acad Sci U S A* (1991) **88**:902–5. doi:10.1073/pnas.88.3.902
11. Kosugi S, Ban T, Akamizu T, Kohn LD. Site-directed mutagenesis of a portion of the extracellular domain of the rat thyrotropin receptor important in autoimmune thyroid disease and nonhomologous with gonadotropin receptors. Relationship of functional and immunogenic domains. *J Biol Chem* (1991) **266**:19413–8.
12. Nakabayashi K, Kudo M, Kobilka B, Hsueh AJW. Activation of the luteinizing hormone receptor following substitution of Ser-277 with selective hydrophobic residues in the ectodomain hinge region. *J Biol Chem* (2000) **275**:30264–71. doi:10.1074/jbc.M005568200
13. Nagayama Y, Russo D, Chazenbalk GD, Wadsworth HL, Rapoport B. Extracellular domain chimeras of the TSH and LH/CG receptors reveal the mid-region (amino acids 171-260) to play a vital role in high affinity TSH binding. *Biochem Biophys Res Commun* (1990) **173**:1150–6. doi:10.1016/S0006-291X(05)80906-4
14. Jaeschke H, Neumann S, Kleinau G, Mueller S, Claus M, Krause G, et al. An aromatic environment in the vicinity of serine 281 is a structural requirement for thyrotropin receptor function. *Endocrinology* (2006) **147**:1753–60. doi:10.1210/en.2005-1138
15. Mueller S, Kleinau G, Jaeschke H, Paschke R, Krause G. Extended hormone binding site of the human thyroid stimulating hormone receptor: distinctive acidic residues in the hinge region are involved in bovine thyroid stimulating hormone binding and receptor activation. *J Biol Chem* (2008) **283**:18048–55. doi:10.1074/jbc.M800449200
16. Mueller S, Kleinau G, Szkudlinski MW, Jaeschke H, Krause G, Paschke R. The superagonistic activity of bovine thyroid-stimulating hormone (TSH) and the human TR1401 TSH analog is determined by specific amino acids in the hinge region of the human TSH receptor. *J Biol Chem* (2009) **284**:16317–24. doi:10.1074/jbc.M109.005710
17. Bonomi M, Busnelli M, Persani L, Vassart G, Costagliola S. Structural differences in the hinge region of the glycoprotein hormone receptors: evidence from the sulfated tyrosine residues. *Mol Endocrinol* (2006) **20**:3351–63. doi:10.1210/me.2005-0521
18. Alvarez CA, Narayan P, Huang J, Puett D. Characterization of a region of the lutropin receptor extracellular domain near transmembrane helix 1 that is important in ligand-mediated signaling. *Endocrinology* (1999) **140**:1775–82. doi:10.1210/endo.140.4.6624
19. Angelova K, de Jonge H, Granneman JC, Puett D, Bogerd J. Functional differences of invariant and highly conserved residues in the extracellular domain of the glycoprotein hormone receptors. *J Biol Chem* (2010) **285**:34813–27. doi:10.1074/jbc.M110.148221
20. Bruysters M, Sultan C, Auger J, Faugeron I, Larue L, Lumbroso S, et al. A new LH receptor splice mutation responsible for male hypogonadism with subnormal sperm production in the propositus, and infertility with regular cycles in an affected sister. *Hum Reprod* (2008) **23**:1917–23. doi:10.1093/humrep/den180
21. Jaeschke H, Gu R, Mueller S. The hinge region of the TSH receptor stabilizes ligand binding and determines different signaling profiles of human and bovine TSH. *Endocrinology* (2011) **152**:3986–96. doi:10.1210/en.2011-1389
22. Schaarschmidt J, Huth S, Meier R, Paschke R, Jaeschke H. Influence of the hinge region and its adjacent domains on binding and signaling patterns of the thyrotropin and follitropin receptor. *PLoS One* (2014) **9**:e111570. doi:10.1371/journal.pone.0111570
23. Bruysters M, Verhoef-Post M, Themmen APN, Technology M. Asp330 and Tyr331 in the C-terminal cysteine-rich region of the luteinizing hormone receptor are key residues in hormone-induced receptor activation. *J Biol Chem* (2008) **283**:25821–8. doi:10.1074/jbc.M804395200
24. Wüller S, Wiesner B, Löffler A, Furkert J, Krause G, Hermosilla R, et al. Pharmacochaperones post-translationally enhance cell surface expression by increasing conformational stability of wild-type and mutant vasopressin V2 receptors. *J Biol Chem* (2004) **279**:47254–63. doi:10.1074/jbc.M408154200
25. Teichmann A, Gibert A, Lampe A, Grzesik P, Rutz C, Furkert J, et al. The specific monomer/dimer equilibrium of the corticotropin-releasing factor receptor type 1 is established in the endoplasmic reticulum. *J Biol Chem* (2014) **289**:24250–62. doi:10.1074/jbc.M114.553644
26. Kleinau G, Haas A-KK, Neumann S, Worth CL, Hoyer I, Furkert J, et al. Signaling-sensitive amino acids surround the allosteric ligand binding

site of the thyrotropin receptor. *FASEB J* (2010) **24**:2347–54. doi:10.1096/fj.09-149146
27. Jiang X, Liu H, Chen X, Chen PH, Fischer D, Sriraman V, et al. Structure of follicle-stimulating hormone in complex with the entire ectodomain of its receptor. *Proc Natl Acad Sci U S A* (2012) **109**:12491–6. doi:10.1073/pnas.1206643109
28. Krause G, Kreuchwig A, Kleinau G. Extended and structurally supported insights into extracellular hormone binding, signal transduction and organization of the thyrotropin receptor. *PLoS One* (2012) **7**:e52920. doi:10.1371/journal.pone.0052920
29. Lapthorn AJ, Harris DC, Littlejohn A, Lustbader JW, Canfield RE, Machin KJ, et al. Crystal structure of human chorionic gonadotropin. *Nature* (1994) **369**:455–61. doi:10.1038/369455a0
30. Zhang Y. Template-based modeling and free modeling by I-TASSER in CASP7. *Proteins* (2007) **69**(Suppl 8):108–17. doi:10.1002/prot.21702
31. Roy A, Kucukural A, Zhang Y. I-TASSER: a unified platform for automated protein structure and function prediction. *Nat Protoc* (2010) **5**:725–38. doi:10.1038/nprot.2010.5
32. Kim DE, Chivian D, Baker D. Protein structure prediction and analysis using the Robetta server. *Nucleic Acids Res* (2004) **32**:W526–31. doi:10.1093/nar/gkh468
33. Roche DB, Buenavista MT, Tetchner SJ, McGuffin LJ. The IntFOLD server: an integrated web resource for protein fold recognition, 3D model quality assessment, intrinsic disorder prediction, domain prediction and ligand binding site prediction. *Nucleic Acids Res* (2011) **39**:W171–6. doi:10.1093/nar/gkr184
34. Källberg M, Margaryan G, Wang S, Ma J, Xu J. RaptorX server: a resource for template-based protein structure modeling. *Methods Mol Biol* (2014) **1137**:17–27. doi:10.1007/978-1-4939-0366-5_2
35. Battey JN, Kopp J, Bordoli L, Read RJ, Clarke ND, Schwede T. Automated server predictions in CASP7. *Proteins* (2007) **69**(Suppl 8):68–82. doi:10.1002/prot.21761
36. Núñez Miguel R, Sanders J, Sanders P, Young S, Clark J, Kabelis K, et al. Similarities and differences in interactions of thyroid stimulating and blocking autoantibodies with the TSH receptor. *J Mol Endocrinol* (2012) **49**:137–51. doi:10.1530/JME-12-0040
37. Costagliola S, Panneels V, Bonomi M, Koch J, Many MC, Smits G, et al. Tyrosine sulfation is required for agonist recognition by glycoprotein hormone receptors. *EMBO J* (2002) **21**:504–13. doi:10.1093/emboj/21.4.504
38. Couch VA, Cheng N, Nambiar K, Fink W. Structural characterization of alpha-helices of implicitly solvated po*ly-alanine*. *J Phys Chem B* (2006) **110**:3410–9. doi:10.1021/jp055209j
39. Ho SC, Van Sande J, Lefort A, Vassart G, Costagliola S. Effects of mutations involving the highly conserved S281HCC motif in the extracellular domain of the thyrotropin (TSH) receptor on TSH binding and constitutive activity. *Endocrinology* (2001) **142**:2760–7. doi:10.1210/endo.142.7.8246
40. Bernard MP, Lin W, Kholodovych V, Moyle WR. Human lutropin (hLH) and choriogonadotropin (CG) are assembled by different pathways: a model of hLH assembly. *J Biol Chem* (2014) **289**:14360–9. doi:10.1074/jbc.M113.535609
41. Kreuchwig A, Kleinau G, Kreuchwig F, Worth CL, Krause G. Research resource: update and extension of a glycoprotein hormone receptors web application. *Mol Endocrinol* (2011) **25**(4):707–12. doi:10.1210/me.2010-0510
42. Majumdar R, Railkar R, Dighe RR, Mujumdar R. Insights into differential modulation of receptor function by hinge region using novel agonistic lutropin receptor and inverse agonistic thyrotropin receptor antibodies. *FEBS Lett* (2012) **586**:810–7. doi:10.1016/j.febslet.2012.01.052

Conflict of Interest Statement: The authors declare that the research was conducted in the absence of any commercial or financial relationships that could be construed as a potential conflict of interest.

frontiers in Endocrinology

MINI REVIEW
published: 13 August 2015
doi: 10.3389/fendo.2015.00127

RXFP1 is targeted by complement C1q tumor necrosis factor-related factor 8 in brain cancer

*Thatchawan Thanasupawat[1], Aleksandra Glogowska[1], Maxwell Burg[1], G. William Wong[2], Cuong Hoang-Vu[3], Sabine Hombach-Klonisch[1,4] and Thomas Klonisch[1,5,6]**

[1] Department of Human Anatomy and Cell Science, Faculty of Health Sciences, College of Medicine, University of Manitoba, Winnipeg, MB, Canada, [2] Department of Physiology, Center for Metabolism and Obesity Research, Johns Hopkins University School of Medicine, Baltimore, MD, USA, [3] Clinics of General, Visceral and Vascular Surgery, Martin Luther University, Halle/Salle, Germany, [4] Department of Obstetrics, Gynecology and Reproductive Medicine, Faculty of Health Sciences, College of Medicine, University of Manitoba, Winnipeg, MB, Canada, [5] Department of Surgery, Faculty of Health Sciences, College of Medicine, University of Manitoba, Winnipeg, MB, Canada, [6] Department of Medical Microbiology and Infectious Diseases, Faculty of Health Sciences, College of Medicine, University of Manitoba, Winnipeg, MB, Canada

OPEN ACCESS

Edited by:
James A. Dias,
University at Albany State University of New York, USA

Reviewed by:
Emma June Petrie,
The Walter and Eliza Hall Institute of Medical Research, Australia
Alexander I. Agoulnik,
Florida International University, USA

***Correspondence:**
Thomas Klonisch,
Faculty of Health Sciences, College of Medicine, University of Manitoba, 130–745 Bannatyne Avenue, Winnipeg, MB R3E 0J9, Canada
thomas.klonisch@umanitoba.ca

Specialty section:
This article was submitted to Molecular and Structural Endocrinology, a section of the journal Frontiers in Endocrinology

Received: 08 June 2015
Accepted: 28 July 2015
Published: 13 August 2015

Citation:
Thanasupawat T, Glogowska A, Burg M, Wong GW, Hoang-Vu C, Hombach-Klonisch S and Klonisch T (2015) RXFP1 is targeted by complement C1q tumor necrosis factor-related factor 8 in brain cancer. Front. Endocrinol. 6:127. doi: 10.3389/fendo.2015.00127

The relaxin-like RXFP1 ligand–receptor system has important functions in tumor growth and tissue invasion. Recently, we have identified the secreted protein, CTRP8, a member of the C1q/tumor necrosis factor-related protein (CTRP) family, as a novel ligand of the relaxin receptor, RXFP1, with functions in brain cancer. Here, we review the role of CTRP members in cancers cells with particular emphasis on CTRP8 in glioblastoma.

Keywords: C1q/TNF-related proteins, RXFP1, CTRP8, cancer, brain tumor

Relaxin-Like Peptides and Cognate Receptors in Cancer: A Brief Overview

Most of the cellular and molecular mechanisms involved in RXFP1-mediated cancer promotion have been established in breast, thyroid, and prostate cancer models. For more detailed reviews on relaxin-like peptides and their cognate receptors, the reader is referred to recent excellent reviews (1–5). Increased expression of relaxin-like peptides has been detected in *breast cancer* (6, 7). Using the ERα-positive human breast cancer cell line MCF-7, the group of Mario Bigazzi showed that highly purified porcine relaxin acted in a dose- and time-dependent manner and promoted proliferation only with short-term exposure at low concentrations. Long-term exposure over up to 7 days reduced proliferation and promoted differentiation of MCF-7 cells as demonstrated with up-regulation of cell surface protein E-cadherin (8, 9). This was accompanied by an increase in inducible NO synthase activity and intracellular NO production (10). In co-culture with myoepithelial cells, relaxin enhanced ultrastructural signs of MCF-7 cell differentiation (11). Exposure to human recombinant RLN2 for 24 h induced S100A4 expression and increased cell migration in ERα-negative MDA-MB-231 triple-negative breast cancer cells, but exposure for more than 3 days downregulated S100A4 levels and reduced cell migration and invasiveness in the same cell model in an RXFP1-dependent manner, leading to reduced tumor xenograft growth *in vivo* (12). In an *in vitro* brain metastasis model, RLN2 promoted the invasion of RXFP1-expressing MCF-7 human breast cancer cells into brain tissue slices (13). These data suggest concentration-, time-, and cell context-dependent actions of relaxin in breast cancer and an essential role for RXFP1 in mediating cell motility and invasion.

Increased expression of RLN2 and RXFP1 was also shown in *thyroid cancer*. RLN2/RXFP1 signaling promotes thyroid cancer motility and invasiveness. RXFP1 mediated the motility-enhancing effect of RLN2 via induction of S100A4 in human thyroid carcinoma cells and

RLN2 enhanced thyroid xenograft angiogenesis (14). RLN2/RXFP1 signaling increased the expression and secretion of the lysosomal proteinases, cathepsin-D and cathepsin-L, resulting in enhanced elastinolytic activity and cell invasion through elastin matrices (15). RXFP1 activation by RLN2 in human thyroid cancer cells increased cell migration and extracellular matrix invasion resulting from enhanced collagenolytic activity through the upregulation of MMP2 and MT1-MMP/MMP14 and the increased secretion of MMP2 (16).

In *prostate cancer*, RLN2/RXFP1 signaling increased cell migration and proliferation in androgen-receptor (AR)-dependent LNCaP and AR-independent PC3 prostate cancer cells (17) and promoted growth in xenografts derived of androgen-independent PC3 prostate cancer cells (18). The siRNA-mediated knockdown of RXFP1 prevented the RLN2-induced increase in prostate cancer cell proliferation and invasiveness and induced apoptosis (19). Injection of siRNA-loaded biodegradable nanoparticles into xenografts of AR-positive LNCaP cells and AR-negative PC3 cells downregulated RXFP1 and resulted in a significant reduction in tumor proliferation and metastasis, implicating RXFP1 as an important growth and survival factor in prostate cancer (20). RXFP1-dependent and RLN2-induced proliferation of prostate carcinoma cells was mediated via a PI3K/Akt signaling pathway. Simultaneous blocking of protein kinase A (PKA) and NF-κB signaling almost completely abolished RLN2-mediated proliferation and colony formation in LNCaP cells (21). The extracellular N-terminal low density lipoprotein A (LDL-A) module of RXFP1 was shown to reduce S100A4, S100P, IGFBP2, and MUC1 expression and inhibit RXFP1-mediated proliferation and invasion of PC3 prostate cancer cells. Similar to RXFP1 knockdown in PC3 cells, LDL-A expression reduced $pAKT^{T308}$ and decreased cell proliferation and colony formation, suggesting LDL-A to block activation of endogenous RXFP1 in PC3 cells (22).

The established role of RXFP1 in cancer and other diseases has prompted attempts to identify specific agonists and antagonists of RXFP1. A recent large high-throughput screen of small molecule libraries yielded RXFP1 agonists (23, 24). The challenging search for RXFP1 antagonists has so far produced few promising candidates. The conversion of the two arginine residues (B13, B17) to lysines (ΔH2) within the receptor binding domain of the B-chain of human RLN2 ("GRELVR") was shown to reduce bioactivity and cAMP production in RXFP1-positive myelo-monocytic THP1 cells and RXFP1 expressing HEK293 cells. This ΔH2 mutant was able to bind to RXFP1 and function as a partial antagonist to functional RLN2 in an *in vivo* xenograft model of prostate cancer (25). In MCF-7 cancer cells and renal myofibroblasts endogenously expressing relaxin, the ΔH2 analog blocked RXFP1 activation and significantly inhibited RLN2-induced MCF-7 cell migration (26). When a chemically synthesized ΔH2 antagonist, named AT-001, was used alone or in combination with the anti-mitotic taxane drug docetaxel, xenografts derived from PC3 androgen-independent prostate cancer cells were reported to show a dramatic 60 and 90% reduction in growth, respectively (18). Although these are promising results, the vulnerability of peptide antagonists to proteolytic attack, size restrictions limiting their tissue penetration, and the difficulty in chemically synthesizing large amounts of ΔH2 derivatives remains challenge. Our recent discovery of a novel RXFP1 ligand that is structurally distinct from relaxin-like peptides may provide new opportunities for developing RXFP1 antagonists. We identified C1q/tumor necrosis factor-related protein (CTRP) family member CTRP8 as a novel RXFP1 ligand. Importantly, a small competitor peptide derived from the closely related C1q/tumor necrosis factor-related factor 6 (CTRP6) was able to disrupt the CTRP8-induced and RXFP1-dependent migration of human glioma cells (27). This suggests a novel and as yet poorly understood regulatory network in which C1q/tumor necrosis factor-related factors, depending on the presence of resident secreting cells, can modulate RXFP1 functions in a tissue-dependent and tumor-specific manner.

Tissue Distribution and Structure of CTRP Family Members

The family of complement C1q/tumor necrosis factor-related proteins is composed of adiponectin and 16 CTRP members (CTRP1-9, 9B, 10−15). All CTRPs are secreted proteins that get assembled into trimers and higher-order oligomers. In co-expression systems, CTRPs can also form heteromeric complexes (28–30). The C-terminal globular domain of CTRPs shares close similarity with the 3D structure of the complement component C1q and the tumor necrosis factor (TNF) homology domain present in members of the TNF family (31–33). Unlike adiponectin, which is produced at high level and almost exclusively by adipocytes, many CTRP members have broad expression profiles. CTRP members were shown to be expressed in various tissues and cell types (28, 34–45). Of particular interest for this review is CTRP8 detected by PCR in the testis and lung (29).

The structure of CTRPs is highly conserved during vertebrate evolution as determined by sequence comparison of orthologous CTRPs from zebrafish, frog, mouse, and human genomes (46). All CTRPs share a common protein structure with adiponectin, with CTRP9 showing the highest homology (54%) in the globular C1q domain to adiponectin (30). *Ctrp8* and *Ctrp9B* are both pseudogenes in the mouse genome (29). The structure of CTRPs consists of four distinct domains (**Figure 1A**). The *N-terminal signal peptide* facilitates protein secretion and is followed by a *short variable region*. The variable region contains one or more conserved cysteine (Cys) residues, which create disulfide bonds to facilitate higher-order multimeric protein assembly and/or secretion (28, 30, 46–49). Next, a *collagen-like domain* contains a variable number of Gly-X–Y (where X and Y indicate any amino acid; often Y is a proline or hydroxyproline) repeats, which are essential for the formation of a left-handed coiled coil structure composed of three collagen-like chains. This collagen triple helix acts as a stabilizing stalk for the formation of CTRP trimers (**Figure 1B**) (32). Located at the C-terminus of each collagen-like domain is a *jelly-roll* β*-sandwich folded globular domain* with 3D structural homology to complement component C1q and the tumor necrosis factor ligand family, hence the name CTRP (28, 45, 46, 50). Connected by the collagenous stalk, three such C1q-like protomers form the globular head typical for CTRP members. The collagen domain not only facilitates trimer formation but also contributes to multimerization of CTRPs into bouquet-like quaternary structures (**Figure 1C**) (32, 51). CTRP4 is unique among the secreted members of the C1qTNF family as it lacks

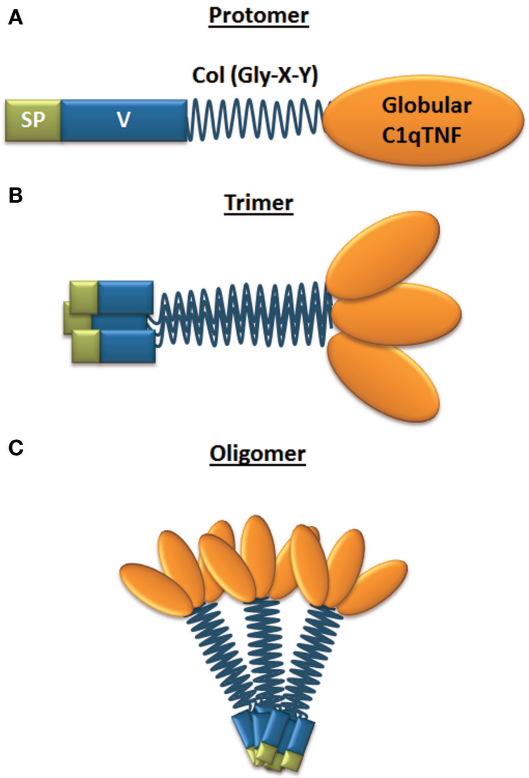

FIGURE 1 | Structure of CTRP family members. (A) Domain structure of a single CTRP protomer, which is composed of a signal peptide (SP), variable region (V), collagen domain (Col – Gly-X-Y), and globular C1q/TNF domain; **(B)** CTRP are secreted and can form homotrimers; **(C)** trimers can form higher-order multimeric 3D structures composed of multiple trimers.

the collagen domain but, instead, contains two tandem globular C1q domains connected by a short non-conserved 18 amino acid linker. CTRP4 protein is encoded by a single exon and its globular C1q domain shows highest homology (44%) to the CTRP member C1qDC1/Caprin-2 (52). The crystal structure of CTRP5 identified residues Y_{152}, F_{230}, and V_{232} within the globular domain as important contributors to the trimer formation and these residues are highly conserved among C1q family proteins (29, 33, 51). Exceptions are CTRP1^{Y230} and CTRP6^{H230} and CTRP8^{H230} where the phenylalanine residue F_{230} of CTRP5 is replaced by less hydrophobic His (H) or Tyr (Y) residues, suggesting potential differences in trimerization and complex stability (51). This finding is intriguing for three reasons: (i) phylogenetic analysis of currently known C1q globular domains of C1q-like family members identified a close relationship of CTRP members 1, 6, and 8 (33, 53); (ii) CTRP1 and CTRP8 share an identical peptide sequence identified as a binding motif for the relaxin receptor RXFP1 (54, 55), and (iii) we described CTRP8 as a novel ligand of RXFP1 (27).

CTRPs are subjected to posttranslational modifications. This includes *N*-linked glycan modifications for CTRP1, CTRP2, CTRP6, CTRP12, and CTRP15, whereas CTRP3, CTRP5, CTRP9, CTRP10, CTRP11, and CTRP13 contain other carbohydrate moieties (28, 30, 46–48, 50, 53, 56, 57). However, N-glycanase-sensitive glycosylation was not detected for CTRP8 (29). Also, bacterially produced (non-glycosylated) recombinant proteins, CTRP1, CTRP6, and CTRP8, retain bioactivity, suggesting that posttranslational glycan modifications are not required for some of their biological effects. Adiponectin, CTRP2, CTRP3, CTRP4, CTRP7, CTRP9, CTRP10 contain Ca^{2+} binding sites, whereas CTRP1, CTRP5, CTRP6, and CTRP8 lack a Ca^{2+}-binding element (32, 49, 51). Ca^{2+} ions were reported to promote stable trimer formation and oligomerization of adiponectin (58, 59).

CTRP Members in Cancer

Research on the role of C1q-TNF-related proteins in cancer is an emerging field and so far CTRP3, CTRP4, and CTRP6 have been associated with tumor-promoting effects. Secreted *CTRP3/cartducin* plays a role in cartilage development. Elevated protein expression of CTRP3/cartducin in mouse osteosarcoma cell lines was shown to promote cell proliferation in a dose-dependent manner. The MAPK/ERK kinase 1/2 (MEK1/2) inhibitor, U0126, prevented the mitogenic effect indicating that CTRP3 induces cell proliferation via ERK1/2-signaling (60). CTRP3 was also shown to induce migration of mouse endothelial cells in an ERK1/2-dependent manner (39) suggesting a role in angiogenesis. The receptor mediating the effects of CTRP3/cartducin is unknown. HeLa and HEK293 cells were used to show that *CTRP4* functions as tumor-promoting inflammatory regulator. CTRP4 overexpression increased NFκB activation in a dose-dependent manner and induced transcriptional activity of the NFκB target TNF-α. In human HepG2 hepatocarcinoma cells, secreted CTRP4 and recombinant CTRP4 caused enhanced STAT3^{Tyr705} phosphorylation and increased IL6 and TNF-α secretion dose-dependently with a maximal stimulation at 4 ng/ml. Interestingly, increased expression of CTRP4 upon IL-6 exposure indicated a positive feedback regulation in cancer cells (61). Immunoreactive *CTRP6* was detected in human hepatocellular carcinoma tissue specimens and was localized to hepatocellular carcinoma cells and to endothelial cells within the tumor. Recombinant CTRP6 increased Akt phosphorylation in isolated liver endothelial cells and this signaling was mediated via the C-terminal C1q domain of CTRP6. Indeed, HepG2 xenografts with exogenous expression of CTRP6 showed increased tumor angiogenesis and reduced necrosis (62).

CTRP8 is a Novel RXFP1 Ligand in Glioblastoma

CTRP8 is evolutionarily highly conserved and secreted as a homotrimer or heterotrimer with the C1qTNF family member C1q-related factor (CRF) (63); the latter also forms heterotrimers with CTRP1, CTRP9, and CTRP10 when co-expressed in cells (29). Until recently, CTRP8 was the least understood C1q-TNF-related protein member, in part, because Ctrp8 is a pseudogene in mice and PCR analysis revealed restricted expression of CTRP8 in human lung and testis (29). We recently identified CTRP8 as a novel ligand for RXFP1 in human

glioblastoma cells (27). Human patient-derived glioblastoma (GB) cells and established GB cell lines express RXFP1, but lack the classical RXFP1 ligands, RLN1 and RLN2. We demonstrated the expression and secretion of CTRP8 in patient GB cells and discovered that RXFP1 serves as a novel receptor for CTRP8 in GB. CTRP8 and RLN2, as well as two biologically active peptides homologous to a peptide sequence within the N-terminal region of the C1q globular domain of human CTRP8, P59, and P74 (54, 55), activated RXFP1 by inducing cAMP signaling and PI3K–PKCζ/PKCδ–ERK1/2 signaling in GB cells. The RXFP1-negative U251 GB cell line and HEK293 cells devoid of RXFP1 with exogenous expression of the related receptor RXFP2 did not respond with increased cAMP levels demonstrating a specific RXFP1-mediated signaling. Furthermore, the increased cell motility by CTRP8, P59, and P74 showed a dose–response and was critically dependent on RXFP1. RXFP1 activation by CTRP8, P59, and P74 increased cathepsin-B protein production and secretion, which mediated the RXFP1-induced enhanced GB cell invasiveness through laminin matrices. Specific inhibitors for PKCζ, PKCδ, PI3K, and cathepsin-B and RNAi-mediated RXFP1 knockdown abolished GB invasiveness. We demonstrated the interaction between RXFP1 and CTRP8 by co-immunoprecipitation of epitope-tagged HA-RXFP1 and CTRP8-His in HEK293 cells. Our structural simulation studies predicted that the amino acid sequence "YAAFSVG" present in the P59 and P74 peptides and located within the N-terminal C1q globular domain of CTRP8 were likely interacting with the leucine-rich repeats (LRR) 7 and 8 of RXFP1 (27). We dismissed the possibility of the formation of CTRP8/CRF heterotrimers because GB cells were devoid of the CTRP8 hetero-oligomerization partner CRF (29). Importantly, competitive binding assays demonstrated that a small peptide derived from the N-terminal region of the globular C1q domain of human CTRP6 successfully blocked the PI3K–PKCζ/PKCδ-mediated increase in cathepsin B secretion and cell motility (27).

Summary and Prospective Goals

The discovery of CTRP8 as RXFP1 agonist in brain cancer is novel for a number of reasons: (i) RXFP1 is the first receptor to be identified for any of the CTRP members; (ii) CTRP8 is the first RXFP1 ligand, which is not structurally related to the relaxin-like family; (iii) the CTRP8–RXFP1 ligand–receptor system is a novel player in brain tumor; (iv) our discovery of a competitor peptide resembling a linear peptide sequence at the transition from the collagen- to the C1q globular domain of CTRP6, a close relative of CTRP8, provides first intriguing evidence for a regulatory network of CTRP factors modulating RXFP1 functions in a tissue-specific context. These findings are the exciting start of an emerging field in CTRP and RXFP1 research with the potential to link metabolic and immunological functions of CTRP members with molecular mechanisms in cancer (45). Future cancer research activities will elucidate the molecular signaling mechanisms and functional relevance of CTRP-derived RXFP1 regulation in a variety of tumors. The use of CTRP-based peptides capable of blocking CTRP8-mediated actions is currently tested for potential clinical applications.

Acknowledgments

Due to space limitations, the authors apologize for not acknowledging all important contributions in the CTRP and relaxin/RXFP1 fields. TK and SH-K are grateful to the Cancer Research Society (CRS), the Natural Sciences and Engineering Research Council of Canada (NSERC), and the Department of Surgery for their generous research support. CH-V and TK are grateful to the German Research Council (DFG, HO 1813/9-4) for funding. GW was supported by a grant from the National Institute of Health (DK084171). The authors thank Dr. Dennis R. Stewart and Corthera Inc. for providing recombinant human relaxin.

References

1. Silvertown JD, Summerlee AJ, Klonisch T. Relaxin-like peptides in cancer. *Int J Cancer* (2003) **107**:513–9. doi:10.1002/ijc.11424
2. Klonisch T, Bialek J, Radestock Y, Hoang-Vu C, Hombach-Klonisch S. Relaxin-like ligand-receptor systems are autocrine/paracrine effectors in tumor cells and modulate cancer progression and tissue invasiveness. *Adv Exp Med Biol* (2007) **612**:104–18. doi:10.1007/978-0-387-74672-2_8
3. Halls ML, Cooper DM. Sub-picomolar relaxin signalling by a pre-assembled RXFP1, AKAP79, AC2, beta-arrestin 2, PDE4D3 complex. *EMBO J* (2010) **29**:2772–87. doi:10.1038/emboj.2010.168
4. Summers RJ. Themed section: molecular pharmacology of GPCRs. *Br J Pharmacol* (2012) **165**:1609–12. doi:10.1111/j.1476-5381.2011.01679.x
5. Halls ML, Bathgate RA, Sutton SW, Dschietzig TB, Summers RJ. International union of basic and clinical pharmacology. XCV. Recent advances in the understanding of the pharmacology and biological roles of relaxin family peptide receptors 1-4, the receptors for relaxin family peptides. *Pharmacol Rev* (2015) **67**:389–440. doi:10.1124/pr.114.009472
6. Tashima LS, Mazoujian G, Bryant-Greenwood GD. Human relaxins in normal, benign and neoplastic breast tissue. *J Mol Endocrinol* (1994) **12**:351–64. doi:10.1677/jme.0.0120351
7. Hombach-Klonisch S, Buchmann J, Sarun S, Fischer B, Klonisch T. Relaxin-like factor (RLF) is differentially expressed in the normal and neoplastic human mammary gland. *Cancer* (2000) **89**:2161–8. doi:10.1002/1097-0142(20001201)89:11<2161::AID-CNCR3>3.0.CO;2-K
8. Bigazzi M, Brandi ML, Bani G, Sacchi TB. Relaxin influences the growth of MCF-7 breast cancer cells. Mitogenic and antimitogenic action depends on peptide concentration. *Cancer* (1992) **70**:639–43. doi:10.1002/1097-0142(19920801)70:3<639::AID-CNCR2820700316>3.0.CO;2-V
9. Sacchi TB, Bani D, Brandi ML, Falchetti A, Bigazzi M. Relaxin influences growth, differentiation and cell-cell adhesion of human breast-cancer cells in culture. *Int J Cancer* (1994) **57**:129–34. doi:10.1002/ijc.2910570123
10. Bani D, Masini E, Bello MG, Bigazzi M, Sacchi TB. Relaxin activates the L-arginine-nitric oxide pathway in human breast cancer cells. *Cancer Res* (1995) **55**:5272–5.
11. Bani D, Riva A, Bigazzi M, Bani Sacchi T. Differentiation of breast cancer cells in vitro is promoted by the concurrent influence of myoepithelial cells and relaxin. *Br J Cancer* (1994) **70**:900–4. doi:10.1038/bjc.1994.417
12. Radestock Y, Hoang-Vu C, Hombach-Klonisch S. Relaxin reduces xenograft tumour growth of human MDA-MB-231 breast cancer cells. *Breast Cancer Res* (2008) **10**:R71. doi:10.1186/bcr2136
13. Binder C, Chuang E, Habla C, Bleckmann A, Schulz M, Bathgate R, et al. Relaxins enhance growth of spontaneous murine breast cancers as well as metastatic colonization of the brain. *Clin Exp Metastasis* (2014) **31**:57–65. doi:10.1007/s10585-013-9609-2
14. Radestock Y, Willing C, Kehlen A, Hoang-Vu C, Hombach-Klonisch S. Relaxin enhances S100A4 and promotes growth of human thyroid carcinoma cell xenografts. *Mol Cancer Res* (2010) **8**:494–506. doi:10.1158/1541-7786.MCR-09-0307
15. Hombach-Klonisch S, Bialek J, Trojanowicz B, Weber E, Holzhausen HJ, Silvertown JD, et al. Relaxin enhances the oncogenic potential of human thyroid carcinoma cells. *Am J Pathol* (2006) **169**:617–32. doi:10.2353/ajpath.2006.050876
16. Bialek J, Kunanuvat U, Hombach-Klonisch S, Spens A, Stetefeld J, Sunley K, et al. Relaxin enhances the collagenolytic activity and in vitro invasiveness by

upregulating matrix metalloproteinases in human thyroid carcinoma cells. *Mol Cancer Res* (2011) **9**:673–87. doi:10.1158/1541-7786.MCR-10-0411
17. Feng S, Agoulnik IU, Li Z, Han HD, Lopez-Berestein G, Sood A, et al. Relaxin/RXFP1 signaling in prostate cancer progression. *Ann N Y Acad Sci* (2009) **1160**:379–80. doi:10.1111/j.1749-6632.2008.03793.x
18. Neschadim A, Pritzker LB, Pritzker KP, Branch DR, Summerlee AJ, Trachtenberg J, et al. Relaxin receptor antagonist AT-001 synergizes with docetaxel in androgen-independent prostate xenografts. *Endocr Relat Cancer* (2014) **21**:459–71. doi:10.1530/ERC-14-0088
19. Feng S, Agoulnik IU, Bogatcheva NV, Kamat AA, Kwabi-Addo B, Li R, et al. Relaxin promotes prostate cancer progression. *Clin Cancer Res* (2007) **13**:1695–702. doi:10.1158/1078-0432.CCR-06-2492
20. Feng S, Agoulnik IU, Truong A, Li Z, Creighton CJ, Kaftanovskaya EM, et al. Suppression of relaxin receptor RXFP1 decreases prostate cancer growth and metastasis. *Endocr Relat Cancer* (2010) **17**:1021–33. doi:10.1677/ERC-10-0073
21. Vinall RL, Mahaffey CM, Davis RR, Luo Z, Gandour-Edwards R, Ghosh PM, et al. Dual blockade of PKA and NF-kappaB inhibits H2 relaxin-mediated castrate-resistant growth of prostate cancer sublines and induces apoptosis. *Horm Cancer* (2011) **2**:224–38. doi:10.1007/s12672-011-0076-4
22. Feng S, Agoulnik AI. Expression of LDL-A module of relaxin receptor in prostate cancer cells inhibits tumorigenesis. *Int J Oncol* (2011) **39**:1559–65. doi:10.3892/ijo.2011.1159
23. Chen CZ, Southall N, Xiao J, Marugan JJ, Ferrer M, Hu X, et al. Identification of small-molecule agonists of human relaxin family receptor 1 (RXFP1) by using a homogenous cell-based cAMP assay. *J Biomol Screen* (2013) **18**:670–7. doi:10.1177/1087057112469406
24. Xiao J, Huang Z, Chen CZ, Agoulnik IU, Southall N, Hu X, et al. Identification and optimization of small-molecule agonists of the human relaxin hormone receptor RXFP1. *Nat Commun* (2013) **4**:1953. doi:10.1038/ncomms2953
25. Silvertown JD, Symes JC, Neschadim A, Nonaka T, Kao JC, Summerlee AJ, et al. Analog of H2 relaxin exhibits antagonistic properties and impairs prostate tumor growth. *FASEB J* (2007) **21**:754–65. doi:10.1096/fj.06-6847com
26. Hossain MA, Samuel CS, Binder C, Hewitson TD, Tregear GW, Wade JD, et al. The chemically synthesized human relaxin-2 analog, B-R13/17K H2, is an RXFP1 antagonist. *Amino Acids* (2010) **39**:409–16. doi:10.1007/s00726-009-0454-1
27. Glogowska A, Kunanuvat U, Stetefeld J, Patel TR, Thanasupawat T, Krcek J, et al. C1q-tumour necrosis factor-related protein 8 (CTRP8) is a novel interaction partner of relaxin receptor RXFP1 in human brain cancer cells. *J Pathol* (2013) **231**:466–79. doi:10.1002/path.4257
28. Wong GW, Krawczyk SA, Kitidis-Mitrokostas C, Revett T, Gimeno R, Lodish HF. Molecular, biochemical and functional characterizations of C1q/TNF family members: adipose-tissue-selective expression patterns, regulation by PPAR-gamma agonist, cysteine-mediated oligomerizations, combinatorial associations and metabolic functions. *Biochem J* (2008) **416**:161–77. doi:10.1042/BJ20081240
29. Peterson JM, Wei Z, Wong GW. CTRP8 and CTRP9B are novel proteins that hetero-oligomerize with C1q/TNF family members. *Biochem Biophys Res Commun* (2009) **388**:360–5. doi:10.1016/j.bbrc.2009.08.014
30. Wong GW, Krawczyk SA, Kitidis-Mitrokostas C, Ge G, Spooner E, Hug C, et al. Identification and characterization of CTRP9, a novel secreted glycoprotein, from adipose tissue that reduces serum glucose in mice and forms heterotrimers with adiponectin. *FASEB J* (2009) **23**:241–58. doi:10.1096/fj.08-114991
31. Shapiro L, Scherer PE. The crystal structure of a complement-1q family protein suggests an evolutionary link to tumor necrosis factor. *Curr Biol* (1998) **8**:335–8. doi:10.1016/S0960-9822(98)70133-2
32. Kishore U, Gaboriaud C, Waters P, Shrive AK, Greenhough TJ, Reid KB, et al. C1q and tumor necrosis factor superfamily: modularity and versatility. *Trends Immunol* (2004) **25**:551–61. doi:10.1016/j.it.2004.08.006
33. Ghai R, Waters P, Roumenina LT, Gadjeva M, Kojouharova MS, Reid KB, et al. C1q and its growing family. *Immunobiology* (2007) **212**:253–66. doi:10.1016/j.imbio.2006.11.001
34. Hayward C, Shu X, Cideciyan AV, Lennon A, Barran P, Zareparsi S, et al. Mutation in a short-chain collagen gene, CTRP5, results in extracellular deposit formation in late-onset retinal degeneration: a genetic model for age-related macular degeneration. *Hum Mol Genet* (2003) **12**:2657–67. doi:10.1093/hmg/ddg289
35. Lee YH, Nair S, Rousseau E, Allison DB, Page GP, Tataranni PA, et al. Microarray profiling of isolated abdominal subcutaneous adipocytes from obese vs non-obese Pima Indians: increased expression of inflammation-related genes. *Diabetologia* (2005) **48**:1776–83. doi:10.1007/s00125-005-1867-3
36. Weigert J, Neumeier M, Schaffler A, Fleck M, Scholmerich J, Schutz C, et al. The adiponectin paralog CORS-26 has anti-inflammatory properties and is produced by human monocytic cells. *FEBS Lett* (2005) **579**:5565–70. doi:10.1016/j.febslet.2005.09.022
37. Akiyama H, Furukawa S, Wakisaka S, Maeda T. Cartducin stimulates mesenchymal chondroprogenitor cell proliferation through both extracellular signal-regulated kinase and phosphatidylinositol 3-kinase/Akt pathways. *FEBS J* (2006) **273**:2257–63. doi:10.1111/j.1742-4658.2006.05240.x
38. Maeda T, Jikko A, Abe M, Yokohama-Tamaki T, Akiyama H, Furukawa S, et al. Cartducin, a paralog of Acrp30/adiponectin, is induced during chondrogenic differentiation and promotes proliferation of chondrogenic precursors and chondrocytes. *J Cell Physiol* (2006) **206**:537–44. doi:10.1002/jcp.20493
39. Akiyama H, Furukawa S, Wakisaka S, Maeda T. CTRP3/cartducin promotes proliferation and migration of endothelial cells. *Mol Cell Biochem* (2007) **304**:243–8. doi:10.1007/s11010-007-9506-6
40. Yamada Y, Ichihara S, Kato K, Yoshida T, Yokoi K, Matsuo H, et al. Genetic risk for metabolic syndrome: examination of candidate gene polymorphisms related to lipid metabolism in Japanese people. *J Med Genet* (2008) **45**:22–8. doi:10.1136/jmg.2007.052415
41. Park SY, Choi JH, Ryu HS, Pak YK, Park KS, Lee HK, et al. C1q tumor necrosis factor alpha-related protein isoform 5 is increased in mitochondrial DNA-depleted myocytes and activates AMP-activated protein kinase. *J Biol Chem* (2009) **284**:27780–9. doi:10.1074/jbc.M109.005611
42. Peterson JM, Wei Z, Wong GW. C1q/TNF-related protein-3 (CTRP3), a novel adipokine that regulates hepatic glucose output. *J Biol Chem* (2010) **285**:39691–701. doi:10.1074/jbc.M110.180695
43. Chavali VR, Khan NW, Cukras CA, Bartsch DU, Jablonski MM, Ayyagari R. A CTRP5 gene S163R mutation knock-in mouse model for late-onset retinal degeneration. *Hum Mol Genet* (2011) **20**:2000–14. doi:10.1093/hmg/ddr080
44. Hofmann C, Chen N, Obermeier F, Paul G, Buchler C, Kopp A, et al. C1q/TNF-related protein-3 (CTRP-3) is secreted by visceral adipose tissue and exerts antiinflammatory and antifibrotic effects in primary human colonic fibroblasts. *Inflamm Bowel Dis* (2011) **17**:2462–71. doi:10.1002/ibd.21647
45. Schaffler A, Buechler C. CTRP family: linking immunity to metabolism. *Trends Endocrinol Metab* (2012) **23**:194–204. doi:10.1016/j.tem.2011.12.003
46. Seldin MM, Tan SY, Wong GW. Metabolic function of the CTRP family of hormones. *Rev Endocr Metab Disord* (2014) **15**:111–23. doi:10.1007/s11154-013-9255-7
47. Wei Z, Lei X, Seldin MM, Wong GW. Endopeptidase cleavage generates a functionally distinct isoform of C1q/tumor necrosis factor-related protein-12 (CTRP12) with an altered oligomeric state and signaling specificity. *J Biol Chem* (2012) **287**:35804–14. doi:10.1074/jbc.M112.365965
48. Wei Z, Seldin MM, Natarajan N, Djemal DC, Peterson JM, Wong GW. C1q/tumor necrosis factor-related protein 11 (CTRP11), a novel adipose stroma-derived regulator of adipogenesis. *J Biol Chem* (2013) **288**:10214–29. doi:10.1074/jbc.M113.458711
49. Tu X, Palczewski K. The macular degeneration-linked C1QTNF5 (S163) mutation causes higher-order structural rearrangements. *J Struct Biol* (2014) **186**:86–94. doi:10.1016/j.jsb.2014.02.001
50. Wong GW, Wang J, Hug C, Tsao TS, Lodish HF. A family of Acrp30/adiponectin structural and functional paralogs. *Proc Natl Acad Sci U S A* (2004) **101**:10302–7. doi:10.1073/pnas.0403760101
51. Tu X, Palczewski K. Crystal structure of the globular domain of C1QTNF5: implications for late-onset retinal macular degeneration. *J Struct Biol* (2012) **180**:439–46. doi:10.1016/j.jsb.2012.07.011
52. Byerly MS, Petersen PS, Ramamurthy S, Seldin MM, Lei X, Provost E, et al. C1q/TNF-related protein 4 (CTRP4) is a unique secreted protein with two tandem C1q domains that functions in the hypothalamus to modulate food intake and body weight. *J Biol Chem* (2014) **289**:4055–69. doi:10.1074/jbc.M113.506956
53. Innamorati G, Bianchi E, Whang MI. An intracellular role for the C1q-globular domain. *Cell Signal* (2006) **18**:761–70. doi:10.1016/j.cellsig.2005.11.004
54. Shemesh R, Toporik A, Levine Z, Hecht I, Rotman G, Wool A, et al. Discovery and validation of novel peptide agonists for G-protein-coupled receptors. *J Biol Chem* (2008) **283**:34643–9. doi:10.1074/jbc.M805181200
55. Shemesh R, Hermesh C, Toporik A, Levine Z, Novik A, Wool A, et al. Activation of relaxin-related receptors by short, linear peptides derived from a

collagen-containing precursor. *Ann N Y Acad Sci* (2009) **1160**:78–86. doi:10.1111/j.1749-6632.2009.03827.x

56. Wei Z, Peterson JM, Wong GW. Metabolic regulation by C1q/TNF-related protein-13 (CTRP13): activation OF AMP-activated protein kinase and suppression of fatty acid-induced JNK signaling. *J Biol Chem* (2011) **286**:15652–65. doi:10.1074/jbc.M110.201087
57. Seldin MM, Peterson JM, Byerly MS, Wei Z, Wong GW. Myonectin (CTRP15), a novel myokine that links skeletal muscle to systemic lipid homeostasis. *J Biol Chem* (2012) **287**:11968–80. doi:10.1074/jbc.M111.336834
58. Banga A, Bodles AM, Rasouli N, Ranganathan G, Kern PA, Owens RJ. Calcium is involved in formation of high molecular weight adiponectin. *Metab Syndr Relat Disord* (2008) **6**:103–11. doi:10.1089/met.2007.0033
59. Min X, Lemon B, Tang J, Liu Q, Zhang R, Walker N, et al. Crystal structure of a single-chain trimer of human adiponectin globular domain. *FEBS Lett* (2012) **586**:912–7. doi:10.1016/j.febslet.2012.02.024
60. Akiyama H, Furukawa S, Wakisaka S, Maeda T. Elevated expression of CTRP3/cartducin contributes to promotion of osteosarcoma cell proliferation. *Oncol Rep* (2009) **21**:1477–81. doi:10.3892/or_00000377
61. Li Q, Wang L, Tan W, Peng Z, Luo Y, Zhang Y, et al. Identification of C1qTNF-related protein 4 as a potential cytokine that stimulates the STAT3 and NF-kappaB pathways and promotes cell survival in human cancer cells. *Cancer Lett* (2011) **308**:203–14. doi:10.1016/j.canlet.2011.05.005
62. Takeuchi T, Adachi Y, Nagayama T. Expression of a secretory protein C1qTNF6, a C1qTNF family member, in hepatocellular carcinoma. *Anal Cell Pathol (Amst)* (2011) **34**:113–21. doi:10.3233/ACP-2011-009
63. Berube NG, Swanson XH, Bertram MJ, Kittle JD, Didenko V, Baskin DS, et al. Cloning and characterization of CRF, a novel C1q-related factor, expressed in areas of the brain involved in motor function. *Brain Res Mol Brain Res* (1999) **63**:233–40. doi:10.1016/S0169-328X(98)00278-2

Conflict of Interest Statement: The authors declare that the research was conducted in the absence of any commercial or financial relationships that could be construed as a potential conflict of interest.

frontiers in Endocrinology

REVIEW
published: 25 August 2015
doi: 10.3389/fendo.2015.00131

LGR4 and its role in intestinal protection and energy metabolism

Ziru Li[1], *Weizhen Zhang*[1,2]* *and Michael W. Mulholland*[1]*

[1] Department of Surgery, University of Michigan Medical Center, Ann Arbor, MI, USA, [2] Department of Physiology and Pathophysiology, Peking University Health Science Center, Beijing, China

Leucine-rich repeat-containing G protein-coupled receptors were identified by the unique nature of their long leucine-rich repeat extracellular domains. Distinct from classical G protein-coupled receptors which act via G proteins, LGR4 functions mainly through Wnt/β-catenin signaling to regulate cell proliferation, differentiation, and adult stem cell homeostasis. LGR4 is widely expressed in tissues ranging from the reproductive system, urinary system, sensory organs, digestive system, and the central nervous system, indicating LGR4 may have multiple functions in development. Here, we focus on the digestive system by reviewing its effects on crypt cells differentiation and stem cells maintenance, which are important for cell regeneration after injury. Through effects on Wnt/β-catenin signaling and cell proliferation, LGR4 and its endogenous ligands, R-spondins, are involved in colon tumorigenesis. LGR4 also contributes to regulation of energy metabolism, including food intake, energy expenditure, and lipid metabolism, as well as pancreatic β-cell proliferation and insulin secretion. This review summarizes the identification of LGR4, its endogenous ligand, ligand–receptor binding and intracellular signaling. Physiological functions include intestinal development and energy metabolism. The potential effects of LGR4 and its ligand in the treatment of inflammatory bowel disease, chemoradiotherapy-induced gut damage, colorectal cancer, and diabetes are also discussed.

Keywords: LGR4, R-spondin, digestive system, energy metabolism, diabetes, colon cancer

OPEN ACCESS

Edited by:
Brian J. Arey,
Bristol-Myers Squibb Co., USA

Reviewed by:
Daniel James Scott,
The University of Melbourne, Australia
Ulla Hansen,
Boston University, USA

***Correspondence:**
Weizhen Zhang,
4618B, MSII, 1150 West Medical Center Drive, Ann Arbor, MI 48109, USA; Department of Physiology and Pathophysiology, Peking University Health Science Center, Beijing 100191, China
weizhenz@umich.edu;
Michael W. Mulholland,
1500 East Medical Center Drive, 2101 Taubman Center SPC 5346, Ann Arbor, MI 48109, USA
micham@umich.edu

Specialty section:
This article was submitted to Molecular and Structural Endocrinology, a section of the journal Frontiers in Endocrinology

Received: *01 June 2015*
Accepted: *10 August 2015*
Published: *25 August 2015*

Citation:
Li Z, Zhang W and Mulholland MW (2015) LGR4 and its role in intestinal protection and energy metabolism. Front. Endocrinol. 6:131. doi: 10.3389/fendo.2015.00131

Introduction

Leucine-rich repeat-containing G protein-coupled receptors (LGRs) are a distinct group of highly conserved proteins of the GPCRs family, characterized by a large extracellular domain (ectodomain) that harbors multiple copies of leucine-rich repeats (LRRs) (1). LRRs represent amphipathic sequences with leucine as the predominant hydrophobic residue and are important for protein–protein interaction (2). The packing of similar repeats allows the formation of a specific hydrogen bond network between neighboring repeats to form a unique tertiary structure (3). LRRs are involved in ligand binding (4), connected via a cysteine-rich region to a seven-transmembrane (TM) domain responsible for heterotrimeric G protein activation (5).

LGRs are divided into three subgroups (groups A–C) (1, 6). Group A receptors include FSH receptor (LGR1), LH receptor (LGR2), and TSH receptor (LGR3), which recognize follicle-stimulating hormone (FSH), luteinizing hormone (LH), and thyroid-stimulating hormone (TSH), respectively (7, 8). These receptors contain seven to nine LRRs in their ectodomains and long hinge regions connecting the LRR domains to TM domains. Group C LGRs have similar number of LRRs but contain a low-density lipoprotein receptor class A domain motif at the N terminus and a short

hinge region between the LRR domain and the 7TM domain. Group C LGRs include RXFP receptor 1 (LGR7) and RXFP receptor 2 (LGR8), recognizing relaxin and INSL3 (insulin-like peptide 3), respectively (1, 7, 8). The group B receptors include LGR4, LGR5, and LGR6, which are characterized by a long ectodomain containing 17 LRR repeats (6, 8) flanked by the N-terminal LRRNT region and the C-terminal LRRCT region (8). Group B receptors play crucial roles in embryonic development and are involved in several types of cancer (9). They have also drawn significant attention recently because of their roles in adult stem cells, especially when LGR5 and LGR6 were identified as stem cells markers in multiple adult tissues (10–12).

The ligands of LGR4-6 remained unidentified for a prolonged time. In 2011, the secreted R-spondin proteins (Rspo1-4) were identified as the endogenous ligands for these receptors to regulate cell proliferation, differentiation, and adult stem cell maintenance through the activation of Wnt signaling pathways (13, 14). Details on the binding between R-spondins and LGRs, and the subsequent intracellular signaling pathways are still under investigation. Recent studies have also revealed a relationship between LGR4 and energy metabolism in areas ranging from food intake and obesity to lipid metabolism.

Identification of LGR4

In 1998, based on the knowledge that large G protein-coupled seven-TM receptors for LH, FSH, and TSH contain LRRs which interact with glycoprotein ligands, and the theory that the putative glycoprotein hormone receptor sequences are conserved in *Drosophila* and sea anemone (15, 16), human sequences related to the sea anemone and *Drosophila* glycoprotein hormone receptors (15, 16) were sought using expression sequence tags. Fragments of two new mammalian receptors in the subfamily of leucine-rich repeat-containing G protein-coupled receptors (LGR) were identified. Adding to the three known LGRs, these two new mammalian receptors were named LGR4 and LGR5 (17).

The full-length cDNAs for these novel receptors were isolated using RT-PCR and repeated screening of sub-libraries from rat ovary or human placenta enriched with each receptor cDNA. LGR4 cDNA from rat ovary consists of 3,504 base pairs with a predicted open reading frame (ORF) of 951 amino acids, whereas LGR5 from human placenta has 4,208 base pairs with a 907 amino acids ORF (17). Similar to three known glycoprotein hormone (LH, FSH, and TSH) receptors, LGR4 and LGR5 are characterized by multiple LRR sequences. The ectodomains of LGR4 and LGR5 are composed of 17 LRR motifs, each 22–24 amino acids in length (17). In contrast to the restricted tissue expression pattern of known gonadotropin and TSH receptors, these new receptors were found in multiple tissues (17).

Identification of this expanding family of LGRs promoted studies to identify putative ligands and to unravel the evolutionary origin of proteins in this subfamily of receptors.

Ligands of LGR4

The R-spondin (Rspo) protein family is a group of four secreted proteins (Rspo1-4) that were isolated as strong potentiators of Wnt/β-catenin signaling (18–20). These proteins share 40–60% identity between each other and a similar structure with a cysteine-rich furin-like domain preceding a thrombospondin-like domain (21, 22). Despite their similarity, the four known Rspos serve in different developmental events. Rspo1 regulates sexual development; Rspo2 modulates development of limbs, lungs, and hair follicles; Rspo3 is involved in placenta development; and Rspo4 affects nail development (23).

Beginning in 2011, several groups have demonstrated that R-spondins (Rspo 1-4) are endogenous ligands for LGR4 and LGR5. A fusion gene construct (mRspo1-Fc), encoding the mature form of mouse Rspo1 and the Fc fragment of mouse IgG2a, is biologically active (24). When incubating cells expressing LGR4 or LGR5 with mRspo1-Fc at 4°C (to prevent internalization), a strong signal indicative of binding was observed on the cell surface. Whole-cell competition binding assay showed that recombinant Rspo1-4 could compete with mRspo1-Fc for binding to LGR4 and LGR5 (25). The results of binding analyses indicate that Rspo1-4 can bind to LGR4 and LGR5 with Rspo2 having the highest affinity to both receptors. Using β-catenin-responsive reporter assay (26), cells transfected with LGR4 or LGR5 displayed a dramatic increase in the potencies of Rspo1-4, ranging from 10- to 1,000-fold, on Wnt/β-catenin signaling in the presence of exogenous Wnt3a (25).

Experiments using an unbiased screening strategy have also identified LGR4 and LGR5 as receptors of Rspo proteins (27). Depletion of LGR4 completely abolishes Rspo1 signaling, while overexpression of LGR4 potentiates Rspo1-4 signaling. Rspo1 interacts with the extracellular domain of LGR4 and LGR5 (27). Further, Rspo1 does not induce coupling between LGR4 and heterotrimeric G proteins, suggesting that LGR4 transmits Rspo signaling through a novel undefined mechanism independent of G protein signaling. This likely contributes to the relatively long time taken to deorphanize LGR4. This study further supports the conclusion that Rspo potentiates Wnt/β-catenin signaling through LGR4 and LGR5, which is described in detail in Section "Intracellular Signaling of LGR4."

Binding of R-Spondins to LGR4/5

The extracelluar domain (ECD) of LGR4 exhibits a twisted horseshoe-like structure. Rspo1 adopts a flat and fold architecture and is bound in the concave surface of LGR4 through electrostatic and hydrophobic interactions (28). All the Rspo1-binding residues are conserved in LGR4-6, suggesting that LGR4-6 bind R-spondins through an identical surface. R-spondin proteins have the same structural organization. They have two adjacent furin-like domains (FU1 and FU2) at the amino terminus, and a thrombospondin (TSP) domain close to the carboxyl terminus (29) (**Figure 1**). Sequence similarities of furin-like domains and TSP domain of four Rspo proteins from different species are high, for example, the identities of Rspo1 protein sequences between human and mouse is 94% (from Pubmed Blast), suggesting R-spondin proteins have conserved functions. A fragment containing two furin-like domains of R-spondin is sufficient to activate Wnt signaling, and both furin-like domains are required for the signaling activity of R-spondin (18, 30). In addition to LGR4/5, various membrane proteins have been reported to bind to R-spondin, including Wnt receptors Frizzled (20) and LRP6 (20,

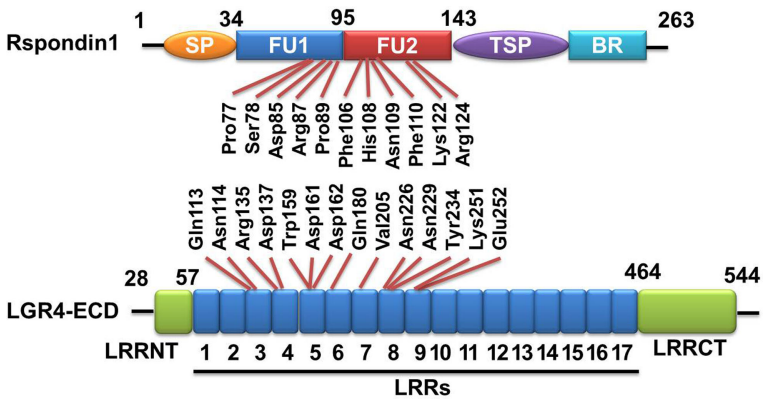

FIGURE 1 | Rspondin1-LGR4 linear sructure illustration. Linear structure of Rspondin1 and LGR4-ECD. Rspondin1 consists of a signal peptide (SP), two adjacent cysteine-rich furin-like domains (FU1/2), a common thrombospondin (TSP-1) motif and a basic amino acid-rich (BR) domain. LGR4 ectodomain (LGR4-ECD) are characterized by 17 leucine-rich repeats (LRRs) flanked by the N-terminal LRRNT region and the C-terminal LRRCT region. The main interacting residues of LGR4-ECD are LRR3-9 [refer to Ref. (4, 5) for detailed information].

31), Kremen (32), Syndecan 4 (33), and membrane E3 ubiquitin ligases ZNRF3/RNF43 (34). For example, Xie et al. reported that mutation of furin-like domain 1 (FU1) (R66A or Q71A) abolished the interaction between Rspo1 and ZNRF3, without affecting the interaction between Rspo1 and LGR4, while mutation of two residues of the furin-like domain 2 (FU2) (F106A or F110A) blocked the interaction between Rspo1 and LGR4, without affecting the interaction between Rspo1 and ZNRF3 (29). These results suggest that Rspo1 binds to ZNRF3 and LGR4 through distinct domains: the FU1 domain is involved in ZNRF3 binding, whereas the FU2 domain is involved in LGR4 binding. In the absence of Rspo, ZNRF3/RNF43 ubiquitinates the FZD receptors for degradation, resulting in low Wnt signaling activity. Rspo1 can bind to both ZNRF3 and LGR4 to induce their dimerization (34). In the R-spondin-LGR4–ZNRF3 complex, LGR4 serves as the engagement receptor to recruit R-spondin to ZNRF3. ZNRF3 serves as the effector receptor. Inhibition of ZNRF3 by R-spondin potentiates Wnt signaling. The R-spondin-LGR4/5–ZNRF3/RNF43 complex represents a fascinating example of a secreted protein regulating receptor turnover by targeting membrane E3 ubiquitin ligases (29) (**Figure 2**).

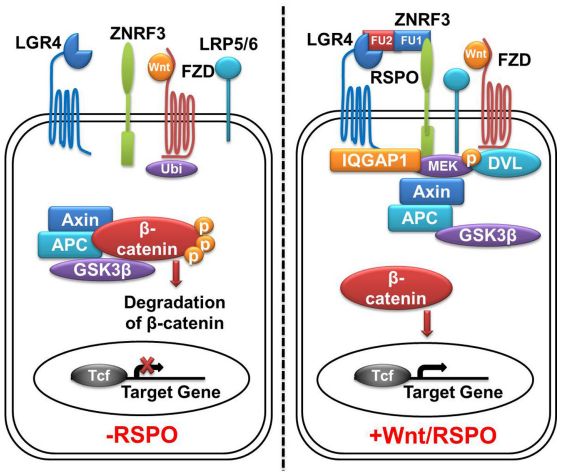

FIGURE 2 | LGR4-Wnt/β-catenin signaling pathway. In the absence of Rspos, membrane E3 ubiquitin ligases ZNRF3/RNF43 ubiquitinates the (Frizzled) FZD receptor for degradation, Wnt signaling activity is blunted. Cytoplasmic β-catenin is degradated by the β-catenin destruction complex, leading to no β-catenin complex formation with T-cell transcription factor (Tcf) and subsequent silence in active transcriptional response. In the presence of Rspos, simultaneous binding of LGR4 and ZNRF3 inhibits the ubiquitination of FZD receptor, meanwhile, LGR4 recruits IQGAP1 and increases its affinity to DVL, leading to the formation of supercomplex with Wnt signalosome. This allows β-catenin accumulation in cytoplasm, followed by translocation into the nucleus and activation of TCF target genes. LGR4, leucine-rich repeat-containing G protein-coupled receptors 4; ZNRF3, zinc and ring finger 3; FZD, Frizzled class receptor; Rspos, R-spondins; LRP5/6, low-density lipoprotein receptor-related protein 5/6; Ubi, ubiquitination; DVL, disheveled.

Intracellular Signaling of LGR4

Studies have suggested that interaction between Rspo proteins and LGR4 potentiates canonical Wnt/β-catenin signaling, but does not activate Gi, Gs, or Gq pathways. Structurally, LGR4 and LGR5 are quite similar to other LRR-containing GPCRs which are coupled to heterotrimeric G protein signaling by ligand binding. The intracellular signaling pathway by which Rspo and LGR4 potentiate Wnt/β-catenin signaling remains largely unknown.

By examining proteins co-immunoprecipitated with LGR4, Kendra et al. identified IQGAP1 and IQGAP3 as potential candidates that could mediate the intracellular signaling of Rspo–LGR4 to the Wnt signalosome (35). Interaction between LGR4 and IQGAP1 occurs between the 7TM domain of LGR4 and the rasGAP-related domain (GRD) of IQGAP1. Stimulation of LGR4 by Rspos increases the affinity of IQGAP1 to disheveled (DVL), leading to the formation of a supercomplex between Rspo–LGR4 and the Wnt signalosome (35). Potentiation of Wnt signaling requires the MEK1/2-binding domain of IQGAP1, which provides the hint that LGR4-bound IQGAP1 brings in MEK1/2 to phosphorylate LRP6. In this configuration, IQGAP1 not only engages MEK1/2 to phosphorylate LRP5/6 but significantly enhance canonical Wnt signaling. IQGAP1 also recruits actin-polymerization complexes through binding to

neural Wiskott–Aldrich syndrome protein (N-WASP) and mDia1 to coordinate actin dynamics (35), which is critical to the control of cell adhesion and migration (36–38). This dual-mechanism model provides an explanation for the pleiotropic functions of Rspo–LGR4 signaling in normal and cancer development, particularly for the crucial role of LGR4 in tubule elongation and branching in multiple organs (**Figure 2**).

Other signaling pathways have also been reported for LGR4. LGR4 (GPR48) participates in the development of the male epididymis and efferent ducts through regulation of ERalpha expression via the cAMP/PKA signaling pathway (39). LGR4 (GPR48) knockout suppressed ATF4, a key transcription factor in erythropoiesis, in midgestation fetal livers through the cAMP–PKA–CREB pathway, suggesting that GPR48 regulates erythropoiesis through ATF4 (40).

LGR4 in Intestinal Development

Expression in Stem Cells

A common feature of the LGR4/5/6 receptors is their expression in distinct types of adult stem cells. LGR5 is a marker for resident stem cells in Wnt-dependent compartments, including the small intestine, colon, stomach, and hair follicles (9). LGR6 serves as a marker of multipotent stem cells in the epidermis (12). LGR4 is widely expressed in proliferating cells (41).

The expression of LGR4 was investigated using an animal model with disrupted LGR4 gene by a trap vector carrying two biological markers, β-geo (a fusion between bacterial β-galactosidase and neomycin phosphotransferase) and a placental alkaline phosphatase (PLAP) (42). Due to the perinatal lethality of homozygosity for this insertion, LacZ and PLAP activity patterns in heterozygous mice were investigated. In embryonic day (E) 14 embryos, LGR4 was strongly labeled in eyes, tongue surface, olfactory epithelium and vomeronasal organ, ribs, esophagus, cartilage condensation of vertebrae, umbilical cord, medulla oblongata, pons, and Rathke's pouch (41). In adults, strong LacZ staining signals were detected in cartilage, kidney, adrenal gland, salivary glands, and testis, while lower intensity was observed in a wide range of organs (41).

LGR4 in Digestive System

At E15 and at birth, LacZ activity was detected in the pseudostratified epithelium and intervillus progenitors, respectively. In adults, epithelial expression of LGR4 was found along the crypts, but not in the villi by using X-gal staining and *in situ* hybridization (41). In the crypts, LGR4 expression was found above the Paneth-cell zone, in the transit-amplifying (TA) cell region, in crypt basal columnar cells, and co-localized with some Paneth cells. Outside the epithelium, LGR4 is expressed in the mesenchyme and smooth-muscle layers, intestinal subepithelial myofibroblasts and enteric neurons. A similar expression pattern was found in the duodenum and colon (41).

Another study has validated the presence of LGR4 immunoreactivity in Paneth cells which were distinguished by large secretory granules in the cytoplasm (43). Similar staining was also noted in crypt stem cells which are sandwiched between Paneth cells (44). No significant staining of LGR4 was found beyond the cells in the crypts. The intense LGR4 positive staining signal observed in Paneth cells and stem cells in the crypt region of mouse intestine were consistent with that of LGR4 mRNA distribution determined using lac-Z alleles (45). In the mouse colon, only diffuse, weak LGR4 immunoreactivity in the cytoplasm was found in all cells from the base to the epithelial surface, with slightly stronger staining at the surface. No distinct staining was found in stem cells located at the crypt base in colon (43).

Intense LGR4 immunoreactivity was also found in the pancreatic islets with no staining in acinar cells. Co-staining of anti-LGR4 and anti-insulin antibody on mouse pancreas sections showed that LGR4 was expressed in all β-cells (43). Moreover, among the three LGR receptors, only LGR4 is expressed in the pancreas based on the analysis of EST data and Northern blotting (46). The intense staining of LGR4 in the islets strongly suggests that LGR4 mediates the effects of its endogenous ligands in the pancreas.

LGR4 in Intestinal Development

Intestinal crypts contain $LGR5^+$ stem cells and their TA daughter cells, as well as terminally differentiated Paneth cells. Cells exiting crypts terminally differentiate into enterocytes, goblet cells, M-cells, Tuft cells, and enteroendocrine cells, and move up the flanks of the villi to undergo apoptosis upon reaching the villus tips (47). Paneth cells escape the crypt–villus flow by migrating to crypt bottoms where they persist for several weeks (48).

Mice homozygous for the gene trap *LacZ* knock-in allele, referred to as "*Lgr4* knockout", displayed a hypomorphic phenotype with intrauterine growth retardation and perinatal lethality. Heterozygous mice with a *LacZ* gene trap knocked in the *Lgr4* locus (42) have also been used. Although the timing of crypt development was normal in *Lgr4*-knockout mice, reduction in the crypt depth and epithelial cell proliferation were obvious from postnatal day (P) 15 (49). Differentiation of absorptive, enteroendocrine, and goblet-cell lineages was not modified significantly. However, defects in Paneth-cell differentiation were observed at all postnatal stages, with reduction in Paneth-cell number at P21 and decreased expression of the terminal differentiation markers P-lyzozyme and cryptdin 4 (49), suggesting a key role for LGR4 in postnatal epithelial cell proliferation and terminal Paneth-cell differentiation.

Ex vivo experiments have demonstrated that LGR4 is required for the maintenance of crypt stem cells. Crypts cultured from P15 wild-type or heterozygous mice differentiated into multi-fingered organoids after 3 days in culture. After generation of hollow spheres containing mainly stem and TA cells (day 0.5–1), structures grown from P15 *Lgr4*-knockout intestine did not increase further in size and became filled with cellular material (days 1.5–2) (49). *Lgr4*-knockout organoids started to disaggregate between days 2 and 3, and died before day 7. The same phenotype was observed in *Lgr4*-knockout progenitors isolated from newborn mice, when fully differentiated Paneth cells are not yet present (49).

LGR4 in Energy Metabolism

The presence of LGR4 in hypothalamic energy homeostatic areas and its co-localization with key energy homeostatic neurons suggests that it may contribute to the regulation of energy

homeostasis. *In situ* hybridization revealed that LGR4 mRNA is highly expressed in the cortex, hippocampus, amygdala, and the hypothalamus (41). In the cortex, LGR4 mRNA is expressed in layers II and III. In the hippocampus, LGR4 is expressed in CA1, CA2, CA3, and the dentate gyrus (DG).The habenular nuclei (Hbs) of the epithalamus also express LGR4. In the amygdala, LGR4 mRNA is expressed with high levels in the medial amygdaloid nucleus, posteroventral nucleus, and basal lateral amygdaloid nucleus (41). In the hypothalamus, LGR4 is expressed in the ventromedial hypothalamus (VMH), the arcuate nucleus (ARC), median eminence (ME), and the ependymocytes lining the third ventricle (50). The ME and ependymocytes have the highest levels of LGR4 expression, followed by VMH and ARC. The expression pattern of LGR4 in the VMH overlaps that of brain-derived neurotrophic factor (BDNF) (51). Double *in situ* hybridization showed that in the ARC, LGR4 is expressed by most neuropeptide Y (NPY) neurons and proopiomelanocortin (POMC) neurons. NPY neurons express higher levels of LGR4 compared with POMC neurons in the ARC. All POMC neurons in the ME express LGR4 at the highest levels. In the VMH, LGR4 is expressed by the majority of BDNF neurons (50).

Rspo1 and Rspo3, ligands of LGR4, are expressed in hypothalamic energy homeostatic areas (50). Their levels were down-regulated by fasting and up-regulated by the satiety factor insulin, indicating that they might be involved in the regulation of energy homeostasis as anorexigenic factors. The inhibition of food intake observed after intracerebroventricular injection of Rspo1 or Rspo3 support this concept (50). Rspo1 is more potent than Rspo3 in inhibiting food intake. Consistent with this observation, Rspo1 binds to LGR4 with an affinity higher than Rspo3 (25).

GPR48 (LGR4) is critical in development, and Gpr48 mutant mice display early neonatal lethality. Wang et al. have established the Gpr48 (LGR4) hypomorphic mutant mice by microinjecting gene trap-mutated Gpr48 ES cells into C57BL/6 blastocysts. The insertion of the trap vector into intron 1 of the Gpr48 gene resulted in approximately 90% knockdown efficiency in the kidney and adrenal gland of adult LGR4 mutant mice. Approximate half of LGR4 mutant newborns died within 28 h after birth, but no further deaths occurred in the following 20 h (52). Studies of the *Lgr4*-knockout mice have revealed a critical role of LGR4 in lipid metabolism. Relative to wild-type mice fed normal chow diet, both male and female *Lgr4* mutant mice exhibited decreased body weight and body fat content, including epididymal white adipose tissue (eWAT) and inguinal WAT (iWAT), whereas brown adipose tissue (BAT) content remained unaltered (53). Consistent with the lean phenotype, *Lgr4* mutant mice showed improved glucose tolerance and reduced fasting total cholesterol levels. When challenged with a high-fat diet (HFD), both male and female *Lgr4* mutant mice showed a resistance to HFD-induced body weight gain, with improved glucose tolerance and insulin sensitivity (53). Higher O_2 consumption, CO_2 production, and body temperature indicated that energy expenditure was elevated in *Lgr4* mutant mice. Compared to the white, large, and unilocular adipocytes comprising WAT in wild-type mice, *Lgr4* mutant mice showed reduced WAT mass with beige color, smaller, and multilocular adipocytes containing increased mitochondrion number. These results indicate an adipocyte phenotype transformation in *Lgr4* mutant mice (52). Consistent with this concept, Ucp1 and other thermogenic genes, including *Pgc-1α*, *Cidea*, *cytochrome c*, *Cpt2*, and *Nrf1*, were significantly increased in eWAT of *Lgr4* mutant mice, and were further enhanced under cold stress or isoprenaline treatment. Beige cell markers CD137 and TMEM26 (54) were also increased in eWAT of *Lgr4* mutant mice after isoprenaline treatment. These results demonstrate that *Lgr4* ablation drives the acquisition of functional brown-like adipocytes in the WAT depots, leading to increased energy expenditure (52).

The association of LGR4 with human obesity has been demonstrated by a case–control study of early-onset obesity in which four SNPs, located in the encoding and flanking regions of the *LGR4* locus, were found to be significantly correlated with body mass index. A low-frequency non-synonymous *LGR4* variant (A750T) was identified more than twice as commonly in obese patients when compared with controls (52). This site in LGRs is highly conserved among different species, and constitutively activated point mutations of the corresponding site in LHR, TSHR, and FSHR have been reported (55–57). The A750T variant showed higher stimulating activity of a CRE-luciferase reporter than wild-type LGR4, suggesting a functional variation. All these observations suggest a contribution of LGR4 to human adiposity.

Another study based on the LGR4 mutant mice described before also indicates a correlation between LGR4 and lipid metabolism (58) in a circadian rhythm-related manner. Resting energy expenditure (RER) is higher in the dark phase than in the light phase in wild type (WT) mice (59), suggesting the existence of a circadian rhythm in substrate utilization for energy during the day, more glucose in the dark phase, and more lipid usage in the light phase. In *Lgr4* mutant mice, the RER was higher than that of their WT littermates during the dark phase with no difference during the light phase (57), suggesting that lack of LGR4 altered the circadian rhythm of lipid metabolism. *Lgr4*-knockout mice consumed less lipids but more sugar compared with WT mice (60, 61). *Lgr4* mutant mice exhibited higher plasma triglyceride levels and lost the rhythmic pattern compared with WT mice. *Lgr4* mutant mice also presented a change in plasma non-esterified fatty acid levels, reflected by lower plasma levels during the light phase and higher levels in the dark phase in comparison with WT mice. Interestingly, loss of LGR4 does not affect clock gene expression in the liver. In WT mice, LGR4 expression in liver was higher during the light phase than the dark phase, presenting a peak at ZT4 and a nadir at ZT16, indicating a circadian rhythm. Lgr4 expression levels in *Lgr4* mutant mice were very low and amplitude was dampened (57). Lack of LGR4 causes an arrhythmic plasma lipid phenotype in mice.

Therapeutics Potential of Rspos-LGR4

Treatment for Inflammatory Bowel Disease

As defective epithelial restitution is an important risk factor for inflammatory bowel disease (IBD), it is not surprising that dysfunction of genes involved in intestinal development, proliferation, and differentiation will increase susceptibility to IBD.

When Lgr4 hypomorphic mice are subjected to the dextran sulfate sodium (DSS)-induced IBD, a more severe colitis developed in *Lgr4* mutant mice than in WT sex-matched littermates. Higher body weight loss, a hallmark of intestinal inflammation, was observed in *Lgr4* mutant mice. This observation was concordant with a more severe anemia (45). Although the small intestine is not the major target of DSS-induced tissue damage (62), the relative length reduction was significantly increased in *Lgr4* mutant mice, indicating critical functions of Lgr4 in the small intestine. Almost all crypts throughout the small intestine were lost in *Lgr4* mutant mice but remained intact in WT littermates. Histological examination showed dramatically increased signs of colitis, which is characterized by the loss of crypts and the infiltration of leukocytes into the colons of *Lgr4* mutant mice (45). Infiltration of neutrophils was significantly higher in the colon of *Lgr4* mutant mice. Additionally, inflammatory cytokines, such as TNFα, IL6, and IL1, were significantly increased in *Lgr4* mutant mice after DSS administration, suggesting a more severe inflammatory response (45). Significant decreases in Ki67-positive proliferating cells were observed in *Lgr4* mutant intestines during tissue regeneration. No significant alteration of apoptosis was observed either in control conditions or in the recovery period, indicating that LGR4 is responsible for epithelial cell proliferation but not apoptosis during DSS-induced tissue regeneration (45).

Human Rspo1 protein effectively increases survival and proliferation of $LGR5^+$ intestinal stem cells *in vitro* through activation of Wnt/β-catenin signaling (63). The mitogenic activity of Rspo1 on intestinal stem cells may be useful in the therapy of IBD because of its stimulating effect on crypt cell growth to accelerate mucosal regeneration. In both acute and chronic phases of colitis in mouse models, administration of Rspo1 protein preserves mucosal integrity in both small and large bowel by stimulating crypt epithelial cell mitosis (64).

Protective Effects of R-Spondin in Chemoradiotherapy-Induced Gut Injury

Stimulation of Wnt/β-catenin signaling with Rspo1 can ameliorate 5-fluorouracil (5-FU) and radiation-induced gut damage, including radiation-induced gastrointestinal syndrome (RIGS) (64–66). Recently, Zhou et al. have found that combination of Slit2 and Rspo1 could potentially protect gut from chemoradiotherapy-induced damage (67). Slit is a secreted protein which functions through the TM protein Roundabout (Robo) receptor as a chemorepellent in axon guidance and neuronal migration, and as an inhibitor in leukocyte chemotaxis (68). The therapeutic dosage of 5-FU (19), a well-characterized chemotherapy agent, markedly shortened villus length, reduced numbers of $LGR5^+$ intestinal stem cells, and $Ki67^+$ transient amplifying cells in jejunum. Using Lgr5–enhanced green fluorescent protein (eGFP)–internal ribosome entry site (IRES)–CreERT2 (Lgr5–GFP) mice to detect the intestine stem cells (10), the lethal dose of 5-FU has been found to abolish >90% of GFP^{high} intestinal stem cells. However, a 3-day treatment of rSlit2 or rRspo1 alone protected 40% of GFP^{high} stem cells. Combination rRspo1 plus rSlit2 preserved 80% of GFP^{high} intestinal stem cells, indicating that Slit2 acts synergistically with Rspo, leading to prolongation of overall survival after exposure to lethal doses of chemotherapy (67).

$Apc^{Min/+}$ mice with spontaneous intestinal adenomas were treated with DSS to induce inflammation-related intestinal carcinogenesis, a murine model of multifactorial human colorectal cancer (CRC) (69). Administration of DSS-treated $Apc^{Min/+}$ mice with rSlit2 or rRspo1 alone led to a 20–30% survival rate upon the lethal dosage of 5-FU. Combination of rSlit2 and rRspo1 led to a 60% survival rate (67), demonstrating functional cooperation between Slit2 and Rspo1. Concomitant prolongations of the villus length, augmentations of $Lgr5^+$ stem cells and $Ki67^+$ transient amplifying cells in the jejunum were observed when animals were treated with a combination of rSlit2 plus rRspo1 (67).

R-Spondin Fusion Protein in the Treatment of Colorectal Cancer

Colorectal cancer is the fourth most prevalent cancer, accounting for over 50,000 deaths per year in the United States. Approximately 15% of CRCs have microsatellite instability arising from defects in the DNA mismatch-repair system, whereas the other 85% of microsatellite-stable CRCs are the result of chromosomal instability (70).

Using RNA-seq data, Seshagiri et al. have identified 36 rearrangements that result in gene fusions (71), including two recurrent ones. The recurrent fusions found in microsatellite-stable samples involve the R-spondin family members, Rspo2 and Rspo3 (70). Both of them were expected to produce functional Rspos protein. The expression of Rspo2 and Rspo3 in colon tumor samples, containing the fusions, was elevated compared with the tumor samples lacking R-spondin fusions (70). Furthermore, all of the Rspo-positive fusion tumors expressed the potential R-spondin receptors LGR4, LGR5, and LGR6. Additionally, alteration of the Rspo2 gene is linked to CRC in a transposon-based genetic screening in mice (72).Consistent with the elevated expression of Rspo genes observed in human tumors, a 20-fold increase in Rspo2 messenger RNA expression in a mouse tumor carrying a transposon insertion near the Rspo2 transcription start site was detected relative to adjacent normal tissue. These observations indicate that the R-spondins may function as drivers in human CRCs (70). Although further studies are required to fully understand the role of R-spondin fusions in CRC development, they represent attractive targets for antibody-based therapy in CRC patients positive for R-spondin fusions. Other therapeutic strategies that target downstream components of the Wnt signaling cascade might be effective against tumors positive for R-spondin fusions.

R-Spondin in the Treatment of Diabetes

The development of type 2 diabetes mellitus (T2DM) usually requires the presence of insulin resistance, impaired β-cell function, and the loss of β-cells (73). Type 1 diabetes mellitus (T1DM) is characterized by autoimmune-mediated destruction of β-cells. Novel therapeutic approaches might include expanding β-cell mass. As reported by Wong et al., Rspo1 enhances insulin mRNA levels after stimulation for 12 h. Rspo1 can also regulate insulin secretion in mouse islets. Static incubation of islets with Rspo1 for 2 h induced a significant increase in insulin secretion in a

TABLE 1 | Roles of LGR4 in intestinal functions and energy metabolism, and summary of the therapeutic potentials of Rspos-LGR4 system.

Roles of LGR4	Physiological functions	Therapeutics potentials
In intestine	1. Postnatal epithelial cell proliferation and terminal Paneth-cell differentiation 2. Maintenance of crypt stem cells	1. Inflammatory bowel disease 2. Chemoradiotherapy-induced gut injury 3. Colorectal cancer
In energy metabolism	1. Inhibition of food intake 2. Acquisition of functional brown-like adipocytes in the WAT depots in *Lgr4*$^{-/-}$ mice 3. Association with human obesity 4. Arrhythmic plasma lipid phenotype in *Lgr4*$^{-/-}$ mice	1. Obesity 2. Diabetes mellitus 3. Lipid metabolism

glucose-independent manner (74). Treatment with recombinant mouse Rspo1 also increases MIN6-cell proliferation. Rspo1 induced an increase in BrdU incorporation in insulin-positive cells (74). When treated MIN6 cells were exposed to a mixture of cytokines for 18 h, the level of activated, cleaved caspase3 was significantly increased. The increase in cleaved caspase 3 was prevented by pretreatment with Wnt3a, as well as by Rspo1. A similar observation was made in dispersed murine β-cells. Treatment with cytokines for 18 h significantly increased the number of TUNEL-positive β-cells; pretreatment with Rspo1 significantly reduced cytokine-induced apoptosis (74). These observations suggest that Rspo1 may be a potential novel molecule for the treatment of patients with T2DM or T1DM.

Conclusion

The importance of LGR4 and its ligands-Rspos in the regulation of canonical and non-canonical Wnt signaling pathways has been established in a variety of *in vitro* and *in vivo* studies using animal models and human genetic analysis. Although significant progress has been made in our understanding of how Rspo binds with LGR4 and regulates the Wnt signaling pathway at the molecular level, the following fundamental questions remain unanswered. How does LGR4 interact with FZD (Wnt receptor) after binding with Rspo proteins? Does LGR4 have a specific intracellular signaling pathway or simply function as a potentiator of Wnt signaling? Additionally, discrepancy between gain and loss of LGR4 function exists. While LGR4-knockout mice showed an improvement in glucose metabolism, Rspo1 has been reported to significantly induce β-cell proliferation and insulin secretion. Further studies on the functions and signaling mechanisms of the LGR4 and Rspo proteins will facilitate the development of therapeutic strategy for human diseases, such as IBD, CRC, and diabetes, by targeting Rspo-LGR4 (**Table 1**).

Author Contributions

ZL, WZ, and MM wrote, discussed, and edited the manuscript.

Acknowledgments

This work was supported by grants from the National Natural Science Foundation of China (81330010, 81390354) and American Diabetes Association grant #1-13-BS-225.

References

1. Luo CW, Hsueh AJ. Genomic analyses of the evolution of LGR genes. *Chang Gung Med J* (2006) **29**:2–8.
2. Kobe B, Deisenhofer J. Crystal structure of porcine ribonuclease inhibitor, a protein with leucine-rich repeats. *Nature* (1993) **366**:751–6. doi:10.1038/366751a0
3. Kajava AV. Structural diversity of leucine-rich repeat proteins. *J Mol Biol* (1998) **277**:519–27. doi:10.1006/jmbi.1998.1643
4. Wang D, Huang B, Zhang S, Yu X, Wu W, Wang X. Structural basis for R-spondin recognition by LGR4/5/6 receptors. *Genes Dev* (2013) **27**:1339–44. doi:10.1101/gad.219360.113
5. Xu K, Xu Y, Rajashankar KR, Robev D, Nikolov DB. Crystal structures of Lgr4 and its complex with R-spondin1. *Structure* (2013) **21**:1683–9. doi:10.1016/j.str.2013.07.001
6. Barker N, Tan S, Clevers H. Lgr proteins in epithelial stem cell biology. *Development* (2013) **140**:2484–94. doi:10.1242/dev.083113
7. Van Loy T, Vandersmissen HP, Van Hiel MB, Poels J, Verlinden H, Badisco L, et al. Comparative genomics of leucine-rich repeats containing G protein-coupled receptors and their ligands. *Gen Comp Endocrinol* (2008) **155**:14–21. doi:10.1016/j.ygcen.2007.06.022
8. Hsu SY, Kudo M, Chen T, Nakabayashi K, Bhalla A, van der Spek PJ, et al. The three subfamilies of leucine-rich repeat-containing G protein-coupled receptors (LGR): identification of LGR6 and LGR7 and the signaling mechanism for LGR7. *Mol Endocrinol* (2000) **14**:1257–71. doi:10.1210/mend.14.8.0510
9. Barker N, Clevers H. Leucine-rich repeat-containing G-protein-coupled receptors as markers of adult stem cells. *Gastroenterology* (2010) **138**:1681–96. doi:10.1053/j.gastro.2010.03.002
10. Barker N, van Es JH, Kuipers J, Kujala P, van den Born M, Cozijnsen M, et al. Identification of stem cells in small intestine and colon by marker gene Lgr5. *Nature* (2007) **449**:1003–7. doi:10.1038/nature06196
11. Jaks V, Barker N, Kasper M, van Es JH, Snippert HJ, Clevers H, et al. Lgr5 marks cycling, yet long-lived, hair follicle stem cells. *Nat Genet* (2008) **40**:1291–9. doi:10.1038/ng.239
12. Snippert HJ, Haegebarth A, Kasper M, Jaks V, van Es JH, Barker N, et al. Lgr6 marks stem cells in the hair follicle that generate all cell lineages of the skin. *Science* (2010) **327**:1385–9. doi:10.1126/science.1184733
13. Clevers H, Nusse R. Wnt/beta-catenin signaling and disease. *Cell* (2012) **149**:1192–205. doi:10.1016/j.cell.2012.05.012
14. Niehrs C. The complex world of WNT receptor signalling. *Nat Rev Mol Cell Biol* (2012) **13**:767–79. doi:10.1038/nrm3470
15. Hauser F, Sondergaard L, Grimmelikhuijzen CJ. Molecular cloning, genomic organization and developmental regulation of a novel receptor from *Drosophila melanogaster* structurally related to gonadotropin-releasing hormone receptors for vertebrates. *Biochem Biophys Res Commun* (1998) **249**:822–8. doi:10.1006/bbrc.1998.9230
16. Nothacker HP, Grimmelikhuijzen CJ. Molecular cloning of a novel, putative G protein-coupled receptor from sea anemones structurally related to members of the FSH, TSH, LH/CG receptor family from mammals. *Biochem Biophys Res Commun* (1993) **197**:1062–9. doi:10.1006/bbrc.1993.2586
17. McDonald T, Wang R, Bailey W, Xie G, Chen F, Caskey CT, et al. Identification and cloning of an orphan G protein-coupled receptor of the glycoprotein hormone receptor subfamily. *Biochem Biophys Res Commun* (1998) **247**:266–70. doi:10.1006/bbrc.1998.8774
18. Kazanskaya O, Glinka A, del Barco Barrantes I, Stannek P, Niehrs C, Wu W. R-spondin2 is a secreted activator of Wnt/beta-catenin signaling and is required for *Xenopus* myogenesis. *Dev Cell* (2004) **7**:525–34. doi:10.1016/j.devcel.2004.07.019
19. Kim KA, Kakitani M, Zhao J, Oshima T, Tang T, Binnerts M, et al. Mitogenic influence of human R-spondin1 on the intestinal epithelium. *Science* (2005) **309**:1256–9. doi:10.1126/science.1112521
20. Nam JS, Turcotte TJ, Smith PF, Choi S, Yoon JK. Mouse cristin/R-spondin family proteins are novel ligands for the frizzled 8 and LRP6 receptors and activate

beta-catenin-dependent gene expression. *J Biol Chem* (2006) **281**:13247–57. doi:10.1074/jbc.M508324200
21. Kim KA, Wagle M, Tran K, Zhan X, Dixon MA, Liu S, et al. R-spondin family members regulate the Wnt pathway by a common mechanism. *Mol Biol Cell* (2008) **19**:2588–96. doi:10.1091/mbc.E08-02-0187
22. Kim KA, Zhao J, Andarmani S, Kakitani M, Oshima T, Binnerts ME, et al. R-spondin proteins: a novel link to beta-catenin activation. *Cell Cycle* (2006) **5**:23–6. doi:10.4161/cc.5.1.2305
23. de Lau WB, Snel B, Clevers HC. The R-spondin protein family. *Genome Biol* (2012) **13**:242. doi:10.1186/gb-2012-13-3-242
24. Ootani A, Li X, Sangiorgi E, Ho QT, Ueno H, Toda S, et al. Sustained in vitro intestinal epithelial culture within a Wnt-dependent stem cell niche. *Nat Med* (2009) **15**:701–6. doi:10.1038/nm.1951
25. Carmon KS, Gong X, Lin Q, Thomas A, Liu Q. R-spondins function as ligands of the orphan receptors LGR4 and LGR5 to regulate Wnt/beta-catenin signaling. *Proc Natl Acad Sci U S A* (2011) **108**:11452–7. doi:10.1073/pnas.1106083108
26. Veeman MT, Slusarski DC, Kaykas A, Louie SH, Moon RT. Zebrafish prickle, a modulator of noncanonical Wnt/Fz signaling, regulates gastrulation movements. *Curr Biol* (2003) **13**:680–5. doi:10.1016/S0960-9822(03)00240-9
27. Ruffner H, Sprunger J, Charlat O, Leighton-Davies J, Grosshans B, Salathe A, et al. R-spondin potentiates Wnt/beta-catenin signaling through orphan receptors LGR4 and LGR5. *PLoS One* (2012) **7**:e40976. doi:10.1371/journal.pone.0040976
28. Xu JG, Huang C, Yang Z, Jin M, Fu P, Zhang N, et al. Crystal structure of LGR4-Rspo1 complex: insights into the divergent mechanisms of ligand recognition by leucine-rich repeat G-protein-coupled receptors (LGRs). *J Biol Chem* (2015) **290**:2455–65. doi:10.1074/jbc.M114.599134
29. Xie Y, Zamponi R, Charlat O, Ramones M, Swalley S, Jiang X, et al. Interaction with both ZNRF3 and LGR4 is required for the signalling activity of R-spondin. *EMBO Rep* (2013) **14**:1120–6. doi:10.1038/embor.2013.167
30. Glinka A, Dolde C, Kirsch N, Huang YL, Kazanskaya O, Ingelfinger D, et al. LGR4 and LGR5 are R-spondin receptors mediating Wnt/beta-catenin and Wnt/PCP signalling. *EMBO Rep* (2011) **12**:1055–61. doi:10.1038/embor.2011.175
31. Wei Q, Yokota C, Semenov MV, Doble B, Woodgett J, He X. R-spondin1 is a high affinity ligand for LRP6 and induces LRP6 phosphorylation and beta-catenin signaling. *J Biol Chem* (2007) **282**:15903–11. doi:10.1074/jbc.M701927200
32. Binnerts ME, Kim KA, Bright JM, Patel SM, Tran K, Zhou M, et al. R-spondin1 regulates Wnt signaling by inhibiting internalization of LRP6. *Proc Natl Acad Sci U S A* (2007) **104**:14700–5. doi:10.1073/pnas.0702305104
33. Ohkawara B, Glinka A, Niehrs C. Rspo3 binds syndecan 4 and induces Wnt/PCP signaling via clathrin-mediated endocytosis to promote morphogenesis. *Dev Cell* (2011) **20**:303–14. doi:10.1016/j.devcel.2011.01.006
34. Hao HX, Xie Y, Zhang Y, Charlat O, Oster E, Avello M, et al. ZNRF3 promotes Wnt receptor turnover in an R-spondin-sensitive manner. *Nature* (2012) **485**:195–200. doi:10.1038/nature11019
35. Carmon KS, Gong X, Yi J, Thomas A, Liu Q. RSPO-LGR4 functions via IQGAP1 to potentiate Wnt signaling. *Proc Natl Acad Sci U S A* (2014) **111**:E1221–9. doi:10.1073/pnas.1323106111
36. Brandt DT, Grosse R. Get to grips: steering local actin dynamics with IQGAPs. *EMBO Rep* (2007) **8**:1019–23. doi:10.1038/sj.embor.7401089
37. Parsons JT, Horwitz AR, Schwartz MA. Cell adhesion: integrating cytoskeletal dynamics and cellular tension. *Nat Rev Mol Cell Biol* (2010) **11**:633–43. doi:10.1038/nrm2957
38. Bensenor LB, Kan HM, Wang N, Wallrabe H, Davidson LA, Cai Y, et al. IQGAP1 regulates cell motility by linking growth factor signaling to actin assembly. *J Cell Sci* (2007) **120**:658–69. doi:10.1242/jcs.03376
39. Li XY, Lu Y, Sun HY, Wang JQ, Yang J, Zhang HJ, et al. G protein-coupled receptor 48 upregulates estrogen receptor alpha expression via cAMP/PKA signaling in the male reproductive tract. *Development* (2010) **137**:151–7. doi:10.1242/dev.040659
40. Song H, Luo J, Luo W, Weng J, Wang Z, Li B, et al. Inactivation of G-protein-coupled receptor 48 (Gpr48/Lgr4) impairs definitive erythropoiesis at midgestation through down-regulation of the ATF4 signaling pathway. *J Biol Chem* (2008) **283**:36687–97. doi:10.1074/jbc.M800721200
41. Van Schoore G, Mendive F, Pochet R, Vassart G. Expression pattern of the orphan receptor LGR4/GPR48 gene in the mouse. *Histochem Cell Biol* (2005) **124**:35–50. doi:10.1007/s00418-005-0002-3
42. Leighton PA, Mitchell KJ, Goodrich LV, Lu X, Pinson K, Scherz P, et al. Defining brain wiring patterns and mechanisms through gene trapping in mice. *Nature* (2001) **410**:174–9. doi:10.1038/35065539
43. Yi J, Xiong W, Gong X, Bellister S, Ellis LM, Liu Q. Analysis of LGR4 receptor distribution in human and mouse tissues. *PLoS One* (2013) **8**:e78144. doi:10.1371/journal.pone.0078144
44. Sato T, van Es JH, Snippert HJ, Stange DE, Vries RG, van den Born M, et al. Paneth cells constitute the niche for Lgr5 stem cells in intestinal crypts. *Nature* (2011) **469**:415–8. doi:10.1038/nature09637
45. Liu S, Qian Y, Li L, Wei G, Guan Y, Pan H, et al. Lgr4 gene deficiency increases susceptibility and severity of dextran sodium sulfate-induced inflammatory bowel disease in mice. *J Biol Chem* (2013) **288**:8794–803. doi:10.1074/jbc.M112.436204
46. Hsu SY, Liang SG, Hsueh AJ. Characterization of two LGR genes homologous to gonadotropin and thyrotropin receptors with extracellular leucine-rich repeats and a G protein-coupled, seven-transmembrane region. *Mol Endocrinol* (1998) **12**:1830–45. doi:10.1210/mend.12.12.0211
47. Clevers H. The intestinal crypt, a prototype stem cell compartment. *Cell* (2013) **154**:274–84. doi:10.1016/j.cell.2013.07.004
48. Bjerknes M, Cheng H. The stem-cell zone of the small intestinal epithelium. I. Evidence from Paneth cells in the adult mouse. *Am J Anat* (1981) **160**:51–63. doi:10.1002/aja.1001600106
49. Mustata RC, Van Loy T, Lefort A, Libert F, Strollo S, Vassart G, et al. Lgr4 is required for Paneth cell differentiation and maintenance of intestinal stem cells ex vivo. *EMBO Rep* (2011) **12**:558–64. doi:10.1038/embor.2011.52
50. Li JY, Chai B, Zhang W, Fritze DM, Zhang C, Mulholland MW. LGR4 and its ligands, R-spondin 1 and R-spondin 3, regulate food intake in the hypothalamus of male rats. *Endocrinology* (2014) **155**:429–40. doi:10.1210/en.2013-1550
51. Larsen MH, Hay-Schmidt A, Ronn LC, Mikkelsen JD. Temporal expression of brain-derived neurotrophic factor (BDNF) mRNA in the rat hippocampus after treatment with selective and mixed monoaminergic antidepressants. *Eur J Pharmacol* (2008) **578**:114–22. doi:10.1016/j.ejphar.2007.08.050
52. Wang J, Li X, Ke Y, Lu Y, Wang F, Fan N, et al. GPR48 increases mineralocorticoid receptor gene expression. *J Am Soc Nephrol* (2012) **23**:281–93. doi:10.1681/ASN.2011040351
53. Wang J, Liu R, Wang F, Hong J, Li X, Chen M, et al. Ablation of LGR4 promotes energy expenditure by driving white-to-brown fat switch. *Nat Cell Biol* (2013) **15**:1455–63. doi:10.1038/ncb2867
54. Wu J, Bostrom P, Sparks LM, Ye L, Choi JH, Giang AH, et al. Beige adipocytes are a distinct type of thermogenic fat cell in mouse and human. *Cell* (2012) **150**:366–76. doi:10.1016/j.cell.2012.05.016
55. Yano K, Saji M, Hidaka A, Moriya N, Okuno A, Kohn LD, et al. A new constitutively activating point mutation in the luteinizing hormone/choriogonadotropin receptor gene in cases of male-limited precocious puberty. *J Clin Endocrinol Metab* (1995) **80**:1162–8. doi:10.1210/jc.80.4.1162
56. Gozu HI, Bircan R, Krohn K, Muller S, Vural S, Gezen C, et al. Similar prevalence of somatic TSH receptor and Gsalpha mutations in toxic thyroid nodules in geographical regions with different iodine supply in Turkey. *Eur J Endocrinol* (2006) **155**:535–45. doi:10.1530/eje.1.02253
57. Achrekar SK, Modi DN, Meherji PK, Patel ZM, Mahale SD. Follicle stimulating hormone receptor gene variants in women with primary and secondary amenorrhea. *J Assist Reprod Genet* (2010) **27**:317–26. doi:10.1007/s10815-010-9404-9
58. Wang F, Zhang X, Wang J, Chen M, Fan N, Ma Q, et al. LGR4 acts as a link between the peripheral circadian clock and lipid metabolism in liver. *J Mol Endocrinol* (2014) **52**:133–43. doi:10.1530/JME-13-0042
59. Tu Y, Thupari JN, Kim EK, Pinn ML, Moran TH, Ronnett GV, et al. C75 alters central and peripheral gene expression to reduce food intake and increase energy expenditure. *Endocrinology* (2005) **146**:486–93. doi:10.1210/en.2004-0976
60. Hems DA, Rath EA, Verrinder TR. Fatty acid synthesis in liver and adipose tissue of normal and genetically obese (ob/ob) mice during the 24-hour cycle. *Biochem J* (1975) **150**:167–73. doi:10.1042/bj1500167
61. Roberts R, Bickerton AS, Fielding BA, Blaak EE, Wagenmakers AJ, Chong MF, et al. Reduced oxidation of dietary fat after a short term high-carbohydrate diet. *Am J Clin Nutr* (2008) **87**:824–31.
62. Elson CO, Sartor RB, Tennyson GS, Riddell RH. Experimental models of inflammatory bowel disease. *Gastroenterology* (1995) **109**:1344–67. doi:10.1016/0016-5085(95)90599-5

63. Sato T, Vries RG, Snippert HJ, van de Wetering M, Barker N, Stange DE, et al. Single Lgr5 stem cells build crypt-villus structures in vitro without a mesenchymal niche. *Nature* (2009) **459**:262–5. doi:10.1038/nature07935
64. Zhao J, de Vera J, Narushima S, Beck EX, Palencia S, Shinkawa P, et al. R-spondin1, a novel intestinotrophic mitogen, ameliorates experimental colitis in mice. *Gastroenterology* (2007) **132**:1331–43. doi:10.1053/j.gastro.2007.02.001
65. Zhao J, Kim KA, De Vera J, Palencia S, Wagle M, Abo A. R-spondin1 protects mice from chemotherapy or radiation-induced oral mucositis through the canonical Wnt/beta-catenin pathway. *Proc Natl Acad Sci U S A* (2009) **106**:2331–6. doi:10.1073/pnas.0805159106
66. Bhanja P, Saha S, Kabarriti R, Liu L, Roy-Chowdhury N, Roy-Chowdhury J, et al. Protective role of R-spondin1, an intestinal stem cell growth factor, against radiation-induced gastrointestinal syndrome in mice. *PLoS One* (2009) **4**:e8014. doi:10.1371/journal.pone.0008014
67. Zhou WJ, Geng ZH, Spence JR, Geng JG. Induction of intestinal stem cells by R-spondin 1 and Slit2 augments chemoradioprotection. *Nature* (2013) **501**:107–11. doi:10.1038/nature12416
68. Wang B, Xiao Y, Ding BB, Zhang N, Yuan X, Gui L, et al. Induction of tumor angiogenesis by Slit-Robo signaling and inhibition of cancer growth by blocking Robo activity. *Cancer Cell* (2003) **4**:19–29. doi:10.1016/S1535-6108(03)00164-8
69. Phutthaphadoong S, Yamada Y, Hirata A, Tomita H, Hara A, Limtrakul P, et al. Chemopreventive effect of fermented brown rice and rice bran (FBRA) on the inflammation-related colorectal carcinogenesis in ApcMin/+ mice. *Oncol Rep* (2010) **23**:53–9. doi:10.3892/or_00000605
70. Seshagiri S, Stawiski EW, Durinck S, Modrusan Z, Storm EE, Conboy CB, et al. Recurrent R-spondin fusions in colon cancer. *Nature* (2012) **488**:660–4. doi:10.1038/nature11282
71. Ozsolak F, Milos PM. RNA sequencing: advances, challenges and opportunities. *Nat Rev Genet* (2011) **12**:87–98. doi:10.1038/nrg2934
72. Starr TK, Allaei R, Silverstein KA, Staggs RA, Sarver AL, Bergemann TL, et al. A transposon-based genetic screen in mice identifies genes altered in colorectal cancer. *Science* (2009) **323**:1747–50. doi:10.1126/science.1163040
73. Butler AE, Janson J, Bonner-Weir S, Ritzel R, Rizza RA, Butler PC. Beta-cell deficit and increased beta-cell apoptosis in humans with type 2 diabetes. *Diabetes* (2003) **52**:102–10. doi:10.2337/diabetes.52.1.102
74. Wong VS, Yeung A, Schultz W, Brubaker PL. R-spondin-1 is a novel beta-cell growth factor and insulin secretagogue. *J Biol Chem* (2010) **285**:21292–302. doi:10.1074/jbc.M110.129874

Conflict of Interest Statement: The authors declare that the research was conducted in the absence of any commercial or financial relationships that could be construed as a potential conflict of interest.

frontiers in Endocrinology

PERSPECTIVE
published: 19 October 2015
doi: 10.3389/fendo.2015.00155

New frontier in glycoprotein hormones and their receptors structure–function

*Mariusz W. Szkudlinski**

Trophogen Inc., Rockville, MD, USA

Last two decades of structure–function studies performed in numerous laboratories provided substantial progress in understanding basic science, physiological, pathophysiological, pharmacological, and comparative aspects of glycoprotein hormones (GPHs) and their cognate receptors. Multiple concepts and models developed based on experimental data in the past stood the test of time and have been, at least in part, confirmed and/or remained compatible with the new structures resolved at the atomic level. Major advances in understanding of the ligand–receptor relationships are heralding the dawn of a new era for GPHs and their receptors, although many basic questions still remain unanswered. This article examines retrospectively several basic science aspects of GPH super-agonists and related "biosuperiors" in a broader context of the advances in the ligand–receptor structure–function relationships and new mechanistic models generated based on the structure elucidation. Due to selective focus of my comments and perspectives in certain parts, the reader is directed to the most relevant publications and reviews in the field for more comprehensive analyses.

Keywords: glycoprotein hormone, glycoprotein hormone receptor, structure–function, protein engineering, charge cluster, super–agonist, biosuperior, biobetter

OPEN ACCESS

Edited by:
James A. Dias, University at Albany State University of New York, USA

Reviewed by:
Emma June Petrie, The Walter and Eliza Hall Institute of Medical Research, Australia
Leigh Stoddart, University of Nottingham, UK

***Correspondence:**
Mariusz W. Szkudlinski, Trophogen Inc., 9714 Medical Center Drive, Rockville, MD, USA
mszkudlinski@trophogen.com

Specialty section:
This article was submitted to Molecular and Structural Endocrinology, a section of the journal Frontiers in Endocrinology

Received: *30 June 2015*
Accepted: *18 September 2015*
Published: *19 October 2015*

Citation:
Szkudlinski MW (2015) New frontier in glycoprotein hormones and their receptors structure–function. Front. Endocrinol. 6:155. doi: 10.3389/fendo.2015.00155

Origins and Evolution of Function

The family of glycoprotein hormones (GPHs) consists of luteinizing hormone (LH), chorionic gonadotropin (CG), follicle-stimulating hormone (FSH), and thyroid-stimulating hormone (TSH), which are heterodimers formed by the non-covalent association of a common alpha (α) and a hormone-specific beta (β) subunit. Structurally, GPHs and their subunit ancestors belong to the cysteine-knot growth factor superfamily and due to relatively high glycosylation are recognized as the most complex protein hormone molecules (1–3). Their cognate GPH receptors (GPHRs) are type A leucine-rich repeat (LRR)-containing G-protein-coupled receptors (LGR) with a large glycoprotein extracellular domain (ECD). Early ancestors of GPHs and their receptors emerged at the origin of metazoan animals (multicellular mitochondrial eukaryotes) (4), although two domains of GPHRs, LRRs and 7-helix transmembrane domain (TMD), have much earlier evolutionary origin and are very well-diversified in extremely large number of functionally unrelated proteins in animals and plants (5). Parallel evolution of GPHs, their subunits, and cognate GPHRs was previously studied and discussed in detail (2, 6, 7). An evolution of the receptor–ligand interface likely progressed through the series of fine-tuning within the concave face of the LRRs and activating configuration within the hinge region located between the LRRs and TMD. Interestingly, as previously proposed (6), numerous early vertebrate GPHRs are functioning at least in part by utilizing their constitutive activity, which is determined in each individual cell by the number of receptors expressed

in its cell membrane. Remarkably, nematode LGRs are constitutively activating only the G_s/cAMP, but not G_q/IP_3 inositol phosphate pathway (8). In addition, comparative analysis of GPHRs signaling may suggest that G_s/cAMP pathway as the only mechanism of the agonist-dependent and -independent receptor activation has evolved into more diversified and complex signaling system (9, 10).

Significant level of inherent constitutive activity is present in various vertebrate GPHRs (11–13), including wild-type (WT) hTSHR. In sharp contrast, human LHRs and FSHRs are activated almost exclusively by their respective ligands and the number of natural or artificial receptor mutations in their respective ECDs causing constitutive activity is very low (14–16). With regard to the TSHR, there is an apparent correlation between a high level of basal constitutive activity and much more relaxed ligand specificity (promiscuity), which is exemplified by the prevalence of hCG-induced subclinical or overt hyperthyroidism in the first trimester of pregnancy (17).

Charge Cluster in the Common α-Subunit

Significant contribution of electrostatic interactions to high affinity receptor binding has been recognized for various ligand–receptor pairs, including different cysteine-knot growth factors and their respective receptors (18). Accordingly, a long-standing postulate held that charge–charge interactions are of major importance in the TSH–TSHR interactions (19). For the entire G-protein-coupled receptor, strong statistical evidence was provided that negatively charged amino acids are enriched in the ECDs, including extracellular loops (ECLs), but positively charged amino acids dominate within the intracellular domains (20). Design and sequential development of human TSH and gonadotropin super-agonists (**Figure 1**) were described previously in details (1, 21, 22). Our early mutagenesis studies, which has been recognized as "the advent of super hormone drugs" (21, 23) focused primarily on the 11–20 region of the human α-subunit. These studies have revealed that a basic charge cluster in this region, which has evolved in vertebrates and disappeared in apes and humans, is an important modulator of hormone–receptor binding and activation. Amino acid substitutions to positively charged lysine (K) or arginine (R) in the 11–20 region individually (T11K/R, Q13K/R, E14K/R, P16K/R, Q20K/R) and in various combinations increased the potency and efficacy of hTSH and hCG (21). Such human analogs remain highly specific for their respective receptors and inactive (up to 1000-fold higher concentration) at the other GPHRs (24). The effect of these substitutions on the *in vitro* bioactivity was highly correlated with their effects on the receptor binding activity. It was repeatedly demonstrated in media and buffers with various salt concentrations, and confirmed by studies in other laboratories (25, 26) as well as by using CHO-TSHR cells with largely depleted pool of the negatively charged cell surface proteoglycans. Notably, mutations to alanine did not alter hormone activity, indicating that only selective substitutions to K or R amino acid residues are causing an enhancement of cAMP and IP_3 production, iodine uptake, proliferation of FRTL-5 cells, thyroxine and progesterone production, respectively (1, 21, 24). All our previous theoretical models of GPH–GPHR interaction derived from super-agonist studies were placing the mutagenized

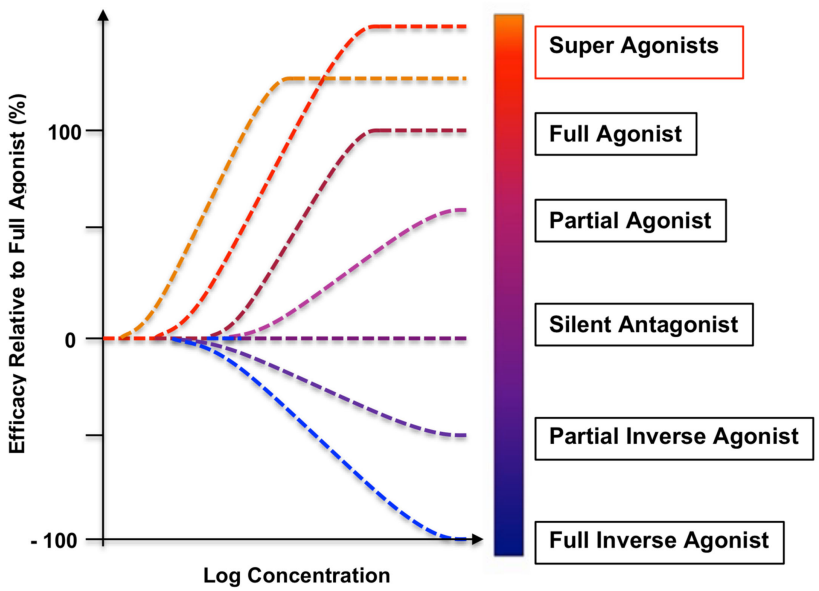

FIGURE 1 | A range of dose–response curves and relative efficacy spectrum of GPHR ligands. The efficacies of the selected classes of ligands are illustrated by the *in vitro* stimulation of cAMP production and comparison with an endogenous, WT agonist (full agonist with 100% intrinsic efficacy). Although the term "super-agonist" has not been yet officially addressed in the NC-IUPHAR nomenclature, super-agonists show higher efficacy than full agonists, variable assay-dependent increases in receptor-binding affinity and potency, differences dependent on the receptor densities, differences related to the degree of signal amplification in the activation cascade, and significant enhancement of clinical efficacy in human and veterinary applications. High affinity super-agonists are especially desirable in various disorders with largely impaired receptor-binding and cell-surface expression (22, 24, 31). Multiple partial agonists of all GPHRs and TSHR-blocking anti-TSHR antibodies (silent or orthosteric antagonists) have been studied (32), but only one human monoclonal anti-TSHR antibody was recognized as an inverse agonist with a significant suppression of the basal constitutive activity of the WT TSHR (33).

α-subunit αL1 and αL3 loops in a close proximity to the hinge region and the ECLs of the receptor TMD (1, 27), very similar to early structural predictions by Jiang et al. (28) and highly compatible with two epitope-mapping studies (29, 30).

Super-agonists of human GPHs, also named as "superactive analogs," have been generated by introduction of positively charged amino acid residues in selected locations of the αL1, αL3, and βL3 beta-hairpin loops (1, 21, 27). Our "signal-enhancing αL1 loop mutations" were described as fully consistent with the model of receptor activation based on the structure of FSH bound to N-terminal cysteine cluster together with the LRRs proposed in 2005 (34). Highly unique position of the α-subunit αL1 13–20 mutations was more recently confirmed by Jiang et al. and the structure of hFSH bound to the entire ECD of hFSHR (35) (**Figure 2**). Moreover, Jiang et al. (36) discovered that such α-subunit αL1 loop amino acid substitutions to K (21) or R (37) are "concentrated near the top right side of the 'activation pocket' generating stronger electrostatic interaction to pull and lift the sulfated-tyrosine 335 (sTyr335) of the FSHR hairpin loop," which is essential in the receptor activation.

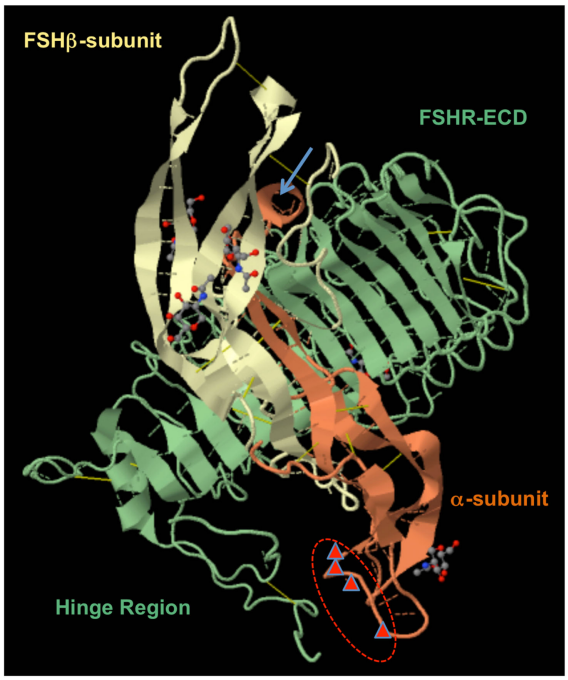

FIGURE 2 | FSH–FSHR/ECD complex (PDB 4AY9) as reported by Jiang et al. (35). The locations of human α-subunit αL1 residues 13, 14, 16, and 20 are marked by red triangles and circled in red. The α-subunit α-helix is seen at the top as a light brown circle and is marked with a blue arrow. LRRs together with the hinge region are forming one large domain interconnected with three disulfide bridges. The recent "two-step model" subdivided this domain into the hormone-binding subdomain (HBSD) and signal-specificity subdomain (SSSD) (36).

GPH Super-Agonists – Tools in Structure–Function Studies

Two step activation mechanism proposed based on FSH–FSHR/ECD complexes (35, 36), and other structure-based models (38, 39) incorporated and explained, at least in part, several our previous findings as described below.

First, the new structure-based model by Jiang et al. (36) is placing much emphasis on the signal-specificity subdomain (SSSD). It explains, at least in part, why positive charge cluster in the αL1 loop, from our studies initiated in 1995, was rescuing (restoring) several major "loss-of-function" mutations including two mutations of K51 in the α-subunit (K51A and K51P) (40), which later have been found to be essential in the formation of salt bridge with highly conserved D153 within the receptor LRRs domain (34) and several others described elsewhere (1, 41) [see also Ref. (3, 38, 42, 43)]. Moreover, largely reduced binding activity and potency of single-chain hCG and its minimized variants were restored using αL1 loop substitutions (α4K and α4R) (25, 26). Remarkably, also the LH activity of the hTSH/hCG "seat-belt" "determinant loop" chimera was further increased by concomitant introduction of a cluster of K residues (α4K) into a highly distant from "seat-belt" αL1 13–20 domain (41). The results of several other published and unpublished studies further reinforced the role of αL1 loop basic charge cluster in the compensatory mechanism functioning within the SSSD.

Second, activation of the TSHR by free or fused homodimeric αL1 α-subunit analogs, but not the WT human α-subunits has been detected in a concentration range only 1–2 log orders higher than that of hTSH-WT (44, 45). Such agonistic activity of α-subunit analogs was observed only in free, non-tethered forms, but not in the yoked subunit-TSHR complexes constrained by the fusion of α-subunit and TSHR. These findings first challenged the most dominant at that time concept that the hormone-induced receptor activation is highly restricted to interactions primarily or exclusively within LRRs. In the light of new structures, the location and configuration of "signal-enhancing substitutions" in the activating complex is important and may not be altered, particularly considering much weaker binding of the free α-subunit analog than the hormone heterodimer. This explanation is also consistent with our data indicating that synthetic linear and cyclic peptides corresponding to the human α-subunit 11–20 residues with α4K substitutions and 10 μM concentrations are not inducing any significant cAMP responses (45).

Third, testing hTSH-WT in comparison to hTSH super-agonist TR1401 with the same α4K substitutions using mutated hTSHR in the hinge region, revealed that non-conservative substitutions E297, E303, and D382 are strongly reducing TR1401 binding and cAMP signaling based on TSHR cell surface expression normalization using FACS analysis (46). Two substitutions to the positively charged K residue (E297K and D382K) led to particularly strong decrease of TR1401 binding and cAMP signaling. Regardless of specific mechanism of electrostatic steering and repulsion involved, and considering well known limitations of simultaneous hormone and receptor mutagenesis (47–49), such studies indicated that the analogs with a limited number of "gain-of activity" substitutions can serve as an excellent tool for probing hormone–receptor interactions. Use of such minimally mutagenized human hTSH analogs (e.g., TR1401 with α4K) together with largely different bovine bTSH-WT (36 amino acid difference) combined with systematic receptor mutagenesis and TSHR

expression normalization allowed to narrow interactions areas within the hinge region and SSSD (49, 50).

Fourth, heterothyrotropic activity of mammalian GPHs can be increased in goldfish by the same α4K substitutions and interactions within the SSSD and hinge region. Such interactions likely evolved long before diversification of LHR and TSHR receptors (51). Co-evolution of early GPHs and their receptors, driven by positive selection within the hormone-binding subdomain (HBSD), related to the need for adaptation of new functions, likely controlled "spillover" of hormone activity to other GPHRs.

Fifth, in addition to supergonists based on selective introduction of positively charged amino acid residues into the αL1 loop, additional substitutions to R or K in the αL3 and βL3 loops led to noticeable increases in the receptor binding both individually and in combination (21, 52–54). The oligomerization of GPHRs was observed in the past, but recent structures provided more convincing evidence for functional relevance of receptors oligomers, dimers, and trimers. An interaction of βL3 loop with three mutations to R (β3R) located in proximity to the FSHR trimer exosite, suggests potential role of such exosites for additional hTSH βL3 loop binding in trimeric receptors (36, 52, 55), which could be affected by the proportion of receptor trimers in different cells and *in vitro* bioassay conditions. Although, the trimeric FSH model does not precisely predicts the extend of cAMP increase due to signal amplification by the adenylate cyclase, it places again the location of both αL1 and αL3 loops near the TMD and predicts that upon dissociation of trimers into monomers both binding and signaling activities of glycosylated WT hFSH should increase threefold. Dual FSHR signaling by monomers and/or by trimers may serve as a part of evolutionarily based protection of reproductive functions, and constitute a possible compensatory mechanism preserving some minimum level of FSH induced signaling in various stress conditions affecting GnRH pulsatile secretion depressing pituitary hFSH production and secretion, observed during chronic malnutrition or starvation (56, 57). hFSHR and likely hLHR signaling by monomers or trimers may also modulate action of elevated endogenous gonadotropins during malignant cell transformation in the menopausal women and their ovarian epithelial and granulosa cells, later associated with the decreased FSHR expression, low receptor number in the cell membrane as well as altered receptor occupancy, trafficking, and biased signaling (58, 59).

Although, activation of GPHRs induces the coupling of different G proteins (60), most of physiological activities are mediated through a $G_{\alpha s}$ protein induced adenyl cyclase catalyzing the conversion of ATP into cAMP (1). However, as suggested by studies on TSHR deletions and others focusing on GPHRs signaling and trafficking, "biased agonism," also referred to as "ligand directed signaling" is likely caused by a spectrum of different ligand–receptor complex conformations in combination with other cell-specific factors (1, 61–63). Recent studies indicated that different GPH glycoforms may have distinct effects on signaling and result in a biased agonism (64). Thus, it is expected that each GPH variant may have different and sometimes completely unique signaling pattern. However, there is also pharmacologically justified possibility that super-agonists are in general less capable of inducing multiple conformations and therefore much less biased (65). Selected super-agonists are known to have an extended receptor-residence time, which in turn may affect GPHR interactions with the cell adapter proteins, endosome signaling, and signal compartmentalization (61, 66–68).

In summary, new investigative strategies including "charge scanning and reversal mutagenesis," "loss-of-function restoration by superagonist," as well as "loss-of-superagonism" with mutated or truncated GPHRs constitute highly valuable tools in the structure-function studies both in the absence and presence of structural information (1, 46, 53, 69). We have first showed directly using large deletions that the ECD suppresses an inherent constitutive activity of the TMD of the human TSHR (14). Such an intrinsic property of the ECD acting on the TMD as a partial inverse agonist was recognized after introduction of the "driver hemagglutinin (HA) tag-sequence" at the N-terminus of the truncated constructs designed to improve and assess cell surface expression (14). We have demonstrated that the presence of such "driver sequence" in the TSHR and other GPHRs constructs with large ECD deletions in the ECD is absolutely necessary for an efficient cell surface expression (1, 14, 70). Similar "driver sequences" were subsequently used to express and normalize expression of various other GPHR constructs with several major ECD deletions, assess their interactions with analogs, and determine their constitutive activities in both cAMP and IP_3 signaling pathways (1, 15, 62). Several newer studies analyzing the role of charged residues in the receptor hinge region attributed an inherent agonistic property to this domain and supported our early concept that the receptor charge clusters adjacent to the TMD are critical in a downstream signal transmission (49, 50, 71).

Development of GPH Biosuperiors and Other Related Molecules

"Biosuperiors" (biobetters or next-generation biological therapeutics) are defined as the second-generation products with substantial advantages over the originator molecules. Biosuperiors have the same receptor target and general mechanism of action as previously approved WT recombinant molecules but include structural changes and/or altered properties that result in an improvement in their clinical profile. GPH biosuperiors can be classified into three main categories: super-agonists, long-acting analogs, and WT molecules with optimized glycosylation, formulation, or delivery.

Long-acting bovine FSH super-agonists with much higher efficacy than all other products in veterinary markets have been developed at Trophogen Inc. and entered clinical trials for superovulation in cows and heifers (72). Human TSH and FSH superagonists for diagnostic and therapeutic applications in the thyroid cancer of follicular origin and the treatment of infertility, including poor responders in the controlled ovarian stimulation (COS), respectively, have entered the late-phases of preclinical development (22, 24, 37, 73). Long-acting analog of WT hFSH (corifollitropin alfa; Elonva^R, Merck) has been approved in Europe for COS. It was constructed by fusion of the carboxy-terminal peptide of the β-subunit of hCG to the β-subunit of

hFSH. Such additional 28 amino acid residues peptide containing 4-5 *O*-linked carbohydrate chains resulted in twofold increase in the FSH plasma half-life. Elonva® substituted for 7 days daily injection of the WT hormone in the standard COS procedure (74–76). Additional post-approval assessments are expected to determine its clinical convenience value and acceptance in the IVF market. Glyco-optimized highly sialylated WT FSH (FSH-GEX™) developed by Glycotope GmbH is based on its production in the human GT-5s cell line providing more optimal glycan structure pattern than standard CHO cell line (77). Similar efforts are now also directed to engineering CHO cells and generation of more homogenous FSH glycosylation, including "human-like" α2,6-terminal sialic acid linkages (78). Recent developments of various GPH biosimilars, improved formulations (79), injection frequency and convenience-focused preparations have not addressed several largely unmet needs for much higher efficacy-based biosuperiors (80, 81).

Clinical utility of thyrostimulin, GPH-related protein found in both vertebrates and invertebrates (82), still awaits full elucidation and rigorous assessment of specificity, selectivity and potential, if any, therapeutic benefits. Small molecules given orally may also lack sufficient specificity, but modified and/or minimized protein variants may provide sufficient balance between specificity, selectivity, half-life and convenience of enteral or topical administration (83). In contrast to large GPHs, there is largely incorrect perception that highly improved affinity of small molecules to GPHRs should result in parallel increase of their specificity. However, the specificity of small molecules is more relative to the degree of non-relevant binding than the strength of their interaction with specific receptor (84). These reservations aside, during the last 10 years, several new advances have been made in the development of GPHR small molecule ligands and allosteric modulators (85–87).

Closing Remarks and Future Perspectives

Glycoprotein hormone–glycoprotein hormone receptor structure–function research is evolving into new highly promising phase, which will likely culminate in elucidation of the entire active and inactive structure(s) of hormone–receptor complexes, including constitutively active receptors, entire receptors bound to super-agonists, antibodies and small molecule ligands. The advent of new optical techniques based on FRET and BRET sensors, as well as single-molecule microscopy, will allow more detailed analysis of real-time receptor activation and direct spatial assessment of signaling in the living cells. Such new optical techniques made already possible detection of TSHR signaling to cAMP after receptor internalization into endosomes (68, 88).

In analogy to human genome sequencing, full benefits of the structure–function achievements may not immediately translate into the new drugs and the third generation of GPH biosuperiors and theranostics. Further progress in the understanding of functional and therapeutic potential of signaling bias, receptor trimerization, trafficking, compartmentalization of signaling as well as detailed elucidation of the mechanism of super-agonists binding and signaling, should move this field to a new very exciting times of personalized drugs with predefined pharmacodynamics (PD), pharmacokinetics (PK), and signaling profiles (89).

Future third-generation recombinant protein biosuperiors will likely have even more advantages related to efficacy, potency and half-life, but also in relation to largely improved stability, formulation, bioavailability, and new methods of administration, eliminating the need for multiple injections (83, 90). New automated single-use sensor-based manufacturing technology platforms of biologics as well as largely improved purification and characterization methods should make a whole development process faster, safer, and more efficient, assuming necessary improvement and streamlining in the regulatory agencies, their flexibility, commitment to a case-by-case considerations and willingness to accept well justified unorthodox development strategies.

It is apparent to many biotechnology experts and market analysts that major biosuperiors, which are largely improved versions of the originator molecules, will be the next big opportunity in the entire field of biologics and GPCR protein ligands (80). It is predicted that biotech and pharma companies, well known for innovation and experience with the first-generation recombinant proteins and biosimilars, will be the best positioned to achieve early success with biosuperiors as well as with the biosuperior-based targeting conjugates and the nanoparticles with theranostic capabilities. New highly exciting frontier of precision medicine combining targeted and personalized interventions is already looming on the horizon. The sense of wonder, excitement, and anticipation of the future progress in the structure–function and novel drug design can be well expressed by Carl Sagan's visionary quote: "Somewhere, something incredible is waiting to be known."

Acknowledgment

The author thanks Dr. Bruce D. Weintraub, President and CEO of Trophogen, Inc., for his visionary leadership, inspiration, and passion in the development of groundbreaking biosuperiors.

References

1. Szkudlinski MW, Fremont V, Ronin C, Weintraub BD. Thyroid-stimulating hormone and thyroid-stimulating hormone receptor structure-function relationships. *Physiol Rev* (2002) **82**(2):473–502. doi:10.1152/physrev.00031.2001
2. Cahoreau C, Klett D, Combarnous Y. Structure-function relationships of glycoprotein hormones and their subunits' ancestors. *Front Endocrinol* (2015) **6**:26. doi:10.3389/fendo.2015.00026
3. Dias JA, Cohen BD, Lindau-Shepard B, Nechamen CA, Peterson AJ, Schmidt A. Molecular, structural, and cellular biology of follitropin and follitropin receptor. *Vitam Horm* (2002) **64**:249–322. doi:10.1016/S0083-6729(02)64008-7
4. Roch GJ, Sherwood NM. Glycoprotein hormones and their receptors emerged at the origin of metazoans. *Genome Biol Evol* (2014) **6**(6):1466–79. doi:10.1093/gbe/evu118
5. Taddese B, Upton GJ, Bailey GR, Jordan SR, Abdulla NY, Reeves PJ, et al. Do plants contain g protein-coupled receptors? *Plant Physiol* (2014) **164**(1):287–307. doi:10.1104/pp.113.228874
6. Farid NR, Szkudlinski MW. Minireview: structural and functional evolution of the thyrotropin receptor. *Endocrinology* (2004) **145**(9):4048–57. doi:10.1210/en.2004-0437
7. Moyle WR, Campbell RK, Myers RV, Bernard MP, Han Y, Wang X. Co-evolution of ligand-receptor pairs. *Nature* (1994) **368**(6468):251–5. doi:10.1038/368251a0

8. Kudo M, Chen T, Nakabayashi K, Hsu SY, Hsueh AJ. The nematode leucine-rich repeat-containing, G protein-coupled receptor (LGR) protein homologous to vertebrate gonadotropin and thyrotropin receptors is constitutively active in mammalian cells. *Mol Endocrinol* (2000) **14**(2):272–84. doi:10.1210/mend.14.2.0422
9. Ulloa-Aguirre A, Crépieux P, Poupon A, Maurel MC, Reiter E. Novel pathways in gonadotropin receptor signaling and biased agonism. *Rev Endocr Metab Disord* (2011) **12**(4):259–74. doi:10.1007/s11154-011-9176-2
10. Landomiel F, Gallay N, Jégot G, Tranchant T, Durand G, Bourquard T, et al. Biased signalling in follicle stimulating hormone action. *Mol Cell Endocrinol* (2014) **382**(1):452–9. doi:10.1016/j.mce.2013.09.035
11. Van Hiel MB, Vandersmissen HP, Proost P, Vanden Broeck J. Cloning, constitutive activity and expression profiling of two receptors related to relaxin receptors in *Drosophila melanogaster*. *Peptides* (2015) **68**:83–90. doi:10.1016/j.peptides.2014.07.014
12. Van Hiel MB, Vandersmissen HP, Van Loy T, Vanden Broeck J. An evolutionary comparison of leucine-rich repeat containing G protein-coupled receptors reveals a novel LGR subtype. *Peptides* (2012) **34**(1):193–200. doi:10.1016/j.peptides.2011.11.004
13. Van Loy T, Vandersmissen HP, Van Hiel MB, Poels J, Verlinden H, Badisco L, et al. Comparative genomics of leucine-rich repeats containing G protein-coupled receptors and their ligands. *Gen Comp Endocrinol* (2008) **155**(1):14–21. doi:10.1016/j.ygcen.2007.06.022
14. Zhang M, Tong KP, Fremont V, Chen J, Narayan P, Puett D, et al. The extracellular domain suppresses constitutive activity of the transmembrane domain of the human TSH receptor: implications for hormone-receptor interaction and antagonist design. *Endocrinology* (2000) **141**(9):3514–7. doi:10.1210/endo.141.9.7790
15. Vassart G, Pardo L, Costagliola S. A molecular dissection of the glycoprotein hormone receptors. *Trends Biochem Sci* (2004) **29**(3):119–26. doi:10.1016/j.tibs.2004.01.006
16. Kreuchwig A, Kleinau G, Kreuchwig F, Worth CL, Krause G. Research resource: update and extension of a glycoprotein hormone receptors web application. *Mol Endocrinol* (2011) **25**(4):707–12. doi:10.1210/me.2010-0510
17. Hershman JM. Physiological and pathological aspects of the effect of human chorionic gonadotropin on the thyroid. *Best Pract Res Clin Endocrinol Metab* (2004) **18**(2):249–65. doi:10.1016/j.beem.2004.03.010
18. Szkudlinski MW, Grossmann M, Weintraub BD. Progress in understanding structure-function relationships of human thyroid-stimulating hormone. *Curr Opin Endocrinol Diabetes* (1997) **4**(5):354–63. doi:10.1097/00060793-199710000-00007
19. Rees Smith B, McLachlan SM, Furmaniak J. Autoantibodies to the thyrotropin receptor. *Endocr Rev* (1988) **9**(1):106–21. doi:10.1210/edrv-9-1-106
20. Wallin E, von Heijne G. Properties of N-terminal tails in G-protein coupled receptors: a statistical study. *Protein Eng* (1995) **8**(7):693–8. doi:10.1093/protein/8.7.693
21. Szkudlinski MW, Teh NG, Grossmann M, Tropea JE, Weintraub BD. Engineering human glycoprotein hormone superactive analogues. *Nat Biotechnol* (1996) **14**(10):1257–63. doi:10.1038/nbt1096-1257
22. Szkudlinski MW. Recombinant human thyrotropins of the twenty-first century. *Expert Opin Pharmacother* (2004) **5**(12):2435–40. doi:10.1517/14656566.5.12.2435
23. Ruddon RW. Super hormones. *Nat Biotechnol* (1996) **14**(10):1224. doi:10.1038/nbt1096-1224
24. Szkudlinski MW. Past, presence and future of thyroid-stimulating hormone (TSH) superactive analogs. *Cancer Treat Res* (2004) **122**:345–56. doi:10.1007/1-4020-8107-3_19
25. Heikoop JC, Huisman-de Winkel B, Grootenhuis PD. Towards minimized gonadotropins with full bioactivity. *Eur J Biochem* (1999) **261**(1):81–4. doi:10.1046/j.1432-1327.1999.00232.x
26. Setlur SR, Dighe RR. Single chain human chorionic gonadotropin, hCGalpha-beta: effects of mutations in the alpha subunit on structure and bioactivity. *Glycoconj J* (2007) **24**(1):97–106. doi:10.1007/s10719-006-9016-x
27. Grossmann M, Weintraub BD, Szkudlinski MW. Novel insights into the molecular mechanisms of human thyrotropin action: structural, physiological, and therapeutic implications for the glycoprotein hormone family. *Endocr Rev* (1997) **18**(4):476–501. doi:10.1210/edrv.18.4.0305
28. Jiang X, Dreano M, Buckler DR, Cheng S, Ythier A, Wu H, et al. Structural predictions for the ligand-binding region of glycoprotein hormone receptors and the nature of hormone-receptor interactions. *Structure* (1995) **3**(12):1341–53. doi:10.1016/S0969-2126(01)00272-6
29. Remy JJ, Couture L, Pantel J, Haertlé T, Rabesona H, Bozon V, et al. Mapping of HCG-receptor complexes. *Mol Cell Endocrinol* (1996) **125**(1–2):79–91. doi:10.1016/S0303-7207(96)03955-X
30. Pantel J, Remy JJ, Salesse R, Jolivet A, Bidart JM. Unmasking of an immunoreactive site on the alpha subunit of human choriogonadotropin bound to the extracellular domain of its receptor. *Biochem Biophys Res Commun* (1993) **195**(2):588–93. doi:10.1006/bbrc.1993.2086
31. Kenakin T. New concepts in drug discovery: collateral efficacy and permissive antagonism. *Nat Rev Drug Discov* (2005) **4**(11):919–27. doi:10.1038/nrd1875
32. Sanders P, Young S, Sanders J, Kabelis K, Baker S, Sullivan A, et al. Crystal structure of the TSH receptor (TSHR) bound to a blocking-type TSHR autoantibody. *J Mol Endocrinol* (2011) **46**(2):81–99. doi:10.1530/JME-10-0127
33. Sanders J, Miguel RN, Furmaniak J, Smith BR. TSH receptor monoclonal antibodies with agonist, antagonist, and inverse agonist activities. *Methods Enzymol* (2010) **485**:393–420. doi:10.1016/B978-0-12-381296-4.00022-1
34. Fan QR, Hendrickson WA. Structure of human follicle-stimulating hormone in complex with its receptor. *Nature* (2005) **433**(7023):269–77. doi:10.1038/nature03206
35. Jiang X, Liu H, Chen X, Chen PH, Fischer D, Sriraman V, et al. Structure of follicle-stimulating hormone in complex with the entire ectodomain of its receptor. *Proc Natl Acad Sci U S A* (2012) **109**(31):12491–6. doi:10.1073/pnas.1206643109
36. Jiang X, Dias JA, He X. Structural biology of glycoprotein hormones and their receptors: insights to signaling. *Mol Cell Endocrinol* (2014) **382**(1):424–51. doi:10.1016/j.mce.2013.08.021
37. Reinfelder J, Maschauer S, Foss CA, Nimmagadda S, Fremont V, Wolf V, et al. Effects of recombinant human thyroid-stimulating hormone superagonists on thyroidal uptake of 18F-fluorodeoxyglucose and radioiodide. *Thyroid* (2011) **21**(7):783–92. doi:10.1089/thy.2010.0394
38. Núñez Miguel R, Sanders J, Chirgadze DY, Blundell TL, Furmaniak J, Rees Smith B. FSH and TSH binding to their respective receptors: similarities, differences and implication for glycoprotein hormone specificity. *J Mol Endocrinol* (2008) **41**(3):145–64. doi:10.1677/JME-08-0040
39. Fan QR, Hendrickson WA. Assembly and structural characterization of an authentic complex between human follicle stimulating hormone and a hormone-binding ectodomain of its receptor. *Mol Cell Endocrinol* (2007) **26**(0–262):73–82. doi:10.1016/j.mce.2005.12.055
40. Szkudlinski MW, Teh NG, Grossmann, M, Tropea JE, Witta, J, Weintraub BD, Role of the 40-51 region of the alpha-subunit in the bioactivity of human thyrotropin and gonadotropins: implications for the design of new hormone analogs based on simultaneous mutagenesis of multiple domains. *Program & Abstracts, Abstract OR1-4. 78th Annual Endocrine Society Meeting*. San Francisco, CA (1996).
41. Grossmann M, Szkudlinski MW, Wong R, Dias JA, Ji TH, Weintraub BD. Substitution of the seat-belt region of the thyroid-stimulating hormone (TSH) beta-subunit with the corresponding regions of choriogonadotropin or follitropin confers luteotropic but not follitropic activity to chimeric TSH. *J Biol Chem* (1997) **272**(24):15532–40. doi:10.1074/jbc.272.24.15532
42. Bhowmick N, Huang J, Puett D, Isaacs NW, Lapthorn AJ. Determination of residues important in hormone binding to the extracellular domain of the luteinizing hormone/chorionic gonadotropin receptor by site-directed mutagenesis and modeling. *Mol Endocrinol* (1996) **10**(9):1147–59. doi:10.1210/mend.10.9.8885249
43. Ulloa-Aguirre A, Zariñán T, Pasapera AM, Casas-González P, Dias JA. Multiple facets of follicle-stimulating hormone receptor function. *Endocrine* (2007) **32**(3):251–63. doi:10.1007/s12020-008-9041-6
44. Angelova K, Fremont V, Jain R, Zhang M, Puett D, Narayan P, et al. Human alpha-subunit analogs act as partial agonists to the thyroid-stimulating hormone receptor: differential effects of free and yoked subunits. *Endocrine* (2004) **24**(1):25–31. doi:10.1385/ENDO:24:1:025
45. Szkudlinski MW, Zhang M, Chen J, Tong KP, Leitolf H, Weintraub BD. Against the dogma: recombinant free alpha-subunit analogs with biological activity: implications for glycoprotein hormone minimization, evolution and hormone-receptor interaction. *Program & Abstracts, Abstract – Hot Topic 9. 81th Annual Meeting of the Endocrine Society*. San Diego, CA (1999).
46. Mueller S, Kleinau G, Szkudlinski MW, Jaeschke H, Krause G, Paschke R. The superagonistic activity of bovine thyroid-stimulating hormone (TSH) and

the human TR1401 TSH analog is determined by specific amino acids in the hinge region of the human TSH receptor. *J Biol Chem* (2009) **284**(24):16317–24. doi:10.1074/jbc.M109.005710
47. Ji I, Zeng H, Ji TH. Receptor activation of and signal generation by the lutropin/choriogonadotropin receptor. Cooperation of Asp397 of the receptor and alpha Lys91 of the hormone. *J Biol Chem* (1993) **268**(31):22971–4.
48. Schaarschmidt J, Huth S, Meier R, Paschke R, Jaeschke H. Influence of the hinge region and its adjacent domains on binding and signaling patterns of the thyrotropin and follitropin receptor. *PLoS One* (2014) **9**(10):e111570. doi:10.1371/journal.pone.0111570
49. Mueller S, Szkudlinski MW, Schaarschmidt J, Günther R, Paschke R, Jaeschke H. Identification of novel TSH interaction sites by systematic binding analysis of the TSHR hinge region. *Endocrinology* (2011) **152**(8):3268–78. doi:10.1210/en.2011-0153
50. Kleinau G, Neumann S, Grüters A, Krude H, Biebermann H. Novel insights on thyroid-stimulating hormone receptor signal transduction. *Endocr Rev* (2013) **34**(5):691–724. doi:10.1210/er.2012-1072
51. Miller TC, Jaques JT, Szkudlinski MW, Mackenzie DS. Thyrotropic activity of recombinant human glycoprotein hormone analogs and pituitary mammalian gonadotropins in goldfish (*Carassius auratus*): insights into the evolution of thyrotropin receptor specificity. *Gen Comp Endocrinol* (2012) **177**(1):70–5. doi:10.1016/j.ygcen.2012.02.012
52. Grossmann M, Leitolf H, Weintraub BD, Szkudlinski MW. A rational design strategy for protein hormone superagonists. *Nat Biotechnol* (1998) **16**(9):871–5. doi:10.1038/nbt0998-871
53. Leitolf H, Tong KP, Grossmann M, Weintraub BD, Szkudlinski MW. Bioengineering of human thyrotropin superactive analogs by site-directed "lysine-scanning" mutagenesis of the common βL3 loop of human glycoprotein hormones. Analysis of cooperative effects within and between peripheral β-hairpin loops. *J Biol Chem* (2000) **275**(35):27457–65. doi:10.1074/jbc.M003707200
54. Szkudlinski MW, Leitolf H, Dong W, Grossmann M, Weintraub BD. Superagonists of human lutropin (hLH) and human chorionic gonadotropin (hCG) obtained by introduction of charged amino acids in the peripheral β hairpin loops. *Program & Abstracts, Abstract OR28-2. 80th Annual Meeting of the Endocrine Society*. New Orleans, LA (1998). 88 p.
55. Jiang X, Fischer D, Chen X, McKenna SD, Liu H, Sriraman V, et al. Evidence for follicle-stimulating hormone receptor as a functional trimer. *J Biol Chem* (2014) **289**(20):14273–82. doi:10.1074/jbc.M114.549592
56. Campbell GA, Kurcz M, Marshall S, Meites J. Effects of starvation in rats on serum levels of follicle stimulating hormone, luteinizing hormone, thyrotropin, growth hormone and prolactin; response to LH-releasing hormone and thyrotropin-releasing hormone. *Endocrinology* (1977) **100**(2):580–7. doi:10.1210/endo-100-2-580
57. Parrott JA, Doraiswamy V, Kim G, Mosher R, Skinner MK. Expression and actions of both the follicle stimulating hormone receptor and the luteinizing hormone receptor in normal ovarian surface epithelium and ovarian cancer. *Mol Cell Endocrinol* (2001) **172**(1–2):213–22. doi:10.1016/S0303-7207(00)00340-3
58. Puett D, Angelova K, da Costa MR, Warrenfeltz SW, Fanelli F. The luteinizing hormone receptor: insights into structure-function relationships and hormone-receptor-mediated changes in gene expression in ovarian cancer cells. *Mol Cell Endocrinol* (2010) **329**(1–2):47–55. doi:10.1016/j.mce.2010.04.025
59. Mertens-Walker I, Baxter RC, Marsh DJ. Gonadotropin signalling in epithelial ovarian cancer. *Cancer Lett* (2012) **324**(2):152–9. doi:10.1016/j.canlet.2012.05.017
60. Laugwitz KL, Allgeier A, Offermanns S, Spicher K, Van Sande J, Dumont JE, et al. The human thyrotropin receptor: a heptahelical receptor capable of stimulating members of all four G protein families. *Proc Natl Acad Sci U S A* (1996) **93**(1):116–20. doi:10.1073/pnas.93.1.116
61. Ulloa-Aguirre A, Dias JA, Bousfield G, Huhtaniemi I, Reiter E. Trafficking of the follitropin receptor. *Methods Enzymol* (2013) **521**:17–45. doi:10.1016/B978-0-12-391862-8.00002-8
62. Fremont V, Zhang M, Weintraub BD, Szkudlinski MW. Novel insights into the molecular mechanism of glycoprotein hormone receptor activation. *FASEB J* (2001) **15**(4):A175.
63. Nechamen CA, Thomas RM, Dias JA. APPL1, APPL2, Akt2 and FOXO1a interact with FSHR in a potential signaling complex. *Mol Cell Endocrinol* (2007) **260–262**:93–9. doi:10.1016/j.mce.2006.08.014
64. Arey BJ, Lopez FJ. Are circulating gonadotropin isoforms naturally occurring biased agonists? Basic and therapeutic implications. *Rev Endocr Metab Disord* (2011) **12**(4):275–88. doi:10.1007/s11154-011-9188-y
65. Langmead CJ, Christopoulos A. Supra-physiological efficacy at GPCRs: superstition or super agonists? *Br J Pharmacol* (2013) **169**(2):353–6. doi:10.1111/bph.12142
66. Szkudlinski MW. Challenges and opportunities of trapping ligands. *Mol Pharmacol* (2007) **72**(2):231–4. doi:10.1124/mol.107.038208
67. Dias JA, Mahale SD, Nechamen CA, Davydenko O, Thomas RM, Ulloa-Aguirre A. Emerging roles for the FSH receptor adapter protein APPL1 and overlap of a putative 14-3-3tau interaction domain with a canonical G-protein interaction site. *Mol Cell Endocrinol* (2010) **329**(1–2):17–25. doi:10.1016/j.mce.2010.05.009
68. Calebiro D, Nikolaev VO, Lohse MJ. Imaging of persistent cAMP signaling by internalized G protein-coupled receptors. *J Mol Endocrinol* (2010) **45**(1):1–8. doi:10.1677/JME-10-0014
69. Szkudlinski MW, Grossmann M, Leitolf H, Weintraub BD. Human thyroid-stimulating hormone: structure-function analysis. *Methods* (2000) **21**(1):67–81. doi:10.1006/meth.2000.0976
70. Vlaeminck-Guillem V, Ho SC, Rodien P, Vassart G, Costagliola S. Activation of the cAMP pathway by the TSH receptor involves switching of the ectodomain from a tethered inverse agonist to an agonist. *Mol Endocrinol* (2002) **16**(4):736–46. doi:10.1210/mend.16.4.0816
71. Chen CR, Salazar LM, McLachlan SM, Rapoport B. The thyrotropin receptor hinge region as a surrogate ligand: identification of loci contributing to the coupling of thyrotropin binding and receptor activation. *Endocrinology* (2012) **153**(10):5058–67. doi:10.1210/en.2012-1376
72. Szkudlinski MW, Fremont V, Wolf V, Han Y, Wu D, Weintraub BD. Novel high affinity and long-acting recombinant bovine FSH analogs for veterinary superovulation. *Program & Abstracts, Abstract 16. 18th Biennial AAVPT Symposium*. Potomac, MD (2013).
73. Galli F, Manni I, Piaggio G, Balogh L, Weintraub BD, Szkudlinski MW, et al. (99m)Tc-labeled-rhTSH analogue (TR1401) for imaging poorly differentiated metastatic thyroid cancer. *Thyroid* (2014) **24**(8):1297–308. doi:10.1089/thy.2013.0429
74. Boime I, Ben-Menahem D. Glycoprotein hormone structure-function and analog design. *Recent Prog Horm Res* (1999) **54**:271–88.
75. Pouwer AW, Farquhar C, Kremer JA. Long-acting FSH versus daily FSH for women undergoing assisted reproduction. *Cochrane Database Syst Rev* (2012) **6**:CD009577. doi:10.1002/14651858.CD009577.pub2
76. Croxtall JD, McKeage K. Corifollitropin alfa: a review of its use in controlled ovarian stimulation for assisted reproduction. *BioDrugs* (2011) **25**(4):243–54. doi:10.2165/11206890-000000000-00000
77. Goletz S, Stockl L. *Recombinant Human Follicle-Stimulating Hormone*. USPTO US Patent Application 201301376636 (2013).
78. Yang Z, Wang S, Halim A, Schulz MA, Frodin M, Rahman SH, et al. Engineered CHO cells for production of diverse, homogeneous glycoproteins. *Nat Biotechnol* (2015) **33**(8):842–4. doi:10.1038/nbt.3280
79. Clark E, Magner J, Skell J. *Formulations for Therapeutic Administration of Thyroid Stimulating Hormone (TSH)*. USPTO, US Patent Application WO2008036271 (2008).
80. Louet S. *Banking on a Big Biobetters Bonanza*. *Cpb Review* (2012) 48–52.
81. Ubaldi F, Vaiarelli A, D'Anna R, Rienzi L. Management of poor responders in IVF: is there anything new? *Biomed Res Int* (2014) **2014**:352098. doi:10.1155/2014/352098
82. Bassett JH, van der Spek A, Logan JG, Gogakos A, Bagchi-Chakraborty J, Murphy E, et al. Thyrostimulin regulates osteoblastic bone formation during early skeletal development. *Endocrinology* (2015) **156**(9):3098–113. doi:10.1210/en.2014-1943
83. Low SC, Nunes SL, Bitonti AJ, Dumont JA. Oral and pulmonary delivery of FSH-Fc fusion proteins via neonatal Fc receptor-mediated transcytosis. *Hum Reprod* (2005) **20**(7):1805–13. doi:10.1093/humrep/deh896
84. Vance D, Martin J, Patke S, Kane RS. The design of polyvalent scaffolds for targeted delivery. *Adv Drug Deliv Rev* (2009) **61**(11):931–9. doi:10.1016/j.addr.2009.06.002
85. Gershengorn MC, Neumann S. Update in TSH receptor agonists and antagonists. *J Clin Endocrinol Metab* (2012) **97**(12):4287–92. doi:10.1210/jc.2012-3080
86. Palmer SS, McKenna S, Arkinstall S. Discovery of new molecules for future treatment of infertility. *Reprod Biomed Online* (2005) **10**(Suppl 3):45–54. doi:10.1016/S1472-6483(11)60390-8

87. Kenakin TP. Biased signalling and allosteric machines: new vistas and challenges for drug discovery. *Br J Pharmacol* (2012) **165**(6):1659–69. doi:10.1111/j.1476-5381.2011.01749.x
88. Calebiro D, Sungkaworn T, Maiellaro I. Real-time monitoring of GPCR/cAMP signalling by FRET and single-molecule microscopy. *Horm Metab Res* (2014) **46**(12):827–32. doi:10.1055/s-0034-1384523
89. Kenakin T. *A Pharmacology Primer: Theory, Applications, and Methods*. London: Academic Press (2010).
90. Szkudlinski MW, et al. Superagonists of human TSH with increased stability and prolonged plasma half-life. *Thyroid* (1997) **7**(Suppl 1):S-8.

Conflict of Interest Statement: The author is Executive Vice President, CSO, and Co-founder of Trophogen, Inc. discovering and developing biosuperior drugs for profit.

frontiers in Endocrinology

ORIGINAL RESEARCH
published: 17 August 2015
doi: 10.3389/fendo.2015.00128

Activation of relaxin family receptor 1 from different mammalian species by relaxin peptide and small-molecule agonist ML290

Zaohua Huang[1†], Courtney Myhr[1†], Ross A. D. Bathgate[2], Brian A. Ho[1], Amaya Bueno[1], Xin Hu[3], Jingbo Xiao[3], Noel Southall[3], Elena Barnaeva[3], Irina U. Agoulnik[4], Juan J. Marugan[3], Marc Ferrer[3] and Alexander I. Agoulnik[1]*

[1] Department of Human and Molecular Genetics, Herbert Wertheim College of Medicine, Florida International University, Miami, FL, USA, [2] Department of Biochemistry and Molecular Biology, Florey Department of Neuroscience and Mental Health, Florey Institute of Neuroscience and Mental Health, The University of Melbourne, Melbourne, VIC, Australia, [3] NIH Chemical Genomics Center, National Center for Advancing Translational Sciences, National Institutes of Health, Rockville, MD, USA, [4] Department of Cellular Biology and Pharmacology, Herbert Wertheim College of Medicine, Florida International University, Miami, FL, USA

OPEN ACCESS

Edited by:
Brian J. Arey,
Bristol-Myers Squibb Co, USA

Reviewed by:
Jeremy Tavare,
University of Bristol, UK
Sophie Jane Bradley,
Medical Research Council, UK

***Correspondence:**
Alexander I. Agoulnik,
Department of Human and Molecular Genetics, Herbert Wertheim College of Medicine, Florida International University, 11200 SW 8th Street, AHCI 419B, Miami, FL 33199, USA
aagoulni@fiu.edu

[†]Zaohua Huang and Courtney Myhr have contributed equally to this work.

Specialty section:
This article was submitted to Molecular and Structural Endocrinology, a section of the journal Frontiers in Endocrinology

Received: 17 June 2015
Accepted: 31 July 2015
Published: 17 August 2015

Citation:
Huang Z, Myhr C, Bathgate RAD, Ho BA, Bueno A, Hu X, Xiao J, Southall N, Barnaeva E, Agoulnik IU, Marugan JJ, Ferrer M and Agoulnik AI (2015) Activation of relaxin family receptor 1 from different mammalian species by relaxin peptide and small-molecule agonist ML290. Front. Endocrinol. 6:128. doi: 10.3389/fendo.2015.00128

Relaxin peptide (RLN), which signals through the relaxin family peptide 1 (RXFP1) GPCR receptor, has shown therapeutic effects in an acute heart failure clinical trial. We have identified a small-molecule agonist of human RXFP1, ML290; however, it does not activate the mouse receptor. To find a suitable animal model for ML290 testing and to gain mechanistic insights into the interaction of various ligands with RXFP1, we have cloned rhesus macaque, pig, rabbit, and guinea pig RXFP1s and analyzed their activation by RLN and ML290. HEK293T cells expressing macaque or pig RXFP1 responded to relaxin and ML290 treatment as measured by an increase of cAMP production. Guinea pig RXFP1 responded to relaxin but had very low response to ML290 treatment only at highest concentrations used. The rabbit RXFP1 amino acid sequence was the most divergent, with a number of unique substitutions within the ectodomain and the seven-transmembrane domain (7TM). Two splice variants of rabbit RXFP1 derived through alternative splicing of the fourth exon were identified. In contrast to the other species, rabbit RXFP1s were activated by ML290, but not with human, pig, mouse, or rabbit RLNs. Using FLAG-tagged constructs, we have shown that both rabbit RXFP1 variants are expressed on the cell surface. No binding of human Eu-labeled RLN to rabbit RXFP1 was detected, suggesting that in this species, RXFP1 might be non-functional. We used chimeric rabbit–human and guinea pig–human constructs to identify regions important for RLN or ML290 receptor activation. Chimeras with the human ectodomain and rabbit 7TM domain were activated by RLN, whereas substitution of part of the guinea pig 7TM domain with the human sequence only partially restored ML290 activation, confirming the allosteric mode of action for the two ligands. Our data demonstrate that macaque and pig models can be used for ML290 testing.

Keywords: relaxin, G protein-coupled receptor, RXFP1, receptor structure–function, small-molecule allosteric agonist

Introduction

The relaxin hormone was discovered by Dr. Frederick Hisaw 90 years ago in experiments involving the injection of serum from pregnant guinea pigs or rabbits into virgin guinea pigs that resulted in the softening of the pubic ligament (1). Further experiments led to the identification of the peptide responsible for this effect. It was the first peptide hormone identified in mammals. The relaxin gene, RLN1, has a relatively simple structure, containing only two exons (2). The mRNA encodes the preprohormone, which is processed by convertases to the mature 6 kDa hormone with A- and B-chains connected to each other by two disulfide bonds. An additional disulfide bond is located within the A-chain. Relaxin (RLN) peptides from various mammalian species show significant variations in amino acid sequence; however, almost all maintain the conserved functional RXXXRXXI/V motif in the B-chain. The analysis of the full genome sequences revealed the presence of only one RLN gene in various species. One exception is primates, where two RLN1 and RLN2 genes coding for almost identical peptides are located next to each other, most likely the result of genomic DNA duplication. It is believed that the RLN2 gene is the functional copy, as only the RLN2 peptide was isolated from the peripheral blood (1).

The cognate receptor for RLN peptide is the G protein-coupled receptor Relaxin Family Peptide Receptor 1, or RXFP1 (3). All *RXFP1* genes cloned to date from various mammalian species have the same conserved 18-exon genomic organization and encode proteins with very similar structures. RXFP1 contains a large extracellular ectodomain, which is unique among G protein-coupled receptors. This domain consists of a single low-density lipoprotein receptor type A module (LDLa) followed by 10 leucine-rich repeats (LRRs). The classical seven-transmembrane (7TM) region of the RXFP1 is well-conserved among different species. Structural studies of RLN and RXFP1 binding and activation have revealed a complex mechanism of their interaction (2). It was established that primary high-affinity binding of RLN occurs within the LRRs, while the secondary low-affinity interaction occurs via the second extracellular loop (ECL) of the 7TM region. The LDLa domain is not necessary for binding but is essential for activation of the receptor signaling, although the detailed mechanism of these interactions is still under investigation. When transfected into HEK293T, CHO, or other cells, human, mouse, and rat RXFP1s respond to RLN treatment by increasing cAMP production. Increased phosphorylation of extracellular signal-regulated kinase 1/2 (ERK1/2), MAPK, tyrosine kinase(s) and activation of nitric oxide (NO) signaling in various RXFP1-transfected cells and cells endogenously expressing RXFP1were also found (2).

Non-reproductive functions of this hormone/receptor pair were identified through analysis of *Rln1*- and *Rxfp1*-deficient transgenic mice, experiments with RLN injection into rodents, and inactivation of RLN signaling using antibodies or peptide antagonists (1, 2). It was shown that RLN behaves as an antifibrotic, antiapoptotic, vasodilatory, and angiogenic factor. This led to the investigation of the therapeutic potential for RLN in several diseases. The most advanced clinical trial to date tested the use of recombinant RLN as a treatment for acute heart failure. The reported analysis suggests that the treatment is well tolerated by patients, safe, and most importantly, results in a reduced 180-day mortality (4).

As with other peptide-based pharmaceuticals, the use of such drugs in chronic conditions is complicated due to their short half-life and the need for intravenous administration. An additional disadvantage is the cost of recombinant peptide production. To overcome these limitations, we have initiated the search for a small-molecule agonist of RXFP1. High throughput screening of a small-molecule library and the subsequent structure activity campaign resulted in the identification of the first series of RXFP1 agonists with preferred biochemical and *in vivo* pharmacokinetic properties, which supported further therapeutic investigation of RLN biology (5, 6). Surprisingly, these compounds, including lead compound, ML290, did not activate the mouse RXFP1 receptor. Using chimeric human–mouse RXFP1 variants and point mutations, we have established that amino acid differences in the third ECL of 7TM are responsible for such specificity (5). This mouse variant is also present in rat and hamster RXFP1s. An overwhelming majority of the preclinical animal testing for RLN treatment includes rodent models, and thus the inability of small-molecule agonists to activate the mouse receptor hampers preclinical studies. To find suitable *in vitro* and *in vivo* models, we have cloned and tested in a functional cAMP assay RXFP1 receptors from four mammalian species: rhesus macaque (Macaca mullata), pig (*Sus scrofa*), European rabbit (*Oryctolagus cuniculus*), and the guinea pig (*Cavia porcellus*). We also tested various chimeric human constructs that had their extracellular or 7TM parts swapped for corresponding guinea pig and rabbit fragments to establish regions responsible for RLN and ML290 activation. For rabbit RXFP1s, which were non-responsive to RLN, we tested surface expression, RLN binding, and activation by RLN peptides from various species. We have concluded that pig and macaque models are suitable for ML290 testing, whereas rodent RXFP1 genes have to be humanized for preclinical studies.

Materials and Methods

Sequence Analysis

Genomic sequences of the RXFP1 genes for different species were obtained from the Ensembl database[1]. The full-length human and mouse RXFP1 cDNA were used to identify exons using the Blast2seq program (7) available from the NCBI website[2]. Multiple sequence alignments and evolutionary tree rendering were performed using the MUSCLE algorithm (8) at the EMBL-EBI website[3].

Production of RXFP1 Expression Constructs From Various Species and Human–Guinea Pig or Rabbit Chimeric RXFP1s

The human, mouse, macaque, and pig RXFP1 cDNA constructs in baculovirus BacMam mammalian expression vector (Invitrogen, Carlsbad, CA, USA) were synthesized at the Eukaryotic

[1]http://www.ensembl.org
[2]www.ncbi.nlm.nih.gov
[3]http://www.ebi.ac.uk/Tools/msa/

Expression Group-Protein Expression laboratory (NCI, Frederick, MD, USA). The PCR primers for RT-PCR were designed to cover the full-length sequence of the open reading frame (ORF). PCR amplifications were performed with *PfuUltra* High-Fidelity DNA polymerase (Agilent Technologies, Santa Clara, CA, USA). Guinea pig *RXFP1* (G-RXFP1) was amplified from guinea pig ovarian cDNA (Zyagen, San Diego, CA, USA). Rabbit *RXFP1* (R1-RXFP1 and R2-RXFP1) cDNAs were amplified from rabbit uterus cDNA (Zyagen). All cloning was performed using the In-Fusion® HD Cloning Kit (Clontech Laboratories, Mountain View, CA, USA). Rabbit and guinea pig *RXFP1*s were cloned into pCR3.1 mammalian expression vector (Invitrogen). In order to study RXFP1 surface expression, rabbit cDNAs were cloned into pcDNA3.1™/Zeo+ mammalian expression vector (Invitrogen), which contained an N-terminal FLAG-tag and a bovine prolactin signal sequence (3). It was shown previously that such additions do not alter receptor activity (14). To make chimeric clones, the human, guinea pig, and rabbit plasmid were used as templates to produce PCR amplicons, which were then used for overlapping PCR and subsequent cloning with the In-Fusion kit. The chimeric guinea pig/human GH-RXFP1 construct contains guinea pig *RXFP1* cDNA (*G-RXFP1*, 1–1499 bp) encoding the ectodomain, TM1, TM2, and part of TM3 (amino acids 1–499 of G-RXFP1), and human RXFP1 (*hRXFP1*, 1509–2274 bp) encoding TM3 to the C-terminal tail of the receptor (amino acids 503–757 of hRXFP1) (**Figure 1A**). The recombinant chimeric human–rabbit HR-RXFP1 was made with the 5′-part of the *hRXFP1* sequence (1–972 bp, LDLa-LRR9, 1–324 aa), with the remainder being the rabbit *RXFP1* sequence (973–2277 bp, LRR9-C-terminal tail, 325–759 aa) (**Figure 1A**). The recombinant chimeric rabbit–human R1H-RXFP1 or R2H-RXFP1 contains the N-terminal rabbit RXFP1 sequence (1–972 bp for *R1-RXFP1* or 975 bp for *R2-RXFP1*), with the remaining sequence being *hRXFP1* (973–2274) (**Figure 1A**). *R1-* and *R2-RXFP1* denote two variants of rabbit *RXFP1* cDNA. All numbers correspond to the full-length cDNAs with the first nucleotide of the ORF.

The rabbit RLN gene SQ10 (9) was synthesized and cloned into pCR2.1-TOPO (Invitrogen) by Eurofins MWG Operon LLC. The SQ10 cDNA was PCR amplified and cloned using In-Fusion kit into a pCR3.1 vector.

At least three independent plasmids were obtained in each cloning experiment. The cDNA inserts were fully sequenced using overlapping primers by Eurofins MWG Operon LLC (Huntsville, AL, USA). GenBank accession numbers are KT149378 (guinea pig RXFP1), KT149379 (rabbit variant 1 RXFP1), and KT149380 (rabbit variant 2 RXFP1).

Relaxin Peptides and Cell Lines

Porcine relaxin peptide (10) was a gift from Dr. O. David Sherwood (University of Illinois at Urbana-Champaign). Human recombinant RLN peptide was obtained from PeproTech Inc. (Rocky Hill, NJ, USA) or from Corthera (San Carlos, CA, USA). Chemically synthesized mouse RLN peptide was a gift from Prof. John D. Wade (Florey Institute of Neuroscience and Mental Health, Melbourne, VIC, Australia). Human embryonic kidney HEK293T cells (ATCC #CRL-1573; American Type Tissue Culture Collection, Manassas, VA, USA) used for transfection experiments were maintained in 37°C, 5% CO_2 in Dulbecco's Modified Eagle medium (DMEM) supplemented with 10% fetal bovine serum (FBS), 1% L-glutamine, and 1% penicillin/streptomycin.

CRE-Luc BacMam Luciferase Assay

GloResponse™ CRE-*luc2P* HEK293T cells stably transfected with cAMP response element-driven luciferase (CRE-Luc) reporter (Promega, Madison, WI, USA) were transduced with human, macaque, pig, and mouse RXFP1 expression BacMam vectors according to the manufacturer's protocol (Invitrogen) and incubated at room temperature for 2 h in the dark with occasional mixing. The volume of the cell culture was adjusted to 1000 cells/μl with DMEM + 10% FBS. Cells (3 μl, 3000 cells) were plated on 1536-well white solid-bottom TC plates and incubated overnight at 37C°, 5% CO_2. Four hundred micromoles Ro 20-1724 (Sigma-Aldrich, St. Louis, MO, USA) in PBS (1 μl) was added in each well. The cells were treated with serial dilutions of either Forskolin (Sigma-Aldrich), ML290 (5) or porcine RLN at final concentrations' range (57 μM–3.5 pM) for Forskolin and ML290, and (8.7 μM–1.8 pM, or 57 ng/μl–0.012 pg/μl] for RLN. After 2 h stimulation at 37°C, 4 μl of detection reagent from Amplite™ Luciferase reporter gene assay kit (AAT Bioquest, Sunnyvale, CA, USA) was added as a mix of 90% Component A, 5% Component C, and 5% Component D, and incubated at room temperature for 5 min. Luminescent signal was measured on Viewlux uHTS Microplate Imager (PerkinElmer, Santa Clara, CA, USA). The data were processed using GraphPad Software (San Diego, CA, USA).

Cell Transfection and cAMP Assays

HEK293T cell transient transfections were performed using Lipofectamine 2000 transfection reagent (Life Technologies, Grand Island, NY, USA) according to the manufacturer's instructions. Cells transiently expressing the RXFP1 receptors were used within 48 h of transfection. Each construct was tested at least three times. For cell-conditioned media stimulation, HEK293T cells were transfected with the rabbit RLN construct (SQ10) or an empty pCR3.1 vector, and cells were cultured for 24 h. The media was used to stimulate HEK293T cells transfected with the RXFP1 receptors.

Direct measurement of cAMP production was performed using the HTRF cAMP HiRange kit (CisBio, Bedford, MA, USA). HEK293T cells transiently transfected with different RXFP1 receptors were stimulated with various concentrations of RLN peptides or ML290 for 60 min at 37°C, 5% CO_2, after which, two HTRF detection reagents (diluted according to assay kit directions in HTRF lysis buffer) were added. The plates were incubated for 60 min at room temperature, and the signal was read on a FLUOstar Omega (BMG Labtech, Cary, NC, USA) plate reader. cAMP levels were calculated according to the manufacturer's instructions against a standard curve. Statistical processing of the data was performed using GraphPad Prism software.

For the indirect cAMP assay, changes in cAMP signaling were measured by co-transfection of receptors with a CRE-β-galactosidase (CRE-β-gal) reporter construct (11). Cells were

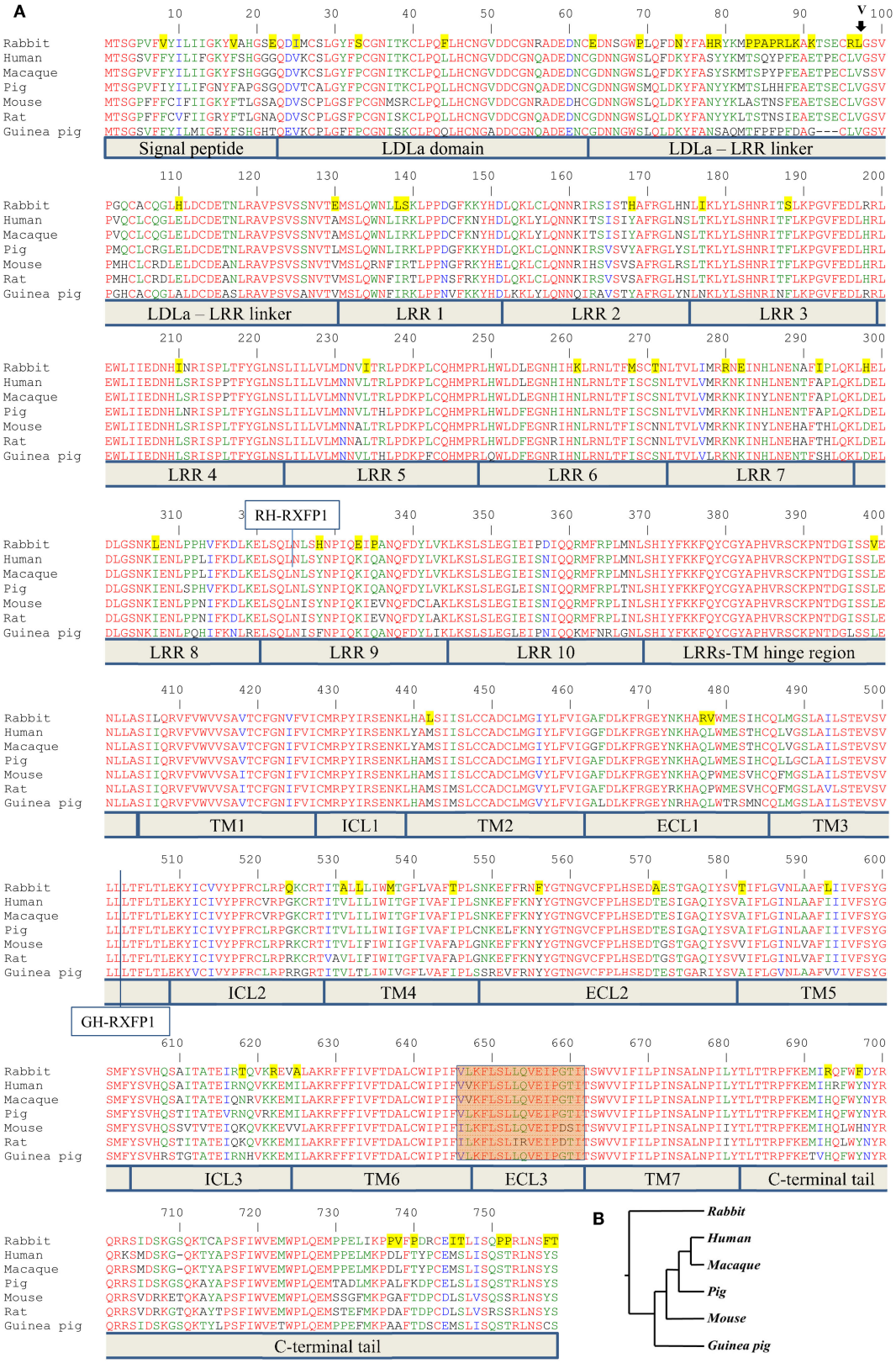

FIGURE 1 | Alignment of RXFP1 proteins from various species.

(Continued)

FIGURE 1 | Continued
(A) Amino acid alignment of RXFP1 receptor sequences. The position of the extra amino acid (V98) in rabbit receptor variant R2 is shown above the sequence with an arrow. Functional domains are shown below the sequences. LDLa is low-density lipoprotein class A domain; LRR is leucine-rich repeat, TM1–7 are transmembrane domains; ICL1–3 are intracellular loops of seven-transmembrane domain; ECL1–3 are extracellular loops of seven-transmembrane domain. The highlighted brown box is the third extracellular loop and adjacent amino acids required for ML290 activation of RXFP1. Amino acids conserved in all seven species are in red; amino acids specific for the rabbit sequence are highlighted in yellow. The vertical line at position 324 indicates the fusion site in chimeric rabbit/human receptor (RH-RXFP1). The vertical line at position 502 indicates the fusion site in chimeric guinea pig/human receptor (GH-RXFP1). **(B)** Evolutionary tree showing the relationship of various RXFP1 proteins. The rabbit sequence is the most diverged.

stimulated for 6 h at 37°C with RLN peptides or ML290 at various concentrations. A non-linear regression sigmoidal dose–response curve was then produced using GraphPad Prism. All experiments were conducted at least three times with three to four replicates each time.

Cell Total and Surface Expression Assay of RXFP1

HEK293T cells were transfected with RXFP1 plasmid DNA or empty vector pCR3.1 as described above. After 24 h incubation at 37°C, cells were harvested in PBS/5 mM EDTA. To determine surface expression, 0.5×10^6 cells were fixed in stain buffer (2% BSA/PBS) containing 3.7% formaldehyde, washed, and incubated with 0.5 μg anti-FLAG M1 Ab (Sigma) for 30 min at 4°C. After washing, the cells were then incubated with 1 μg Alexa Fluor 488 goat anti-mouse IgG (Life Technologies) for 20 min at 4°C. Cells were washed and resuspended in stain buffer for analysis on an Accuri C6 flow cytometer (BD Biosciences, San Jose, CA, USA). For total expression, 0.2% Tween-20 (Bio-Rad) was added to the stain buffer at all steps and the cells were processed identically. Cells transfected with empty vector were used as the negative cut-off to determine RXFP1 expression. All experiments were repeated three times in triplicates. Differences in receptor expression were quantified as the ratios of surface expression to total expression, and analyzed with a one-way ANOVA.

Ligand-Binding Assays

Saturation-binding studies using Eu-labeled human H2 RLN (Eu-H2 RLN) were performed on whole cells as described previously (12). Cells stably expressing RXFP1 (13) or with a semi-stable transfection of R1-RXFP1 selected using FACS (14) were used in this experiment. Increasing concentrations of Eu-H2 RLN (0.1–50 nM) were utilized and non-specific binding was determined in presence of 1 μM of unlabeled H2 RLN. Readings were taken in triplicate and read on a BMG PolarStar plate reader in clear-bottomed, opaque-walled 96-well plates (PerkinElmer). All experiments were repeated three times. Data were analyzed using GraphPad PRISM and presented as the mean percentage specific binding ± SEM of independent experiments. A non-linear regression one-site binding curve was then fitted and resulting pKd, and Bmax values were subjected to one-way ANOVA and uncorrected Fisher's LSD comparison test. In this experiment, the cell total and surface expression was analyzed using a previously described method (15). Differences in receptors expression were assessed using a Student's *t*-test.

Results

RXFP1 Genes

The ENSEMBL sequence of rhesus macaque RXFP1 (RXFP1-202 ENSMMUT00000041571) had high homology to the human RXFP1 sequence at both the mRNA and amino acid level. The 18-exon structure encoded 757 amino acids with 99% identity to the human protein after removing 22 extra amino acids at the N-terminus (**Figure 1**). Of the 10 substitutions identified, two were located in the N-terminal signal peptide. The LDLa and LRRs were identical between the two species, as well as ECL3, which is important for the ML290 response. Analysis of the pig RXFP1 annotated sequence revealed the absence of the first exon, but three additional 5′ small exons with no homology to the human or mouse sequence. Using human exon 1 as a probe, we performed a BLAST search of the 50 kb pig genomic sequence upstream of the putative *RXFP1* exon 2. The search revealed exon 1 of pig *RXFP1*, separated from exon 2 by a 42 kb intron, a size comparable to hRXFP1 intron 1. All intron–exon boundaries contained conserved GT and AG sequences at the 5′- and 3′-ends of the introns, which are required for proper RNA splicing. Alignment of the resulting full-length 2277 bp sequence with human cDNA showed 91% identity. The pig RXFP1 758 aa protein sequence was 92% identical to the human sequence (**Figure 1A**). The second valine in the TM6 domain, adjacent to ECL3, was substituted for leucine in the pig sequence (*V L/V* K F L S L L Q V E I P *G T*). As both macaque and pig cDNAs showed high homology to the human sequence, we chemically synthesized corresponding cDNAs and cloned them into a BacMam vector. Mouse and human cDNA expression BacMam vectors were also produced.

Analysis of the guinea pig annotated RXFP1 genomic sequence and cDNA sequences identified 17 exons with high homology to the corresponding human exons. A BLAST search of the upstream genomic sequence revealed that exon 1 was separated from exon 2 by a 42.8 kb intron. The putative full-length *G-RXFP1* cDNA was 2268 bp long, encoding a 755 aa protein. At the amino acid level, the guinea pig RXFP1 sequence was 84 and 80% identical to the human and mouse RXFP1 proteins, respectively (**Figure 1A**). The ECL3 sequence was identical to the pig sequence. Since the guinea pig sequence was more divergent from the human and mouse sequences, we used RT-PCR with primers designed from the established first and last exons to generate full-length cDNA. The RT-PCR fragments were obtained from total ovarian guinea pig RNA. Comparison of the sequenced cDNA clones with the genomic sequence from GenBank identified only one synonymous substitution.

Next, we analyzed rabbit genomic DNA. Both the cDNA and predicted protein sequence of rabbit RXFP1 were quite different

from the human and mouse sequences, with the 3′ exons not well defined. We used RT-PCR with primers designed from the first and the last exons and total uterine rabbit RNA to obtain the expected 2.3 kb full-length sequence of *R-RXFP1*. The fragments were cloned into pCR3.1 vector, and sequencing of the resultant cDNA clones revealed two variants differing by 3 bp in the 5′end (**Figure 2**). Comparison with the genomic sequence suggested that the variant with the additional TAG sequence was a result of alternative splicing at the 5′-end of exon 4. We performed direct sequencing of the RT-PCR products to confirm the presence of both variants in total mRNA. As shown in **Figure 2**, the chromatogram depicts a single sequence at the end of exon 3, followed by two overlapping sequences present at equal ratios, as evident by the heights of the overlapping nucleotide picks. Alignment with the genomic sequence showed that the 2277 bp (or 2280 bp) cDNA was encoded by the 18 exons as in other species. When compared to GenBank genomic sequence, all putative exon–intron boundaries, with the exception of the beginning of exon 4, were conserved in rabbit cDNAs. Four synonymous differences were found in our cDNA versus GenBank genomic sequence. At the amino acid level, rabbit RXFP1 sequence was 84 and 79% identical to human and mouse proteins, respectively. The ECL3 sequence was identical to the pig sequence (**Figure 1A**).

Multiple sequence analysis showed the primate and rodent RXFP1s grouped together, with the pig RXFP1 sequence situated between them (**Figure 1B**). Rabbit RXFP1 was the most diverged. In rabbit RXFP1, there were multiple substitutions in amino acid positions conserved among the other species, including in the extracellular, 7TM, and C-terminal part (**Figure 1A**).

Macaque and Pig RXFP1 Receptors Respond to RLN and ML290 in a CRE-Reporter cAMP Assay

To analyze the functional activity of the synthesized macaque and pig RXFP1s, we used a CRE-Luc BacMam luciferase assay (**Figure 3**). Human and mouse RXFP1s were used in these experiments as controls. The cells were stimulated for 2 h, and the elevation of cAMP production was detected by increased luciferase activity. All four receptors showed similar EC50 when treated with porcine RLN (**Figure 3A**). Human, macaque, and pig RXFP1s also responded strongly to ML290 stimulation (**Figure 3B**; **Table 1**). Previously, we did not see an increase of cAMP in cells transfected with the mouse receptor in a direct cAMP HTRF assay (5). In this experiment, there was significant increase in luciferase activity in cells expressing mouse RXFP1 receptor in response to the highest concentrations of ML290.

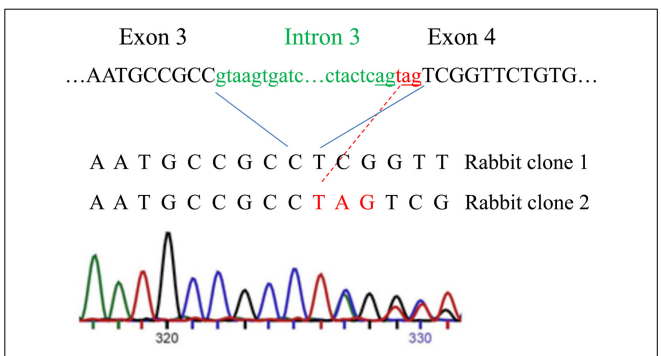

FIGURE 2 | Alternative splicing of the intron 3 and exon 4 in rabbit RXFP1 genomic DNA. The upper sequence shows the intron (green) and exon (black) boundaries in the genomic DNA. Three additional nucleotides (in red) are added to the mRNA as result of alternative splicing, as shown with the red line. Below is the sequencing chromatogram showing the presence of two sequences after the alternative splicing site. Note an equal size of the peaks in the overlapping sequence, indicating an equal representation of the two variants in the total mRNA pool.

Characterization of Guinea Pig RXFP1

G-RXFP1 response to RLN and ML290 treatment was tested by measuring cAMP production in HEK293T cells transiently transfected with receptor. A direct HTRF assay to measure cAMP concentration was used in these experiments, and cells transfected

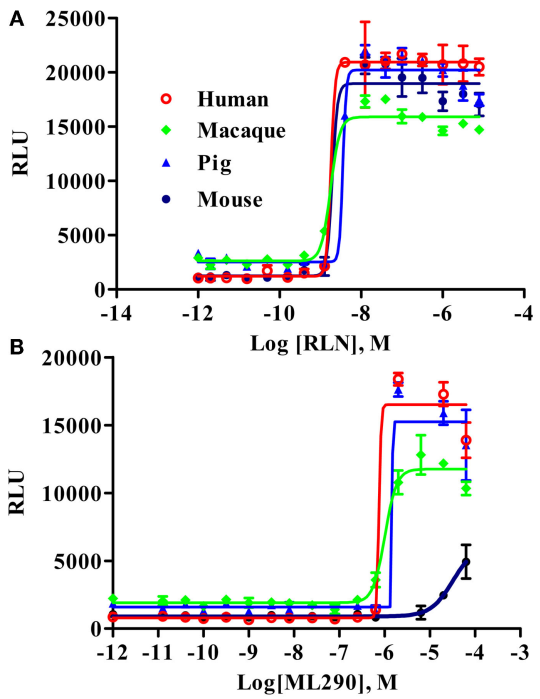

FIGURE 3 | Activation of macaque and pig RXFP1 receptors by RLN and ML290. **(A)** Porcine RLN-induced cAMP response. **(B)** ML290-induced cAMP response. HEK293T cells with CRE-luc reporter were transduced with BacMam RXFP1 expression vectors. RLU, relative luciferase units. Data are expressed as mean ± SEM.

TABLE 1 | Activation of RXFP1 receptors with relaxin and ML290.

Ligand	RLN	ML290
Receptor		
Human	***	***
Macaque	***	***
Pig	***	***
Guinea pig	***	No
Guinea pig/human	***	*
Rabbit 1 and 2	No	**
Human/rabbit	**	**
Rabbit 1(2)/human	No	**
Mouse	***	No

**Weak, **intermediate, ***strong activation of the receptor.*

with hRXFP1 were used as a control. As shown in **Figure 4**, G-RXFP1 responded to porcine RLN, although the maximum response was lower than that of hRXFP1. There was small response to ML290 only at highest concentration of compound used. A chimeric guinea pig receptor containing the TM3-C-terminal end of human RXFP1 was created (**Figure 1**); analysis of cAMP production in cells transfected with the chimeric receptor GH-RXFP1 showed ML290 responsiveness, albeit to a much lower level than in hRXFP1 ($p < 0.001$) (**Figure 4**; **Table 1**).

Characterization of Rabbit RXFP1

Two variants of rabbit *RXFP1* cDNA with and without the additional amino acid in the LDLa-LRRs linker (R1-RXFP1 and R2-RXFP1, respectively) were used in a transient transfection of HEK293T cells, and the cAMP response to ligand treatment was measured. Both failed to respond to porcine RLN, but generated an increase in cAMP after stimulation with ML290 (data not shown). One explanation for the lack of receptor activation could be poor expression of the rabbit receptors on the cell membrane. To test for cell surface expression, we used modified R1- and R2-constructs with a FLAG-tag at the N-terminal part of the receptor. Both receptors were expressed at the same or greater levels relative to a FLAG-tagged human RXFP1 (**Figure 5**). The HTRF assay on FLAG-tagged rabbit receptors failed to detect cAMP production when they were stimulated by porcine RLN. Stimulation with ML290 produced a cAMP increase in cells transfected with both rabbit receptors, albeit with lesser efficacy than hRXFP1 (**Figure 6**).

Two chimeric constructs were created to identify the region of the rabbit receptor responsible for its lack of RLN response: R1H-RXFP1 and R2H-RXFP1, which contain most of the ectodomain of the two rabbit receptors and the 7TM domain of hRXFP1; and HR-RXFP1, which contains most of the hRXFP1 ectodomain and rabbit 7TM (**Figure 1**). The N-terminus contains LRR4, 5, 6, and 8, which have been identified as the sites of RLN binding (2). As shown in **Figure 6A**, R1H-and R2H-RXFP1 were inactive when stimulated with porcine RLN, whereas HR-RXFP1 responded at a low level to RLN stimulation. While all three receptors respond to ML290, the level of activation of R1H- and R2H-RXFP1 was higher than that of R1-, R2-, or HR-RXFP1-transfected cells (**Figure 6B**; **Table 1**).

In addition to porcine RLN, we analyzed the response of the two rabbit RXFP1 variants to human and mouse RLN in the HTRF cAMP assay (**Figure 7A**). In all cases, 10 nM of peptide failed to stimulate cAMP production in cells transiently transfected with rabbit receptors, whereas they responded to 5 μM of ML290. Human receptor was active with all ligands.

To test the activity of rabbit receptor versus rabbit RLN (SQ10), we designed an expression construct of the latter gene. HEK293T cells were transfected with SQ10, and conditioned medium was used for activation of cells expressing rabbit, human, and guinea pig RXFP1s. Cells transfected with the latter two receptors responded to SQ10 treatment with cAMP production measured by the HTRF assay (**Figure 7B**). No response was recorded from cells transfected with R1- or R2-RXFP1, suggesting that rabbit RLN does not induce cAMP production through RXFP1 in rabbits.

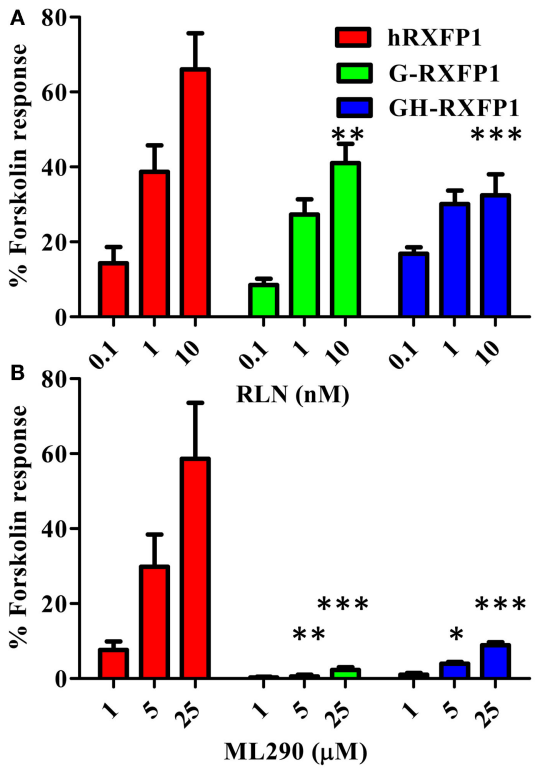

FIGURE 4 | Activation of guinea pig and guinea pig–human chimeric receptors by RLN and ML290. **(A)** Porcine RLN-induced cAMP response. **(B)** ML290-induced cAMP response. HEK293T cells were transiently transfected with RXFP1 expression vectors and cAMP was determined using HTRF cAMP assay. cAMP activity is expressed as the percentage of 10 μM Forskolin-stimulated response. Data are expressed as mean ± SEM, each point represent triplicate measurements. The experiment was repeated three times. *$p < 0.05$, **$p < 0.01$, ***$p < 0.001$ compared to hRXFP1.

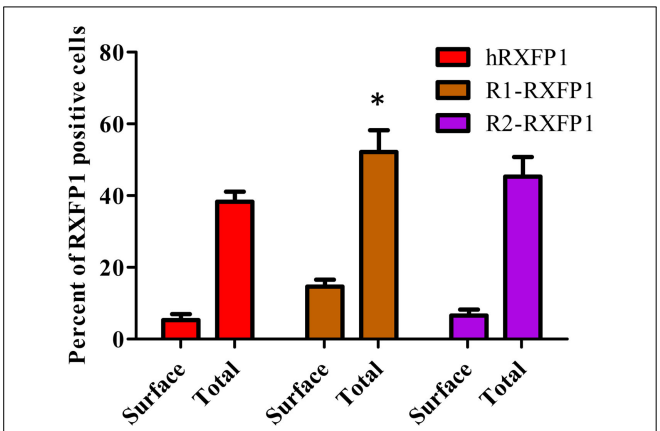

FIGURE 5 | Expression of two rabbit RXFP1 receptors compared to human RXFP1. Shown is the total and cell surface RXFP1 expression in transiently transfected HEK293T cells. Data are expressed as mean ± SEM, each point represent triplicate measurements. The experiment was repeated three times. *$p < 0.05$ compared to hRXFP1.

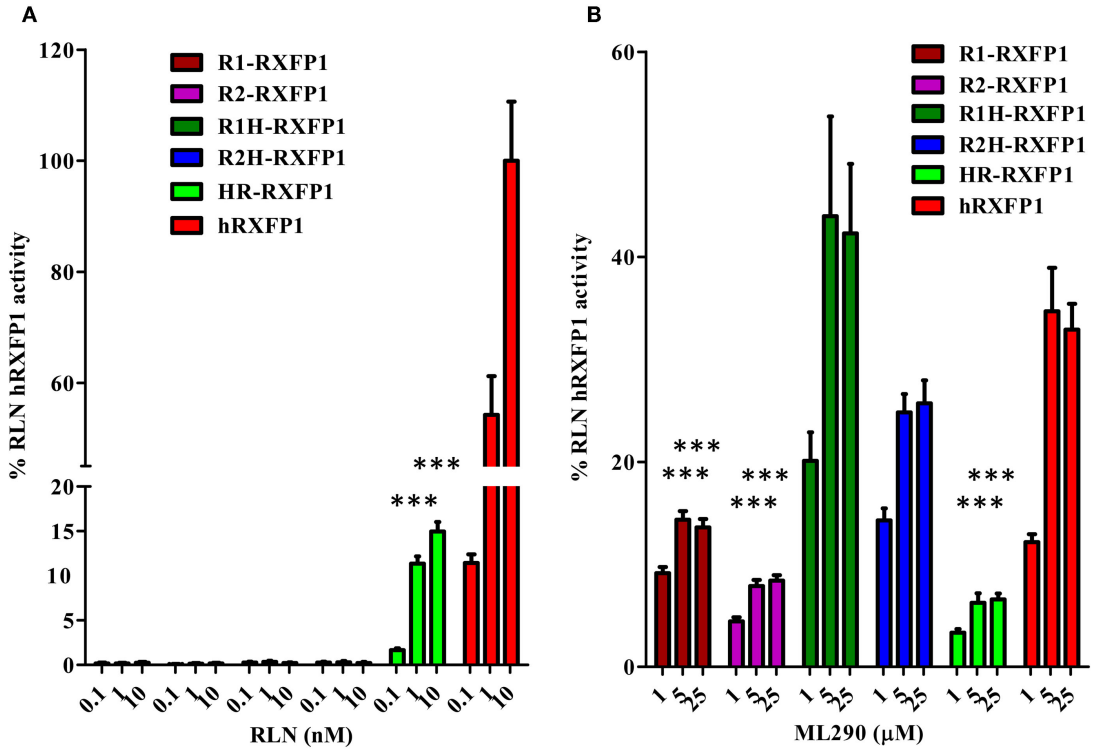

FIGURE 6 | Activation of rabbit and rabbit–human chimeric receptors by RLN and ML290. (A) Porcine RLN-induced cAMP response. **(B)** ML290-induced cAMP response. HEK293T cells were transiently transfected with RXFP1 expression vectors and cAMP was determined using the HTRF cAMP assay. cAMP activity is expressed as the percentage of hRXFP1 cAMP activation by 10 nM of RLN. Data are expressed as mean ± SEM; each point represents triplicate measurements. The experiment was repeated at least three times. ***$p < 0.001$ compared to hRXFP1.

Binding of Eu-human RLN to the rabbit R1-RXFP1 receptor was evaluated in a saturation binding assay using selected HEK293T cells with a high level of RXFP1 (**Figure 8**). The R1-RXFP1 was well-expressed on the cell surface membrane, with an even somewhat higher level than hRXFP1 (**Figure 8A**), similar to what was detected in transiently transfected cells. These cells were used in human RLN-binding experiments. While strong binding of labeled RLN was detected with human RXFP1, no binding to rabbit R1-RXFP1 receptor was found (**Figure 8B**). In the CRE-reporter-based cAMP assay, hRXFP1 and R1-RXFP1 were stimulated with human RLN and ML290. For ML290 treatment, the cAMP response in cells transfected with rabbit receptor measured using this approach was comparable to hRXFP1. At very high concentrations of RLN (>1 μM), there was some increase in β-gal activity for R1-RXFP1-transfected cells (**Figures 8C,D**).

Discussion

Due to its vasodilatory, antifibrotic, and cytoprotective properties, among others, RLN hormone induces pleotropic responses in multiple normal and diseased tissues and organs (2). In animal models, treatment with RLN has shown therapeutic effects in induced liver, pulmonary, kidney, and heart fibrosis, as well as diabetes, ischemia–perfusion injury, wound healing, and other common diseases. Most of these studies were performed with rodents, although other species were used to a lesser degree. However, there are noted differences in the physiology of this hormone in other species; for instance, the concentration of RLN during pregnancy in mice is 100 times higher than in women (1). The largest clinical trial of the therapeutic use of RLN was in acute heart failure patients (4). The data indicated the possible benefits of even short-term intravenous RLN administration. We have recently reported the discovery of the first small-molecule agonist series for the RLN receptor (5, 6). This has raised the possibility of developing a therapeutic agent with high stability, activity, specificity, and potentially oral delivery. However, we have shown that the identified compounds did not activate the mouse RLN receptor. Using chimeric human–mouse receptors and site-specific mutagenesis, we have determined that the amino acid sequence of the ECL3 of the 7TM determines the receptor selectivity. The mutation of four amino acids in the mouse receptor ECL3 made it responsive to small agonist treatment. Analysis of the available sequences in GenBank revealed that both rat and hamster RXFP1s have the mouse variant of ECL3, and thus these rodents could not be used for the analysis of small molecules. Here, we have cloned and tested the functional activation of RXFP1s from mammals of four different orders, Primates (rhesus macaque), Artodactyla (pig), Lagomorpha (rabbit), and Rodentia (guinea pig). The data show that the RXFP1 receptors from the first two species are fully activated by RLN and ML290 and hence, the corresponding animal models can

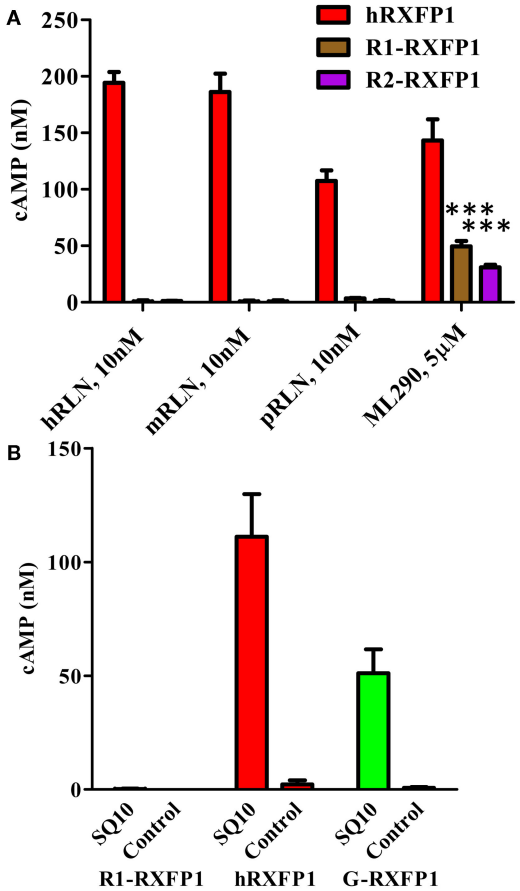

FIGURE 7 | Activation of rabbit receptors by relaxin peptides from different species. **(A)** Activation of two rabbit receptor variants (R1- and R2-RXFP1) and hRXFP1with 10 nM of human (hRLN), mouse (mRLN), and porcine (pRLN) relaxin peptides, and by 5 μM of ML290. Treatments of rabbit RXFP1 are statistically significant compared to hRXFP1, $^{***}p < 0.001$. **(B)** Activation of rabbit (R1-), human (h), and guinea pig (G-) RXFP1s with rabbit relaxin SQ10. Conditioned media from HEK293T cells transfected with SQ10 and control empty vector was used for cell stimulation. cAMP activity is expressed as the percentage of 10 μM Forskolin stimulation for each type of cells. Data are expressed as mean ± SEM; each point represents triplicate measurements. The experiment was repeated at least three times. Treatment of R1-RXFP1 is statistically significant ($p < 0.0001$) compared to hRXFP1 or G-RXFP1.

be used for RLN and ML290 studies. Guinea pig RXFP1 does not respond to ML290. The use of rabbit in studies of RLN biology should be further critically assessed as in our experiments RLN did not bind to the rabbit RXFP1 receptors nor did it activate cAMP response at physiologically relevant concentrations (**Table 1**).

The availability of genome sequencing data allows quick retrieval of gene information. However, a critical appraisal of this information is required. In the case of RXFP1, the genomic structure of cloned human, mouse, and rat receptors is well-established and each comprises 18 coding exons (16). The same conserved structure was annotated for macaque and pig genes. In the case of guinea pig and rabbit, we identified the missing first exon using a BLAST search of the genomic DNA. The correct assembly of the ORFs was further confirmed by RT-PCR isolation of the full-length cDNAs, cloning, and sequencing. We found two splice variants of the rabbit receptor mRNA, an apparent consequence of a mutation in the splice site of the intron 3/exon 4 boundary, which results in one extra amino acid in the LDL–LRR linker. While splice variants of hRXFP1 affecting full exons were described (13, 17, 18), such additional insertion of only three nucleotides is unique for rabbit RXFP1.

Comparison of the various sequences indicated that pig, rabbit, and guinea pig receptors share the same ECL3 sequence, differing from the human and monkey sequence by only one amino acid (V647). Multiple substitutions were found in the rabbit sequence, including three unique substitutions in the LDLa domain, numerous changes in the LDLa–LRR linker (17 unique amino acids) and in several LRR repeats. Notably, all previously identified amino acids essential for the structural and functional integrity of human RXFP1 remained conserved in the rabbit receptor: amino acids required for the coordination of Ca^{2+} binding and receptor activation in the LDLa domain (19, 20), previously described LRR amino acids important for primary RLN binding by the RXFP1 ectodomain (2), and the sites crucial for secondary binding of RLN peptide to the ECL1 or ECL2 (21). However, there is a substitution of serine at amino acid 33, which is proline in all the other RXFP1 receptors. This residue is located next to one of the crucial cysteine residues in the LDLa module that are essential for its function. It is possible that this substitution results in a structural perturbation in the LDLa module. Additionally, there are numerous proline substitutions in the LDLa–LRR linker region which would result in structural changes in this domain. Recent studies have suggested that this linker region may have an important role in receptor activation by the LDLa module (14).

Analysis of RLN response measured by cAMP production revealed RLN activity in all but the rabbit receptor. Neither of the two rabbit RXFP1 variants responded to stimulation with RLN peptides from various mammalian species, including previously described rabbit RLN homolog SQ10 (22). Moreover, we were not able to detect binding of labeled human recombinant RLN to the rabbit receptor. Taken together, the homology of the isolated rabbit clones with other species RXFP1s, almost identical sequence of our cDNAs to the GenBank genomic DNA, and identity of the cloned cDNA with the DNA obtained by direct sequencing of the isolated RT-PCR fragments all suggest that we have isolated the correct full-length rabbit RXFP1 clones. The rabbit receptors were activated by ML290, indicating their functionality.

It was recently suggested that there are five copies of the RLN gene in the rabbit genome, which raises the question of whether the rabbit RLN peptide used in our experiments is correct (23). Putative translation of two rabbit RLN genes produced identical peptides. The three other RLN genes encoding putative rabbit RLN peptides each differ from the first two by a single evolutionary non-conserved amino acid (23). The sequence of the first peptide was also identical to the previously reported sequence encoded by SQ10 cDNA obtained by RT-PCR (9) and partial protein sequencing (24). Therefore, we decided to use SQ10 cDNA in our experiments to generate rabbit RLN. Importantly, it activated

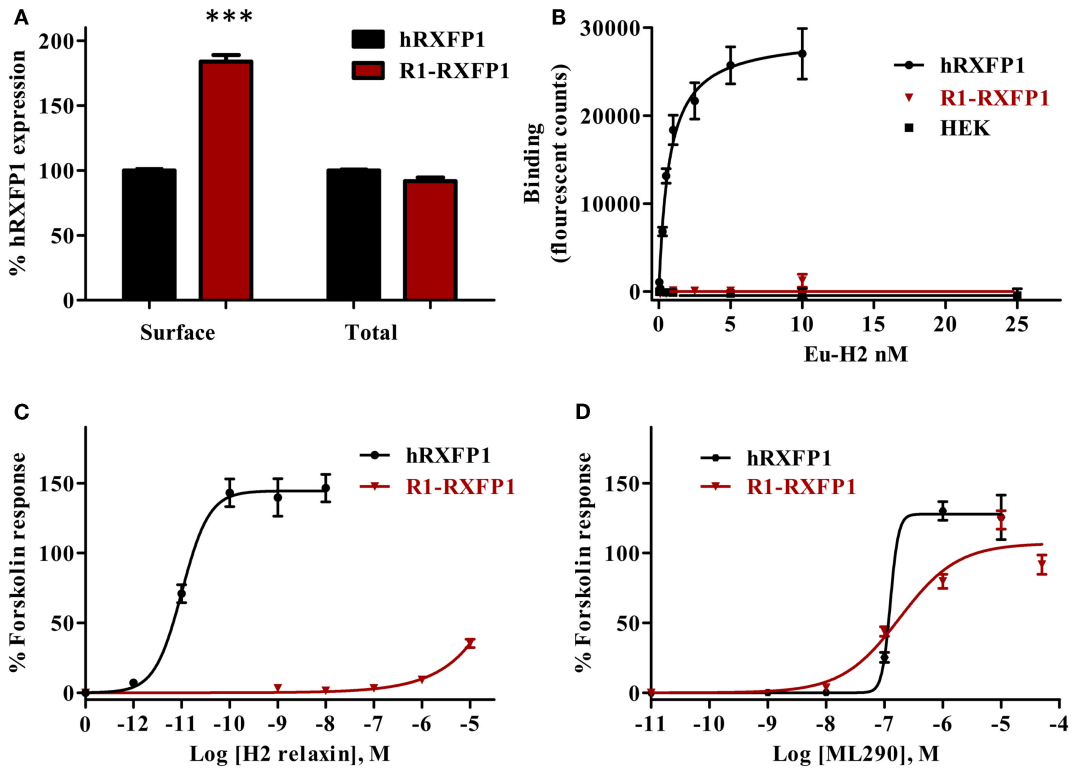

FIGURE 8 | Rabbit RXFP1 does not bind relaxin peptide. **(A)** Total and cell surface expression of hRXFP1 and R1-RXFP1. Expression is normalized to the expression of human receptor. ***$p < 0.001$ compared to hRXFP1. **(B)** Saturation binding using Eu-labeled H2 RLN. **(C)** Human RLN-induced cAMP response. **(D)** ML290-induced cAMP response. cAMP activity is expressed as the percentage of the 5 μM Forskolin-stimulated response for each receptor. Data are expressed as mean ± SEM; each point represents triplicate measurements. The experiment was repeated at least three times.

human and guinea pig receptors and thus was fully functional. Taking into account that there is only a single amino acid difference between the SQ10 sequence and other three putative peptides, it seems highly unlikely that the latter RLNs will activate rabbit RXFP1.

Surprisingly, in an indirect assay, activation of a CRE-reporter was detected when RLN was used at a concentration far exceeding the detected serum RLN range in rabbits (25). Similarly, activation of the CRE-reporter was observed with high-dose ML290 treatment on the mouse receptor, despite no activation being seen in the direct HTRF cAMP assay. One explanation is that ligand interactions with the receptor triggered signaling pathways other than cAMP in both CRE-reporter assays, which then affected CRE transcriptional activity (26). It was demonstrated that RLN activated various signaling pathways in cells expressing RXFP1 (27, 28). It should be noted, however, that the fact that we were not able to detect human RLN binding to the rabbit receptor in our assays contradicts this suggestion.

Another possible explanation for the loss of activity of rabbit receptors is that the activation of rabbit receptor by RLN requires dimerization or interaction with other GPCRs or other cellular partners. It is possible that such partners might be rabbit-specific or that the receptor works only in rabbit cells. Such interactions have been shown; for instance, RXFP1 can directly interact with the angiotensin II type 2 receptor to regulate downstream cellular signaling (29). It is also possible that rabbit RLNs do not signal through RXFP1, and other ligands activate this receptor. In any of these scenarios, the question of whether rabbit is an appropriate model for RLN studies should be carefully examined. One might wonder if treatment of rabbits rather than guinea pigs with serum from the pregnant animals in Dr. Hisaw's original experiments would have led to the discovery of RLN.

The rabbit and guinea pig receptors provide new structural templates for analysis of RLN and ML290 activation of RXFP1. Using chimeric human and rabbit receptors, we showed here that the extracellular part of the rabbit receptor is responsible for the failure of RLN activation. Indeed, it was shown that primary binding of RLN to RXFP1 involve sites within LRR4, 5, 6, and 8 (2). In contrast, the 7TM region of RXFP1, which is the site of allosteric small-molecule agonist binding, is functional in rabbits. The opposite was true for guinea pig RXFP1: despite having the same ECL3 sequence as pig or rabbit RXFP1, the receptor was activated by ML290 only at highest concentration of ML290 and with much lower efficacy than hRXFP1. As noted above, one potential site of ML290 interaction with the receptor is ECL3 (5). To further define the region of interaction, we substituted the C-terminus guinea pig fragment with human sequence in chimeric GH-RXFP1. This part contained peptide regions adjacent to ECL3: TM3–7, ICL2–3, and ECL2–3. The data showed that the efficacy of ML290 stimulation was improved, however,

it was still lower than in hRXFP1-transfected cells. Thus, specific amino acids in the guinea pig TM1–3, or their interaction with TM3–7 amino acids might be responsible for ML290 binding or activation. Importantly, a modified mouse receptor with humanized ECL3 is activated by ML290 (5). Thus, amino acid substitutions unique for the guinea pig 7TM domain and not present in other species might be responsible for the lack of activation with ML290. Identification of such sites might help in understanding the structural basis of ML290 and RXFP1 interactions. Collectively, our data demonstrate that different parts of the receptor are important for RLN- or ML290-induced activation and thus indicate the allosteric mode of activation by two ligands.

In summary, the information derived from this study may help in the selection of appropriate animal models to study the biological effects of RLN and ML290. The comparisons of RXFP1 sequences have provided further insights into the structural basis, mechanism of activation, and selectivity of peptide and small-molecule agonists for RXFP1.

Acknowledgments

The authors thank Dr. O. David Sherwood, University of Illinois, for providing porcine relaxin; Prof. John D. Wade, Florey Institute of Neuroscience and Mental Health, Melbourne, VIC, Australia, for providing mouse relaxin peptide; Corthera, Inc. (San Mateo, CA, USA) for providing recombinant human relaxin and Sharon Layfield and Tania Ferraro for technical assistance with studies at the Florey and Shashank Pawitwar and Supurna Dhar for their help in cloning rabbit and guinea pig receptors. This research was supported by Florida Department of Health, James and Esther King Biomedical Research Program grant 3KFO1, and National Cancer Institute grant 1U01CA177711 (AA). Research at the Florey was supported by National Health and Medical Research Council of Australia project grants 628427 and 1043750 and by the Victorian Government Operational Infrastructure Support Program. RADB is a recipient of an NHMRC Research Fellowship. BH is a recipient of a MARC U*STAR program fellowship at the Florida International University.

References

1. Sherwood OD. Relaxin's physiological roles and other diverse actions. *Endocr Rev* (2004) **25**:205–34. doi:10.1210/er.2003-0013
2. Halls ML, Bathgate RA, Sutton SW, Dschietzig TB, Summers RJ. International Union of Basic and Clinical Pharmacology. XCV. Recent advances in the understanding of the pharmacology and biological roles of relaxin family peptide receptors 1-4, the receptors for relaxin family peptides. *Pharmacol Rev* (2015) **67**:389–440. doi:10.1124/pr.114.009472
3. Hsu SY, Nakabayashi K, Nishi S, Kumagai J, Kudo M, Sherwood OD, et al. Activation of orphan receptors by the hormone relaxin. *Science* (2002) **295**:671–4. doi:10.1126/science.1065654
4. Teerlink JR, Cotter G, Davison BA, Felker GM, Filippatos G, Greenberg BH, et al. Serelaxin, recombinant human relaxin-2, for treatment of acute heart failure (RELAX-AHF): a randomised, placebo-controlled trial. *Lancet* (2013) **381**:29–39. doi:10.1016/S0140-6736(12)61855-8
5. Xiao J, Huang Z, Chen CZ, Agoulnik IU, Southall N, Hu X, et al. Identification and optimization of small-molecule agonists of the human relaxin hormone receptor RXFP1. *Nat Commun* (2013) **4**:1953. doi:10.1038/ncomms2953
6. Chen CZ, Southall N, Xiao J, Marugan JJ, Ferrer M, Hu X, et al. Identification of small-molecule agonists of human relaxin family receptor 1 (RXFP1) by using a homogenous cell-based cAMP assay. *J Biomol Screen* (2013) **18**:670–7. doi:10.1177/1087057112469406
7. Tatusova TA, Madden TL. BLAST 2 Sequences, a new tool for comparing protein and nucleotide sequences. *FEMS Microbiol Lett* (1999) **174**:247–50. doi:10.1111/j.1574-6968.1999.tb13575.x
8. Edgar RC. MUSCLE: a multiple sequence alignment method with reduced time and space complexity. *BMC Bioinformatics* (2004) **5**:113. doi:10.1186/1471-2105-5-113
9. Fields P, Kondo S, Tashima L, Bryant-Greenwood G, Greenwood F. Expression of SQ10 (a preprorelaxin-like gene) in the pregnant rabbit placenta and uterus. *Biol Reprod* (1995) **53**:1139–45. doi:10.1095/biolreprod53.5.1139
10. Sherwood CD, O'Byrne EM. Purification and characterization of porcine relaxin. *Arch Biochem Biophys* (1974) **160**:185–96. doi:10.1016/S0003-9861(74)80025-1
11. Chen W, Shields TS, Stork PJ, Cone RD. A colorimetric assay for measuring activation of Gs- and Gq-coupled signaling pathways. *Anal Biochem* (1995) **226**:349–54. doi:10.1006/abio.1995.1235
12. Shabanpoor F, Bathgate RA, Belgi A, Chan LJ, Nair VB, Wade JD, et al. Site-specific conjugation of a lanthanide chelator and its effects on the chemical synthesis and receptor binding affinity of human relaxin-2 hormone. *Biochem Biophys Res Commun* (2012) **420**:253–6. doi:10.1016/j.bbrc.2012.02.141
13. Scott DJ, Layfield S, Yan Y, Sudo S, Hsueh AJ, Tregear GW, et al. Characterization of novel splice variants of LGR7 and LGR8 reveals that receptor signaling is mediated by their unique low density lipoprotein class A modules. *J Biol Chem* (2006) **281**:34942–54. doi:10.1074/jbc.M602728200
14. Bruell S, Kong RC, Petrie EJ, Hoare B, Wade JD, Scott DJ, et al. Chimeric RXFP1 and RXFP2 receptors highlight the similar mechanism of activation utilizing their N-terminal low-density lipoprotein class A modules. *Front Endocrinol* (2013) **4**:171. doi:10.3389/fendo.2013.00171
15. Yan Y, Scott DJ, Wilkinson TN, Ji J, Tregear GW, Bathgate RA. Identification of the N-linked glycosylation sites of the human relaxin receptor and effect of glycosylation on receptor function. *Biochemistry* (2008) **47**:6953–68. doi:10.1021/bi800535b
16. Scott DJ, Layfield S, Riesewijk A, Morita H, Tregear GW, Bathgate RA. Identification and characterization of the mouse and rat relaxin receptors as the novel orthologues of human leucine-rich repeat-containing G-protein-coupled receptor 7. *Clin Exp Pharmacol Physiol* (2004) **31**:828–32. doi:10.1111/j.1440-1681.2004.04075.x
17. Muda M, He C, Martini PG, Ferraro T, Layfield S, Taylor D, et al. Splice variants of the relaxin and INSL3 receptors reveal unanticipated molecular complexity. *Mol Hum Reprod* (2005) **11**:591–600. doi:10.1093/molehr/gah205
18. Kern A, Hubbard D, Amano A, Bryant-Greenwood GD. Cloning, expression, and functional characterization of relaxin receptor (leucine-rich repeat-containing g protein-coupled receptor 7) splice variants from human fetal membranes. *Endocrinology* (2008) **149**:1277–94. doi:10.1210/en.2007-1348
19. Kern A, Agoulnik AI, Bryant-Greenwood GD. The low-density lipoprotein class A module of the relaxin receptor (leucine-rich repeat containing G-protein coupled receptor 7): its role in signaling and trafficking to the cell membrane. *Endocrinology* (2007) **148**:1181–94. doi:10.1210/en.2006-1086
20. Kong RC, Petrie EJ, Mohanty B, Ling J, Lee JC, Gooley PR, et al. The relaxin receptor (RXFP1) utilizes hydrophobic moieties on a signaling surface of its N-terminal low density lipoprotein class A module to mediate receptor activation. *J Biol Chem* (2013) **288**:28138–51. doi:10.1074/jbc.M113.499640
21. Diepenhorst NA, Petrie EJ, Chen CZ, Wang A, Hossain MA, Bathgate RA, et al. Investigation of interactions at the extracellular loops of the relaxin family peptide receptor 1 (RXFP1). *J Biol Chem* (2014) **289**:34938–52. doi:10.1074/jbc.M114.600882
22. Eldridge RK, Fields PA. Rabbit placental relaxin: purification and immunohistochemical localization. *Endocrinology* (1985) **117**:2512–9. doi:10.1210/endo-117-6-2512
23. Arroyo JI, Hoffmann FG, Opazo JC. Gene duplication and positive selection explains unusual physiological roles of the relaxin gene in the European rabbit. *J Mol Evol* (2012) **74**:52–60. doi:10.1007/s00239-012-9487-2
24. Fields PA, Lee VH, Jetten A, Chang SM, Fields MJ. B-chain sequence and in situ hybridization of the rabbit placental relaxin-like gene product. *Biol Reprod* (1999) **61**:527–32. doi:10.1095/biolreprod61.2.527

25. Kikkawa Y, Matsuo S, Kurogi R, Nakamizo A, Mizoguchi M, Sasaki T. Upregulation of relaxin after experimental subarachnoid hemorrhage in rabbits. *Biomed Res Int* (2014) **2014**:836397. doi:10.1155/2014/836397
26. Lonze BE, Ginty DD. Function and regulation of CREB family transcription factors in the nervous system. *Neuron* (2002) **35**:605–23. doi:10.1016/S0896-6273(02)00828-0
27. Hashem G, Zhang Q, Hayami T, Chen J, Wang W, Kapila S. Relaxin and beta-estradiol modulate targeted matrix degradation in specific synovial joint fibrocartilages: progesterone prevents matrix loss. *Arthritis Res Ther* (2006) **8**:R98. doi:10.1186/ar1978
28. Kapila S, Xie Y, Wang W. Induction of MMP-1 (collagenase-1) by relaxin in fibrocartilaginous cells requires both the AP-1 and PEA-3 promoter sites. *Orthod Craniofac Res* (2009) **12**:178–86. doi:10.1111/j.1601-6343.2009.01451.x
29. Chow BS, Kocan M, Bosnyak S, Sarwar M, Wigg B, Jones ES, et al. Relaxin requires the angiotensin II type 2 receptor to abrogate renal interstitial fibrosis. *Kidney Int* (2014) **86**:75–85. doi:10.1038/ki.2013.518

Conflict of Interest Statement: The authors declare that the research was conducted in the absence of any commercial or financial relationships that could be construed as a potential conflict of interest.

frontiers in Endocrinology

REVIEW
published: 14 September 2015
doi: 10.3389/fendo.2015.00142

Discovery and development of small molecule allosteric modulators of glycoprotein hormone receptors

Selvaraj G. Nataraja[1], Henry N. Yu[1,2] and Stephen S. Palmer[1]*

[1] TocopheRx Inc., Burlington, MA, USA, [2] EMD Serono Research and Development Institute Inc., Billerica, MA, USA

OPEN ACCESS

Edited by:
James A. Dias, University at Albany State University of New York, USA

Reviewed by:
Smita D. Mahale, National Institute for Research in Reproductive Health, India
John S. S. Davis, University of Nebraska Medical Center, USA

***Correspondence:**
Selvaraj G. Nataraja, TocopheRx Inc., 15 New England Executive Park, Suite 1087, Burlington, MA 01803, USA selva@tocopherx.com

Specialty section:
This article was submitted to Molecular and Structural Endocrinology, a section of the journal Frontiers in Endocrinology

Received: *01 June 2015*
Accepted: *31 August 2015*
Published: *14 September 2015*

Citation:
Nataraja SG, Yu HN and Palmer SS (2015) Discovery and development of small molecule allosteric modulators of glycoprotein hormone receptors. Front. Endocrinol. 6:142. doi: 10.3389/fendo.2015.00142

Glycoprotein hormones, follicle-stimulating hormone (FSH), luteinizing hormone (LH), and thyroid-stimulating hormone (TSH) are heterodimeric proteins with a common α-subunit and hormone-specific β-subunit. These hormones are dominant regulators of reproduction and metabolic processes. Receptors for the glycoprotein hormones belong to the family of G protein-coupled receptors. FSH receptor (FSHR) and LH receptor are primarily expressed in somatic cells in ovary and testis to promote egg and sperm production in women and men, respectively. TSH receptor is expressed in thyroid cells and regulates the secretion of T3 and T4. Glycoprotein hormones bind to the large extracellular domain of the receptor and cause a conformational change in the receptor that leads to activation of more than one intracellular signaling pathway. Several small molecules have been described to activate/inhibit glycoprotein hormone receptors through allosteric sites of the receptor. Small molecule allosteric modulators have the potential to be administered orally to patients, thus improving the convenience of treatment. It has been a challenge to develop a small molecule allosteric agonist for glycoprotein hormones that can mimic the agonistic effects of the large natural ligand to activate similar signaling pathways. However, in the past few years, there have been several promising reports describing distinct chemical series with improved potency in preclinical models. In parallel, proposal of new structural model for FSHR and *in silico* docking studies of small molecule ligands to glycoprotein hormone receptors provide a giant leap on the understanding of the mechanism of action of the natural ligands and new chemical entities on the receptors. This review will focus on the current status of small molecule allosteric modulators of glycoprotein hormone receptors, their effects on common signaling pathways in cells, their utility for clinical application as demonstrated in preclinical models, and use of these molecules as novel tools to dissect the molecular signaling pathways of these receptors.

Keywords: small molecule allosteric modulators, follicle-stimulating hormone, leutinizing hormone/chorionic gonadotropin, thyroid-stimulating hormone, G protein-coupled receptor, glycoprotein hormone receptors, leucine-rich repeat

Introduction

Glycoprotein hormones, FSH, LH, and TSH, are secreted from the anterior pituitary gland (1, 2). These hormones are composed of two subunits, a common α-subunit and a hormone-specific β-subunit (2, 3). Specificity of the hormone for receptor binding is determined by the β-subunit (4, 5). Chorionic gonadotropin (CG), a homolog of LH, is secreted from the placenta of primates during pregnancy (6, 7). Human CG β-subunit (beta-hCG) gene has evolved from LH β-subunit by gene duplication and reading through into the 3′ untranslated region (8–10). Beta-hCG differs from LH β-subunit at the C-terminal end of the protein, which contains additional 34 amino acids called the C-terminal peptide (CTP) (11). Glycoprotein hormones are characterized by glycosylation of both subunits (11, 12). The common α-subunit carries two N-linked glycans and the β-subunits of all three glycoproteins have one or two N-linked glycans (13). Human CGβ has additional four O-linked glycans in their CTP (14). The N-linked oligosaccharide chains have a minor role in receptor binding of glycoprotein hormones, but they are critical for bioactivity (15). Glycoprotein hormones lacking N-linked oligosaccharides behave as antagonists (16–19). On the other hand, it was suggested that the four O-linked oligosaccharides play an important role in the survival of hCG in circulation, and thus increasing the half-life of the protein (15, 20). Naturally occurring glycosylation variants of hFSH and hCG with differing activity in human granulosa cells have been described (14, 21–23).

Stimulation of FSH and LH secretion is controlled by gonadotropin-releasing hormone (GnRH), released from the hypothalamus (24, 25). FSH and LH secretion from the pituitary is also modulated by gonadal feedback through steroid and protein factors (26–28). Gonadotropins, FSH and LH, play critical roles in regulating reproduction. In females, FSH induces follicular development, while LH stimulates egg maturation and ovulation in ovaries, and subsequently supports the corpus luteum (29, 30). In males, FSH supports early stages of sperm production in testes and LH stimulates final maturation of sperm through stimulation of testosterone from Leydig cells (31).

Thyrotrophin-releasing hormone (TRH), released from the hypothalamus, regulates TSH secretion with fine tuning by the feedback action of thyroxine (T4) and tri-iodo-thyronine (T3) (32, 33). The primary role of TSH is in stimulating the growth of thyrocytes and biosynthesis of thyroid hormone (T3/T4) through increased uptake of iodide by thyrocytes (34–36). TSHR is also a major autoantigen for autoimmune processes in Grave's disease (37–41).

Receptors for the glycoprotein hormones belong to the large family of G protein-coupled receptors (GPCRs) that play crucial roles in cellular homeostasis. While GPCRs account for only 3% of the human functional genes, this class of proteins have proven to be extremely valuable as targets for drug discovery with >30% of the small molecule therapeutics developed to date modulating this class of membrane proteins (42–44). Common features shared by GPCRs are their hepta-helical or 7-transmembrane domain (7TM) that links an N-terminal extracellular domain with a C-terminal intracellular domain. The 7TM domain of GPCRs have, in common, three extracellular loops and three intracellular loops that have been shown to be involved in transmission of hormone-binding events into cellular signaling responses (45). GPCRs are activated by variety of stimuli, such as glycoproteins, peptides, neurotransmitters, and ions (46).

The GPCR superfamily can be divided into subfamilies on the basis of phylogenetic analysis of the sequence (47). Glycoprotein hormone receptors belong to the leucine-rich repeat containing GPCR (LGR) subfamily (48). The LGR subfamily is part of the larger Family-A or rhodopsin like GPCR (42, 49). LGRs differ from other Family-A receptors through their extracellular domain. While non-LGRs have a short extracellular region and bind small molecules (e.g., aminergic receptor, opioid receptor, etc.), LGRs have exceptionally large extracellular domains with the leucine-rich repeats (LRRs) of about 340–420 amino acids (50). Binding of glycoprotein hormone to their receptor leads to activation of the receptor by stabilizing the active confirmation (51). Active receptor, in turn, communicates the extracellular event to intracellular signal transducers primarily through a G-protein heterodimer leading to the dissociation of the α and β, γ subunits (52, 53). Following dissociation, the α-subunit stimulates adenylate cyclase, and consequently increases cAMP (54). Increase in intracellular cAMP results in activation of PKA (54). In parallel, the β, γ subunits recruit GPCR-kinases (GRK) to phosphorylate the receptor. This, in turn, leads to the recruitment of β-arrestin to the receptor, resulting in downregulation of the receptor (53, 55–57). In addition to the classical intracellular signal, cAMP, activated glycoprotein hormone receptors have also been shown to invoke other signaling pathways like Ca^{2+}, MAPK, and Akt (**Figure 1**) (54, 58–60). In summary, glycoprotein hormones or FSH, as shown in **Figure 1**, provokes a complex pattern of gene expression through actions of many different signaling cascades culminating in their physiological response.

Structure of Glycoprotein Hormone and Their Receptor

Structural determination of glycoprotein heterodimers bound to their cognate GPCRs is extremely challenging. However, several groups have utilized improved technological advances in molecular biology, structural biology, and impressive crystallization methods to stabilize and anchor GPCRs to obtain quality crystals. Solving the crystal structure of hCG was a major milestone in the early quest for elucidating the structure for glycoprotein hormones (61, 62). Subsequently, Fox et al. determined the crystal structure of βThr26Ala hFSHR, a partially deglycosylated protein (63). These studies interestingly revealed that both subunits of glycoprotein hormones are folded into elongated non-globular structures belonging to the cysteine-knot superfamily, which includes some growth factors. The heterodimer is stabilized by a segment of the beta subunit, which wraps around the alpha subunit and is covalently linked like a seat belt (61–63). Based on charge distribution, β93–100 (determinant loop), located at the center of the "seatbelt" of beta-hCG conferred specificity of the hormone binding to the receptor. This has been confirmed experimentally by several groups (64–66). In addition to the determinant loop, a second site in the β subunit, L2β has also been implicated in hormone binding to the receptor (67–69). In α-subunit, the CTP 88–92, is required for receptor activation of

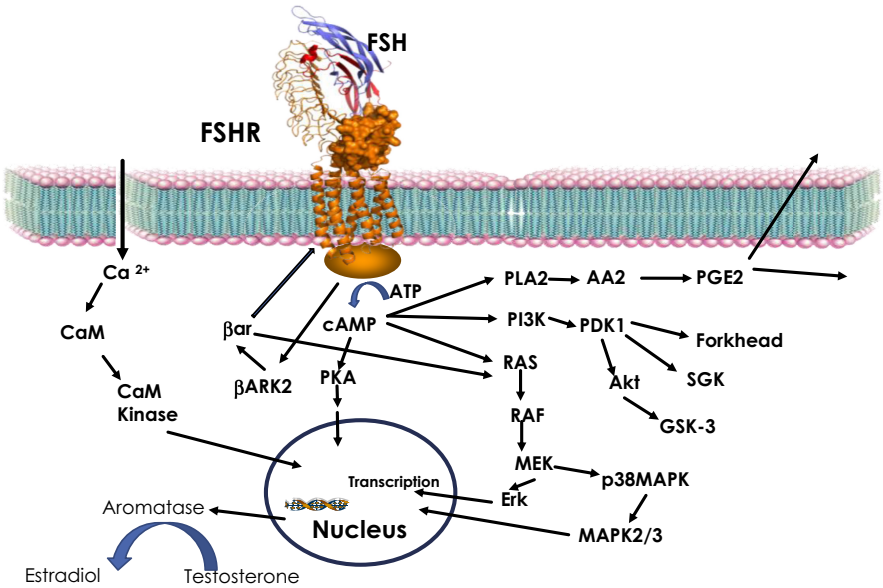

FIGURE 1 | FSH signaling. Activation of FSHR by FSH leads to increase in intracellular cAMP through Gs-adenylate cyclase. Increased cAMP leads to PKA activation, which regulate expression of several genes through phosphorylation of transcription factors like CREBP. FSH also causes increase in Ca^{2+} by depolarization of Ca channels. Increased Ca^{2+} can upregulate calmodulin kinase leading to modulation of downstream effectors. In addition to cAMP, FSH has also been shown to modulate PLA, Erk, p38 MAPK, and PI3Kinase pathways. Activated FSHR is phosphorylated by BARK, which in turn recruits β-arrestin to the receptor and lead to down regulation of FSHR, in addition, β-arrestin independently can activate Erk pathway.

intracellular signals (70–72). Thus, these three regions of the hormone, the determinant loop, the L2β loop of the β-subunit, and the CTP of the α-subunit, are the major contributors of receptor binding and activation.

Extracellular domain of these receptors can be further divided into two distinct regions, the N-terminal LRR domains, and the hinge region that connects the LRRs to the TMD. In 1990s, several groups identified the importance of the LRR of the extracellular domain of glycoprotein hormone receptor for ligand interaction (73–75). Elucidation of the crystal structure of FSH complexed with truncated FSHR in 2005 by Fan and Hendrickson revealed a detailed interaction of the hormone with the extracellular domain of the receptor (76). The crystal structure revealed that FSH binds to FSHR like "a handclasp" (76). According to their hypothesis, the basal receptor exists as a monomer and ligand binding induces formation of an activated dimer. Recent crystal structure analysis of the complete ectodomain of FSHR confirms that the heterodimeric FSH is bound into the concave surface of LRR in a "handclasp" fashion similar to that described by Fan and Hendrickson (77).

The concave high-affinity hormone-binding surface in the LRR region is a common feature among other members of this family of LRR-GPCRs. TSH and the TSHR stimulating monoclonal antibody M22 bind to the corresponding concave surface of TSHR in the complex (78, 79). Very recently crystal structure of R-spondin with LGR4 and LGR5 revealed that the concave surface of these LGRs is the sole interacting site for R-spondin (50, 80).

The role of the hinge domain in hormone binding and signal transduction has been intensively investigated (81–86). Jiang and co-workers identified a critical function for the sulfated Tyr-335 (sTyr) in the FSHR hinge region as a second interaction site with FSH (**Figure 2**) (77). According to their findings, binding of FSH to the high-affinity inner concave face of the ECD is a transitory event. This first binding event is followed by the formation of sTyr-binding pocket at the interface of α and β subunits of FSH. Then, sTyr is drawn into the pocket lifting the hairpin loop. The lift of the loop releases the inhibitory nature of the hairpin loop and activation of the transmembrane domain. A sulfated tyrosine located in the hinge domain of both LH/CGR and TSHR is also essential for the activation of the hairpin loop domain by their respective ligands (87, 88), suggesting that glycoprotein receptors utilize a common two-step mechanism for ligand recognition and activation.

Glycoprotein hormone receptors have been proposed to undergo dimerization in living cells (86, 89–92). The previous crystal structure of FSH with the extracellular domain of FSHR, lacking the hinge domain, proposed that the dimeric FSH-FSHR may be involved in receptor signaling (76). Evidence supporting intermolecular co-operativity as a component of transactivation of receptor has been cited as supportive evidence for the activated form of the receptor to be a dimer for all three glycoprotein receptors (86, 90, 93, 94). In a very elegant series of genetic models, Huhtaniemi's group demonstrated that in LHR deficient mice co-expressing equal ratios of both binding deficient and signaling-deficient forms of LHR receptor transactivation can reestablish normal LHR function through intermolecular interaction to restore spermatogenesis (95). In contrast, in transgenic mice expressing only the binding deficient receptor or the signaling-deficient receptor, males were spermatogenically incompetent.

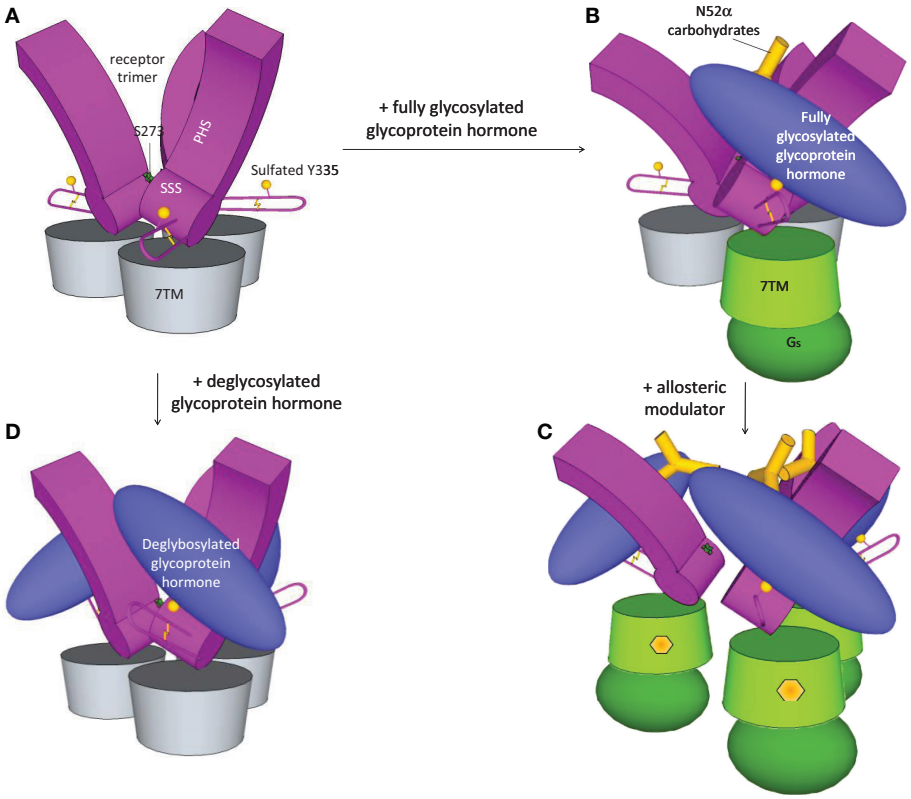

FIGURE 2 | Activation of FSHR. Based on the recent crystal structure (77), FSHR exists as trimer in the basal state **(A)**. FSH binding leads to dissociation and activation of the receptor **(B)**. Due to the bulky glycan, only one FSH can bind to the trimeric FSHR. Small molecule modulators by binding to the allosteric site in the transmembrane domain opens up the receptor and enables three FSH binding **(C)**. On the other hand, three deglycosylated FSH can bind to the trimeric receptor without dissociation and activation of the receptor **(D)**.

Further, single-molecule analysis of these mutant receptors reveal diverse structural assembly of LHR with varying degree of oligomerization that can regulate signaling of the receptor (96).

Zonen and co-workers propose that ligand binding induces strong negative cooperativity within the glycoprotein hormone receptor (86). At physiological concentrations, a single ligand binds a dimer, leading to transmission of the intracellular signal before horizontally causing a negative impact on the transmembrane domain of the other protomer. This leads to lowering of the binding affinity of the second protomer, providing allosteric cooperativity across the receptors (86). Very recently, single-molecule analysis of FSHR/LHR co-expressed in HK293 cells demonstrates heterodimeric interaction between FSHR and LHR (97). This heterodimeric interaction results in attenuation of LH-induced signaling through LHR and attenuation of FSH-mediated signaling through FSHR. The authors propose that heterodimerization of glycoprotein receptors could play a significant role in fine tuning the signaling event of FSH and LH during granulosa cell differentiation. However, it will be critical to demonstrate heterodimerization in primary cell systems and in *in vivo* models where the receptor expression is at low level compared to the overexpression system.

The recent crystal structure of the FSH complexed with the complete extracellular domain of FSHR challenged the previous view of the structural changes imposed on this receptor upon ligand binding (98). According to this model, in basal state, FSHR exists as a trimer (**Figure 2A**), and only a single unit of fully glycosylated FSH bind the trimeric receptor (**Figure 2B**), leading to dissociation and activation of the ligand-bound monomeric receptor. On the other hand, due to the lack of bulky glycans, three deglycosylated hormones can bind to the receptor keeping it in the trimeric inactive state (**Figure 2D**). Although the trimer model of FSHR in FSH recognition could well explain some observation in biochemical and functional studies, the *in vivo* relevance of the FSHR-FSH trimerization and the actual oligomerization form in living cells still need to be determined.

Small Molecule Modulators of Glycoprotein Hormone Receptors

Development of drugs that target the ligand-binding domain has been highly successful for agonists or antagonists that address the large superfamily of GPCRs. Unfortunately, many of the current GPCR-based drugs produce unwanted dose-limiting side effects due to cross reactivity with other related receptors that share structurally conserved features. Yet, another challenge for developing innovative drugs targeting GPCRs is that many of the synthetic molecules that replace peptide or protein ligands have been intractable (not "drug-able") largely because the molecules

must fit into highly lipophylic regions of the GPCR transmembrane domains (99). However, for the past several decades, it has been realized that receptors can be regulated by allosteric sites that are distinct from the ligand-binding orthosteric site (100). Accordingly, there is now ample evidence over the past decade and half that a GPCR response to endogenous ligand can be modulated by synthetic small molecules targeting allosteric sites (101–105). These allosteric modulators can exert negative or positive effects on endogenous ligand signaling. There are four types of allosteric ligands, antagonist known as negative allosteric modulators (NAMs), potentiators also called positive allosteric modulators (PAMs), allosteric agonists (allo-agonists), and finally silent modulators (SAMs) (106). For glycoprotein hormone receptors, since the ligands are very large and involve multiple binding sites at the receptor, a small molecule binding the orthosteric site cannot be envisaged. The advent of allosteric modulators in other GPCR programs has encouraged the incorporation of drug discovery strategies to screen for allosteric modulators that modulate glycoprotein hormone receptors.

The primary market driver invoked by drug discoverers to pursue allosteric modulators for glycoprotein hormones over available injectable proteins is patient convenience. A secondary motivation is the hope that a new mechanism of action for allosteric agonists can improve the biological response relative to "glyco-uniform" biotherapeutics. As the number and quality of allosteric modulators increases, subtle advantages of PAMs or NAMs over the injectable proteins are beginning to emerge. In the late 1990s, recombinant therapeutic proteins were developed to provide superior consistency than could be obtained by purification of hormones from natural sources. However, the recombinant proteins continue to be administered by injections, which are inconvenient and results in low patient engagement for infertility treatment. Recombinant proteins are also constrained by regulatory requirements for uniform post-translational modifications, such as glycosylation. The preference of patients and physicians for orally active therapeutics has motivated development of replacements for injectable treatments in rheumatoid arthritis (anti-TNF agents vs JAK inhibitors) (107, 108) and multiple sclerosis (interferons vs Fingolimod or Teriflunomide) (109, 110). For infertility patients, the motivation is similar; it is more desirable to have small molecule agonists of glycoprotein hormones that can be used as an oral therapy. Secondarily, if the allosteric agonist can amplify the receptor response to endogenous biodiverse glycoprotein forms, this may provide a preferred therapeutic over suppressing endogenous glycoprotein production followed by replacement with a bio-constrained uniformly glycosylated glycoprotein. A NAM of FSHR and/or LHR may lead to development of a highly specific oral contraceptive with lesser side effects than the currently available steroidal-based drugs. In addition, glycoprotein hormone receptor small molecule antagonists may have a better long-term safety than steroidal contraceptives (111–113).

Developing small molecule agonists or antagonists for glycoprotein hormone receptors has been challenging for medicinal chemists; however, in the last few years, great strides have been achieved in developing chemical scaffolds targeting the glycoprotein receptors through advances in screening tools, access to larger diverse library of small molecule compounds and robotic systems to conduct high-throughput campaign. Most of the new allosteric modulators have been identified through high-throughput screening (HTS) campaigns using cell-based assays (114–117). The availability of a wide range of assays from overexpressed isolated proteins to engineered cell culture systems measuring second messengers, to primary cell cultures, and to *ex vivo* animal tissues has made it critical to identify the appropriate system for screening as well as various transitions to more physiologically relevant models. The key objective of the optimal screen is to quickly filter false positives identified because of the artificial system and confirm their activity in physiologic cellular responses that address the therapeutic goal (118).

In our own drug discovery experience, there has been an evolution in the approaches we have used to identify and develop small molecule agonists of glycoprotein hormone receptors. In the process, we learned three key lessons: (a) molecules that stimulate cAMP in immortalized cell systems expressing FSH receptor (FSHR) as a primary screen do not necessarily reflect the compound requirements to stimulate follicular development; (b) the diversity of intracellular and intrafollicular events stimulated by FSH cannot be reproduced by measuring single endpoints in single cell types *in vitro;* and (c) the highest potency compound *in vitro* does not always correlate with best efficacy *in vivo*. In the next several sections, we will highlight how these lessons influenced our current discovery process.

Molecules that Stimulate cAMP in Immortalized Cell Systems Expressing FSH Receptor as a Primary Screen Do Not Necessarily Reflect the Compound Requirements to Stimulate Follicular Development

It is intuitively obvious that it is a huge challenge to engineer a small molecule (molecular weight 500–600) that can replicate the integrated biochemical response of a large protein (molecular weight 33,000). A small molecule glycoprotein hormone receptor agonist cannot occupy the same space in the extracellular ligand-binding domain of the FSHR. Therefore, binding assays were discarded as a primary screen in these programs, but instead were applied to understand changes in receptor conformations induced by the small molecule. Cell-based assays using physiologically reasonable levels of expression of the appropriate receptor and intracellular signaling cascades are important to interpret screening results. Exaggerated overexpression systems can make a weakly active compound look more potent than it really is. FSHR expression in our CHO-cell system, as detected by FSH binding to receptors, was approximately threefold greater than expression in primary granulosa cells. It has been demonstrated that receptor density at the plasma membrane can control the balance between distinct signal transduction pathways (56).

Diversity of Intracellular and Intrafollicular Events Stimulated by FSH Cannot be Reproduced by Measuring Single Cell, Single Outputs in Cell Culture

It is imperative to confirm changes in second messengers induced by allosteric modulators, in subsequent primary cell culture systems that measure physiologically relevant products associated with the same intracellular pathways. In the earliest attempts

to identify FSHR agonists, compounds with activity in FSHR-expressing CHO cells were quickly advanced into *in vivo* models without evaluation in primary granulosa cells. Over several iterations of screening, we learnt that the structure–activity relationship (SAR) from immortalized CHO cells does not translate well to activity in rat granulosa cells or human granulosa cells. Compounds active in the immortalized cell screen were tested in relevant functional assays using rat granulosa cell cultures and measuring estradiol secreted in the media. Responses of the compounds varied between CHO-hFSHR cells and in granulosa cells (**Table 1**). Among compounds that were moderately potent in CHO cells (EC50 between 10–49.9 nM and 50–250 nM) ~30% of compounds were ineffective in stimulating estradiol in the functional assay (**Table 1**). Furthermore, among compounds that were potent in CHO-FSHR cells (1–4.9 nM and 5–9.9 nM EC50), ~25% of the compounds were unable to stimulate estradiol production in granulosa cell culture. Among the most potent compounds (EC50 < 1 nM), only 7% of compounds were inactive in granulosa cells (**Table 1**). This data suggests that the result obtained from overexpression system should be treated with caution, as response in functional assay at the beginning of the lead optimization effort had nearly 30% false positive rate.

The converse relationship between physiological activity in granulosa cells and signaling activity in immortalized cells was observed for FSHR NAMs. An FSHR NAM was shown capable to partially reduce cAMP induced by FSH in HEK293 cells, but it was very effective in blocking cAMP and progesterone production in a primary granulosa cell system (119). This clearly highlights that the SAR developed in an immortalized cell system is not always transferable to the physiologically relevant functional cell model. It is imperative to test molecules in a therapeutically relevant cell very early on in the screening program before progressing molecules to animal models.

Highest Potency Compound *In Vitro* Does Not Always Correlate with Best Efficacy *In Vivo*

The correlation between granulosa cell activity and *in vivo* activity is much lower, and is affected by multiple variables. Compounds in our program as well as compounds from other efforts [thiazolidinones (TZDs)] that are very potent (EC50 < 1 nM) are poorly absorbed and/or extensively metabolized following oral exposure (117, 120). In general, these molecules have very high log*D* values, and are metabolized faster. One has to balance the desire for highly potent compounds with candidates that can be orally available. Highly potent compounds frequently share undesirable absorption, distribution, and metabolism (ADME) properties. There are some excellent reviews published on the small molecule allosteric modulators of glycoprotein hormone receptors (121–123). We will focus on the most recent advances made in this exciting field.

TABLE 1 | Not all compounds active in CHO-hFSR cells can stimulate estradiol secretion in primary rat granulosa cells.

EC50 in CHO-hFSHR (nM)	Rat granulosa cell assay (GC)		
	No. of compounds		
	Tested in GC	No activity	% Inactive
<1	44	3	7
1–4.99	97	20	21
5–9.99	52	15	29
10–49.9	84	30	36
50–250	10	3	30

FSH Receptor Modulators

Among the three glycoprotein hormones used in infertility treatment, FSH is the major value driver for therapeutic intervention. Without the FSH treatment, there is no ovarian hyperstimulation. As expected, there are several publications on FSHR modulators and fewer reports on development of LHR and TSHR modulators. The first report of FSHR agonist was published as a patent in 2001 by Serono (124), describing a piperidine carboxyamide, which had an EC50 of 3.9 nM in CHO-hFSHR cells measuring cAMP. These molecules were originally identified through HTS of a compound library. Unfortunately, piperidine carboximides lacked *in vivo* activity. In this program, there was virtually no systematic structure-based optimization of the lead through iterative Med Chem efforts using granulosa cell cultures to guide their development. Since then, several groups have followed up with various chemical scaffolds targeting FSHR, including TZDs (125–127), substituted gamma-lactam (128), diketopiperazines (129, 130), N-alkylated sulfonyl piperazine (131), tetrahydroquinolines (132), hexahydroquinoline (133), thienopyrimidines (134), and benzamides (117). Chemical structures for some of these are provided in **Figure 3**. For more detailed review on chemical nature of other series, please refer to van Straten and Timmers (123). The cellular and physiological effects of specific chemical classes are summarized below.

Thiazolidinones Agonists

Thiazolidinones were identified through a combinatorial library screening (126–128). The initial hit obtained through screening had an EC50 of 20 μM in CHO-hFSHR cells, but this potency was optimized over 10,000-fold during lead optimization (127). In addition to their effects in immortalized cells, TZDs were capable of stimulating estradiol production in functional rat granulosa cells (127). These authors further explored the site within the receptor where these compounds might be working. Using multiple reconstitutions of FSHR and TSHR transmembrane domain chimeras, they identified that TZDs activated FSHR through the transmembrane domain 1–3 (127). They also observed a range of biochemical features of this series of compounds from PAM to mixed modulators and to negative modulators (125), suggesting that a small change in the TZD scaffold can provide FSHR analogs of differing pharmacology. The agonists stimulated cAMP and estradiol in granulosa cells. On the other hand, the negative modulators were completely devoid of agonistic activity and inhibited FSH-induced cAMP and steroidogenesis, through activation of Gi pathway. The mixed modulators at lower concentrations behaved as agonist stimulating cAMP through Gs, while at higher concentration, the compound activated Gi pathway and reduced cAMP demonstrating negative cooperativity as was demonstrated within cells expressing constitutively active glycoprotein receptors (86, 125). These molecules provide evidence that it is possible to selectively trigger specific signaling pathways

A *Agonists*

1. Thiazolidinone (Compound 5, Yanofsky *et al.* 2006)

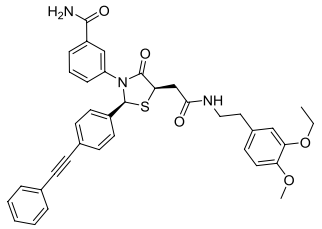

Compound 5

2. Hexahydroquinolines (Org214444-0, van Koppen *et al.* 2013)

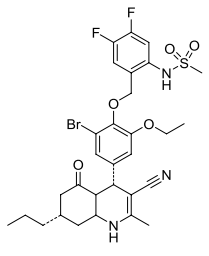

Org 21444-0

3. Benzamide (Compound 9K, Yu *et al.* 2014)

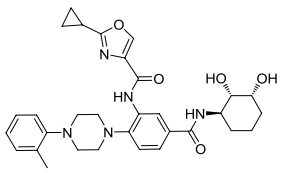

Compound 9k

B *Antagonists*

1. Thiazolidinone (Compound 3, Arey *et al.* 2008)

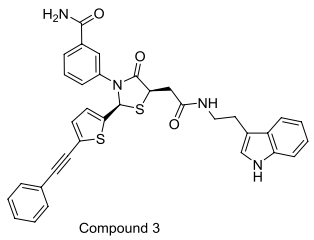

Compound 3

2. Dimethoxybenzamide (ADX68692, Dias *et al.* 2014)

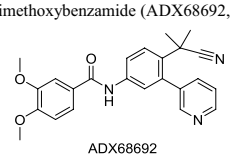

ADX68692

3. Aminoalkyamine (van Straten *et al.* 2005)

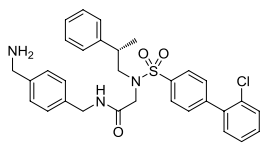

FIGURE 3 | Chemical structure of selected small molecule modulators of FSHR. **(A)** Agonists: (1) thiazolidinone [compound 5 (127)], (2) hexahydroquinolines [Org214444-0 (135)], and (3) benzamide [compound 9K (117)]. **(B)** Antagonists: (1) thiazolidinone [compound 3 (125)], (2) dimethoxybenzamide [ADX68692 (147)], and (3) aminoalkyamine (132).

of the receptor. Recently, our group demonstrated that the TZD compound was capable of stimulating multiple signaling pathways, in addition to cAMP, in an integrated cellular signal very similar to FSH (120). These molecules behaved as "allo-agonists," in that they can potentiate FSH action in the presence of low FSH, and also directly activate FSHR in rat granulosa cells (120). In relevant physiological cellular models, TZD stimulated cumulus expansion of granulosa cells, and induced *in vitro* follicular growth. Due to extremely low oral bioavailability, TZD was not suitable as orally active therapeutics; however, the compound was quite effective in stimulating follicular development in immature rat when delivered continuously by Alzet pump (120).

Hexahydroquinoline Agonists

A series of hexahydroquinolines with nanomolar activity in CHO cells were reported (133). Cyclocondensation reaction of hexahydroquinolines resulted in mixtures of four diastereoisomers with EC50 <1 nM. One such compound, Org214444-0, was highly lipophilic and stereoselective on FSHR over related LHR and TSHR (135). Org214444-0 was quite potent in stimulating rat and human granulosa cells. In binding experiment with ^{125}I-FSH, this compound was able to increase FSH binding affinity by 6.5-fold, while in CHO-CRE luciferase assay, a three to fivefold increase in potency was observed, behaving as "allo agonist." They also demonstrated oral bioactivity as measured by increased follicular development and ovulation in mature rats (135). This is the first report of an orally active FSHR molecule. In an attempt to reduce the lipophilicity, several pyridyl- and sulfonamide-substituted hexahydroquinolines were prepared (136). The compounds had moderate *in vitro* activity but there is no report on their *in vivo* potency.

FSHR Antagonists

In addition to the pursuit of the development of small molecule FSHR agonists to promote fertility, several novel series of compounds have shown potential to suppress fertility as contraceptives. Contraceptives have played a significant role in avoiding unwanted pregnancy, for family planning, and for slowing population growth. Currently the widely used contraceptives are steroid based and have a number of side effects, so developing a safer method of contraceptive is a significant unmet medical need (137, 138). FSH plays a critical role in follicular development and the onset of sperm production (139–142). Thus, blocking FSH action with a receptor antagonist can be a novel non-steroidal-based approach with specific activity in ovary and testes without affecting other peripheral and central tissue.

The first report of an FSHR antagonist for use in contraception was reported in 2002 (143). The compound inhibited FSH-induced cAMP and steroid production. *In vivo* at 100 mg/kg, provided by ip, the compound blocked increases in ovarian weight and ovulation (143). Aminoalkylamides were described in 2003 to have antagonistic activity against FSHR (144). Two compounds were tested for their ability to interrupt estrous cycle in female rats and their effect on spermatogenesis in male, but in both cases, the compounds were not very effective (144). Organon later reported identification of tetrahydroquinolines agonists from HTS with EC50 on FSHR at 4.4 μM (132). Hit optimization of this series led

to switch from agonist to antagonist with IC50 of 5 nM (132). This compound showed antagonistic activity in granulosa cells and inhibited *in vitro* follicle growth and ovulation (132). However, *in vivo* efficacy of this molecule was not reported. Antagonists with greater potency were obtained with dimeric compounds (145). Connection of two weakly antagonistic molecules with a spacer of sufficient length generated antagonists with much better activity *in vitro* (145).

Small molecule FSHR agonists have varying pharmacokinetics properties, hence shown to have quite different half-life. A clever approach was used by van de Lagemaat to develop a contraceptive using a FSHR agonist with a very short half-life (146). Follicle stimulation in mammals is achieved when the circulating concentration of FSH is sustained above the threshold for sufficiently long time. Thus in rats, optimal follicular growth occurs only when FSH is administered twice a day for 2 days due to its short half-life, in contrast to a single injection of PMSG, which has longer half-life and remains in the circulation for a longer duration (119). Van de Lagemaat et al. observed that oral administration of the short-acting FSHR agonist inhibited ovulation by inducing premature luteinization of unruptured follicles in rat and guinea pig (146). This effect was reversible; therefore, this novel approach of short follicular stimulation followed by premature withdrawal presents a unique mechanism of contraceptive action relative to that used by steroidal hormones, which blocks the entire ovarian follicular phase. However, in cynomolgus monkey, the effect of the compound was partial as only about 40% of animals showed luteinized unruptured follicle. Due to the variation in response in non-human primate, this molecule was not pursued for development, but the approach is quite novel. Thus, having allosteric modulators with differing pharmacology can be a useful tool for both stimulating and controlling fertility.

Investigators from Addex, in collaboration with Dias and co-workers, characterized three of the NAM identified from their drug discovery effort. These are low molecular weight compounds effective in blocking FSH-induced cAMP production in CHO-hFSHR and rat granulosa cells. In the first paper, they demonstrate ADX61623 to increase the affinity of ^{125}I-hFSH binding to the receptor (119). In rat granulosa cells, FSH-induced progesterone secretion was inhibited by ADX61623, but not estradiol, demonstrating biased antagonism on FSH signaling. This molecule was only partially effective in blocking FSH-induced follicular development and ovulation in rats (119). Results with ADX61623 provide proof that small molecule modulator of FSHR can be used to dissect the signaling pathways of the receptor. In a more recent publication, Dias et al. have tested two other NAMs, ADX68692 and its analog ADX68693 (147). ADX68692 inhibited FSH-induced progesterone and estradiol production in granulosa cells. *In vivo*, this compound blocked FSH-mediated follicular maturation and ovulation in immature rats (147). While in mature cycling rats, though ADX68692 disrupted estrous cycle, it had only a partial effect in blocking pregnancy following mating (147). Its contraceptive efficacy in mature rat remained lower than that can be achieved with steroidal contraceptives. ADX68693, on the other hand, showed biased antagonistic activity on FSH-mediated steroid production like ADX61623 by inhibiting FSH-stimulated progesterone, but rather stimulating estradiol secretion in granulosa cells and no significant effect in blocking ovulation in immature rat (147). These studies demonstrate that, for an effective contraception, it is critical to inhibit both arms of FSH-induced steroidogenesis, i.e., progesterone and estradiol biosynthesis. At present, the available FSH antagonists lack pharmacological properties that would justify development as alternatives to steroidal contraceptives.

LH Receptor Modulators

The first series of small molecule LHR agonist reported in literature were thienopyrimidines (116). An HTS campaign followed by hit optimization resulted in Org41841 with EC50 of 20 nM in CHO-hLHR assay. This compound stimulated testosterone in mouse Leydig cells. Org41841 at 50 mg/kg administered orally induced ovulation in 40% of immature mice primed with FSH (116). This was the first report of oral activity of LHR analog. Intensive medchem optimization of thienopyrimidines led to the identification of several potent molecules. One compound, a trifluoroacetic acid salt form of thienopyrimidine, Org42599 behaved as a pharmacochaperone of mutant LHR (148). In previous work, mutations in LH receptors (LHRs) at two locations, A593P and S616Y, cause misfolding of the receptor and these receptors fail to get trafficked to the plasma membrane. Org42599 facilitated expression of the mutant receptors to the plasma membrane behaving as pharmacochaperone and rescued the stimulatory response to LH (148). This approach may have translational application for treatment of patients bearing such mutation.

A series of pyrazole compounds with mixed FSH/LH activity was reported (149). Compound 5 was described to have an EC50 of 20 nM (efficacy 53%) in CHO-hLHR and an EC50 value of 130 nM (efficacy 73%) in CH-hFSHR assays (122). This compound stimulated testosterone production in rat (122, 149), though its effect on follicular development was not reported. Bonger et al. obtained a highly selective LHR agonist by linking a dual LHR/FSHR molecule to a previously characterized FSHR antagonist (115, 150).

Another interesting molecule from optimization of thienopyrimidine is Org43553. This molecule stimulated LHR to produce cAMP with EC50 3.4 nM, while FSHR was activated at 110 nM (151). LH at higher concentration can activate phospholipase C (PLC), but Org43553 inhibited LH-induced PLC, showing biased agonism on LHR (152). Pharmacokinetic analysis showed that the compound had high oral bioavailability with short half-life (151). Oral administration of Org43553 induced ovulation in female (immature mice and adult rat) and serum testosterone in male rat (151). Since the half-life of this molecule was shorter than that of hCG, it can potentially reduce the risk of ovarian hyperstimulation syndrome (OHSS), a condition believed to be induced by hCG (153–155). In fact, in rat, Org43553 induced ovulation without the increased vascular permeability or increased expression of vascular endothelial growth factor (VEGF), caused by hCG (156). At present, it is unclear if it is biased agonism or short half-life of the Org43553 that is able to induce ovulation, but reduce the risk of OHSS (156). Finally, in the most exciting study, Org43553 and another molecule Org43902 were well

tolerated in normal healthy women and demonstrated that single oral administration of the small molecule agonist induced ovulation of gonadotropin-stimulated, mature follicles in pituitary-suppressed women (157). This represents a giant stride toward the demonstration of proof of concept for development of an orally active small molecule modulator of glycoprotein hormone receptor in human.

Antagonist

Development of LHR antagonists is very limited. A binding assay using small molecule radioligand ^{3}H-Org43553 (LHR agonist, described above) was used as a screening tool to identify LHR antagonists (158). Binding of ^{3}H-Org43553 with hLHR membrane was saturable with K_d of 2.4 nM and B_{max} of 1.6 pmol/mg protein (159). Five small molecule agonists evaluated in this assay showed good correlation between binding affinity relative to Org43553 and their potency in cellular assay (159). Using this binding assay as the screening tool, terphenyl derivatives were identified to inhibit ^{3}H-Org43553 binding to the membrane (158). Interestingly, one of the derivatives, compound 24 (LUF5771) was able to increase the K_d of ^{3}H-Org43553 by 3.3-fold. In a functional assay, LUF5771 inhibited the activation of the receptor by hLH and Org43553. *In vivo* efficacy of LUF5771 as an allosteric inhibitor was not demonstrated. **Figure 4** illustrates the chemical structure of some of the interesting LHR modulators.

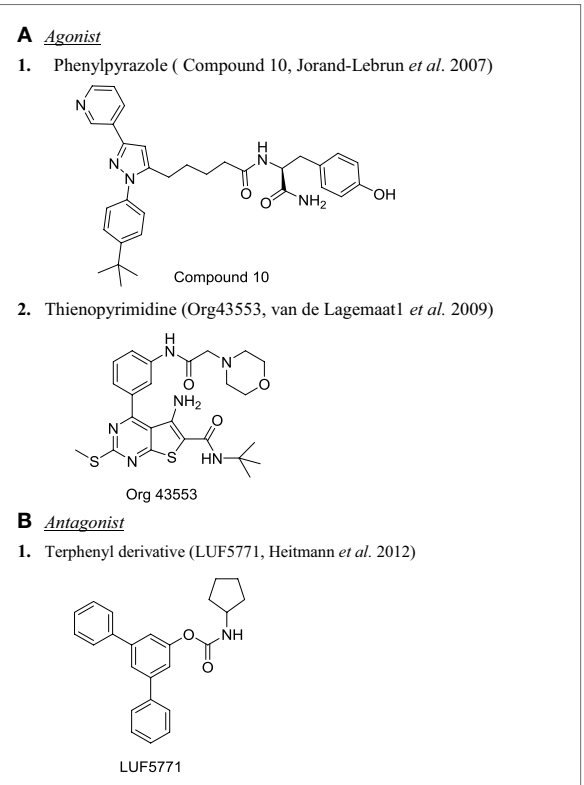

FIGURE 4 | Chemical structure of LHR modulators. **(A)** Agonist: (1) phenylpyrazole [compound 10 (149)] and (2) thienopyrimidine [Org43553 (151)]. **(B)** Antagonist: (1) terphenyl derivative [LUF5771 (158)].

TSH Receptor Modulators

For the past few years, there are reports on the development of small molecule allosteric modulators for TSHR (160, 161). The chemical structure of few of the TSHR allosteric modulators are shown in **Figure 5**. The first TSHR agonist started from a thienopyrimidine, Org41841, the LHR agonist (116). Due to high homology between TMD of LHR and TSHR, it was predicted that Org41841 would bind to TSHR. This prediction was confirmed by docking studies, and eventually experimental results identified Org41841 as a partial agonist (162). Further, HTS and optimization of a hit resulted in identification of compound 2 (C2), which was a full agonist at TSHR with an EC50 of 40 nM and no activity at FSHR or LHR (163). More importantly, C2 was

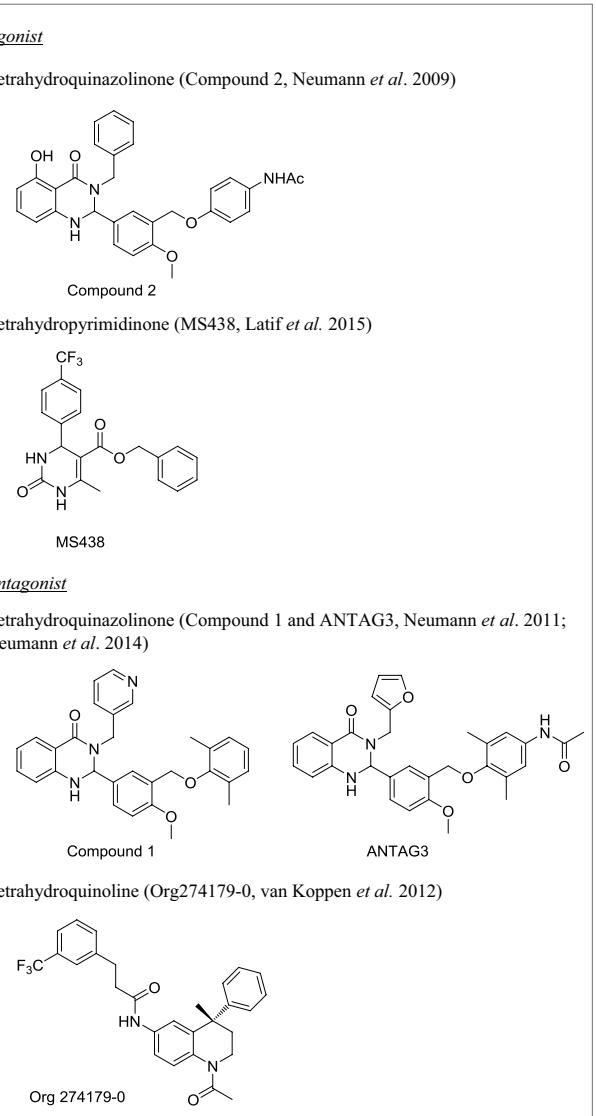

FIGURE 5 | Chemical structure of TSHR modulators. **(A)** Agonist: (1) tetrahydroquinazolinone [compound 2 (163)] and (2) tetrahydropyrimidinone [MS438 (114)]. **(B)** Antagonist: (1) tetrahydroquinazolinone [compound 1 and ANTAG3 (165, 169)] and (2) tetrahydroquinoline [Org274179-0 (167)].

active in a physiologically relevant cell system, primary human thyrocyte culture. C2 stimulated serum thyroxine (T4) in mice when administered orally (163). This is the first proof of principle study that a small molecule agonist for TSHR is active in an *in vivo* preclinical model. However, there is no report on further development of the compound. Very recently, Latif et al. described two molecules, MS437 and MS438, with potent activity on TSHR and thyrocytes (114). Both these molecules demonstrated *in vivo* activity in stimulating thyroxine in male rats when administered intraperitoneally. It is not known if these molecules are orally active. Molecular docking studies showed that these compounds bind to the TMD3 of TSHR (114).

The first antagonist against TSHR also had its origin from Org41841. Based on the model of Org41841–TSHR complex, it was predicted that elongated analogs would bind differently to the receptor, so a long propylene-methyl-ether group was added at the para position of the aromatic moiety to obtain compound 52 (164). This compound inhibited TSH-stimulated cAMP by 71% with an IC50 of 4.2 μM and blocked antibody-induced thyroperoxidase mRNA in primary thyrocytes, suggesting it could be used in pathological condition like Grave's disease (164). However, due to its weak potency, it could only be used as a starting point to make more potent analogs to develop as therapeutics. This group also described developing a TSHR inverse agonist with antagonistic activity that can block TSHR antibody-induced orbital fibroblast functions (165, 166). Van Koppen et al. reported development of Org274179-0 as nanomolar potent allosteric antagonist capable of inhibiting M22-induced cAMP production in orbital fibroblast, but this compound was equally effective in inhibiting FSHR as well (167, 168). Perhaps, the most potent and selective TSHR antagonist, ANTAG3, inhibited TSH and M22-induced elevation of serum-free T4 and mRNAs for thyroperoxidase and sodium-iodide cotransporter *in vivo* (169). Availability of several chemical series of small molecule modulators of TSHR opens an exciting opportunity for developing novel therapy for pathological conditions as well as to use them as research tools to understand the basic biology of TSHR signaling.

Mechanism of Action of Small Molecule Modulators

Small molecule modulators of glycoprotein hormone identified to date, except for stilbene bisulfonic acid 20 (143), do not displace the binding of the protein ligand. Several chemotypes have been demonstrated experimentally to bind to the transmembrane domains of the receptors (127, 162, 170). Molecular modeling and mutagenesis studies have helped us to understand the functional mechanism of allosterism of small molecule modulators of the glycoprotein receptors. The structure of rhodopsin is adopted as a general model for elucidating the functional domains of all GPCRs. Using this approach, it is proposed that there are two pockets of allosteric binding sites in the transmembrane regions of glycoprotein receptors (121, 170). Pocket1 (P1) is formed between TMD III, IV, V, and VI, while the 2nd pocket (P2) is formed by TMD I, II, III, and VII (121, 170, 171). P1 has been suggested to be the site of interaction of pyrazole, pyrimidine, and tetrahydroquinoline chemotypes (121, 162). Using chimeric FSHR–TSHR hybrid receptors, activity of TZD on FSHR was dependent on presence of transmembrane regions I, II, and III, suggesting this chemical series interacts with the P2 pocket of the receptor (121, 127).

Based on the docking studies and experimental evidence with Org43553 and two other small molecules (LUF5771 and LUF5419), Heitman et al. confirmed two binding sites in the transmembrane region of LHR for small molecule modulators (170). By *in silico* docking studies, the binding site for LUF5771 was proposed to be in the pocket created by TMDs 1, 2, 3, 6, and extra cellular loop 2, corresponding to site P2 [reviewed in Ref. (121)]. Org43553 interaction was restricted to site P1 (170). LUF5771, the allosteric inhibitor, strongly overlapped with the binding site of LUF5419, an allosteric enhancer of Org43553. However, the antagonist interacts with additional residues in TM2 and 7, which are likely to restrict the receptor in an inactive conformation (170). It is noteworthy to mention that similar structural constraint is induced by compound 52 on TSHR to behave as an antagonist (161). The existence of multiple allosteric sites on glycoprotein hormone receptors provides opportunities to design and develop new compounds with improved selectivity and therapeutic value.

Recent crystal structure of FSH with FSHR extracellular domain provided evidence for the existence of trimer in the basal state (**Figure 2A**) (98). Receptor trimerization is mediated by both the transmembrane domains and the ectodomain. Binding of one fully glycosylated FSH to the basal trimer results in dissociation of a single monomer from the trimer, resulting in the activation of the single monomer (**Figure 2B**). Based on this model of hormone receptor activation, refined through the use of several small molecule ligands, the mechanism proposed is that small molecules induce 1–3 active monomers in concentration-dependent manner that can be monitored by binding of three glycosylated FSH heterodimers to the dissociated monomers (**Figure 2C**) (98). Increased binding of FSH in the presence of the modulators confirms this observation (119, 135, 172). An important question is whether the FSHR trimer described by the new crystal structure is functionally relevant in physiological systems.

Summary

With greater understanding of GPCR biology and improved methods to develop allosteric modulators, several chemical series have emerged. Currently, we are pursuing a new chemical series for FSHR modulator, which has shown great promise in preclinical models including DMPK, safety, and toxicology studies. Successful development of an oral LH/hCG as well as GnRH antagonist modulator in clinical studies has kindled our hopes to have an oral therapy for fertility treatment in assisted reproductive technology. Encouraging progress in the development of allosteric modulators of GPCRs can transform the dream of physicians and patients for having a more convenient therapy associated with infertility treatment into reality. Access to an orally active glycoprotein hormone agonist provides hope for patients that are considering dropping out of the treatment due to the stress involved in injection of the drugs. Similarly, for

contraceptive development, a new chemical series of antagonists have emerged, which are quite encouraging for future. The availability of small molecule ligands for TSHR would widen the therapeutic interventions for thyroid cancer and patients with hyperthyroidism. Both agonists and antagonists of glycoprotein hormones will be useful as pharmacological tools to conduct further basic and applied research in understanding the molecular regulation in hormone binding, signal transduction, and biased signaling. The future holds special promise for development of novel oral allosteric modulators of glycoprotein hormone receptors as the third generation therapeutics after purified and recombinant hormones.

References

1. Albanese C, Colin IM, Crowley WF, Ito M, Pestell RG, Weiss J, et al. The gonadotropin genes: evolution of distinct mechanisms for hormonal control. *Recent Prog Horm Res* (1996) **51**:23–58.
2. Ryan RJ, Charlesworth MC, McCormick DJ, Milius RP, Keutmann HT. The glycoprotein hormones: recent studies of structure-function relationships. *FASEB J* (1988) **2**(11):2661–9.
3. Pierce JG, Parsons TF. Glycoprotein hormones: structure and function. *Annu Rev Biochem* (1981) **50**:465–95. doi:10.1146/annurev.bi.50.070181.002341
4. Pierce JG, Faith MR, Giudice LC, Reeve JR. Structure and structure-function relationships in glycoprotein hormones. *Ciba Found Symp* (1976) **41**:225–50.
5. Stockell Hartree A, Renwick AG. Molecular structures of glycoprotein hormones and functions of their carbohydrate components. *Biochem J* (1992) **287**(Pt 3):665–79. doi:10.1042/bj2870665
6. Canfield RE, O'Connor JF. Biological markers on human pregnancy. *Biomed Environ Sci* (1991) **4**(1–2):56–68.
7. Hearn JP, Webley GE, Gidley-Baird AA. Chorionic gonadotrophin and embryo-maternal recognition during the peri-implantation period in primates. *J Reprod Fertil* (1991) **92**(2):497–509. doi:10.1530/jrf.0.0920497
8. Fiddes JC, Goodman HM. The cDNA for the beta-subunit of human chorionic gonadotropin suggests evolution of a gene by readthrough into the 3'-untranslated region. *Nature* (1980) **286**(5774):684–7. doi:10.1038/286684a0
9. Jameson JL, Lindell CM, Habener JF. Evolution of different transcriptional start sites in the human luteinizing hormone and chorionic gonadotropin beta-subunit genes. *DNA* (1986) **5**(3):227–34. doi:10.1089/dna.1986.5.227
10. Li MD, Ford JJ. A comprehensive evolutionary analysis based on nucleotide and amino acid sequences of the alpha- and beta-subunits of glycoprotein hormone gene family. *J Endocrinol* (1998) **156**(3):529–42. doi:10.1677/joe.0.1560529
11. Boime I, Ben-Menahem D. Glycoprotein hormone structure-function and analog design. *Recent Prog Horm Res* (1999) **54**:271–88.
12. Sairam MR. Role of carbohydrates in glycoprotein hormone signal transduction. *FASEB J* (1989) **3**(8):1915–26.
13. Matzuk MM, Boime I. Mutagenesis and gene transfer define site-specific roles of the gonadotropin oligosaccharides. *Biol Reprod* (1989) **40**(1):48–53. doi:10.1095/biolreprod40.1.48
14. Fournier T, Guibourdenche J, Evain-Brion D. Review: hCGs: different sources of production, different glycoforms and functions. *Placenta* (2015) **36**(Suppl 1):S60–5. doi:10.1016/j.placenta.2015.02.002
15. Fares F. The role of O-linked and N-linked oligosaccharides on the structure-function of glycoprotein hormones: development of agonists and antagonists. *Biochim Biophys Acta* (2006) **1760**(4):560–7. doi:10.1016/j.bbagen.2005.12.022
16. Bishop LA, Robertson DM, Cahir N, Schofield PR. Specific roles for the asparagine-linked carbohydrate residues of recombinant human follicle stimulating hormone in receptor binding and signal transduction. *Mol Endocrinol* (1994) **8**(6):722–31. doi:10.1210/me.8.6.722
17. Fares FA, Gruener N, Kraiem Z. The role of the asparagine-linked oligosaccharides of the alpha-subunit in human thyrotropin bioactivity. *Endocrinology* (1996) **137**(2):555–60. doi:10.1210/endo.137.2.8593802
18. Matzuk MM, Keene JL, Boime I. Site specificity of the chorionic gonadotropin N-linked oligosaccharides in signal transduction. *J Biol Chem* (1989) **264**(5):2409–14.
19. Ulloa-Aguirre A, Timossi C, Damian-Matsumura P, Dias JA. Role of glycosylation in function of follicle-stimulating hormone. *Endocrine* (1999) **11**(3):205–15. doi:10.1385/ENDO:11:3:205
20. Kalyan NK, Bahl OP. Role of carbohydrate in human chorionic gonadotropin. Effect of deglycosylation on the subunit interaction and on its in vitro and in vivo biological properties. *J Biol Chem* (1983) **258**(1):67–74.
21. Davis JS, Kumar TR, May JV, Bousfield GR. Naturally occurring follicle-stimulating hormone glycosylation variants. *J Glycomics Lipidomics* (2014) **4**(1):e117. doi:10.4172/2153-0637.1000e117
22. Jiang C, Hou X, Wang C, May JV, Butnev VY, Bousfield GR, et al. Hypoglycosylated hFSH has greater bioactivity than fully glycosylated recombinant hFSH in human granulosa cells. *J Clin Endocrinol Metab* (2015) **100**(6):E852–60. doi:10.1210/jc.2015-1317
23. Crochet JR, Shah AA, Schomberg DW, Price TM. Hyperglycosylated human chorionic gonadotropin does not increase progesterone production by luteinized granulosa cells. *J Clin Endocrinol Metab* (2012) **97**(9):E1741–4. doi:10.1210/jc.2012-2027
24. Clayton RN. Mechanism of GnRH action in gonadotrophs. *Hum Reprod* (1988) **3**(4):479–83.
25. Plant TM. Hypothalamic control of the pituitary-gonadal axis in higher primates: key advances over the last two decades. *J Neuroendocrinol* (2008) **20**(6):719–26. doi:10.1111/j.1365-2826.2008.01708.x
26. Evans JJ. Modulation of gonadotropin levels by peptides acting at the anterior pituitary gland. *Endocr Rev* (1999) **20**(1):46–67. doi:10.1210/edrv.20.1.0355
27. Padmanabhan V, Karsch FJ, Lee JS. Hypothalamic, pituitary and gonadal regulation of FSH. *Reprod Suppl* (2002) **59**:67–82.
28. Shupnik MA. Gonadotropin gene modulation by steroids and gonadotropin-releasing hormone. *Biol Reprod* (1996) **54**(2):279–86. doi:10.1095/biolreprod54.2.279
29. Channing CP, Hillensjo T, Schaerf FW. Hormonal control of oocyte meiosis, ovulation and luteinization in mammals. *Clin Endocrinol Metab* (1978) **7**(3):601–24. doi:10.1016/S0300-595X(78)80011-5
30. Schwartz NB, McCormack CE. Reproduction: gonadal function and its regulation. *Annu Rev Physiol* (1972) **34**:425–72. doi:10.1146/annurev.ph.34.030172.002233
31. de Kretser DM. Endocrinology of male infertility. *Br Med Bull* (1979) **35**(2):187–92.
32. Chiamolera MI, Wondisford FE. Minireview: thyrotropin-releasing hormone and the thyroid hormone feedback mechanism. *Endocrinology* (2009) **150**(3):1091–6. doi:10.1210/en.2008-1795
33. Persani L. Hypothalamic thyrotropin-releasing hormone and thyrotropin biological activity. *Thyroid* (1998) **8**(10):941–6. doi:10.1089/thy.1998.8.941
34. Brabant G, Ocran K, Ranft U, von zur Muhlen A, Hesch RD. Physiological regulation of thyrotropin. *Biochimie* (1989) **71**(2):293–301. doi:10.1016/0300-9084(89)90066-7
35. Licht P, Denver RJ. Regulation of pituitary thyrotropin secretion. *Prog Clin Biol Res* (1990) **342**:427–32.
36. Postiglione MP, Parlato R, Rodriguez-Mallon A, Rosica A, Mithbaokar P, Maresca M, et al. Role of the thyroid-stimulating hormone receptor signaling in development and differentiation of the thyroid gland. *Proc Natl Acad Sci U S A* (2002) **99**(24):15462–7. doi:10.1073/pnas.242328999
37. Bahn RS. Autoimmunity and Graves' disease. *Clin Pharmacol Ther* (2012) **91**(4):577–9. doi:10.1038/clpt.2012.10
38. Davies TF, Ando T, Lin RY, Tomer Y, Latif R. Thyrotropin receptor-associated diseases: from adenomata to Graves disease. *J Clin Invest* (2005) **115**(8):1972–83. doi:10.1172/JCI26031
39. Dong YH, Fu DG. Autoimmune thyroid disease: mechanism, genetics and current knowledge. *Eur Rev Med Pharmacol Sci* (2014) **18**(23):3611–8.
40. Muldoon BT, Mai VQ, Burch HB. Management of Graves' disease: an overview and comparison of clinical practice guidelines with actual practice trends. *Endocrinol Metab Clin North Am* (2014) **43**(2):495–516. doi:10.1016/j.ecl.2014.02.001
41. Weetman AP. Thyroid abnormalities. *Endocrinol Metab Clin North Am* (2014) **43**(3):781–90. doi:10.1016/j.ecl.2014.05.006

42. Fredriksson R, Schioth HB. The repertoire of G-protein-coupled receptors in fully sequenced genomes. *Mol Pharmacol* (2005) **67**(5):1414–25. doi:10.1124/mol.104.009001
43. Overington JP, Al-Lazikani B, Hopkins AL. How many drug targets are there? *Nat Rev Drug Discov* (2006) **5**(12):993–6. doi:10.1038/nrd2199
44. Wise A, Gearing K, Rees S. Target validation of G-protein coupled receptors. *Drug Discov Today* (2002) **7**(4):235–46. doi:10.1016/S1359-6446(01)02131-6
45. Kristiansen K. Molecular mechanisms of ligand binding, signaling, and regulation within the superfamily of G-protein-coupled receptors: molecular modeling and mutagenesis approaches to receptor structure and function. *Pharmacol Ther* (2004) **103**(1):21–80. doi:10.1016/j.pharmthera.2004.05.002
46. Premont RT, Gainetdinov RR. Physiological roles of G protein-coupled receptor kinases and arrestins. *Annu Rev Physiol* (2007) **69**:511–34. doi:10.1146/annurev.physiol.69.022405.154731
47. Venkatakrishnan AJ, Deupi X, Lebon G, Tate CG, Schertler GF, Babu MM. Molecular signatures of G-protein-coupled receptors. *Nature* (2013) **494**(7436):185–94. doi:10.1038/nature11896
48. Van Loy T, Vandersmissen HP, Van Hiel MB, Poels J, Verlinden H, Badisco L, et al. Comparative genomics of leucine-rich repeats containing G protein-coupled receptors and their ligands. *Gen Comp Endocrinol* (2008) **155**(1):14–21. doi:10.1016/j.ygcen.2007.06.022
49. Alexander SP, Benson HE, Faccenda E, Pawson AJ, Sharman JL, Spedding M, et al. The concise guide to PHARMACOLOGY 2013/14: G protein-coupled receptors. *Br J Pharmacol* (2013) **170**(8):1459–581. doi:10.1111/bph.12445
50. Kumar KK, Burgess AW, Gulbis JM. Structure and function of LGR5: an enigmatic G-protein coupled receptor marking stem cells. *Protein Sci* (2014) **23**(5):551–65. doi:10.1002/pro.2446
51. Jiang X, Dias JA, He X. Structural biology of glycoprotein hormones and their receptors: insights to signaling. *Mol Cell Endocrinol* (2014) **382**(1):424–51. doi:10.1016/j.mce.2013.08.021
52. Kleinau G, Krause G. Thyrotropin and homologous glycoprotein hormone receptors: structural and functional aspects of extracellular signaling mechanisms. *Endocr Rev* (2009) **30**(2):133–51. doi:10.1210/er.2008-0044
53. Ulloa-Aguirre A, Crepieux P, Poupon A, Maurel MC, Reiter E. Novel pathways in gonadotropin receptor signaling and biased agonism. *Rev Endocr Metab Disord* (2011) **12**(4):259–74. doi:10.1007/s11154-011-9176-2
54. Ulloa-Aguirre A, Zarinan T, Pasapera AM, Casas-Gonzalez P, Dias JA. Multiple facets of follicle-stimulating hormone receptor function. *Endocrine* (2007) **32**(3):251–63. doi:10.1007/s12020-008-9041-6
55. Krishnamurthy H, Galet C, Ascoli M. The association of arrestin-3 with the follitropin receptor depends on receptor activation and phosphorylation. *Mol Cell Endocrinol* (2003) **204**(1–2):127–40. doi:10.1016/S0303-7207(03)00088-1
56. Tranchant T, Durand G, Gauthier C, Crepieux P, Ulloa-Aguirre A, Royere D, et al. Preferential beta-arrestin signalling at low receptor density revealed by functional characterization of the human FSH receptor A189 V mutation. *Mol Cell Endocrinol* (2011) **331**(1):109–18. doi:10.1016/j.mce.2010.08.016
57. Ulloa-Aguirre A, Dias JA, Bousfield G, Huhtaniemi I, Reiter E. Trafficking of the follitropin receptor. *Methods Enzymol* (2013) **521**:17–45. doi:10.1016/B978-0-12-391862-8.00002-8
58. Hunzicker-Dunn M, Maizels ET. FSH signaling pathways in immature granulosa cells that regulate target gene expression: branching out from protein kinase A. *Cell Signal* (2006) **18**(9):1351–9. doi:10.1016/j.cellsig.2006.02.011
59. Walker WH, Cheng J. FSH and testosterone signaling in sertoli cells. *Reproduction* (2005) **130**(1):15–28. doi:10.1530/rep.1.00358
60. Landomiel F, Gallay N, Jegot G, Tranchant T, Durand G, Bourquard T, et al. Biased signalling in follicle stimulating hormone action. *Mol Cell Endocrinol* (2014) **382**(1):452–9. doi:10.1016/j.mce.2013.09.035
61. Lapthorn AJ, Harris DC, Littlejohn A, Lustbader JW, Canfield RE, Machin KJ, et al. Crystal structure of human chorionic gonadotropin. *Nature* (1994) **369**(6480):455–61. doi:10.1038/369455a0
62. Wu H, Lustbader JW, Liu Y, Canfield RE, Hendrickson WA. Structure of human chorionic gonadotropin at 2.6 A resolution from MAD analysis of the selenomethionyl protein. *Structure* (1994) **2**(6):545–58. doi:10.1016/S0969-2126(00)00054-X
63. Fox KM, Dias JA, Roey PV. Three-dimensional structure of human follicle-stimulating hormone. *Mol Endocrinol* (2001) **15**(3):378–89. doi:10.1210/mend.15.3.0603
64. Campbell RK, Dean-Emig DM, Moyle WR. Conversion of human choriogonadotropin into a follitropin by protein engineering. *Proc Natl Acad Sci U S A* (1991) **88**(3):760–4. doi:10.1073/pnas.88.3.760
65. Dias JA, Zhang Y, Liu X. Receptor binding and functional properties of chimeric human follitropin prepared by an exchange between a small hydrophilic intercysteine loop of human follitropin and human lutropin. *J Biol Chem* (1994) **269**(41):25289–94.
66. Huang J, Ujihara M, Xia H, Chen F, Yoshida H, Puett D. Mutagenesis of the 'determinant loop' region of human choriogonadotropin beta. *Mol Cell Endocrinol* (1993) **90**(2):211–8. doi:10.1016/0303-7207(93)90154-C
67. Chen F, Puett D. Contributions of arginines-43 and -94 of human choriogonadotropin beta to receptor binding and activation as determined by oligonucleotide-based mutagenesis. *Biochemistry* (1991) **30**(42):10171–5. doi:10.1021/bi00106a014
68. Weiss J, Axelrod L, Whitcomb RW, Harris PE, Crowley WF, Jameson JL. Hypogonadism caused by a single amino acid substitution in the beta subunit of luteinizing hormone. *N Engl J Med* (1992) **326**(3):179–83. doi:10.1056/NEJM199201163260306
69. Roth KE, Dias JA. Scanning-alanine mutagenesis of long loop residues 33-53 in follicle stimulating hormone beta subunit. *Mol Cell Endocrinol* (1995) **109**(2):143–9. doi:10.1016/0303-7207(95)03494-R
70. Chen F, Wang Y, Puett D. The carboxy-terminal region of the glycoprotein hormone alpha-subunit: contributions to receptor binding and signaling in human chorionic gonadotropin. *Mol Endocrinol* (1992) **6**(6):914–9. doi:10.1210/me.6.6.914
71. Grossmann M, Szkudlinski MW, Zeng H, Kraiem Z, Ji I, Tropea JE, et al. Role of the carboxy-terminal residues of the alpha-subunit in the expression and bioactivity of human thyroid-stimulating hormone. *Mol Endocrinol* (1995) **9**(8):948–58. doi:10.1210/mend.9.8.7476992
72. Sen Gupta C, Dighe RR. Biological activity of single chain chorionic gonadotropin, hCGalphabeta, is decreased upon deletion of five carboxyl terminal amino acids of the alpha subunit without affecting its receptor binding. *J Mol Endocrinol* (2000) **24**(2):157–64. doi:10.1677/jme.0.0240157
73. Jiang X, Dreano M, Buckler DR, Cheng S, Ythier A, Wu H, et al. Structural predictions for the ligand-binding region of glycoprotein hormone receptors and the nature of hormone-receptor interactions. *Structure* (1995) **3**(12):1341–53. doi:10.1016/S0969-2126(01)00272-6
74. Kajava AV, Vassart G, Wodak SJ. Modeling of the three-dimensional structure of proteins with the typical leucine-rich repeats. *Structure* (1995) **3**(9):867–77. doi:10.1016/S0969-2126(01)00222-2
75. Moyle WR, Campbell RK, Rao SN, Ayad NG, Bernard MP, Han Y, et al. Model of human chorionic gonadotropin and lutropin receptor interaction that explains signal transduction of the glycoprotein hormones. *J Biol Chem* (1995) **270**(34):20020–31. doi:10.1074/jbc.270.34.20020
76. Fan QR, Hendrickson WA. Structure of human follicle-stimulating hormone in complex with its receptor. *Nature* (2005) **433**(7023):269–77. doi:10.1038/nature03206
77. Jiang X, Liu H, Chen X, Chen PH, Fischer D, Sriraman V, et al. Structure of follicle-stimulating hormone in complex with the entire ectodomain of its receptor. *Proc Natl Acad Sci U S A* (2012) **109**(31):12491–6. doi:10.1073/pnas.1206643109
78. Sanders J, Chirgadze DY, Sanders P, Baker S, Sullivan A, Bhardwaja A, et al. Crystal structure of the TSH receptor in complex with a thyroid-stimulating autoantibody. *Thyroid* (2007) **17**(5):395–410. doi:10.1089/thy.2007.0041
79. Kleinau G, Neumann S, Gruters A, Krude H, Biebermann H. Novel insights on thyroid-stimulating hormone receptor signal transduction. *Endocr Rev* (2013) **34**(5):691–724. doi:10.1210/er.2012-1072
80. Xu JG, Huang C, Yang Z, Jin M, Fu P, Zhang N, et al. Crystal structure of LGR4-Rspo1 complex: insights into the divergent mechanisms of ligand recognition by leucine-rich repeat G-protein-coupled receptors (LGRs). *J Biol Chem* (2015) **290**(4):2455–65. doi:10.1074/jbc.M114.599134
81. Agrawal G, Dighe RR. Critical involvement of the hinge region of the follicle-stimulating hormone receptor in the activation of the receptor. *J Biol Chem* (2009) **284**(5):2636–47. doi:10.1074/jbc.M808199200
82. Dias JA, Van Roey P. Structural biology of human follitropin and its receptor. *Arch Med Res* (2001) **32**(6):510–9. doi:10.1016/S0188-4409(01)00333-2
83. Mizutori Y, Chen CR, McLachlan SM, Rapoport B. The thyrotropin receptor hinge region is not simply a scaffold for the leucine-rich domain but

contributes to ligand binding and signal transduction. *Mol Endocrinol* (2008) **22**(5):1171–82. doi:10.1210/me.2007-0407
84. Mueller S, Jaeschke H, Gunther R, Paschke R. The hinge region: an important receptor component for GPHR function. *Trends Endocrinol Metab* (2010) **21**(2):111–22. doi:10.1016/j.tem.2009.09.001
85. Szkudlinski MW, Fremont V, Ronin C, Weintraub BD. Thyroid-stimulating hormone and thyroid-stimulating hormone receptor structure-function relationships. *Physiol Rev* (2002) **82**(2):473–502. doi:10.1152/physrev.00031.2001
86. Zoenen M, Urizar E, Swillens S, Vassart G, Costagliola S. Evidence for activity-regulated hormone-binding cooperativity across glycoprotein hormone receptor homomers. *Nat Commun* (2012) **3**:1007. doi:10.1038/ncomms1991
87. Costagliola S, Panneels V, Bonomi M, Koch J, Many MC, Smits G, et al. Tyrosine sulfation is required for agonist recognition by glycoprotein hormone receptors. *EMBO J* (2002) **21**(4):504–13. doi:10.1093/emboj/21.4.504
88. Bonomi M, Busnelli M, Persani L, Vassart G, Costagliola S. Structural differences in the hinge region of the glycoprotein hormone receptors: evidence from the sulfated tyrosine residues. *Mol Endocrinol* (2006) **20**(12):3351–63. doi:10.1210/me.2005-0521
89. Guan R, Feng X, Wu X, Zhang M, Zhang X, Hebert TE, et al. Bioluminescence resonance energy transfer studies reveal constitutive dimerization of the human lutropin receptor and a lack of correlation between receptor activation and the propensity for dimerization. *J Biol Chem* (2009) **284**(12):7483–94. doi:10.1074/jbc.M809150200
90. Urizar E, Montanelli L, Loy T, Bonomi M, Swillens S, Gales C, et al. Glycoprotein hormone receptors: link between receptor homodimerization and negative cooperativity. *EMBO J* (2005) **24**(11):1954–64. doi:10.1038/sj.emboj.7600686
91. Segaloff DL. Regulatory processes governing the cell surface expression of LH and FSH receptors. *Subcell Biochem* (2012) **63**:113–29. doi:10.1007/978-94-007-4765-4_7
92. Guan R, Wu X, Feng X, Zhang M, Hebert TE, Segaloff DL. Structural determinants underlying constitutive dimerization of unoccupied human follitropin receptors. *Cell Signal* (2010) **22**(2):247–56. doi:10.1016/j.cellsig.2009.09.023
93. Ji I, Lee C, Jeoung M, Koo Y, Sievert GA, Ji TH. Trans-activation of mutant follicle-stimulating hormone receptors selectively generates only one of two hormone signals. *Mol Endocrinol* (2004) **18**(4):968–78. doi:10.1210/me.2003-0443
94. Lee C, Ji I, Ryu K, Song Y, Conn PM, Ji TH. Two defective heterozygous luteinizing hormone receptors can rescue hormone action. *J Biol Chem* (2002) **277**(18):15795–800. doi:10.1074/jbc.M111818200
95. Rivero-Muller A, Chou YY, Ji I, Lajic S, Hanyaloglu AC, Jonas K, et al. Rescue of defective G protein-coupled receptor function in vivo by intermolecular cooperation. *Proc Natl Acad Sci U S A* (2010) **107**(5):2319–24. doi:10.1073/pnas.0906695106
96. Jonas KC, Fanelli F, Huhtaniemi IT, Hanyaloglu AC. Single molecule analysis of functionally asymmetric G protein-coupled receptor (GPCR) oligomers reveals diverse spatial and structural assemblies. *J Biol Chem* (2015) **290**(7):3875–92. doi:10.1074/jbc.M114.622498
97. Mazurkiewicz JE, Herrick-Davis K, Barroso M, Ulloa-Aguirre A, Lindau-Shepard B, Thomas RM, et al. Single-molecule analyses of fully functional fluorescent protein-tagged follitropin receptor reveal homodimerization and specific heterodimerization with lutropin receptor. *Biol Reprod* (2015) **92**(4):100. doi:10.1095/biolreprod.114.125781
98. Jiang X, Fischer D, Chen X, McKenna SD, Liu H, Sriraman V, et al. Evidence for follicle-stimulating hormone receptor as a functional trimer. *J Biol Chem* (2014) **289**(20):14273–82. doi:10.1074/jbc.M114.549592
99. Conn PJ, Christopoulos A, Lindsley CW. Allosteric modulators of GPCRs: a novel approach for the treatment of CNS disorders. *Nat Rev Drug Discov* (2009) **8**(1):41–54. doi:10.1038/nrd2760
100. Changeux JP. Allosteric receptors: from electric organ to cognition. *Annu Rev Pharmacol Toxicol* (2010) **50**:1–38. doi:10.1146/annurev.pharmtox.010909.105741
101. Bridges TM, Lindsley CW. G-protein-coupled receptors: from classical modes of modulation to allosteric mechanisms. *ACS Chem Biol* (2008) **3**(9):530–41. doi:10.1021/cb800116f
102. De Amici M, Dallanoce C, Holzgrabe U, Trankle C, Mohr K. Allosteric ligands for G protein-coupled receptors: a novel strategy with attractive therapeutic opportunities. *Med Res Rev* (2010) **30**(3):463–549. doi:10.1002/med.20166
103. Keov P, Sexton PM, Christopoulos A. Allosteric modulation of G protein-coupled receptors: a pharmacological perspective. *Neuropharmacology* (2011) **60**(1):24–35. doi:10.1016/j.neuropharm.2010.07.010
104. Wang CI, Lewis RJ. Emerging opportunities for allosteric modulation of G-protein coupled receptors. *Biochem Pharmacol* (2013) **85**(2):153–62. doi:10.1016/j.bcp.2012.09.001
105. Rees S, Morrow D, Kenakin T. GPCR drug discovery through the exploitation of allosteric drug binding sites. *Receptors Channels* (2002) **8**(5–6):261–8. doi:10.1080/10606820214640
106. Burford NT, Watson J, Bertekap R, Alt A. Strategies for the identification of allosteric modulators of G-protein-coupled receptors. *Biochem Pharmacol* (2011) **81**(6):691–702. doi:10.1016/j.bcp.2010.12.012
107. Hansen RB, Kavanaugh A. Novel treatments with small molecules in psoriatic arthritis. *Curr Rheumatol Rep* (2014) **16**(9):443. doi:10.1007/s11926-014-0443-6
108. Lundquist LM, Cole SW, Sikes ML. Efficacy and safety of tofacitinib for treatment of rheumatoid arthritis. *World J Orthop* (2014) **5**(4):504–11. doi:10.5312/wjo.v5.i4.504
109. Lorefice L, Fenu G, Frau J, Coghe GC, Marrosu MG, Cocco E. Oral agents in multiple sclerosis. *Antiinflamm Antiallergy Agents Med Chem* (2015) **14**(1):15–25. doi:10.2174/1871523014999150415130224
110. Safavi M, Nikfar S, Abdollahi M. A systematic review of drugs in late-stage development for the treatment of multiple sclerosis: a focus on oral synthetic drugs. *Inflamm Allergy Drug Targets* (2015) **13**(6):351–66. doi:10.2174/1871528114666150529102613
111. Brynhildsen J. Combined hormonal contraceptives: prescribing patterns, compliance, and benefits versus risks. *Ther Adv Drug Saf* (2014) **5**(5):201–13. doi:10.1177/2042098614548857
112. Hannaford PC. Combined oral contraceptives: do we know all of their effects? *Contraception* (1995) **51**(6):325–7. doi:10.1016/0010-7824(95)00095-R
113. Thomin A, Keller V, Darai E, Chabbert-Buffet N. Consequences of emergency contraceptives: the adverse effects. *Expert Opin Drug Saf* (2014) **13**(7):893–902. doi:10.1517/14740338.2014.921678
114. Latif R, Ali MR, Ma R, David M, Morshed SA, Ohlmeyer M, et al. New small molecule agonists to the thyrotropin receptor. *Thyroid* (2015) **25**(1):51–62. doi:10.1089/thy.2014.0119
115. Bonger KM, van den Berg RJ, Knijnenburg AD, Heitman LH, van Koppen CJ, Timmers CM, et al. Discovery of selective luteinizing hormone receptor agonists using the bivalent ligand method. *ChemMedChem* (2009) **4**(7):1189–95. doi:10.1002/cmdc.200900058
116. van Straten NC, Schoonus-Gerritsma GG, van Someren RG, Draaijer J, Adang AE, Timmers CM, et al. The first orally active low molecular weight agonists for the LH receptor: thienopyr(im)idines with therapeutic potential for ovulation induction. *Chembiochem* (2002) **3**(10):1023–6. doi:10.1002/1439-7633(20021004)3:10<1023::AID-CBIC1023>3.0.CO;2-9
117. Yu HN, Richardson TE, Nataraja S, Fischer DJ, Sriraman V, Jiang X, et al. Discovery of substituted benzamides as follicle stimulating hormone receptor allosteric modulators. *Bioorg Med Chem Lett* (2014) **24**(9):2168–72. doi:10.1016/j.bmcl.2014.03.018
118. Kenakin TP. Cellular assays as portals to seven-transmembrane receptor-based drug discovery. *Nat Rev Drug Discov* (2009) **8**(8):617–26. doi:10.1038/nrd2838
119. Dias JA, Bonnet B, Weaver BA, Watts J, Kluetzman K, Thomas RM, et al. A negative allosteric modulator demonstrates biased antagonism of the follicle stimulating hormone receptor. *Mol Cell Endocrinol* (2011) **333**(2):143–50. doi:10.1016/j.mce.2010.12.023
120. Sriraman V, Denis D, de Matos D, Yu H, Palmer S, Nataraja S. Investigation of a thiazolidinone derivative as an allosteric modulator of follicle stimulating hormone receptor: evidence for its ability to support follicular development and ovulation. *Biochem Pharmacol* (2014) **89**(2):266–75. doi:10.1016/j.bcp.2014.02.023
121. Arey BJ. Allosteric modulators of glycoprotein hormone receptors: discovery and therapeutic potential. *Endocrine* (2008) **34**(1–3):1–10. doi:10.1007/s12020-008-9098-2
122. Guo T. Small molecule agonists and antagonists for the LH and FSH receptors. *Expert Opin Ther Pat* (2005) **15**(11):1555–64. doi:10.1517/13543776.15.11.1555

123. van Straten N, Timmers CM. Non-Peptide ligands for the gonadotropin receptors. *Annu Rep Med Chem* (2009) **44**:171–88. doi:10.1016/S0065-7743(09)04408-X
124. El Tayer N., Reddy A., Buckler D, S. M, Inventors; Applied Research Systems ARS Holding N.A., assignee. *FSH Mimetics for the Treatment of Infertility*. Unites States patent US 6,235,755 (2001).
125. Arey BJ, Yanofsky SD, Claudia Perez M, Holmes CP, Wrobel J, Gopalsamy A, et al. Differing pharmacological activities of thiazolidinone analogs at the FSH receptor. *Biochem Biophys Res Commun* (2008) **368**(3):723–8. doi:10.1016/j.bbrc.2008.01.119
126. Wrobel J, Jetter J, Kao W, Rogers J, Di L, Chi J, et al. 5-Alkylated thiazolidinones as follicle-stimulating hormone (FSH) receptor agonists. *Bioorg Med Chem* (2006) **14**(16):5729–41. doi:10.1016/j.bmc.2006.04.012
127. Yanofsky SD, Shen ES, Holden F, Whitehorn E, Aguilar B, Tate E, et al. Allosteric activation of the follicle-stimulating hormone (FSH) receptor by selective, nonpeptide agonists. *J Biol Chem* (2006) **281**(19):13226–33. doi:10.1074/jbc.M600601200
128. Pelletier JC, Rogers J, Wrobel J, Perez MC, Shen ES. Preparation of highly substituted gamma-lactam follicle stimulating hormone receptor agonists. *Bioorg Med Chem* (2005) **13**(21):5986–95. doi:10.1016/j.bmc.2005.07.025
129. Guo T, Adang AE, Dolle RE, Dong G, Fitzpatrick D, Geng P, et al. Small molecule biaryl FSH receptor agonists. Part 1: lead discovery via encoded combinatorial synthesis. *Bioorg Med Chem Lett* (2004) **14**(7):1713–6. doi:10.1016/j.bmcl.2004.01.043
130. Guo T, Adang AE, Dong G, Fitzpatrick D, Geng P, Ho KK, et al. Small molecule biaryl FSH receptor agonists. Part 2: lead optimization via parallel synthesis. *Bioorg Med Chem Lett* (2004) **14**(7):1717–20. doi:10.1016/j.bmcl.2004.01.043
131. Magar S., Goutopoulos A., Liao Y., Schwarz M., R.J. T, Inventors; Merck Serono SA, assignee. *Piperazine Derivatives and Methods of Use*. United States patent US WO2004/031182 (2004).
132. van Straten NC, van Berkel TH, Demont DR, Karstens WJ, Merkx R, Oosterom J, et al. Identification of substituted 6-amino-4-phenyltetrahydroquinoline derivatives: potent antagonists for the follicle-stimulating hormone receptor. *J Med Chem* (2005) **48**(6):1697–700. doi:10.1021/jm049676l
133. Grima Poveda PM, Karstens Willem FJ, Timmers CM, Inventors; N.V. Organon, assignee. *4-Phenyl-5-Oxo-1,4,5,6,7,8-Hexahydroquinoline Derivatives for the Treatment of Infertility*. United States patent US 8,022,218 (2006).
134. Hanssen RGJM, Timmers CM, Inventors. *Preparation of Thienopyrimidines with Combined FSH and LH Activity* (2003).
135. van Koppen CJ, Verbost PM, van de Lagemaat R, Karstens WJ, Loozen HJ, van Achterberg TA, et al. Signaling of an allosteric, nanomolar potent, low molecular weight agonist for the follicle-stimulating hormone receptor. *Biochem Pharmacol* (2013) **85**(8):1162–70. doi:10.1016/j.bcp.2013.02.001
136. Timmers CM, Karstens WF, Grima Poveda PM, Inventors; N.V. Organon, assignee. *4-Phenyl-5-Oxo-1,4,5,6,7,8-Hexahydroquinoline Derivatives as Medicaments for the Treatment of Infertility*. United States patent US WO2006/117370 (2006).
137. Bahamondes L, Bahamondes MV. New and emerging contraceptives: a state-of-the-art review. *Int J Womens Health* (2014) **6**:221–34. doi:10.2147/IJWH.S46811
138. Warren AM, Gurvich C, Worsley R, Kulkarni J. A systematic review of the impact of oral contraceptives on cognition. *Contraception* (2014) **90**(2):111–6. doi:10.1016/j.contraception.2014.03.015
139. Palermo R. Differential actions of FSH and LH during folliculogenesis. *Reprod Biomed Online* (2007) **15**(3):326–37. doi:10.1016/S1472-6483(10)60347-1
140. Vegetti W, Alagna F. FSH and folliculogenesis: from physiology to ovarian stimulation. *Reprod Biomed Online* (2006) **12**(6):684–94. doi:10.1016/S1472-6483(10)61080-2
141. Weinbauer GF, Behre HM, Fingscheidt U, Nieschlag E. Human follicle-stimulating hormone exerts a stimulatory effect on spermatogenesis, testicular size, and serum inhibin levels in the gonadotropin-releasing hormone antagonist-treated nonhuman primate (*Macaca fascicularis*). *Endocrinology* (1991) **129**(4):1831–9. doi:10.1210/endo-129-4-1831
142. Moudgal NR, Sairam MR, Krishnamurthy HN, Sridhar S, Krishnamurthy H, Khan H. Immunization of male bonnet monkeys (*M. radiata*) with a recombinant FSH receptor preparation affects testicular function and fertility. *Endocrinology* (1997) **138**(7):3065–8. doi:10.1210/endo.138.7.5381
143. Arey BJ, Deecher DC, Shen ES, Stevis PE, Meade EH Jr, Wrobel J, et al. Identification and characterization of a selective, nonpeptide follicle-stimulating hormone receptor antagonist. *Endocrinology* (2002) **143**(10):3822–9. doi:10.1210/en.2002-220372
144. Coats SJ, Fitzpatrick LJ, Hlasta DJ, Lanter CL, Macielag MJ, Pan K, et al., Inventors; Ortho-McNeill Pharmaceutical, Inc., assignee. *Substituted Aminoalkylamide Derivatives as Antagonists of Follicle Stimulating Hormone*. United States patent US 6,583,179 B2 (2003).
145. Bonger KM, Hoogendoorn S, van Koppen CJ, Timmers CM, Overkleeft HS, van der Marel GA. Synthesis and pharmacological evaluation of dimeric follicle-stimulating hormone receptor antagonists. *ChemMedChem* (2009) **4**(12):2098–102. doi:10.1002/cmdc.200900344
146. van de Lagemaat R, van Koppen CJ, Krajnc-Franken MA, Folmer BJ, van Diepen HA, Mulders SM, et al. Contraception by induction of luteinized unruptured follicles with short-acting low molecular weight FSH receptor agonists in female animal models. *Reproduction* (2011) **142**(6):893–905. doi:10.1530/REP-11-0234
147. Dias JA, Campo B, Weaver BA, Watts J, Kluetzman K, Thomas RM, et al. Inhibition of follicle-stimulating hormone-induced preovulatory follicles in rats treated with a nonsteroidal negative allosteric modulator of follicle-stimulating hormone receptor. *Biol Reprod* (2014) **90**(1):19. doi:10.1095/biolreprod.113.109397
148. Newton CL, Whay AM, McArdle CA, Zhang M, van Koppen CJ, van de Lagemaat R, et al. Rescue of expression and signaling of human luteinizing hormone G protein-coupled receptor mutants with an allosterically binding small-molecule agonist. *Proc Natl Acad Sci U S A* (2011) **108**(17):7172–6. doi:10.1073/pnas.1015723108
149. Jorand-Lebrun C, Brondyk B, Lin J, Magar S, Murray R, Reddy A, et al. Identification, synthesis, and biological evaluation of novel pyrazoles as low molecular weight luteinizing hormone receptor agonists. *Bioorg Med Chem Lett* (2007) **17**(7):2080–5. doi:10.1016/j.bmcl.2006.12.062
150. Bonger KM, Hoogendoorn S, van Koppen CJ, Timmers CM, van der Marel GA, Overkleeft HS. Development of selective LH receptor agonists by heterodimerization with a FSH receptor antagonist. *ACS Med Chem Lett* (2011) **2**(1):85–9. doi:10.1021/ml100229v
151. van de Lagemaat R, Timmers CM, Kelder J, van Koppen C, Mosselman S, Hanssen RG. Induction of ovulation by a potent, orally active, low molecular weight agonist (Org 43553) of the luteinizing hormone receptor. *Hum Reprod* (2009) **24**(3):640–8. doi:10.1093/humrep/den412
152. van Koppen CJ, Zaman GJ, Timmers CM, Kelder J, Mosselman S, van de Lagemaat R, et al. A signaling-selective, nanomolar potent allosteric low molecular weight agonist for the human luteinizing hormone receptor. *Naunyn Schmiedebergs Arch Pharmacol* (2008) **378**(5):503–14. doi:10.1007/s00210-008-0318-3
153. Binder H, Dittrich R, Einhaus F, Krieg J, Muller A, Strauss R, et al. Update on ovarian hyperstimulation syndrome: part 1 – incidence and pathogenesis. *Int J Fertil Womens Med* (2007) **52**(1):11–26.
154. Vlahos NF, Gregoriou O. Prevention and management of ovarian hyperstimulation syndrome. *Ann N Y Acad Sci* (2006) **1092**:247–64. doi:10.1196/annals.1365.021
155. Kashyap S, Parker K, Cedars MI, Rosenwaks Z. Ovarian hyperstimulation syndrome prevention strategies: reducing the human chorionic gonadotropin trigger dose. *Semin Reprod Med* (2010) **28**(6):475–85. doi:10.1055/s-0030-1265674
156. van de Lagemaat R, Raafs BC, van Koppen C, Timmers CM, Mulders SM, Hanssen RG. Prevention of the onset of ovarian hyperstimulation syndrome (OHSS) in the rat after ovulation induction with a low molecular weight agonist of the LH receptor compared with hCG and rec-LH. *Endocrinology* (2011) **152**(11):4350–7. doi:10.1210/en.2011-1077
157. Gerrits M, Mannaerts B, Kramer H, Addo S, Hanssen R. First evidence of ovulation induced by oral LH agonists in healthy female volunteers of reproductive age. *J Clin Endocrinol Metab* (2013) **98**(4):1558–66. doi:10.1210/jc.2012-3404
158. Heitman LH, Narlawar R, de Vries H, Willemsen MN, Wolfram D, Brussee J, et al. Substituted terphenyl compounds as the first class of low molecular weight allosteric inhibitors of the luteinizing hormone receptor. *J Med Chem* (2009) **52**(7):2036–42. doi:10.1021/jm801561h
159. Heitman LH, Oosterom J, Bonger KM, Timmers CM, Wiegerinck PH, Ijzerman AP. [3H]Org 43553, the first low-molecular-weight agonistic and

allosteric radioligand for the human luteinizing hormone receptor. *Mol Pharmacol* (2008) **73**(2):518–24. doi:10.1124/mol.107.039875
160. Davies TF, Latif R. Targeting the thyroid-stimulating hormone receptor with small molecule ligands and antibodies. *Expert Opin Ther Targets* (2015) **19**(6):835–47. doi:10.1517/14728222.2015.1018181
161. Neumann S, Raaka BM, Gershengorn MC. Human TSH receptor ligands as pharmacological probes with potential clinical application. *Expert Rev Endocrinol Metab* (2009) **4**(6):669. doi:10.1586/eem.09.36
162. Jaschke H, Neumann S, Moore S, Thomas CJ, Colson AO, Costanzi S, et al. A low molecular weight agonist signals by binding to the transmembrane domain of thyroid-stimulating hormone receptor (TSHR) and luteinizing hormone/chorionic gonadotropin receptor (LHCGR). *J Biol Chem* (2006) **281**(15):9841–4. doi:10.1074/jbc.C600014200
163. Neumann S, Huang W, Titus S, Krause G, Kleinau G, Alberobello AT, et al. Small-molecule agonists for the thyrotropin receptor stimulate thyroid function in human thyrocytes and mice. *Proc Natl Acad Sci U S A* (2009) **106**(30):12471–6. doi:10.1073/pnas.0904506106
164. Neumann S, Kleinau G, Costanzi S, Moore S, Jiang JK, Raaka BM, et al. A low-molecular-weight antagonist for the human thyrotropin receptor with therapeutic potential for hyperthyroidism. *Endocrinology* (2008) **149**(12):5945–50. doi:10.1210/en.2008-0836
165. Neumann S, Eliseeva E, McCoy JG, Napolitano G, Giuliani C, Monaco F, et al. A new small-molecule antagonist inhibits Graves' disease antibody activation of the TSH receptor. *J Clin Endocrinol Metab* (2011) **96**(2):548–54. doi:10.1210/jc.2010-1935
166. Turcu AF, Kumar S, Neumann S, Coenen M, Iyer S, Chiriboga P, et al. A small molecule antagonist inhibits thyrotropin receptor antibody-induced orbital fibroblast functions involved in the pathogenesis of Graves ophthalmopathy. *J Clin Endocrinol Metab* (2013) **98**(5):2153–9. doi:10.1210/jc.2013-1149
167. van Koppen CJ, de Gooyer ME, Karstens WJ, Plate R, Conti PG, van Achterberg TA, et al. Mechanism of action of a nanomolar potent, allosteric antagonist of the thyroid-stimulating hormone receptor. *Br J Pharmacol* (2012) **165**(7):2314–24. doi:10.1111/j.1476-5381.2011.01709.x
168. van Zeijl CJ, van Koppen CJ, Surovtseva OV, de Gooyer ME, Plate R, Conti P, et al. Complete inhibition of rhTSH-, Graves' disease IgG-, and M22-induced cAMP production in differentiated orbital fibroblasts by a low-molecular-weight TSHR antagonist. *J Clin Endocrinol Metab* (2012) **97**(5):E781–5. doi:10.1210/jc.2011-2931
169. Neumann S, Nir EA, Eliseeva E, Huang W, Marugan J, Xiao J, et al. A selective TSH receptor antagonist inhibits stimulation of thyroid function in female mice. *Endocrinology* (2014) **155**(1):310–4. doi:10.1210/en.2013-1835
170. Heitman LH, Kleinau G, Brussee J, Krause G, Ijzerman AP. Determination of different putative allosteric binding pockets at the lutropin receptor by using diverse drug-like low molecular weight ligands. *Mol Cell Endocrinol* (2012) **351**(2):326–36. doi:10.1016/j.mce.2012.01.010
171. Schwartz TW, Frimurer TM, Holst B, Rosenkilde MM, Elling CE. Molecular mechanism of 7TM receptor activation – a global toggle switch model. *Annu Rev Pharmacol Toxicol* (2006) **46**:481–519. doi:10.1146/annurev.pharmtox.46.120604.141218
172. Janovick JA, Maya-Nunez G, Ulloa-Aguirre A, Huhtaniemi IT, Dias JA, Verbost P, et al. Increased plasma membrane expression of human follicle-stimulating hormone receptor by a small molecule thienopyr(im)idine. *Mol Cell Endocrinol* (2009) **298**(1–2):84–8. doi:10.1016/j.mce.2008.09.015

Conflict of Interest Statement: Selvaraj G. Nataraja, Henry N. Yu, and Stephen S. Palmer are founders and employees of TocopheRx; Henry N. Yu is also an employee of EMD Serono Research and Development Institute Inc.

frontiers in Endocrinology

REVIEW
published: 29 September 2015
doi: 10.3389/fendo.2015.00152

Genetic models for the study of luteinizing hormone receptor function

*Prema Narayan**

Department of Physiology, School of Medicine, Southern Illinois University, Carbondale, IL, USA

The luteinizing hormone/chorionic gonadotropin receptor (LHCGR) is essential for fertility in men and women. LHCGR binds luteinizing hormone (LH) as well as the highly homologous chorionic gonadotropin. Signaling from LHCGR is required for steroidogenesis and gametogenesis in males and females and for sexual differentiation in the male. The importance of LHCGR in reproductive physiology is underscored by the large number of naturally occurring inactivating and activating mutations in the receptor that result in reproductive disorders. Consequently, several genetically modified mouse models have been developed for the study of LHCGR function. They include targeted deletion of LH and LHCGR that mimic inactivating mutations in hormone and receptor, expression of a constitutively active mutant in LHCGR that mimics activating mutations associated with familial male-limited precocious puberty and transgenic models of LH and hCG overexpression. This review summarizes the salient findings from these models and their utility in understanding the physiological and pathological consequences of loss and gain of function in LHCGR signaling.

Keywords: luteinizing hormone receptor, gonadotropins, inactivating and activating mutations, genetic models, knockout mice, knockin mice, transgenic mice

OPEN ACCESS

Edited by:
Brian J. Arey, Bristol-Myers Squibb Company, USA

Reviewed by:
Emma June Petrie, The Walter and Eliza Hall Institute of Medical Research, Australia
Chengcheng "Alec" Zhang, University of Texas Southwestern Medical Center, USA

***Correspondence:**
Prema Narayan, Department of Physiology, School of Medicine, Southern Illinois University, LSIII, 1135 Lincoln Drive, Carbondale, IL 62901, USA
pnarayan@siumed.edu

Specialty section:
This article was submitted to Molecular and Structural Endocrinology, a section of the journal Frontiers in Endocrinology

Received: *17 July 2015*
Accepted: *11 September 2015*
Published: *29 September 2015*

Citation:
Narayan P (2015) Genetic models for the study of luteinizing hormone receptor function. Front. Endocrinol. 6:152. doi: 10.3389/fendo.2015.00152

Introduction

The luteinizing hormone/chorionic gonadotropin receptor (LHCGR), together with the glycoprotein hormone receptors, follicle-stimulating hormone receptor (FSHR) and thyroid stimulating hormone receptor (TSHR), belongs to the G protein-coupled receptor superfamily (1). LHCGR is the target receptor for the pituitary-derived luteinizing hormone (LH) and the highly homologous placental chorionic gonadotropin (CG). The fully processed human LHCGR is 675 amino acid residues long and is characterized by a large extracellular domain that is sufficient for hormone binding (2). The LHCGR has 11 exons with the first 10 exons encoding the extracellular domain and exon 11 encoding the C-terminal tail of the hinge region of the extracellular domain, the transmembrane helices with the connecting extra- and intracellular loops, and the cytoplasmic tail (1, 2). Functional LHCGR is essential for sex differentiation in the fetus and reproductive function in the adult. During fetal development in males, LHCGR present in the interstitial fetal Leydig cells of the testis binds to placental CG to produce testosterone required for male sexual differentiation (3, 4). Postnatally, LH stimulates LHCGR in the Leydig cells to produce testosterone required for development of puberty, male secondary sexual characteristics, and spermatogenesis. Female fetal sex differentiation does not require LH or steroid hormones. Postnatally, in females, LHCGR is present in the theca cells lining the follicle, mature granulosa cells, stromal cells, and luteinized cells. LH activation of LHCGR in the

theca cells stimulates androgen production, thereby providing the substrate for conversion to estradiol by follicle-stimulating hormone (FSH) induced aromatase in granulosa cells and triggering puberty (5). LHCGR activation is required for ovulation and subsequent progesterone production by the corpus luteum (6). The canonical signaling pathway mediated by LHCGR for steroidogenesis is the Gαs/cAMP/protein kinase A pathway. However, LHCGR can also activate additional pathways, including the Gαq/inositol phosphate/protein kinase C, protein kinase B, and ERK1/2 pathways (6–10). In the testis, the ERK1/2 cascade modulates androgen synthesis as well as proliferation/survival of Leydig cells (11–15). In the ovary, LHCGR-mediated activation of the EGF network and ERK1/2 cascade via Gαs/cAMP is required for resumption of meiosis, cumulus expansion, and luteinization, whereas follicular rupture is dependent on both Gαs and Gαq/11 (6, 16).

Naturally Occurring Mutations in *LHCGR* and *LHB* Genes

The large number of naturally occurring mutations and polymorphisms in the LHCGR gene that result in disorders of sexual development and reproductive function (4, 17) highlights the critical role of this receptor in reproduction. Mutations are inactivating, resulting in loss of receptor function, or activating resulting in constitutive activation of the receptor. These mutations have been particularly useful in elucidating the molecular mechanisms of LHCGR activation. Inactivating mutations are present in all domains of the receptor and may be missense mutations, insertions, deletions, and nonsense mutations. As a result, there may be partial inactivation or complete loss of receptor function caused by premature truncation of the receptor protein or failure to traffic to the cell surface (18). The mutations are recessive (19) and patients are either homozygous or compound heterozygous carriers. In males, inactivating mutations result in failure of testicular Leydig cell differentiation, resulting in the disorder called Leydig cell hypoplasia (LCH). Two types of Leydig cell hypoplasia are identified. The severe form is caused by mutations that result in loss of receptor protein, failure of receptor to traffic to cell surface, or failure to transduce a signal. This results in 46,XY male pseudohermaphroditism with female external genitalia, undescended testes, low testosterone, and high LH levels. The milder form, caused by mutations that allow partial LHR function, results in micropenis and hypospadia (4, 17, 20). Testicular histology showed hyalinized basement membrane in the seminiferous tubules with Sertoli cells but few or no germ cells (4). Females with inactivating mutations exhibit amenorrhea and infertility, but normal feminization at puberty indicating that LH is not essential for pubertal development. Activating mutations resulting in single amino acid replacements in LHCGR were the first to be described in patients with familial male-limited precocious puberty (FMPP) (21, 22). This is a rare disorder affecting upto 9/million (Orphanet/NIH, Office of Rare Diseases). In early studies, before the availability of molecular analyses, this disorder was called familial testotoxicosis (23, 24). These mutations are heterozygous and inherited in an autosomal dominant male-limited pattern although a few sporadic cases have been reported (25). Clinically, these boys present with precocious puberty by 3–4 years of age, Leydig cell hyperplasia, and high circulating levels of testosterone in the context of prepubertal levels of LH (26–28). Surprisingly, female carriers of activating mutations are normal. The mutations are limited to exon 11 and clustered in transmembrane helix 6 and the third intracellular loop with aspartic acid at position 578 most commonly mutated to glycine (D578G) (22, 28). This mutation is found in about 62% of all FMPP cases and 29% of all sporadic cases of male-limited precocious puberty (29). Only one activating somatic mutation (D578H) has been identified so far in boys with precocious puberty and Leydig cell adenomas (30–32) and this mutation has not been identified in boys with FMPP.

In contrast to the large number of activating and inactivating mutations in LHCGR, no germ line mutations in the common α-subunit or hCGβ subunits and no gain-of-function mutations in LHβ have been identified. Only three inactivating mutations in LHβ resulting in complete loss of bioactive LH have been reported in four men and one woman (33–35). In all cases, the males were normally masculinized at birth but later presented with delayed or lack of spontaneous puberty, hypogonadism, low testosterone levels, and infertility. Testicular biopsy revealed absence of complete spermatogenesis and mature Leydig cells (33, 34). This suggests that LH is not required for male sexual differentiation. Fetal testosterone production begins autonomously and then becomes dependent on maternal hCG activation of LHCGR. Postnatal testicular development and function is, however, dependent on pituitary LH. Treatment with exogenous LH and hCG resulted in an increase in testosterone, indicating that receptor function was normal (33). The single female patient showed normal pubertal development but presented with secondary amenorrhea and infertility (35). The normal pubertal development is similar to that seen in women with a homozygous inactivating mutation in the LHCGR gene (36–39). A fourth mutation resulting in a deletion of amino acid residues 10–12 of LHβ was reported in a man and his sister (40). In spite of undetectable levels of LH and low serum and intratesticular testosterone, the man had complete spermatogenesis and normal sperm count. The low residual activity of the mutant LH detected *in vitro* was apparently sufficient for normal spermatogenesis. The single female patient underwent normal puberty, but developed secondary amenorrhea and infertility (35).

Genetic Models to Study LHCGR Function

Several mouse models have been developed that model human reproductive disorders involving LHCGR signaling. They include knockout models of LH and LHCGR to mimic the inactivating LHβ and LHCGR mutations (41–43) and knockin mice expressing a constitutively active mutant LHCGR (44, 45) to mimic the activating LHCGR mutations. In addition, several transgenic models of enhanced LH/hCG action have been generated. They include mice expressing the LHβ-CGβ carboxyl terminal peptide (CTP) fusion protein under the control of the bovine common α subunit promoter (46), mice expressing hCG under the control of the ubiquitin C (47, 48) or metallothionein promoter (49), and mice expressing a yoked hCG–LHCGR fusion protein and

D556H rat LHCGR under the control of the inhibin α subunit promoter (50).

LHβ Knockout Mice

Phenotype of Male Mice

LHβ knockout mice were generated by deleting the coding sequence of the *Lhb* gene (43). Heterozygous mice were fertile and homozyous male and female mice were infertile. Serum levels of LH were undetectable, while serum FSH levels were normal. Male mice had significantly smaller testes and accessory glands consistent with reduced levels of serum and testicular testosterone. Testes contained very few Leydig cells, which were mostly fetal and immature adult Leydig cells as indicated by increased levels of serum androstenedione and upregulation of the fetal Leydig cell marker, thrombospondin. Spermatogenesis in the mutant mice was arrested at the round spermatid stage, indicating that LH and/or testosterone are required for the last step in spermatogenesis. Some Sertoli cell markers (FSHR) and inhibin α were unchanged in the knockout mice, while others (anti-mullerian hormone and the inhibin β subunits) were upregulated, indicating that lack of LHβ caused both somatic and germ cell defects. Sexual differentiation and fetal gonadal development was normal in the knockout mice, indicating that pituitary LH is not required for fetal testosterone production and gonadal development. A similar result was seen in mice lacking the common alpha subunit (α-GSU) for gonadotropin hormones (51).

Phenotype of Female Mice

Female KO mice were also infertile with abnormal estrous cycles. Serum estradiol and progesterone were greatly reduced. Primary and secondary follicles were present in the ovary, but healthy antral, preovulatory, and corpora lutea (CL) were absent. Antral follicles contained degenerating oocytes. However, the theca cell layer appeared normal, indicating that the differentiation of this layer was independent of LH signaling. Expression of steroidogenic enzyme genes was reduced in both sexes consistent with the reduction in steroid hormone levels. Treatment of the knockout mice with hCG rescued the phenotype in both male and female mice, indicating that receptor responsiveness was normal.

LHCGR Knockout Mice (LuRKO)

Two groups independently reported the development of the LHCGR knockout mice by deleting part of the promoter region and exon 1 (41) or exon 11 encoding the transmembrane and intracellular domain of the receptor (42). Both models showed a complete loss of functional receptor resulting in infertility in both sexes. The reproductive phenotypes described by the two groups were similar.

Phenotype of Male Mice

Sexual differentiation was normal, demonstrating again that, unlike in humans, fetal testosterone production required for masculinization is gonadotropin independent in mice, as previously shown with the LHβ and the common alpha subunit (αGSU) knockout models (43, 51). The mice were phenotypically normal at birth. Postnatally, the mice exhibited cryptorchidism, reduced testis size, poorly developed accessory sex glands, and micropenis. Testosterone levels were dramatically reduced while levels of both serum LH and FSH were increased. The testis had dramatically reduced Leydig cell numbers and spermatogenesis was arrested in the round spermatid stage (41, 42). The slightly elevated FSH levels in the LuRKO mice apparently stimulated spermatogenesis to the round spermatid stage. Further analysis revealed that the testicular histology of the LuRKO mice was similar to wild type (WT) mice until about 3 weeks of age. After 3 weeks, the growth rate of the testis was dramatically decreased (52) and the interstitium lacked adult-type Leydig cells. Leydig cell-specific and steroidogenic enzyme genes showed similar level of expression in the neonatal WT and LuRKO mice but the LuRKO did not show the pubertal increase seen in WT mice. Testicular testosterone levels were similar between the genotypes at birth. Expression of the fetal Leydig cell marker *Tsp2* was similar between the genotypes but the adult Leydig cell markers, *Hsd3b6* and *Hsd17b3*, were downregulated at postpubertal ages. Together, these data suggested that testosterone production by fetal Leydig cells and initial differentiation of the adult Leydig cell population are not dependent on LHCGR action. However, differentiation to the mature Leydig cells with steroidogenic potential requires LHCGR signaling.

Testosterone replacement therapy at puberty restored full spermatogenesis and testicular descent, but failed to restore adult-type Leydig cells (53, 54), indicating that androgen-independent actions of LH are required for adult Leydig cell differentiation. However, the fertility of the mice could not be completely restored (54, 55). The subfertile phenotype was determined to be due to reduced epididymal sperm counts and low ejaculatory frequency. Additionally, inflammation in the prostate and vas deferens was observed (54). Interestingly, additional studies by Zhang et al. (56) reveal that complete spermatogenesis with the appearance of elongated spermatids can be observed in the LuRKO mice at 12 months of age although intratesticular testosterone levels remained suppressed and similar to the levels in 2-month-old mice. This result suggested that the low level of constitutively produced intratesticular testosterone was sufficient for differentiation of round to elongated spermatids.

Phenotype of Female Mice

Female KO mice were phenotypically normal at birth, which is not surprising since female sexual differentiation is independent of ovarian function and ovarian LHCGR expression begins after birth (57, 58). The age of vaginal opening was delayed in the KO mice and they did not exhibit normal estrous cyclicity. The uterus was atrophic with a thinning of all layers and lack of endometrial glands. Serum levels of estradiol and progesterone were suppressed but not absent (41). Estradiol and progesterone replacement therapy of 4-week-old KO mice for a period of 3 weeks stimulated vaginal growth and increased uterine size (55). However, the number of endometrial glands remained low and fertility was not restored. The ovaries were greatly reduced in size and ovaries contained preantral and antral follicles but no preovulatory follicles or CL (41, 42). This indicates that both ovulation and the maturation of antral to preovulatory follicles require LH action. The requirement of LHCGR action for follicle

maturation beyond the antral stage was novel and was further investigated in the LuRKO mice (59). This study showed that progression of folliculogenesis beyond the antral stage and induction of ovulation could not be achieved by hCG or recombinant FSH in the absence of LHCGR.

Knockin Mice Expressing the Constitutively Active Mutant D582G LHCGR (KiLHR^{D582G})

We have recently generated mice expressing a constitutively active Asp582Gly (D582G) mutant in the mouse LHCGR (44). The mice are heterozygous with one WT allele replaced by the mutant allele as seen in patients with FMPP. Expression from both WT and mutant alleles could be detected in the testis. This mutation is analogous to the most prevalent Asp578G mutation in humans with FMPP. When tested in cell culture, the mouse D582G LHCGR showed a similar binding affinity as WT LHCGR. However, the basal level of cAMP was 23-fold higher in cells expressing the mutant receptor compared to WT. These levels are much higher than the three- to fourfold increase in basal cAMP seen with the human LHCGR (22, 60), and similar to that obtained with the D578H mutation found in Leydig cell adenomas (30).

Phenotype of Male Mice

KiLHR^{D582G} mice exhibited precocious puberty as shown by the advancement of balanopreputial separation and the early detection of mouse urinary proteins in the urine by 15 days compared to 22 days for WT mice (44). Both are androgen-dependent events and indicators of puberty in mice (61, 62). Testosterone levels were elevated as early as 7 days of age while gonadotropin levels were suppressed. The high testosterone levels resulted in enlarged seminal vesicles and prostate but not in significantly higher body weights. Several of the Leydig cell-specific genes involved in the steroidogenic pathway, including *Lhcgr* were upregulated. In spite of the precocious puberty, no advancement in the timing of spermatogenesis was seen. Spermatogenesis and Sertoli cell development and function appeared unaffected although testis size was decreased in the KiLHR^{D582G} mice presumably due to the suppressed FSH levels. Significantly, Leydig cell hyperplasia was detected as early as 7 days (**Figure 1**). The hyperplasia was patchy with a higher prevalence around the periphery of the testis. Precocious maturation of adult Leydig cells occurred in the mutant mice leading to the hyperplasia. The severity of the hyperplasia appeared to increase in the older animals (**Figure 1**). Interestingly, the KiLHR^{D582G} mice became progressively infertile and were unable to produce litter after an average age of 5–6 months. This was not due to a defect in spermatogenesis as the number of total and motile sperm from the cauda epididymis of 6-month-old KiLHR^{D582G} mice was not different from the WT mice.

Phenotype of Female Mice

Female KiLHR^{D582G} mice exhibited precocious puberty and the age of vaginal opening was advanced by 2 weeks compared to WT mice (45). Mutant mice demonstrated irregular estrous cyclicity and were infertile. A temporal study from 2 to 24 weeks of age demonstrated elevated levels of androstenedione, testosterone, estradiol, and progesterone in the serum of KiLHR^{D582G} mice compared to WT mice. Consequently, gonadotropin levels were suppressed. The ovaries and uterus of the KiLHR^{D582G} mice were enlarged and large cysts were apparent in the gross morphology of the ovaries. The ovarian histology was normal in the 2-week-old KiLHR^{D582G} mice. However, degenerating follicles and hemorrhagic cysts were observed starting at 3 weeks of age (**Figure 2**). Follicles did not progress beyond the preantral stage likely due to lack of FSH stimulation. CL were not present indicating anovulation. Extensive stromal cell hypertrophy and hyperplasia with luteinization was apparent. In 6-month-old mice, granulosa cell tumors were evident in 50% of the KiLHR^{D582G} mice. Interestingly, the anovulatory phenotype could

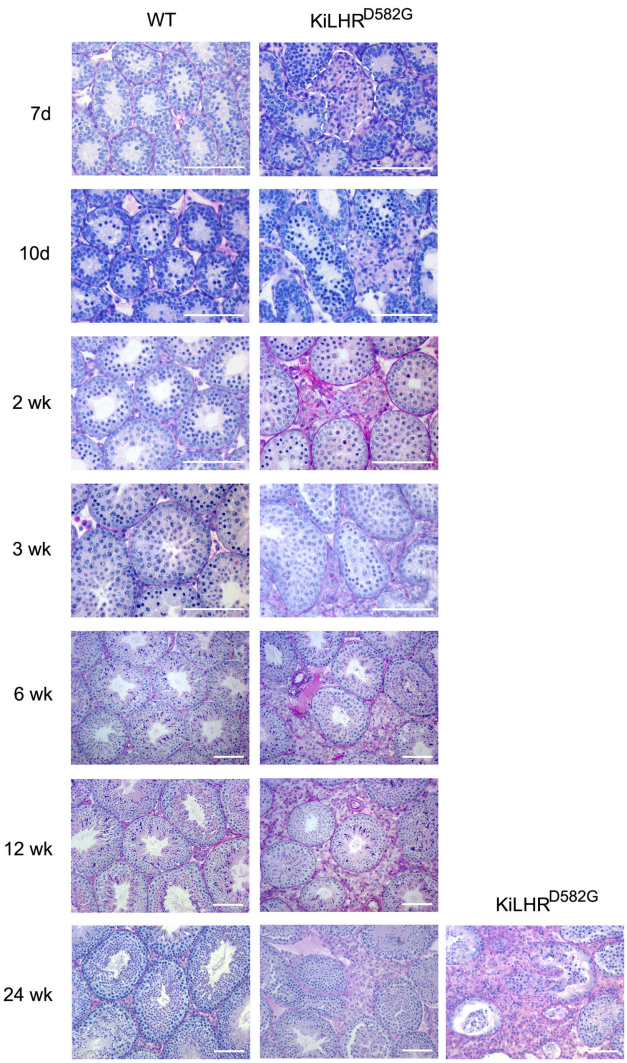

FIGURE 1 | Leydig cell hyperplasia in KiLHR^{D582G} mice. Representative photomicrographs of PASH stained testis sections of WT and KiLHR^{D582G} from 7 days to 24 weeks of age. At least three animals per age and genotype were examined. The Leydig cell interstitium is marked by the dashed lines in sections from the 7-day-old mice. Sections of testis from two 24-week-old KiLHR^{D582G} mice shows variation in the severity of the Leydig cell hyperplasia. Bar = 100 μm. From McGee and Narayan (44).

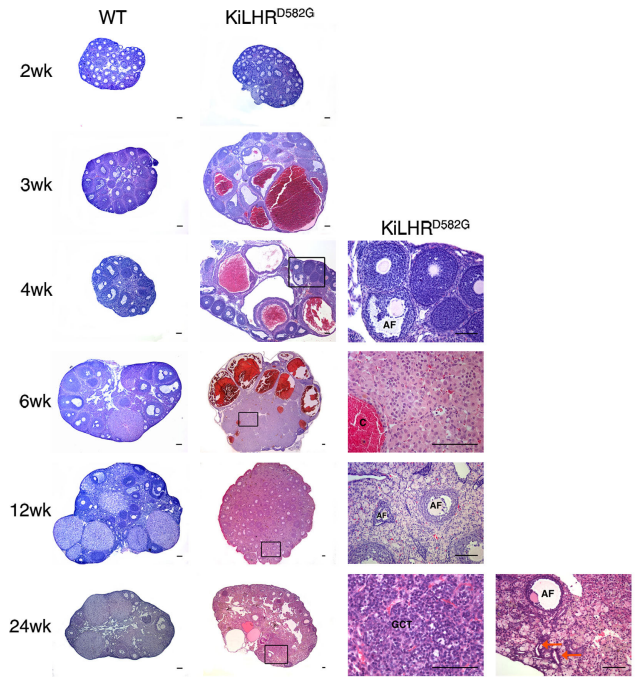

FIGURE 2 | Ovarian pathology in KiLHR^{D582G} mice. Representative photomicrographs of H&E stained ovary sections of WT and KiLHR^{D582G} mice. At least three animals per age and genotype were examined. Higher magnification of the boxed areas in sections of KiLHR^{D582G} mice at 4, 6, 12, and 24 weeks are shown in the last column. C, hemorrhagic cyst; GCT, granulosa cell tumor; AF, atretic follicle. Arrow indicates tubulostromal hyperplasia. Scale bars represent 100 μm. From Hai et al. (45).

not be rescued by superovulation with pregnant mare serum gonadotropin (PMSG) and hCG. Although preovulatory follicles with oocytes could be detected in the ovaries of the KiLHR^{D582G} mice, they did not rupture to form CL. This result suggests that neither the WT or D582G mutant LHCGR is able to respond to exogenous gonadotropins. LH-dependent induction of Gαs/cAMP is required for the activation of the EGF network and the ERK1/2 cascade responsible for oocyte maturation and cumulus expansion while LH activation of Gαq/11 and Gαs is required for ovulation (6, 16). Coexpression of a constitutively active hLHR (L457R) that was unresponsive to additional hormone stimulation, with the WT LHR in cell culture, caused an attenuation of the hCG/Gαs stimulated cAMP production by WT LHCGR (63). This attenuation was not due to a decrease in the cell surface expression of the WT receptor, but due to the activation of phosphodiesterase 4D3 resulting in decreased levels of cAMP. Perhaps a similar mechanism occurs *in vivo* in the granulosa cells of the KiLHR^{D582G} mice to inhibit ovulation. The body weights of KiLHR^{D582G} mice were higher than that of WT mice. However, there were no changes in body fat composition or insulin resistance as seen in experimentally induced hyperandrogenic rodent models of polycystic ovarian syndrome (PCOS).

LHβ Overexpressing Transgenic Mice

Transgenic mice expressing a chimeric protein (bLHβ-CTP) consisting of the bovine LHβ subunit fused in frame to the C-terminal peptide of hCGβ subunit driven by the pituitary-specific bovine glycoprotein α-subunit (α-GSU) promoter was first reported by Risma et al. (46). The addition of the CTP increased the circulatory half-life of LH resulting in constitutive high levels (5- to 10-fold) in the female but not male mice. Preliminary observations with the male mice showed reduced fertility and smaller testis in spite of normal hormone levels and the mice were not characterized further. Female LHβCTP mice presented with precocious puberty, elevated levels of testosterone, and estradiol and infertility due to anovulation (64). The predominant ovarian phenotype was the presence of hemorrhagic cysts with widespread luteinization of the interstitial tissue. Accelerated depletion of primordial follicles was also observed (65). Although anovulation could be reversed by treatment with exogenous gonadotropins, pregnancy could not be maintained due to defects in uterine receptivity and mid-gestation pregnancy failure (66). Additional ovarian defects included granulosa cell tumors by 5 months of age only in the genetic background of CF-1 mice (67). In a hybrid background, the phenotype resembled the luteoma of pregnancy and it was shown that three genes likely control the different phenotypes (67). In addition to the ovarian tumors, the LHβCTP mice also developed mammary gland tumors (68). An interesting non-reproductive phenotype resulting from the elevated LH in the LHβCTP mice is adrenal hyperplasia and induction of LHCGR expression and activity in the adrenal gland. As a result, corticosterone production is stimulated (69). This phenotype was dependent on the dysfunctional ovaries of the transgenic mice as gonadectomy abolished the adrenocortical hyperfunction. LHβCTP mice also have elevated levels of prolactin caused by the enhanced estrogen synthesis (69). It has been suggested that prolactin synergizes with LH in the induction of LHCGR expression in the adrenal glands. Additionally, LHβCTP female mice are obese (70). Obesity was associated with hyperphagia, increased intra-abdominal fat, increased levels of serum leptin and insulin, and reduced thermogenic activity of brown adipose tissue. The elevated androgens and corticosterone most likely contribute to the obesity seen in the LHβCTP females as ovariectomy normalized corticosterone levels and reversed the obesity and hyperphagia (70). Transgenic females also developed renal abnormalities, including enlarged bladders, dilated ureters, and hydronephrosis presumably due to the elevated steroids (46).

hCG Overexpressing Mice

Additional models of enhanced LH/hCG action were independently developed by two groups. Supraphysiological levels of hCG were expressed using the human ubiquitin C promoter or the mouse metallothionein-1 (MT-1) promoter (47–49). Transgenic mice expressing only the hCGβ subunit or both the common α subunit and hCGβ from multiple tissues were examined in both sexes.

Phenotype of Male Mice

In male mice expressing only the hCGβ subunit (hCGβ^{+}) under the human ubiquitin C promoter, circulating levels of dimeric hCG were detected, indicating that the hCGβ subunit associated with the endogenously produced α subunit in the pituitary (48).

However, dimeric hCG levels were only 3-4 fold higher than WT mice because the amount of endogenous α−GSU produced by the pituitary is rate-limiting. These mice were fertile and presented with only a mild reproductive phenotype of smaller testes (48). By contrast, mice expressing the hCGβ subunit under the mouse MT-1 promoter were infertile although hCG dimer could not be detected in the serum of these mice and the testes were morphologically and physiologically normal (49). This was surprising as individual subunits of hCG are devoid of activity (71).

Mice expressing both subunits (hCGαβ$^+$) under the control of the ubiquitin C promoter produced extremely high levels of dimeric hCG with about 2000-fold increase in circulating LH/hCG bioactivity in male mice (48). Serum and testicular testosterone and progesterone were elevated in spite of down regulation of receptor expression. Male mice were infertile and vaginal plugs were not observed when mice were mated with superovulated females in spite of motile and morphologically normal sperm in the cauda epididymis. Adult mice at 2–6 months of age showed smaller testes with normal tubular structure. However, progressive degenerative changes in the seminiferous tubules were observed. Mice developed focal Leydig cell hyperplasia/hypertrophy but not adenomas. Subsequent studies in prepubertal mice showed Leydig cell adenomas that were of fetal Leydig cell origin and disappeared at puberty (72). No sign of precocious puberty was observed in these young mice in spite of elevated levels of testosterone. The seminal vesicle and prostate were enlarged. The distention and sperm accumulation in the distal vas deferens as well as the dilated urinary bladder and ureters and enlarged kidneys pointed to a functional uretheral obstruction caused by the overproduction of secretory fluids or impaired emptying of the accessory glands. This may be a likely cause of infertility in these mice. Aggressive behavior of the males toward the females during mating may also contribute to the infertile phenotype.

Matzuk et al. used the MT-1 promoter to generate transgenic mice expressing low and high levels of the dimeric hCG (49). Males with low levels of heterodimer expression showed progressive infertility of unknown etiology. Adult males with high expression levels had similar reproductive defects as described above, including reduced testis size, Leydig cell hyperplasia, enlarged fluid-filled seminal vesicles, elevated testosterone levels, and infertility. Males were very aggressive toward both transgenic and non-transgenic males or females.

Phenotype of Female Mice

In contrast to male mice, female transgenic hCGβ$^+$ mice using the ubiquitin C promoter associated with the endogenously expressed mouse α-subunit to produce a 40-fold increase in bioactive LH/hCG compared to WT females (47). Although female hCGαβ$^+$ mice expressing both subunits as transgenes produced a 2000-fold elevation in bioactive LH/hCG, the phenotype of the hCGβ$^+$ and hCGαβ$^+$ mice were similar. Mice presented with precocious puberty, disrupted estrous cycles, and infertility. Adult mice were obese due to abdominal fat accumulation. Transiently elevated estradiol and persistent elevation of testosterone and progesterone were observed in the transgenic mice. The ovaries were significantly enlarged with massive luteinization, resembling luteomas, which may explain the transient increase in estradiol. Hemorrhagic cysts and CL were present. Females also developed macroprolactinomas and mammary gland tumors at 9–12 months of age. Serum prolactin was greatly elevated and may help maintain the ovarian luteinization and progesterone production. Metastasis of the mammary tumors to the liver, spleen, and lung was seen in about 47% of the mice. The mammary gland and pituitary tumors were dependent of ovarian function and ovariectomy prevented their development even when hCG levels were high. Subsequent studies (73) showed that the hCGαβ$^+$ mice with the 2000-fold elevation in bioactive LH/hCG develop teratomas.

Mice overexpressing only the hCGβ subunit under the MT-1 promoter were infertile although heterodimer could not be detected in the serum (49). These mice also had ovarian defects, including block in folliculogenesis and cysts. Mice with low levels of hCG dimer became progressively infertile. Mice expressing high levels of hCG dimer had elevated estradiol levels and developed enlarged cystic and hemorrhagic ovaries with stromal cell proliferation and enlarged thecal cell layers. Degenerating kidneys were also evident. These mice did not develop mammary gland or pituitary tumors.

Yoked Hormone Receptor and Rat D556H LHCGR Transgenic Mice

Transgenic mice expressing a yoked hormone receptor (YHR$^+$) genetically engineered by covalently linking hCG to LHCGR was generated to create a model for constitutively active LHCGR mutations. In cell culture, YHR exhibited an increase in the basal level of both cAMP and inositol phosphate similar to that seen with constitutively active mutants (50, 74). The transgene was expressed under the control of the gonadal-specific inhibin α-subunit promoter and male mice were fertile (75). Serum and testicular testosterone levels were elevated in YHR$^+$ mice at prepubertal ages of 3 and 5 weeks, but not at 8 and 12 weeks of age. Consistent with the increased testosterone was the increase in seminal vesicle weights. However, there was no evidence of precocious puberty. Serum levels of LH and FSH were decreased due to elevated testosterone. Testis size was decreased at all ages in YHR$^+$ mice and histological analysis showed a significant decrease in the cross-sectional area of the tubules. Spermatogenesis was not initiated earlier and Leydig cell hyperplasia, as seen in patients with constitutively active LHCGR, was also not observed. Further characterization of the male phenotype showed a reduction in the number of Leydig cells in YHR$^+$ mice accompanied by a reduction in the expression of several Leydig cell specific genes (76). The difference in the phenotype of the YHR$^+$ mice from humans with activating LHCGR mutations is likely because the inhibin α-subunit promoter did not faithfully mimic the spatial and temporal expression of LHCGR.

Female YHR$^+$ mice exhibited precocious puberty and were subfertile. Increased levels of estradiol and progesterone were observed at 5 weeks of age. However, the hormonal changes were no longer apparent in adult mice. Increased folliculogenesis and CL were observed in 5-week-old mice and interstitial cell hypertrophy, degenerating follicles, and follicular cysts were observed in adult mice.

Transgenic mice expressing the rat D556H LHCGR under the control of the inhibin α-subunit promoter was also generated

(50). This mutation corresponds to the somatic D578H mutation found in Leydig cell adenomas (30–32). Unfortunately, male and female mice expressing the transgene were infertile which prevented their further characterization. Preliminary analysis of two infertile founder male mice did not show testicular adenomas.

Comparison of the Mouse Models with Human Reproductive Pathologies of LHCGR Function

Inactivating Mutations and Knockout Models

The mouse models of inactivation of LHCGR function have verified existing knowledge, but more importantly have provided new information on the function of LH. Although the homozygous inactivating mutations in the *LHB* gene result in single amino acid, changes they cause result complete loss of bioactivity similar to the deletion of the *Lhb* gene in the mouse. The phenotype of the homozygous LHβ knockout male and female mice closely mimics that of humans with the inactivating LHβ mutations (**Table 1**). In males, sexual differentiation is normal in humans and mice. However, in humans, testosterone required for masculinization *in utero* is dependent on placental hCG stimulating LHCGR while in mice it is independent of LH action. LH is critical postnatally and both humans and mice show hypogonadism, low testosterone levels, arrest of spermatogenesis, Leydig cell hypoplasia, and infertility.

Female LHβ knockout mice displayed several characteristics similar to the single female patient with LHβ inactivating mutation identified thus far. Folliculogenesis was arrested at the antral

TABLE 1 | Summary of genetic models for the study of LHCGR function.

Gene (mutation/ mouse model)	Major human phenotypes	Major mouse phenotypes	Reference
A. COMPARISON OF HUMAN AND MOUSE PHENOTYPES FOR INACTIVATING AND ACTIVATING MUTATIONS IN LH AND LHCGR			
LHB (inactivating/ knockout)	Male: infertility, delayed puberty, hypogonadism, Leydig cell hypoplasia, spermatogenic arrest, normal sexual differentiation	Male: infertility, hypogonadism, Leydig cell hypoplasia, spermatogenesis arrested at round spermatid stage, normal sexual differentiation	(43)
	Female: normal pubertal development, normal uterus, folliculogenesis blocked at antral stage, secondary amenorrhea, infertility	Female: hypogonadal, folliculogenesis blocked at antral stage, hypoplastic uterus, infertility	
LHCGR (inactivating/ knockout)	Male: micropenis, hypospadia, pseudohermaphroditism, Leydig cell hypoplasia, germ cell defects	Male: infertility, Leydig cell hypoplasia, underdeveloped sex organs, spermatogenesis arrested at round spermatid stage, normal sexual differentiation	(41, 42)
	Female: normal pubertal development, amenorrhea, folliculogenesis blocked at antral stage, infertility	Female: delayed puberty, underdeveloped accessory glands, follicles arrested at antral stage, infertility	
LHCGR (activating/ knockin)	Male: precocious puberty, Leydig cell hyperplasia, high testosterone	Male: precocious puberty, Leydig cell hyperplasia, high testosterone, progressive infertility	(44, 45)
	Female: normal	Female: precocious puberty, cystic hemorrhagic ovaries with stromal cell hyperplasia with luteinization, granulosa cell tumors, infertility	
Construct	**Major phenotypes**		**Reference**
B. TRANSGENIC MOUSE MODELS OF ENHANCED LH/hCG ACTION			
α-GSU promoter/ bLHβ-CTP	Males: subfertility, smaller testis		(46, 66, 67)
	Females: precocious puberty, infertility, polycystic ovaries, stromal cell luteinization, granulosa cell tumors, mammary gland tumors, hydronephrosis		
Ubiquitin C promoter/ hCGβ	Males: no phenotype		(47, 48)
	Females: precocious puberty, infertility, luteinized cystic ovaries, prolactinomas, mammary gland tumors		
Ubiquitin C promoter/ hCGαβ	Males: infertility, adult Leydig cell hyperplasia, fetal Leydig cell adenomas, urethral obstruction, and kidney defects		(48, 73)
	Females: infertility, ovarian teratomas		
MT-1 promoter/hCGβ	Males: infertility		(49)
	Females: infertility, cystic, and hemorrhagic ovaries		
MT-1 promoter/hCGαβ	Males: infertility, Leydig cell hyperplasia		(49)
	Females: infertility, cystic, and hemorrhagic ovaries, degenerating kidneys		
Inhibin α-subunit promoter/YHR	Males: fertile, elevated testosterone with smaller testis, and Leydig cell hypoplasia		(75)
	Females: subfertile, precocious puberty, interstitial cell hypertrophy		

stage resulting in infertility. Surprisingly, this patient had normal puberty, with normal sized ovaries and breast and uterine development. Presumably, the low level of estradiol was sufficient for normal breast and uterine development (35).

Inactivating mutations in LHCGR in human males have a more severe phenotype, resulting from abnormal sexual differentiation, that those in LHβ emphasizing the importance of LHCGR signaling in sexual development and postnatal pubertal development. By contrast, the LuRKO mouse demonstrates that LHCGR signaling is not essential for mouse sexual differentiation, highlighting a major species difference. LHCGR activation is, however, important for postnatal development in both species. The phenotypes of the LHβ and LHCGR knockout male mice are very similar. Spermatogenic arrest at the round spermatid stage in both models indicates that FSH alone is not sufficient for full spermatogenesis and that testosterone produced by LH signaling is required for postmeiotic germ cell maturation. A novel observation that resulted from studies on the LHCGR knockout mice was that at 12 months of age, qualitatively complete spermatogenesis was possible in the absence of LH stimulated high testosterone production (56). This process, however, requires a long priming period. From a clinical standpoint, this finding may explain why men treated with testosterone for contraceptive purposes are not azoospermic (56).

Women with inactivating LHCGR and LHβ mutations have normal pubertal development, indicating that LH signaling is not essential for puberty in women. This process is more dependent on FSH signaling as demonstrated by lack of pubertal development in women with inactivating mutations in the FSHβ or FSHR (77). LH signaling is, however, required in the mouse where absence of LHCGR delays pubertal development (**Table 1**). There is a remarkable similarity in the ovarian phenotype of women with inactivating LHβ and LHCGR mutations, LHβ knockout and LuRKO mice showing a block in folliculogenesis at the antral stage. The studies from these mouse models clearly showed for the first time that, in addition to its well-known role in ovulation, LH is also required for the final stage of follicular maturation before ovulation. Studies with the LuRKO mice (59) also clarified that ovulation could not be induced by FSH in the absence of functional LHCGR as has been previously suggested (78, 79).

Activating Mutations and Knockin Models

The most common mutation in FMPP is the D578G mutation in transmembrane helix 6. In the mouse model (KiLHR^{D582G}) generated in our laboratory, the corresponding D582G mutation was introduced into the WT *Lhcgr* gene (44). The male mouse is a good phenocopy of men with constitutively activating LHCGR mutations as shown by the development of precocious puberty, Leydig cell hyperplasia and high testosterone (**Table 1**). A major difference between the mouse model and FMPP patients is that spermatogenesis is not advanced in the KiLHR^{D582G} mouse. Presumably, the seminiferous cycle of 35 days is at a minimum in mice and cannot be shortened further even with premature testosterone production. Furthermore, spermatogenic development requires the expression of the androgen receptor in Sertoli cells and significant levels are not detected till around postnatal day 15 in mice (80). It has been demonstrated that premature expression of the androgen receptor in Sertoli cells can accelerate spermatogenic development (80). Two new findings form the mouse model, not previously reported or confirmed in FMPP cases, are that the hyperplasia is not uniform throughout the testis and that it results from the precocious development of adult Leydig cells. The progressive infertility and hyperplasia seen in the KiLHR^{D582G} mice suggest that FMPP patients may be susceptible to infertility and perhaps tumor development later in life. There is only one report of a FMPP patient with the D578G mutation who was diagnosed with nodular Leydig cell hyperplasia (81), primarily due to lack of long-term follow-up of FMPP patients past puberty.

The phenotype of female KiLHR^{D582G} mice (45) is distinctly different from women with activating mutations who are normal (82–84). Mice undergo precocious puberty and are infertile with significant ovarian pathology of hemorrhagic cysts, stromal cell hyperplasia, and granulosa cell tumors. The reason for this discrepancy is unclear. The low level of LHCGR expression in prepubertal girls, the requirement for the activation of both LHCGR and FSHR for puberty, and less efficient androgen synthesis in theca cells compared to Leydig cells (4, 82). A higher magnitude of LHCGR activation may be required for development of ovarian pathology. In this context, the mouse LHCGR has a higher level of constitutive activation than the human receptor and the phenotype of the female KiLHR^{D582G} mice is similar to transgenic models of LH and hCG overexpression. A novel finding from the study of KiLHR^{D582G} mice is the dominant negative effect of the mutant receptor on the function of the WT receptor. The lack of rescue of the anovulatory phenotype by the administration of PMSG and hCG indicated that D582G LHCGR inhibits signaling of the WT receptor and is the first report of such an effect *in vivo*.

In general, the knockout and knockin mouse models are close phenocopies of the human disorders; however, species differences in LHCGR function clearly exist. Although these differences provide useful knowledge on LHCGR physiology, they should be considered when the mice are used as models of human diseases.

Transgenic Models of Enhanced LH/hCG Action

Activating mutations in LH or hCG have not been identified. However, there are physiological and pathological states when these hormone levels are elevated. hCG is produced in high amounts in the first trimester of pregnancy and in gestational trophoblastic disease (1). In men and women, hCGβ, hyperglycosylated hCGβ, and occasionally hCG dimer are secreted from a variety of tumors (1). Gonadotroph adenomas induce high gonadotropin levels and hypersecretion of LH is observed in pathological conditions such as PCOS. Chronic elevation of gonadotropins occurs in menopause and this is proposed as risk factor for ovarian cancer (85).

A comparison of the phenotypes of the overexpressing LH/hCG mice is shown in **Table 1**. The LHβ-CTP model was the first overexpressing model described. Hormone levels were not elevated in male mice because the α-GSU promoter is inefficient in the male. Overexpression of dimer hCG driven by either the ubiquitin C or MT promoter resulted in similar male phenotypes

of infertility and Leydig cell hyperplasia with high testosterone levels. Aggressive behavior of the males toward the females was observed in both hCG models and this may contribute in part to the infertile phenotype. The infertility in the ubiquitin C promoter-driven hCG mice was not due to defects in sperm but possibly due to the urethral obstruction (48).

The pathological changes seen in the female LHβ-CTP and hCG overexpressing mice were similar with precocious puberty and infertility. Significant pathology was seen in all models, with cystic, hemorrhagic, and luteinized ovaries. Granulosa cell tumors were seen in the LHβ-CTP mice, but ubiquitin C promoter-hCG mice had ovarian luteomas and teratomas and no tumors were found in the MT-hCG mice. Both LHβ-CTP and ubiquitin C promoter-hCG mice develop mammary gland tumors, but the latter also develop prolactinomas in older mice. This indicates that chronic high levels of gonadotropins promote tumor formation in gonadal and non-gonadal tissues. The pituitary and mammary gland tumors are secondary effects of aberrant gonadal function. The inhibin α-subunit promoter-YHR mice did not exhibit the robust changes seen in the overexpressing mice in either males or females.

The LH/hCG overexpressing models and the inhibin α-subunit promoter-YHR mice were expected to mimic the activating LHCGR mutations by precocious activation of the receptor. Comparison of the male KiLHR^{D582G} mice with the transgenic mouse models of LH/hCG overexpression showed similar phenotypes of Leydig cell hyperplasia and high testosterone. Similar to the ubiquitin C promoter-hCG mice, the progressive infertility in the KiLHR^{D582G} mice was not due to sperm defects. However, there were distinct differences as well. The overexpressing models did not exhibit precocious puberty and Leydig cell adenomas in the ubiquitin promoter-hCG mice were of fetal origin rather than from adult Leydig cells as seen in the KiLHR^{D582G} mice. The inhibin α-subunit promoter-YHR mice did not exhibit phenotypes similar to either the KiLHR^{D582G} mice or LH/hCG overexpressing mice except for the increase in testosterone. Presumably, the promoter used was regulated differently from the endogenous LHCGR.

The reproductive (precocious puberty, infertility) and ovarian phenotypes (cystic, hemorrhagic ovaries, interstitial cell hypertrophy with luteinization, granulosa cell tumors) of the KiLHR^{D582G} mice are similar to the LH/hCG overexpressing mice. The luteomas, teratomas (47), and enlarged thecal cell layer are specific to the hCG overexpressing mice (49, 73). The extra-gonadal phenotypes of pituitary and mammary gland tumors are not also seen in the KiLHR^{D582G} mice. The obese phenotype seen in the LHβ-CTP and ubiquitin-hCG overexpressing mice is not evident in the KiLHR^{D582G} mice. In contrast to the KiLHR^{D582G} mice, the anovulatory phenotype of the LHβ-CTP could be rescued by exogenous gonadotropins (66), further confirming an inhibition of WT LHCGR function in the KiLHR^{D582G} mice. The differences in the phenotypes between the overexpressing models and KiLHR^{D582G} mice, particularly the extra-gonadal phenotypes, are likely due to the high levels of LH/hCG secreted by transgenes that were expressed ubiquitously under the control of promoters that do not mimic the spatial or temporal expression of LHCGR. Some of the differences between the three overexpressing models may be the result of different levels of hormone production, different promoters, and genetic background. However, the remarkable number of similarities between the models emphasizes the importance of LH/LHCGR action on reproductive physiology and pathophysiology.

Future Perspectives

Mouse models are now available that can mimic the genetic alterations in LH and LHCGR and physiological and pathological states of hormone excess. These models have reinforced the well-established roles of LH and LHCGR but have also uncovered novel functions. The KiLHR^{D582G} mice can be used to investigate the long-term reproductive and non-reproductive abnormalities that result from constitutive LHCGR activity, particularly the mechanism of the progressive infertility. This information will be useful in predicting the long-term health of FMPP patients. This mouse model will be valuable to test new therapeutic agents that can block constitutive activity and to further determine the *in vivo* mechanism of the dominant negative effect of the mutant receptor on WT receptor function. Based on the phenotypic changes seen in the models of enhanced LH/hCG action, it appears that female physiology is more sensitive to changes in LH-mediated signaling. In particular, these models can be used to better understand the signaling mechanisms important in the development of ovarian and extra-gonadal tumors and understand the role of LH in obesity and related metabolic changes. The models can be helpful in sorting out the controversies and conflicting data regarding the extra-gonadal actions of LHCGR. In general, all the described models are amenable to large-scale gene expression profiling to better understand LHCGR signaling mechanisms.

An area that has not been explored extensively is the neurological changes associated with LHCGR signaling. Testosterone is important in brain development and sexual differentiation. Behavioral studies have shown that FMPP patients are susceptible to attention deficit hyperactivity disorder and a higher rate of anxiety disorder (86). The KiLHR^{D582G} mice are an ideal animal model to assess cognitive and behavioral changes associated with FMPP. There is also increasing evidence that elevated levels of LH can exacerbate age-related cognitive decline in Alzheimer's disease (87, 88). LHβ-CTP mice exhibit cognitive deficits (89). Considering that functional LHCGR is expressed in the brain (90), it will be of interest to determine if cognitive and behavioral changes are due to direct LHCGR signaling in the brain or indirectly due to its activity in gonads. These mechanisms and the contributions of direct vs. indirect effects on the brain can be teased out with the mouse models. Clearly, these mouse models have the potential to uncover novel aspects of LHCGR signaling.

Acknowledgments

Work in the author's laboratory was supported by National Institutes of Health grant HD044119 and a Research Seed Grant from School of Medicine, Southern Illinois University.

References

1. Ascoli M, Narayan P. The gonadotropin hormones and their receptors. 7th ed. In: Strauss JL, Barbieri RL, editors. *Yen and Jaffe's Reproductive Endocrinology*. Philadelphia, PA: Elsevier (2013). p. 27–44.
2. Ascoli M, Fanelli F, Segaloff DL. The lutropin/choriogonadotropin receptor, a 2002 perspective. *Endocr Rev* (2002) **23**:141–74. doi:10.1210/edrv.23.2.0462
3. Huhtaniemi IT, Korenbrot CC, Jaffe RB. HCG binding and stimulation of testosterone biosynthesis in the human fetal testis. *J Clin Endocrinol Metab* (1977) **44**:963–7. doi:10.1210/jcem-44-5-963
4. Themmen APN, Huhtaniemi IT. Mutations of gonadotropins and gonadotropin receptors: elucidating the physiology and pathophysiology of pituitary-gonadal function. *Endocr Rev* (2000) **21**:551–83. doi:10.1210/edrv.21.5.0409
5. Richards JS. Hormonal control of gene expression in the ovary. *Endocr Rev* (1994) **15**:725–51. doi:10.1210/edrv-15-6-725
6. Breen SM, Andric N, Ping T, Xie F, Offermans S, Gossen JA, et al. Ovulation involves the luteinizing hormone-dependent activation of G(q/11) in granulosa cells. *Mol Endocrinol* (2013) **27**:1483–91. doi:10.1210/me.2013-1130
7. Richards JS, Russell DL, Ochsner S, Hsieh M, Doyle KH, Falender AE, et al. Novel signaling pathways that control ovarian follicular development, ovulation, and luteinization. *Recent Prog Horm Res* (2002) **57**:195–220. doi:10.1210/rp.57.1.195
8. Andric N, Ascoli M. A delayed gonadotropin-dependent and growth factor-mediated activation of the extracellular signal-regulated kinase 1/2 cascade negatively regulates aromatase expression in granulosa cells. *Mol Endocrinol* (2006) **20**:3308–20. doi:10.1210/me.2006-0241
9. Richards JS, Pangas SA. The ovary: basic biology and clinical implications. *J Clin Invest* (2010) **120**:963–72. doi:10.1172/JCI41350
10. Conti M, Hsieh M, Zamah AM, Oh JS. Novel signaling mechanisms in the ovary during oocyte maturation and ovulation. *Mol Cell Endocrinol* (2012) **356**:65–73. doi:10.1016/j.mce.2011.11.002
11. Martinelle N, Holst M, Soder O, Svechnikov K. Extracellular signal-regulated kinases are involved in the acute activation of steroidogenesis in immature rat Leydig cells by human chorionic gonadotropin. *Endocrinology* (2004) **145**:4629–34. doi:10.1210/en.2004-0496
12. Shiraishi K, Ascoli M. Lutropin/choriogonadotropin stimulate the proliferation of primary cultures of rat Leydig cells through a pathway that involves activation of the extracellularly regulated kinase 1/2 cascade. *Endocrinology* (2007) **148**:3214–25. doi:10.1210/en.2007-0160
13. Evaul K, Hammes SR. Cross-talk between G protein-coupled and epidermal growth factor receptors regulates gonadotropin-mediated steroidogenesis in Leydig cells. *J Biol Chem* (2008) **283**:27525–33. doi:10.1074/jbc.M803867200
14. Tai P, Shiraishi K, Ascoli M. Activation of the lutropin/choriogonadotropin receptor inhibits apoptosis of immature Leydig cells in primary culture. *Endocrinology* (2009) **150**:3766–73. doi:10.1210/en.2009-0207
15. Yamashita S, Tai P, Charron J, Ko C, Ascoli M. The Leydig cell MEK/ERK pathway is critical for maintaining a functional population of adult Leydig cells and for fertility. *Mol Endocrinol* (2011) **25**:1211–22. doi:10.1210/me.2011-0059
16. Fan H-Y, Liu Z, Shimada M, Sterneck E, Johnson PF, Hedrick SM, et al. MAPK3/1 (ERK1/2) in ovarian granulosa cells are essential for female fertility. *Science* (2009) **324**:938–41. doi:10.1126/science.1171396
17. Themmen APN. An update of the pathophysiology of human gonadotrophin subunit and receptor gene mutations and polymorphisms. *Reproduction* (2005) **130**:263–74. doi:10.1530/rep.1.00663
18. Martens JW, Verhoef-Post M, Abelin N, Ezabella M, Toledo SP, Brunner HG, et al. A homozygous mutation in the luteinizing hormone receptor causes partial Leydig cell hypoplasia: correlation between receptor activity and phenotype. *Mol Endocrinol* (1998) **12**:775–84. doi:10.1210/mend.12.6.0124
19. Saldanha PH, Arnhold IJ, Mendonca BB, Bloise W, Toledo SP. A clinico-genetic investigation of Leydig cell hypoplasia. *Am J Med Genet* (1987) **26**:337–44. doi:10.1002/ajmg.1320260212
20. Latronico AC, Segaloff DL. Naturally occurring mutations of the luteinizing-hormone receptor: lessons learned about reproductive physiology and G protein-coupled receptors. *Am J Hum Genet* (1999) **65**:949–58. doi:10.1086/302602
21. Kremer H, Mariman E, Otten BJ, Moll GW Jr, Stoellnga GBA, Wit JM, et al. Cosegregation of missense mutations of the luteinizing hormone receptor gene with familial male-limited precocious puberty. *Hum Mol Genet* (1993) **2**:1779–83. doi:10.1093/hmg/2.11.1779
22. Shenker A, Laue L, Kosugi S, Merendino JJ Jr, Minegishi T, Cutler GB Jr. A constitutively activating mutation of the luteinizing hormone receptor in familial male precocious puberty. *Nature* (1993) **365**:652–4. doi:10.1038/365652a0
23. Egli CA, Rosenthal SM, Grumbach MM, Montalvo JM, Gondos B. Pituitary gonadotropin-independent male-limited autosomal dominant sexual precocity in nine generations: familial testotoxicosis. *J Pediatr* (1985) **106**:33–40. doi:10.1016/S0022-3476(85)80460-1
24. Gondos B, Egli CA, Rosenthal SM, Grumbach MM. Testicular changes in gonadotropin-independent familial male sexual precocity. Familial testotoxicosis. *Arch Pathol Lab Med* (1985) **109**:990–5.
25. Gromoll J, Partsch CJ, Simoni M, Nordhoff V, Sippell WG, Nieschlag E, et al. A mutation in the first transmembrane domain of the lutropin receptor causes male precocious puberty. *J Clin Endocrinol Metab* (1998) **83**:476–80. doi:10.1210/jcem.83.2.4579
26. Schedewie HK, Reiter EO, Beitins IZ, Seyed S, Wooten VD, Jimenez JF, et al. Testicular Leydig cell hyperplasia as a cause of familial sexual precocity. *J Clin Endocrinol Metab* (1981) **52**:271–8. doi:10.1210/jcem-52-2-271
27. Rosenthal SM, Grumbach MM, Kaplan SL. Gonadotropin-independent familial sexual precocity with premature Leydig and Germinal cell maturation (familial testotoxicosis): effects of a potent luteinizing hormone-releasing factor agonist and medroxyprogesterone acetate therapy in four cases. *J Clin Endocrinol Metab* (1983) **57**:571–9. doi:10.1210/jcem-57-3-571
28. Laue L, Chan W, Hsueh A, Kudo M, Hsu S, Wu S, et al. Genetic heterogeneity of constitutively activating mutations of the human luteinizing hormone receptor in familial male-limited precocious puberty. *Proc Natl Acad Sci U S A* (1995) **92**:1906–10. doi:10.1073/pnas.92.6.1906
29. Wu SM, Leschek EW, Rennert OM, Chan WY. Luteinizing hormone receptor mutations in disorders of sexual development and cancer. *Front Biosci* (2000) **5**:D343–52. doi:10.2741/Wu
30. Liu G, Duranteau L, Carel JC, Monroe J, Doyle DA, Shenker A. Leydig-cell tumors caused by an activating mutation of the gene encoding the luteinizing hormone receptor. *N Engl J Med* (1999) **341**:1731–6. doi:10.1056/NEJM199912023412304
31. Canto P, Soderlund D, Ramon G, Nishimura E, Mendex JP. Mutational analysis of the luteinizing hormone receptor gene in two individuals with Leydig cell tumors. *Am J Med Genet* (2001) **108**:148–52. doi:10.1002/ajmg.10218
32. Richter-Unruh A, Wessels HT, Menken U, Bergmann M, Schmittmann-Ohters K, Schaper J, et al. Male LH-independent sexual precocity in a 3.5-year-old boy caused by a somatic activating mutation of the LH receptor in a Leydig cell tumor. *J Clin Endocrinol Metab* (2002) **87**:1052–6. doi:10.1210/jc.87.3.1052
33. Weiss J, Axelrod L, Whitcomb RW, Harris PE, Crowley WF, Jameson JL. Hypogonadism caused by a single amino acid substitution in the b-subunit of luteinizing hormone. *N Engl J Med* (1992) **326**:179–83. doi:10.1056/NEJM199201163260306
34. Valdes-Socin H, Salvi R, Daly AF, Gaillard RC, Quatresooz P, Tebeu P, et al. Brief report: hypogonadism in a patient with a mutation in the luteinizing hormone beta-subunit gene. *N Engl J Med* (2004) **351**:2619–25. doi:10.1056/NEJMoa040326
35. Lofrano-Porto A, Barra GB, Giacomini LA, Nascimento PP, Latronico AC, Casulari LA, et al. Luteinizing hormone beta mutation and hypogonadism in men and women. *N Engl J Med* (2007) **357**:897–904. doi:10.1056/NEJMoa071999
36. Latronico AC, Anasti J, Arnhold IJ, Rapaport R, Mendonca BB, Bloise W, et al. Brief report: testicular and ovarian resistance to luteinizing hormone caused by inactivating mutations of the luteinizing hormone-receptor gene. *N Engl J Med* (1996) **334**:507–12. doi:10.1056/NEJM199602223340805
37. Toledo SP, Brunner HG, Kraaij R, Post M, Dahia PL, Hayashida CY, et al. An inactivating mutation of the luteinizing hormone receptor causes amenorrhea in a 46,XX female. *J Clin Endocrinol Metab* (1996) **81**:3850–4. doi:10.1210/jcem.81.11.8923827
38. Latronico AC, Chai Y, Arnhold IJ, Liu X, Mendonca BB, Segaloff DL. A homozygous microdeletion in helix 7 of the luteinizing hormone receptor associated with familial testicular and ovarian resistance is due to both decreased cell surface expression and impaired effector activation by the cell surface receptor. *Mol Endocrinol* (1998) **12**:442–50. doi:10.1210/mend.12.3.0077

39. Stavrou SS, Zhu YS, Cai LQ, Katz MD, Herrera C, Defillo-Ricart M, et al. A novel mutation of the human luteinizing hormone receptor in 46XY and 46XX sisters. *J Clin Endocrinol Metab* (1998) **83**:2091–8. doi:10.1210/jcem.83.6.4855
40. Achard C, Courtillot C, Lahuna O, Meduri G, Soufir JC, Liere P, et al. Normal spermatogenesis in a man with mutant luteinizing hormone. *N Engl J Med* (2009) **361**:1856–63. doi:10.1056/NEJMoa0805792
41. Lei ZM, Mishra S, Zou W, Xu B, Foltz M, Li X, et al. Targeted disruption of luteinizing hormone/human chorionic gonadotropin receptor gene. *Mol Endocrinol* (2001) **15**:184–200. doi:10.1210/mend.15.1.0586
42. Zhang F-P, Poutanen M, Wilbertz J, Huhtaniemi I. Normal prenatal but arrested postnatal sexual development of luteinizing hormone receptor knockout (LuRKO) mice. *Mol Endocrinol* (2001) **15**:172–83. doi:10.1210/mend.15.1.0582
43. Ma X, Dong Y, Matzuk MM, Kumar TR. Targeted disruption of luteinizing hormone beta-subunit leads to hypogonadism, defects in gonadal steroidogenesis, and infertility. *Proc Natl Acad Sci U S A* (2004) **101**:17294–9. doi:10.1073/pnas.0404743101
44. McGee SR, Narayan P. Precocious puberty and Leydig cell hyperplasia in male mice with a gain of function mutation in the LH receptor gene. *Endocrinology* (2013) **154**:3900–13. doi:10.1210/en.2012-2179
45. Hai L, McGee SR, Rabideau AC, Paquet M, Narayan P. Infertility in female mice with a gain-of-function mutation in the luteinizing hormone receptor is due to irregular estrous cyclicity, anovulation, hormonal alterations, and polycystic ovaries. *Biol Reprod* (2015) **93**(16):11–11. doi:10.1095/biolreprod.115.129072
46. Risma KA, Clay CM, Nett TM, Wagner T, Yun J, Nilson JH. Targeted overexpression of luteinizing hormone in transgenic mice leads to infertility, polycystic ovaries, and ovarian tumors. *Proc Natl Acad Sci U S A* (1995) **92**:1322–6. doi:10.1073/pnas.92.5.1322
47. Rulli SB, Kuorelahti A, Karaer O, Pelliniemi LJ, Poutanen M, Huhtaniemi I. Reproductive disturbances, pituitary lactotrope adenomas, and mammary gland tumors in transgenic female mice producing high levels of human chorionic gonadotropin. *Endocrinology* (2002) **143**:4084–95. doi:10.1210/en.2002-220490
48. Rulli SB, Ahtiainen P, Makela S, Toppari J, Poutanen M, Huhtaniemi I. Elevated steroidogenesis, defective reproductive organs, and infertility in transgenic male mice overexpressing human chorionic gonadotropin. *Endocrinology* (2003) **144**:4980–90. doi:10.1210/en.2003-0403
49. Matzuk MM, Demayo FJ, Hadsell LA, Kumar TR. Overexpression of human chorionic gonadotropin causes multiple reproductive defects in transgenic mice. *Biol Reprod* (2003) **69**:338–46. doi:10.1095/biolreprod.102.013953
50. Meehan TP, Narayan P. Constitutively active luteinizing hormone receptors: consequences of in vivo expression. *Mol Cell Endocrinol* (2007) **260-262**:294–300. doi:10.1016/j.mce.2006.03.045
51. Kendall SK, Samuelson LC, Saunders TL, Wood RI, Camper SA. Targeted disruption of the pituitary glycoprotein hormone a-subunit produces hypogonadal and hypothyroid mice. *Genes Dev* (1995) **9**:2007–19. doi:10.1101/gad.9.16.2007
52. Zhang F-P, Pakarainen T, Zhu F, Poutanen M, Huhtaniemi I. Molecular characterization of postnatal development of testicular steroidogenesis in luteinizing hormone receptor knockout mice. *Endocrinology* (2004) **145**:1453–63. doi:10.1210/en.2003-1049
53. Lei ZM, Mishra S, Ponnuru P, Li X, Yang ZW, Rao CV. Testicular phenotype in luteinizing hormone receptor knockout animals and the effect of testosterone replacement therapy. *Biol Reprod* (2004) **71**:1605–31. doi:10.1095/biolreprod.104.031161
54. Pakarainen T, Zhang F-P, Makela S, Poutanen M, Huhtaniemi I. Testosterone replacement therapy induces spermatogenesis and partially restores fertility in luteinizing hormone receptor knockout mice. *Endocrinology* (2005) **146**:596–606. doi:10.1210/en.2004-0913
55. Rao CV, Lei ZM. Consequences of targeted inactivation of LH receptors. *Mol Cell Endocrinol* (2002) **187**:57–67. doi:10.1016/S0303-7207(01)00694-3
56. Zhang FP, Pakarainen T, Poutanen M, Toppari J, Huhtaniemi I. The low gonadotropin-independent constitutive production of testicular testosterone is sufficient to maintain spermatogenesis. *Proc Natl Acad Sci U S A* (2003) **100**:13692–7. doi:10.1073/pnas.2232815100
57. Sokka TA, Hamalainen TM, Kaipia A, Warren DW, Huhtaniemi IT. Development of luteinizing hormone action in the perinatal rat ovary. *Biol Reprod* (1996) **55**:663–70. doi:10.1095/biolreprod55.3.663
58. O'Shaughnessy PJ, McLelland D, McBride MW. Regulation of luteinizing hormone-receptor and follicle-stimulating hormone-receptor messenger ribonucleic acid levels during development in the neonatal mouse ovary. *Biol Reprod* (1997) **57**:602–8. doi:10.1095/biolreprod57.3.602
59. Pakarainen T, Zhang FP, Nurmi L, Poutanen M, Huhtaniemi I. Knockout of luteinizing hormone receptor abolishes the effects of follicle-stimulating hormone on preovulatory maturation and ovulation of mouse graafian follicles. *Mol Endocrinol* (2005) **19**:2591–602. doi:10.1210/me.2005-0075
60. Kosugi S, Mori T, Shenker A. The role of Asp^{578} in maintaining the inactive conformation of the human lutropin/choriogonadotropin receptor. *J Biol Chem* (1996) **271**:31813–7. doi:10.1074/jbc.271.50.31813
61. Korenbrot CC, Huhtaniemi IT, Weiner RI. Preputial separation as an external sign of pubertal development in the male rat. *Biol Reprod* (1977) **17**:298–303. doi:10.1095/biolreprod17.2.298
62. Knopf JL, Gallagher JF, Held WA. Differential, multihormonal regulation of the mouse major urinary protein gene family in the liver. *Mol Cell Biol* (1983) **3**:2232–40.
63. Shinozaki H, Butnev V, Tao YX, Ang KL, Conti M, Segaloff DL. Desensitization of Gs-coupled receptor signaling by constitutively active mutants of the human lutropin/choriogonadotropin receptor. *J Clin Endocrinol Metab* (2003) **88**:1194–204. doi:10.1210/jc.2002-021051
64. Risma KA, Hirshfield AN, Nilson JH. Elevated luteinizing hormone in prepubertal transgenic mice causes hyperandrogenemia, precocious puberty, and substantial ovarian pathology. *Endocrinology* (1997) **138**:3540–7. doi:10.1210/endo.138.8.5313
65. Flaws JA, Abbud R, Mann RJ, Nilson JH, Hirshfield AN. Chronically elevated luteinizing hormone depletes primordial follicles in the mouse ovary. *Biol Reprod* (1997) **57**:1233–7. doi:10.1095/biolreprod57.5.1233
66. Mann RJ, Keri RA, Nilson JH. Transgenic mice with chronically elevated luteinizing hormone are infertile due to anovulation, defects in uterine receptivity, and midgestation pregnancy failure. *Endocrinology* (1999) **140**:2592–601. doi:10.1210/endo.140.6.6927
67. Keri RA, Lozada KL, Abdul-Karim FW, Nadeau JH, Nilson JH. Luteinizing hormone induction of ovarian tumors: oligogenic differences between mouse strains dictates tumor disposition. *Proc Natl Acad Sci U S A* (2000) **97**:383–7. doi:10.1073/pnas.97.1.383
68. Milliken EL, Ameduri RK, Landis MD, Behrooz A, Abdul-Karim FW, Keri RA. Ovarian hyperstimulation by LH leads to mammary gland hyperplasia and cancer predisposition in transgenic mice. *Endocrinology* (2002) **143**:3671–80. doi:10.1210/en.2002-220228
69. Kero J, Poutanen M, Zhang FP, Rahman N, McNicol AM, Nilson JH, et al. Elevated luteinizing hormone induces expression of its receptor and promotes steroidogenesis in the adrenal cortex. *J Clin Invest* (2000) **105**:633–41. doi:10.1172/JCI7716
70. Kero JT, Savontaus E, Mikola M, Pesonen U, Koulu M, Keri RA, et al. Obesity in transgenic female mice with constitutively elevated luteinizing hormone secretion. *Am J Physiol Endocrinol Metab* (2003) **285**:E812–8. doi:10.1152/ajpendo.00367.2002
71. Narayan P, Gray J, Puett D. Yoked complexes of human choriogonadotropin and the lutropin receptor: evidence that monomeric individual subunits are inactive. *Mol Endocrinol* (2002) **16**:2733–45. doi:10.1210/me.2002-0208
72. Ahtiainen P, Rulli SB, Shariatmadari R, Pelliniemi LJ, Toppari J, Poutanen M, et al. Fetal but not adult Leydig cells are susceptible to adenoma formation in response to persistently high hCG level: a study on hCG overexpressing transgenic mice. *Oncogene* (2005) **24**:7301–9. doi:10.1038/sj.onc.1208893
73. Huhtaniemi I, Rulli S, Ahtiainen P, Poutanen M. Multiple sites of tumorigenesis in transgenic mice overproducing hCG. *Mol Cell Endocrinol* (2005) **234**:117–26. doi:10.1016/j.mce.2004.10.013
74. Wu C, Narayan P, Puett D. Protein engineering of a novel constitutively active hormone-receptor complex. *J Biol Chem* (1996) **271**:31638–42. doi:10.1074/jbc.271.49.31638
75. Meehan TP, Harmon BG, Overcast ME, Yu KK, Camper SA, Puett D, et al. Gonadal defects and hormonal alterations in transgenic mice expressing a single chain human chorionic gonadotropin-lutropin receptor complex. *J Mol Endocrinol* (2005) **34**:489–503. doi:10.1677/jme.1.01669
76. Coonce MM, Rabideau AC, McGee S, Smith K, Narayan P. Impact of a constitutively active luteinizing hormone receptor on testicular gene expression

and postnatal Leydig cell development. *Mol Cell Endocrinol* (2009) **298**:33–41. doi:10.1016/j.mce.2008.10.016
77. Layman LC, McDonough PG. Mutations of follicle stimulating hormone-beta and its receptor in human and mouse: genotype/phenotype. *Mol Cell Endocrinol* (2000) **161**:9–17. doi:10.1016/S0303-7207(99)00217-8
78. Tapanainen JS, Lapolt PS, Perlas E, Hsueh AJ. Induction of ovarian follicle luteinization by recombinant follicle-stimulating hormone. *Endocrinology* (1993) **133**:2875–80. doi:10.1210/endo.133.6.8243314
79. Wang XN, Greenwald GS. Human chorionic gonadotropin or human recombinant follicle-stimulating hormone (FSH)-induced ovulation and subsequent fertilization and early embryo development in hypophysectomized FSH-primed mice. *Endocrinology* (1993) **132**:2009–16. doi:10.1210/endo.132.5.8477652
80. Hazra R, Corcoran L, Robson M, McTavish KJ, Upton D, Handelsman DJ, et al. Temporal role of sertoli cell androgen receptor expression in spermatogenic development. *Mol Endocrinol* (2013) **27**:12–24. doi:10.1210/me.2012-1219
81. Leschek EW, Chan WY, Diamond DA, Kaefer M, Jones J, Barnes KM, et al. Nodular Leydig cell hyperplasia in a boy with familial male-limited precocious puberty. *J Pediatr* (2001) **138**:949–51. doi:10.1067/mpd.2001.114477
82. Rosenthal IM, Refetoff S, Rich B, Barnes RB, Sunthornthepvarakul T, Parma J, et al. Response to challenge with gonadotropin-releasing hormone agonist in a mother and her two sons with a constitutively activating mutation of the luteinizing hormone receptor – a clinical research center study. *J Clin Endocrinol Metab* (1996) **81**:3802–6. doi:10.1210/jc.81.10.3802
83. Ignacak M, Hilczer M, Zarzycki J, Trzeciak WH. Substitution of M398T in the second transmembrane helix of the LH receptor in a patient with familial male-limited precocious puberty. *Endocr J* (2000) **47**:595–9. doi:10.1507/endocrj.47.595
84. Ignacak M, Starzyk J, Dziatkowiak H, Trzeciak WH. Study of the family of a patient with male-limited precocious puberty (MPP) due to T1193C transition in exon 11 of LH receptor gene. *J Endocrinol Invest* (2002) **25**:259–63. doi:10.1007/BF03344001
85. Choi JH, Wong AS, Huang HF, Leung PC. Gonadotropins and ovarian cancer. *Endocr Rev* (2007) **28**:440–61. doi:10.1210/er.2006-0036
86. Mueller SC, Ng P, Sinaii N, Leschek EW, Green-Golan L, Vanryzin C, et al. Psychiatric characterization of children with genetic causes of hyperandrogenism. *Eur J Endocrinol* (2010) **163**:801–10. doi:10.1530/EJE-10-0693
87. Burnham VL, Thornton JE. Luteinizing hormone as a key player in the cognitive decline of Alzheimer's disease. *Horm Behav* (2015). doi:10.1016/j.yhbeh.2015.05.010
88. Barron AM, Verdile G, Martins RN. The role of gonadotropins in Alzheimer's disease: potential neurodegenerative mechanisms. *Endocrine* (2006) **29**:257–69. doi:10.1385/ENDO:29:2:257
89. Casadesus G, Webber KM, Atwood CS, Pappolla MA, Perry G, Bowen RL, et al. Luteinizing hormone modulates cognition and amyloid-beta deposition in Alzheimer APP transgenic mice. *Biochim Biophys Acta* (2006) **1762**:447–52. doi:10.1016/j.bbadis.2006.01.008
90. Apaja PM, Harju KT, Aatsinki JT, Petaja-Repo UE, Rajaniemi HJ. Identification and structural characterization of the neuronal luteinizing hormone receptor associated with sensory systems. *J Biol Chem* (2004) **279**:1899–906. doi:10.1074/jbc.M311395200

Conflict of Interest Statement: The author declares that the research was conducted in the absence of any commercial or financial relationships that could be construed as a potential conflict of interest.

frontiers in Endocrinology

ORIGINAL RESEARCH
published: 27 August 2015
doi: 10.3389/fendo.2015.00130

Assessing gonadotropin receptor function by resonance energy transfer-based assays

Mohammed Akli Ayoub[1,2,3,4,5]*, *Flavie Landomiel*[1,2,3,4], *Nathalie Gallay*[1,2,3,4], *Gwenhael Jégot*[1,2,3,4], *Anne Poupon*[1,2,3,4], *Pascale Crépieux*[1,2,3,4] and *Eric Reiter*[1,2,3,4]

[1] Biologie et Bioinformatique des Systèmes de Signalisation (BIOS) Group, INRA, UMR85, Unité Physiologie de la Reproduction et des Comportements, Nouzilly, France, [2] CNRS, UMR7247, Nouzilly, France, [3] Université François Rabelais, Tours, France, [4] L'Institut français du cheval et de l'équitation (IFCE), Nouzilly, France, [5] LE STUDIUM ® Loire Valley Institute for Advanced Studies, Orléans, France

OPEN ACCESS

Edited by:
Brian J. Arey,
Bristol-Myers Squibb, USA

Reviewed by:
Daniel James Scott,
The Florey Institute and The University of Melbourne, Australia
Jonathan Janssens,
University of Antwerp, Belgium

***Correspondence:**
Mohammed Akli Ayoub,
Institut National de la Recherche Agronomique (INRA) UMR85, CNRS-Université François Rabelais UMR7247, Physiologie de la Reproduction et des Comportements (PRC) - Nouzilly 37380, France
Mohammed.Ayoub@tours.inra.fr

Specialty section:
This article was submitted to Molecular and Structural Endocrinology, a section of the journal Frontiers in Endocrinology

Received: 11 June 2015
Accepted: 10 August 2015
Published: 27 August 2015

Citation:
Ayoub MA, Landomiel F, Gallay N, Jégot G, Poupon A, Crépieux P and Reiter E (2015) Assessing gonadotropin receptor function by resonance energy transfer-based assays. Front. Endocrinol. 6:130. doi: 10.3389/fendo.2015.00130

Gonadotropin receptors belong to the super family of G protein-coupled receptors and mediate the physiological effects of follicle-stimulating hormone (FSHR) and luteinizing hormone (LHR). Their central role in the control of reproductive function has made them the focus of intensive studies. Upon binding to their cognate hormone, they trigger complex signaling and trafficking mechanisms that are tightly regulated in concentration, time, and space. Classical cellular assays often fail to capture all these dynamics. Here, we describe the use of various bioluminescence and fluorescence resonance energy transfer (BRET and FRET) assays to investigate the activation and regulation of FSHR and LHR in real-time, in living cells (i.e., transiently expressed in human embryonic kidney 293 cells). Indeed, the dynamics of hormone-mediated heterotrimeric G protein activation, cyclic adenosine-monophosphate (cAMP) production, calcium release, β-arrestin 2 recruitment, and receptor internalization/recycling was assessed. Kinetics and dose–response analyses confirmed the expected pharmacological and signaling properties of hFSHR and hLHR but revealed interesting characteristics when considering the two major pathways (cAMP and β-arrestin 2) of the two receptors assessed by BRET. Indeed, the EC_{50} values were in picomolar range for cAMP production while nanomolar range was observed for β-arrestin 2 recruitment as well as receptor internalization. Interestingly, the predicted receptor occupancy indicates that the maximal G protein activation and cAMP response occur at <10% of receptor occupancy whereas >90% of activated receptors is required to achieve full β-arrestin 2 recruitment and subsequent receptor internalization. The rapid receptor internalization was also followed by a recycling phase. Collectively, our data reveal that β-arrestin-mediated desensitization, internalization, and the subsequent fast recycling of receptors at the plasma membrane may provide a mechanistic ground to the "spare receptor" paradigm. More generally, the novel tools described here will undoubtedly provide the scientific community investigating gonadotropin receptors with powerful means to decipher their pharmacology and signaling with the prospect of pathophysiological and drug discovery applications.

Keywords: gonadotropins, FSHR, LHR, GPCRs, G proteins, arrestins, BRET, FRET

Introduction

The gonadotropin receptors play a central role in the control of mammal reproduction by mediating the physiological responses of the two major pituitary glycoprotein hormones, follicle-stimulating hormone (FSH) and luteinizing hormone (LH). Their respective receptors, follicle-stimulating hormone receptor (FSHR) and luteinizing hormone receptor (LHR), are mainly expressed in the gonads where they control the ovarian and testicular functions in females and males, respectively, by regulating both steroidogenesis and gametogenesis (1, 2). Both FSHR and LHR belong to a subgroup of class A (rhodopsin-like) G protein-coupled receptors (GPCRs) characterized by the presence of multiple leucine-rich repeats (LRRs) in their extracellular amino-terminal domain. This subgroup also includes the thyroid-stimulating hormone receptor (TSHR) and the receptors for the peptidic hormone relaxin and INSL3 (RXFP1 and 2). The LRRs containing region in FSHR has been shown to be determinant for its interaction with FSH (3–5). In terms of the intracellular signaling, FSHR and LHR are known to mediate the canonical G protein-mediated signaling pathway through coupling to heterotrimeric Gαs proteins, which activates the adenylate cyclase, resulting in an increase in intracellular cyclic adenosine-monophosphate (cAMP) levels and activation of protein kinase A (PKA) as well as the exchange protein directly activated by cAMP (EPAC). This in turn triggers the activation of multiple downstream kinases that modulate the nuclear activity of cAMP response element-binding protein (CREB) and the expression of the genes involved in the physiological responses of the gonadotropins. However, recent evidences point to a multiplicity of the signaling that can be mediated by FSHR and LHR by engaging additional G protein-dependent and independent pathways [for review, see Ref. (6–9)], including β-arrestin-dependent pathways (10–13). As a consequence, similar to most other GPCRs, these receptors' pharmacology and signaling involve highly diverse and complex mechanisms. Therefore, the use of recent innovative technologies to investigate these receptors could certainly help understanding better their activation mode.

Among the emerging methods to study GPCRs, the focus is on energy transfer-based assays that rely on the biophysical bioluminescence and fluorescence resonance energy transfer (BRET and FRET) technologies. These approaches link the concept of distance/proximity, in space and time, between an energy donor and an energy acceptor to the biological question of interest according to Förster's Law in both static and dynamic configurations (14–16). Since their development, BRET and FRET have been extensively used to study different cellular and molecular aspects related to the function and regulation of cell surface receptors, such as GPCRs and tyrosine kinase receptors (TKRs) (17, 18). In fact, GPCRs constitute the research field of choice where BRET/FRET are elegantly used and are being the subject of permanent development and improvement (16, 19–21). Indeed, by using BRET and FRET, it is now possible to quantitatively address, in real-time and live cells, different questions about the functioning of GPCRs including ligand binding, receptor activation, G protein coupling, intracellular downstream signaling, β-arrestin recruitment, receptor trafficking, and oligomerization (16, 19–26). In this context, BRET and FRET significantly contributed to major recent advances in the field with the emergence of new concepts, such as receptor heteromerization, receptor/G protein preassembly, and biased signaling. Even though these advances further illustrate the complexity of the GPCR functioning, they pushed the scientific community one step further in understanding better the involvement of GPCRs in physiology and pathophysiology. However, the application of BRET and FRET approaches to the gonadotropin receptors has remained limited to date. In this study, we report the application of a series of novel BRET and FRET assays to study the activation and regulation of the human gonadotropin receptors, hFSHR and hLHR/hCGR (here designed as hLHR), when they are transiently expressed in HEK 293 cells. Kinetics and dose–response analyses using various assays were performed in 96- and 384-well formats in real-time and live cells.

Materials and Methods

Materials and Plasmid Constructions

The plasmid encoding human FSHR was generated as previously described (12). The other plasmids encoding the different BRET/FRET sensors and fusion proteins were generously provided as follows: hLHR from A. Ulloa-Aguirre (Universidad Nacional Autónoma de México, México, Mexico), different Rluc8- and Venus-fused G proteins from J. P. Pin (Functional Genomics Institute, Montpellier, France) and K. D. Pfleger (Harry Perkins Institute of Medical Research, Perth, WA, Australia) (also hV2R–Rluc8), Rluc8-fused hFSHR and hLHR from A. Hanyaloglu (Imperial College, London, UK), yPET-β-arrestin 2 from M. G. Scott (Cochin Institute, Paris, France), Aequorin-GFP from B. Lambolez (Pierre et Marie Curie University, Paris, France), CAMYEL from L. I. Jiang (University of Texas, TX, USA), ICUE from J. Zhang (The Johns Hopkins University, Baltimore, MD, USA), and Venus-KRas from N. A. Lambert (Georgia Health Sciences University, Augusta, GA, USA). Recombinant hFSH was kindly gifted by Merck-Serono (Darmstadt, Germany), hCG was kindly donated by Y. Combarnous (CNRS, Nouzilly, France), forskolin and DDAVP were purchased from Sigma-Aldrich (St. Louis, MO, USA). All the 96- and 384-well white microplates were from Greiner Bio-One (Courtaboeuf, France). Coelenterazine h substrate was purchased from Interchim (Montluçon, France).

Cell Culture and Transfection

HEK 293 cells were grown in complete medium (DMEM supplemented with 10% (v/v) fetal bovine serum, 4.5 g/l glucose, 100 U/ml penicillin, 0.1 mg/ml streptomycin, and 1 mM glutamine) (all from Invitrogen, Carlsbad, CA, USA). Transient transfections were performed by reverse transfection in 96-well plates using Metafectene PRO (Biontex, München, Germany) following the manufacturer's protocol. Briefly, for each well, the different combinations of coding plasmids were used as follows: 200 ng of total plasmid per well were resuspended in 25 µl of serum-free DMEM and mixed with Metafectene PRO (0.5 µl/well) previously preincubated 5 min at room temperature in 25 µl serum-free DMEM (2 × 25 µl/well). Then the two solutions of serum-free DMEM-containing plasmids and Metafectene

PRO were mixed and incubated for 20 min at room temperature. Cells (10^5 in 200 µl/well) in DMEM supplemented with 10% FCS were then incubated with the final plasmid-Metafectene PRO mix (50 µl/well). Transfection efficiency was typically in the 60–70% range and the correct expression of the different fusion proteins used for BRET and FRET was examined by fluorescence and luminescence measurements using a Mithras LB 943 plate reader (Berthold Technologies GmbH and Co. Wildbad, Germany).

BRET Measurements

Forty-eight hours after transfection, cells were washed with PBS and BRET measurements were performed depending on the experiments as described previously (27). For the endpoint dose–response analysis, cells were first preincubated 30 min at 37°C in 40 µl/well of PBS 1×, HEPES 5 mM, 200 µM IBMX (for cAMP assays) containing or not increasing concentrations of hFSH or hCG as indicated. Then BRET measurements were performed upon addition of 10 µl/well of coelenterazine h (5 µM final) using a Mithras LB 943 plate reader. For the real-time BRET kinetics, cells were first resuspended in 60 µl/well of PBS-HEPES 10 mM (+IBMX 200 µM for cAMP assays) and then BRET measurements were immediately performed upon addition of 10 µl/well of coelenterazine h (5 µM final) and 10 µl/well of the sub-maximal concentrations of hFSH or hCG (fivefold concentrated).

Calcium Measurements Using Aequorin-GFP

Forty-eight hours after transfection, cells co-expressing hFSHR and aequorin-GFP (AEQ-GFP) were incubated for 3 h with 40 µl/well of coelenterazine h substrate (5 µM final) in PBS 1×, HEPES 10 mM, BSA 0.1%, in the dark, and at 37°C to allow aequorin reconstitution. Luminescence emission at 480 and 540 nm was then measured in each well individually every 0.05 s before and after the rapid injection of 10 µl/well of hFSH (fivefold concentrated) or of vehicle, using the injection system and the dual emission detection of a Mithras LB 943 plate reader.

cAMP Accumulation Measured by HTRF®

Intracellular cAMP levels were measured using a homogeneous time-resolved fluorescence (HTRF®) cAMP dynamic 2 assay kit (CisBio Bioassays, Bagnol sur Cèze, France) (28). Forty-eight hours post-transfection cells were detached and seeded into white 384-well microplates with 5,000 cells/well in 5 µl of stimulation buffer (PBS 1×, 200 µM IBMX, 5 mM HEPES, 0.1% BSA). For their stimulation, 5 µl/well of the stimulation buffer containing or not different doses of hFSH and hCG as indicated were added. Then, cells were incubated for 30 min at 37°C and then lysed by addition of 10 µl/well of the supplied conjugate-lysis buffer containing d2-labeled cAMP and Europium cryptate-labeled anti-cAMP antibody, both reconstituted according to the manufacturer's instructions. Plates were incubated for 1 h in the dark at room temperature and time-resolved fluorescence signals were measured at 620 and 665 nm, respectively, 50 ms after excitation at 320 nm using a Mithras LB 943 plate reader.

cAMP Accumulation Measured by Microscopic FRET Assay

Forty-eight hours after transfection, cells co-expressing the cAMP sensor (ICUE) with either hFSHR or hLHR were plated in imaging dishes and imaged in the dark at 37°C on a temperature-controlled stage using a Leica DM IRB (Leica Microsystems) microscope with a CoolSnap fx cooled charge-coupled device camera (Ropper Scientific) controlled by METAFLUOR 7.5 (Universal Imaging Corporation, Downingtown, PA, USA). Dual emission ratio imaging was carried out using a 436DF10 excitation filter, a 436–510 DBDR dichroic mirror, and 480-AF30 and 550-AF30 emission filters for CFP and YFP, respectively. Exposure time was 400 ms and images were taken every 30 s. Typically, equal sensor-positive cells and non-specific areas were chosen in the field of the microscope. The evolution of fluorescence was recorded individually in each area for the whole duration of the experiments. Several independent plates were analyzed according to this procedure, and the specific FRET signal of each cell (positive minus negative area) was pooled. Cells displaying a whole range of intensities were selected and analyzed without any impact of the expression level of the sensor on the responsiveness being noticed. After 5 min of baseline measurement, cells were stimulated with either 1 nM of hFSH or hCG, and 1 µM of forskolin was added as a positive control after 20 min of stimulation. A low hormone dose has been chosen in order to avoid saturation of the ICUE sensor, which has a limited dynamic range compared to BRET assays. Fluorescent intensity of non-specific areas was subtracted to the intensity of fluorescent cells expressing the sensor in order to quantify the specific signal. The FRET ratio (CFP/YFP) was calculated for each individual cell. Data represent the mean ± SEM of at least 20 individual cell responses measured in three independent experiments.

β-arrestin Recruitment Assessed by TANGO Assay

This assay was carried out as previously described by Barnea et al. (29). We generated HTLA cells (HEK293T-derived cell line containing a stably integrated tTA-dependent firefly luciferase reporter gene) stably expressing FSHR/AVPR2-CT chimera, and β-arrestin 2-TEV fusion protein. Growing HTLA hFSHR cells were plated in white 96-well assay plates at 4×10^4 cells per well in MEM, supplemented with 10% FBS, glutamine, and antibiotic cocktail. Twenty-four hours after plating, increasing concentrations of hFSH were added and cells were cultured for 14–20 h before measuring reporter gene activity. Luciferase activity was determined by using the Bright-Glo luciferase assay system (Promega, Charbonnieres, France), following the manufacturer's protocol, and using a POLARstar OPTIMA luminometer (BMG Labtech, Ortenberg, Germany).

Data Analysis

Bioluminescence resonance energy transfer data are represented either as 480 nm/540 nm (ICUE sensor), 540 nm/480 nm (β-arrestin and internalization kinetics), or as hFSH/hCG-induced BRET changes by subtracting the ratio 540 nm/480 nm of luminescence in a well of PBS-treated cells from the same ratio in wells where the cells were treated with hFSH or hCG. In

this calculation, only ligand-induced BRET changes (increase or decrease) are represented and the PBS-treated cell sample represents the background eliminating the requirement for measuring an Rluc-only control sample since fast kinetics and dose–response analyses were performed. Kinetic and dose–response curves were fitted following the appropriate non-linear regression equations using Prism GraphPad software (San Diego, CA, USA). Statistical analyses were performed using two-way ANOVA included in Prism GraphPad software.

Results

Receptor-Mediated cAMP Production

First, we examined cAMP response by hFSHR and hLHR since they are both known to couple to heterotrimeric Gs protein, leading to adenylyl cyclase activation and ultimately to an increase in the intracellular cAMP levels. To this end, we used the BRET-based cAMP sensor, CAMYEL, developed by Jiang et al. (30) (**Figure 1A**), which allows the assessment of intracellular cAMP changes in real-time and live cells. Under basal conditions, a high-BRET signal occurs between the donor (*Renilla* luciferase or Rluc) and the acceptor (green fluorescent protein or GFP) due to the favorable conformation and proximity/orientation of the Rluc and GFP within the Epac motif composing the sensor. In contrast, an increase in the cytosolic cAMP concentrations and its binding to Epac induce changes in the conformation of Rluc-Epac-GFP sensor, resulting in a significant decrease in the BRET signal (**Figure 1A**). The receptors were transiently co-expressed with CAMYEL in HEK 293 cells and real-time kinetics were conducted (**Figures 1B,C**) at different doses allowing the inference of sigmoidal dose–response curves (**Figures 1D,E**). Kinetic analyses showed a relatively fast cAMP response ($t_{1/2}$ of 3.2 and 1.7 min for FSHR and LHR, respectively) (**Table 1**) upon stimulation with 5 nM of gonadotropins with a plateau reached after ~10 min for both hFSHR (**Figure 1B**) and hLHR (**Figure 1C**). As expected, both hormones, hFSH (**Figure 1D**) and hCG (**Figure 1E**), showed very potent effects on their specific receptors with EC_{50} values in the picomolar range (**Table 1**). Similar results were obtained using HTRF®-based cAMP assay (28) on both hFSHR (**Figure 1F**) and hLHR (**Figure 1G**) either wildtype or Rluc8-fused receptors. This indicates that both Rluc8-fused receptors retained correct expression and function and can therefore be used in BRET assays for the recruitment of β-arrestin 2 and receptor internalization (**Figures 5** and **6**).

We also used a FRET-based cAMP sensor (ICUE) allowing real-time measurements of cAMP production as previously shown (31) (**Figure 2A**) using both real-time FRET measurements in 96-well plate format every 0.5 s as well as individual cell analysis with the appropriate fluorescence microscopy setting. The 96-well plate format clearly allowed to measure very rapid changes in the FRET signals in cells co-expressing ICUE and hFSHR and challenged with 1 μM of forskolin (**Figure 2B**) or 5 nM of hFSH (**Figure 2C**). These changes were specific to hFSH/forskolin-induced cAMP production since vehicle injection did not induce any change in the FRET signal (**Figure 2D**). In parallel, the FRET analysis by fluorescence microscopy on individual stimulated cells co-expressing ICUE and either hFSHR or hLHR showed a time-dependent increase of cAMP production induced by 1 nM of hFSH or hCG, respectively, as well as 1 μM of forskolin (**Figure 2E**), as previously reported (12).

Receptor-Gαs Protein Coupling Assessed by BRET

Next, we examined the functional coupling of hFSHR and hLHR to the heterotrimeric G protein (Gαs and Gβγ) in real-time and live cells by measuring BRET changes between the different G protein subunits as previously reported (27, 32–36). In this assay, a change (in this case a decrease) in the proximity/association between the Gα subunit and Gβγ dimer as well as their conformation upon receptor activation is assessed in time-dependent manner reflecting the functional coupling of the receptor with its cognate heterotrimeric G protein (**Figure 3A**). Gαs-Rluc8 was transiently co-expressed with either Venus-Gγ2 (**Figures 3B,C**) or Venus-Gβ1 (**Figures 3D,E**) in the presence of hFSHR or hLHR as indicated. BRET changes were then rapidly assessed every 0.5 s before and after receptor activation by the injection of 10 nM of hFSH or hCG. As shown, hFSH nicely induced a very rapid and significant BRET decrease between Gαs-Rluc8 and Venus-Gγ2 (**Figure 3B**) and Venus-Gβ1 (**Figure 3D**) co-expressed with hFSHR. Similar albeit noisier effects were observed with 10 nM of hCG on BRET between Gαs-Rluc8 and Venus-Gγ2 (**Figure 3C**) and Venus-Gβ1 (**Figure 3E**) in the context of hLHR expressing cells. Such BRET changes likely reflect the activation of Gαs protein by the hFSHR and hLHR and are consistent with the cAMP measurements shown in **Figures 1** and **2**. Our data are consistent with the previous BRET data reported for other GPCRs, showing a decrease of the BRET signals between Gαs and Gβ/γ subunits (32, 33, 35, 36). As expected, the observed kinetics with these sensors was much faster than the one measured for cAMP (i.e., $t_{1/2}$ between 10 and 16 s) (**Table 1**).

Receptor-Mediated Calcium Release

We also assessed the intracellular calcium release mediated by the activation of gonadotropin receptors as previously reported (37, 38). For this, we used an aequorin-dependent calcium assay (AEQ-GFP) based on luminescence and BRET increase upon binding of calcium to the aequorin protein fused to GFP (39, 40) (**Figure 4A**). In the presence of calcium, aequorin emits luminescence at 480 nm part of which is transferred to GFP due to their sufficient proximity leading to GFP excitation and light emission at 540 nm. As shown in **Figure 4B**, in cells co-expressing AEQ-GFP and hFSHR, a significant and rapid increase in light emission at 540 nm occurred upon cell stimulation with 10 nM of hFSH (**Figure 4B**) indicating intracellular calcium increase. However, in cells co-expressing AEQ-GFP and hLHR, a significant basal emission at 540 nm was observed and stimulation with 10 nM hCG only induced weaker response (**Figure 4C**) as compared to hFSH on its receptor (**Figure 4B**). Such an effect was specific to gonadotropins since no increase in light emission was observed in AEQ-GFP and hFSHR co-expressing cells upon vehicle injection (**Figure 4D**) and the hFSH-promoted luminescence increase was dose-dependent (**Figure 4E**). Moreover, no significant light emission was measured in cells expressing AEQ-GFP alone and stimulated with 10 nM of hFSH (data not shown).

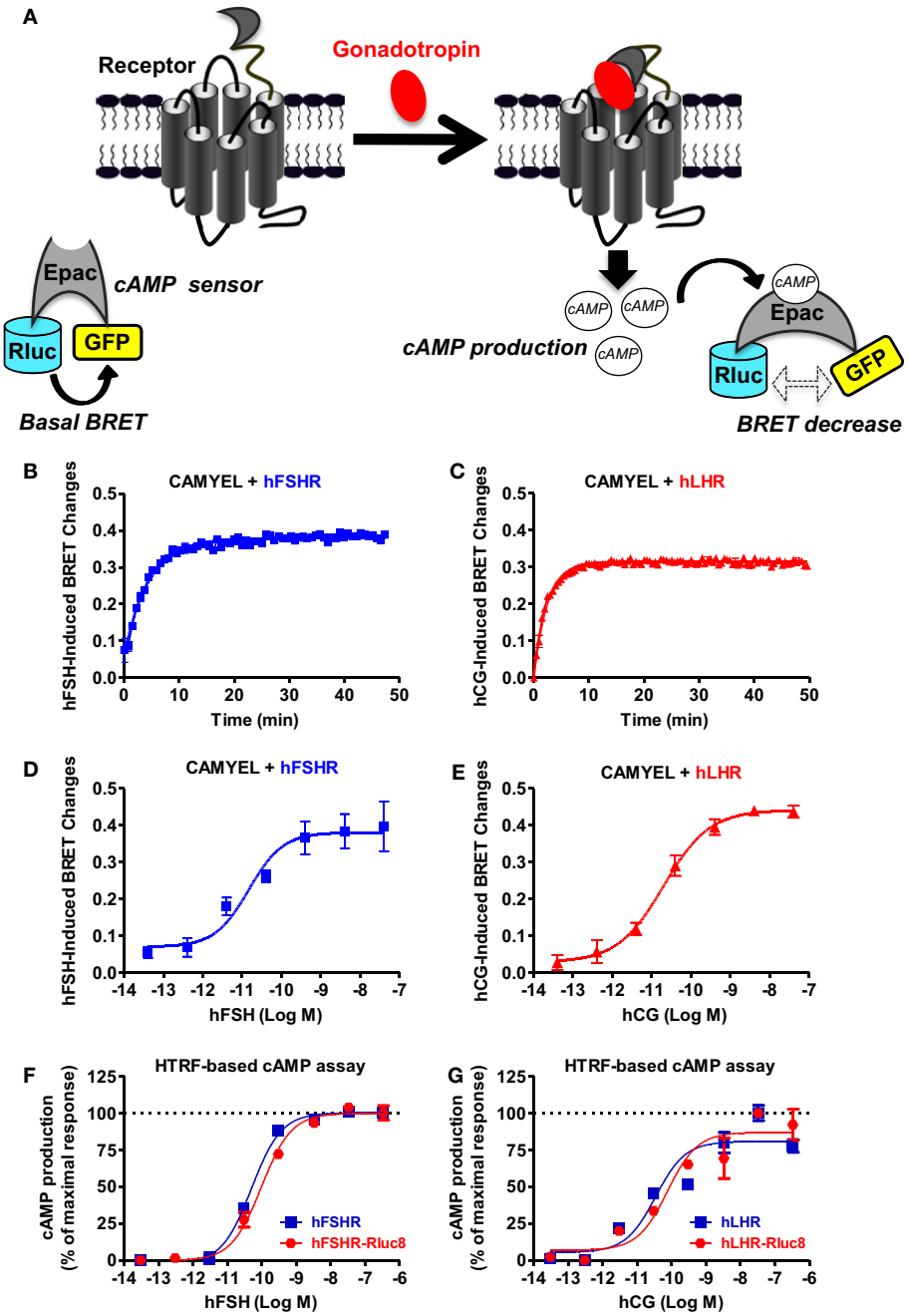

FIGURE 1 | BRET- and HTRF-based cAMP production assays. **(A)** Principle of the BRET-based cAMP assay (CAMYEL sensor). HEK 293 cells transiently expressing the indicated proteins (wildtype receptors and CAMYEL for BRET; wildtype or Rluc8-tagged receptors for HTRF) were stimulated with either 5 nM (for kinetics) or increasing concentrations (for dose–response curves) of hFSH **(B,D,F)** or hCG **(C,E,G)** as indicated. Then BRET and HTRF measurements format were performed as described in the Section "Materials and Methods" in 96-well and 384-well plates, respectively. Data are means ± SEM of three experiments performed either in a single point or triplicate.

Recruitment of β-arrestin 2 Assessed by BRET

The role of β-arrestins not only in desensitization/internalization but also in signaling of GPCRs is now well established (41–43) and this has been previously reported for the FSHR (10, 11, 13, 44) and LHR (45). Here, we examined for the first time the recruitment of β-arrestins to activated hFSHR and hLHR in real-time and live cells using BRET technology as illustrated in **Figure 5A**. Indeed, under the inactive conformation of the receptors, β-arrestins are mostly cytosolic. Upon activation, the receptors are phosphorylated by G protein-coupled receptor kinases (GRKs) leading to

TABLE 1 | EC_{50} and $t_{1/2}$ values for gonadotropin-promoted cAMP production, β-arrestin 2 recruitment and receptor internalization/recycling of hFSHR and hLHR.

Receptors	cAMP production			BRET G proteins	β-arrestin 2 recruitment			Internalization	Recycling
	EC_{50} (pM) BRET	EC_{50} (pM) HTRF	$t_{1/2}$ (min) BRET	$t_{1/2}$ (s) BRET	EC_{50} (nM) BRET	EC_{50} (nM) TANGO	$t_{1/2}$ (min) BRET	EC_{50} (nM) BRET	$t_{1/2}$ (min) BRET
hFSHR	3.0 ± 1.2	1.4 ± 0.1	3.2 ± 0.3	16.8 ± 11.7[a] 10.9 ± 0.3[b]	3.7 ± 2.0*	5.7 ± 2.6*	4.8 ± 0.3	2.6 ± 1.0*	10.5 ± 0.2
hLHR	3.5 ± 2.2	1.9 ± 0.3	1.7 ± 0.1	ND	2.0 ± 0.1	ND	6.6 ± 0.2	4.9 ± 1.9	8.6 ± 0.3

Data are means ± SEM of three to four independent experiments.

[a]*BRET between Gαs-Rluc8 and Venus-Gγ2.*

[b]*BRET between Gαs-Rluc8 and Venus-Gβ1, both calculated by fitting the curves in* **Figures 3B,D** *using "plateau then one phase decay equation."*

**$p < 0.05$ versus EC_{50} values measured in cAMP production assay.*

the translocation of β-arrestins from the cytosol to the intracellular domains of the receptors triggering their desensitization, internalization, and signaling. The BRET increase between the receptors and β-arrestins is used to assess this process in real-time and living cells. For this purpose, the receptors were fused to BRET donor (Receptor-Rluc8) and co-expressed with β-arrestin 2 fused to BRET acceptor (here yPET as a GFP variant) and the translocation of β-arrestin 2 to the receptor was then measured before and after receptor activation (**Figure 5A**). The functionality of FSHR-Rluc8 and hLHR-Rluc8 is verified by the cAMP assay shown in **Figures 1F,G**. Dose–response and kinetics experiments were carried out in cells co-expressing yPET-β-arrestin 2 and either hFSHR-Rluc8 (**Figures 5B,E**) or hLHR-Rluc8 (**Figures 5C,F**). Real-time kinetic analyses showed a significant BRET increase over the basal signal with hFSHR-Rluc8 (**Figure 5B**) or hLHR-Rluc8 (**Figure 5C**) and yPET-β-arrestin 2 upon stimulation with 10 nM of hFSH or hCG, respectively. The BRET increase occurred in a time-dependent manner with a sustained plateau reached after 20–30 min of receptor activation indicating a class B profile according to the common GPCR classification with respect to β-arrestin association (46). We used the human vasopressin V2 receptor (hV2R–Rluc8) as a prototype for class B GPCR in our BRET assay and observed a similar kinetic profile compared to hFSHR and hLHR (**Figure 5D**). Moreover, the effects were dose-dependent for both hFSH (**Figure 5E**) and hCG (**Figure 5F**) on their respective receptors with EC_{50} values largely higher (i.e., nanomolar range) than those observed for cAMP signaling (**Figure 1**; **Table 1**). Such shift in the hormone potencies is not due to the effect of fusion of the receptors with Rluc8 since these constructs showed cAMP responses similar to that observed with their corresponding wild type receptors (**Figures 1F,G**). Moreover, dose–response experiments were also performed using an indirect TANGO assay on hFSHR bearing the vasopressin receptor 2 (V2R) C-terminus and showed similar potency of hFSH on hFSHR/β-arrestin 2 association as assessed by BRET (**Figure 5G**).

Receptor Internalization and Recycling Assessed by BRET

Finally, we examined gonadotropin-induced receptor internalization in real-time and live cells using BRET between the Rluc8-tagged receptors (BRET donor) and a plasma membrane marker, KRas, fused to BRET acceptor (Venus, another GFP variant), as recently described (47). This assay is based on the changes in the physical proximity between KRas and the receptors at the plasma membrane upon receptor activation and thereby internalization as illustrated in **Figure 6A**. The agonist-induced decrease in the high basal BRET signals was assessed in cells co-expressing Venus-KRas with either hFSHR-Rluc8 or hLHR-Rluc8 (**Figure 6A**). We observed a very rapid decrease in the BRET signal between hFHSR-Rluc8 and Venus-KRas following cell stimulation with 10 nM of hFSH to reach the maximal decrease up to 2–5 min post-stimulation, indicating the rapid internalization of hFSHR under our conditions (**Figure 6B**). Interestingly, we observed a recovery phase of the BRET signal after 5–10 min of stimulation, which returns back to the basal level after 20 min suggesting recycling of the internalized receptors (**Figure 6B**). To confirm this observation on both hFSHR and hLHR, we performed time-course analysis where cells were first preincubated with hFSH or hCG at different times at 37°C before BRET signals were measured. The BRET measurements showed a maximal internalization of both receptors after 2–5 min and a total recovery of the BRET signals after 20 min (**Figure 6C**). Interestingly, the recovery phase continued to increase after 30 min to reach maximal BRET signals even higher than the basal levels after 45–60 min (**Figure 6C**), suggesting the recycling of the internalized receptors and/or the recruitment of an intracellular pool of receptors. Such behavior was specific to hFSHR and hLHR, since it was not observed for the human vasopressin 2 receptor (hV2R–Rluc8) activated with 1 μM of AVP (**Figure 6C**). In fact, these data are consistent with a delayed internalization (maximum after 30 min) and absence of recycling to the plasma membrane after internalization as it is well documented for V2R (48–50). Moreover, in order to estimate the kinetic parameter of the receptor recycling, we normalized the part of the curves corresponding to the recovery phase of hFSHR and hLHR shown in **Figure 6C** by taking 0 and 100% of the maximal BRET changes measured after 2 (maximal internalization) and 60 min of stimulation (maximal recycling), respectively (**Figure 6D**). As a result, both receptors recycled with similar kinetics with a half-time of about 10 min (**Table 1**), indicating that the recycling of hFSHR and hLHR was slower than their internalization, at least in our system. Finally, we performed BRET dose–response experiments after 5 min of stimulation showing the decrease in the BRET signals between Rluc8-tagged receptors and Venus-KRas in a dose-dependent manner with no significant differences between the two receptors (**Figure 6E**). It is worth noting that the potencies of hFSH and hCG on receptor

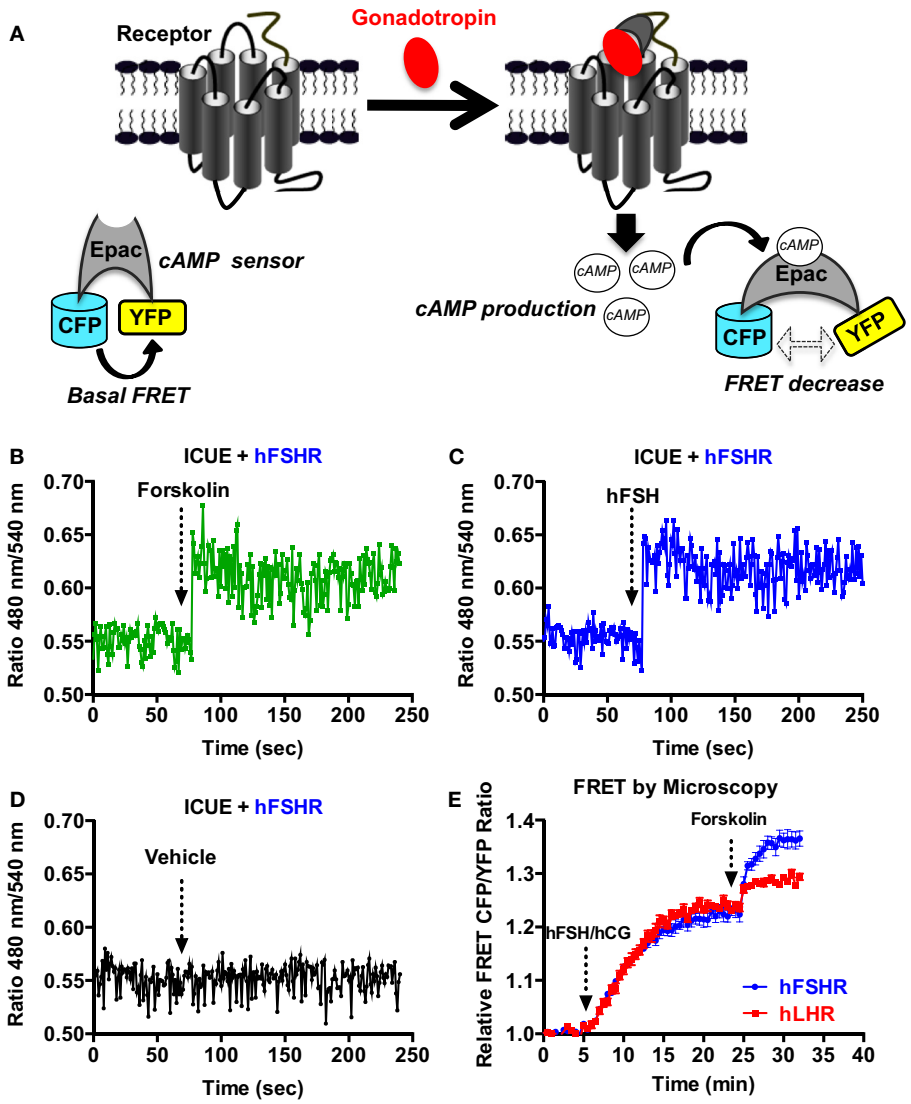

FIGURE 2 | FRET-based cAMP production assays. **(A)** Principle of the FRET-based cAMP assay (ICUE sensor). HEK 293 cells transiently co-expressing ICUE sensor with either hFSHR or hLHR **(E)** were used for FRET measurements using either 96-well format **(B–D)** or microscopy on individual cells **(E)**. Cells were stimulated with either 1 μM of forskolin **(B,E)**, 5 nM of hFSH **(C)**, 1 nM of hFSH or hCG **(E)**, or vehicle **(D)** as indicated. Then FRET measurements were performed as described in the Section "Materials and Methods." Data are representative of three independent experiments performed in single points **(B–D)** or 16 individual cells **(E)**.

internalization were similar to that observed for the recruitment of β-arrestin 2 (**Figures 5D,E**; **Table 1**), consistent with the notion that both events may be linked.

Discussion

In this study, we provide new insights on the activation and regulation of gonadotropin receptors by applying energy transfer-based technologies (BRET and FRET). These aspects were studied in real-time in live HEK 293 cells in dose- and time-dependent manners using various BRET configurations and BRET/FRET sensors. This allowed us to cover critical steps in the signaling of hFSHR and hLHR going from their intimate coupling to the heterotrimeric Gαs/Gβγ proteins at the membrane to the accumulation of cytosolic cAMP and calcium as well as β-arrestin 2 recruitment, receptor internalization, and recycling. Together, our data illustrate the robustness of the different BRET and FRET assays used to examine such components of GPCR activation and signaling with exquisite precision. In our hand, FRET, which gives beautiful results in fluorescence microscopy, is less suited to multiwell plate measurements than BRET since it displayed highly reduced amplitude of response. However, FRET sensors combined with microscopy offers the advantage of measuring individual cell responses.

The set of data presented in this study on hFSHR and hLHR confirm and expand previous reports from the literature using conventional approaches in terms of G protein-dependent signaling,

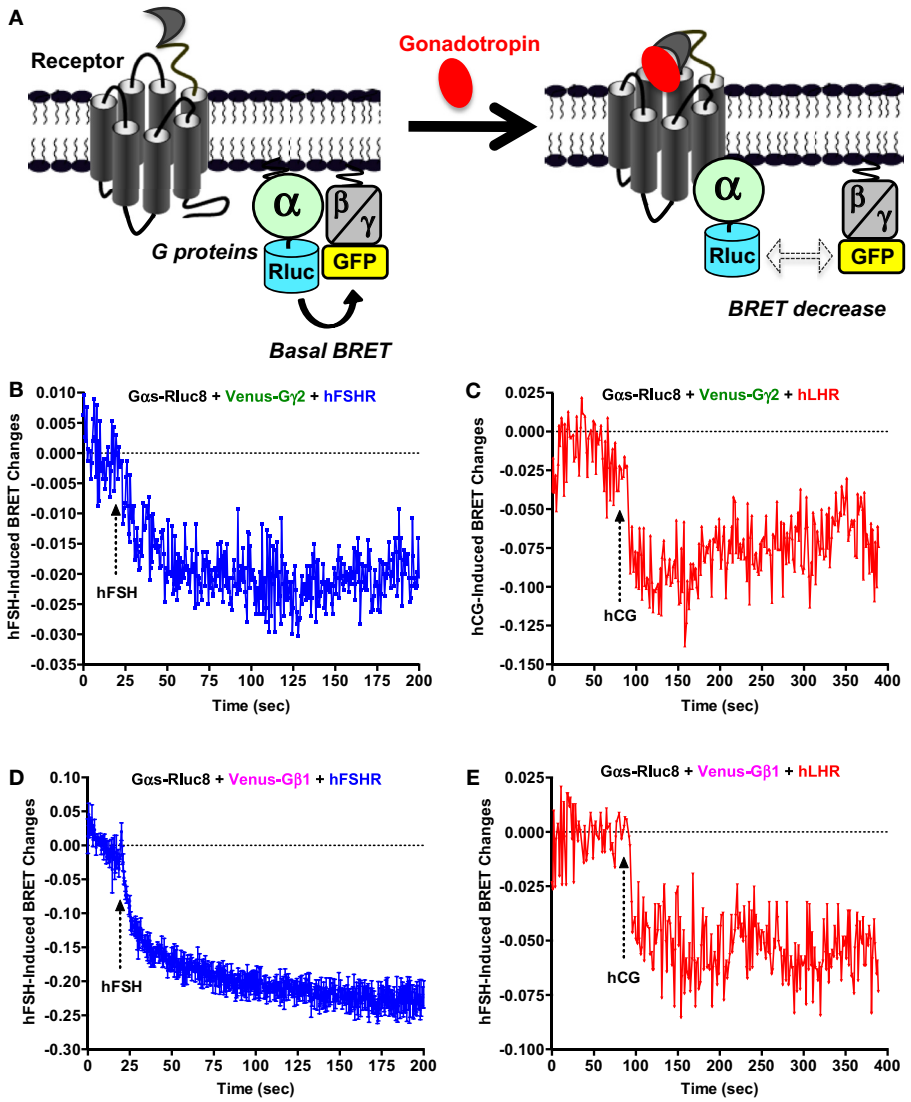

FIGURE 3 | G protein activation assessed by BRET. **(A)** Principle of the BRET-based G protein assay. HEK 293 cells transiently co-expressing the indicated Rluc8- and Venus-fused G protein subunits with either hFSHR **(B,D)** or hLHR **(C,E)** were used for BRET measurements using 96-well format performed before and after injection of 10 nM hFSH or hCG as described in the Section "Materials and Methods." Data are representative of three independent experiments performed in single points.

β-arrestin recruitment, and receptor trafficking. Indeed, a high potency (picomolar range) (**Table 1**) was classically observed for both hFSH and hCG with respect to the activation of the canonical Gs/cAMP signaling pathway, which is thought to account for the most physiological responses of FSH and LH in the gonads, hence in the control of reproduction (1, 2, 8). BRET measurements between the Gαs and Gβγ subunits activated by hFSHR and hLHR showed relatively rapid BRET changes upon receptor activation consistent with previous observations using similar BRET assays on different heterotrimeric G proteins and GPCRs (32, 33, 35, 36, 51). Moreover, BRET-based calcium sensor allowed the assessment of rapid and transient calcium release in response to the hormones confirming previous reports of FSHR- and LHR-mediated calcium response (37, 38). Moreover, our data suggest differences between the two receptors in terms of the basal calcium response, and further investigation will be needed to better understand this aspect of FSHR/LHR signaling. One possible explanation could be that the higher basal level observed in LHR-transfected cells is a reflexion of the fact that this receptor leads to significant constitutive activity while FSHR does not (52, 53).

Interestingly, our BRET data provide the first direct evidence for the dynamics of receptor/β-arrestin association, in real-time and live cells, in response to FSH and hCG stimulation. We confirmed the accuracy of the measurements for hFSHR/β-arrestin association using an indirect TANGO assay, both data sets being also consistent with those recently reported on FSHR using the PathHunter β-arrestin assay from DiscoverRx (4, 5). This commercial assay, similar to our home-made TANGO assay,

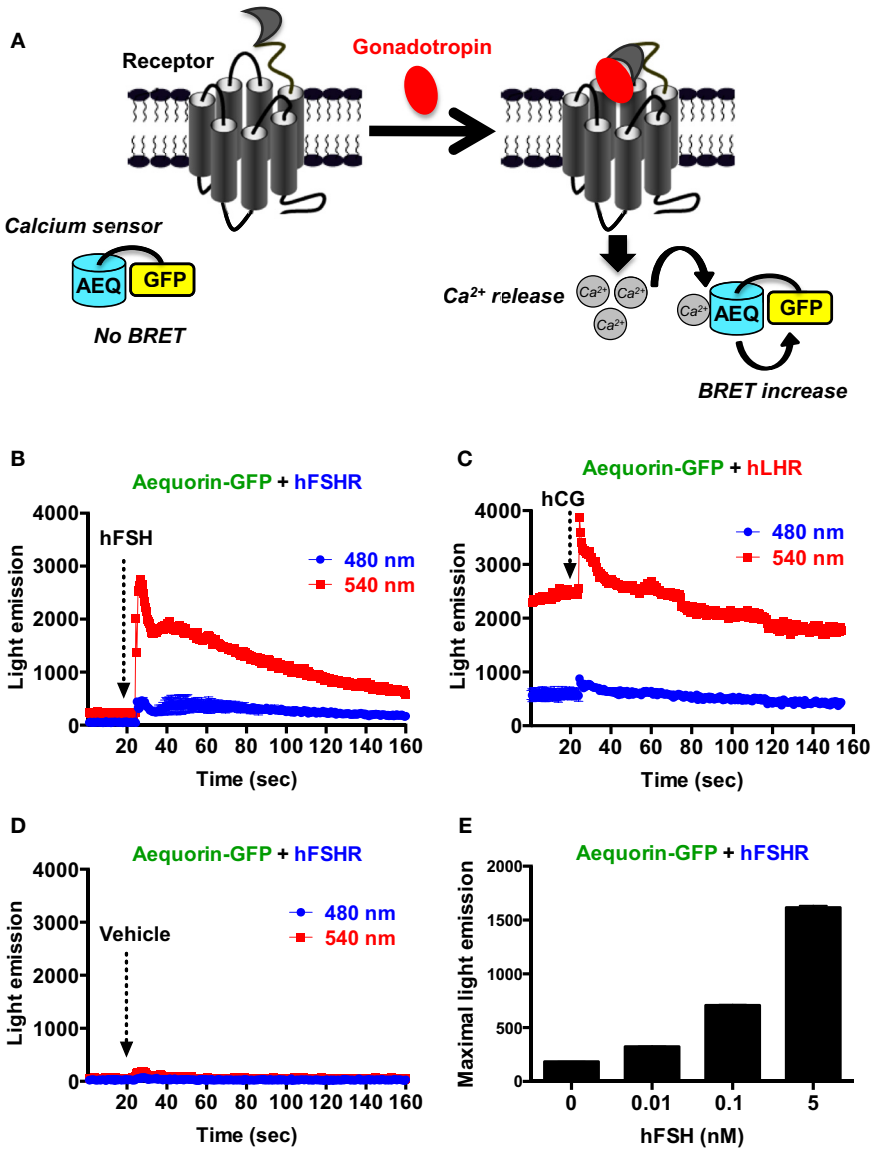

FIGURE 4 | BRET-based calcium assay. **(A)** Principle of the BRET-based calcium assay. HEK 293 cells transiently co-expressing the AEQ-GFP sensor with either hFSHR **(B,D,E)** or hLHR **(C)** were used for light emission measurements using 96-well format before and after injection of vehicle **(D)** 10 nM hFSH or hCG or various doses of hFSH **(E)** as described in the Section "Materials and Methods." Data are representative of three independent experiments performed in single points.

precludes real-time measurements since 90 min of agonist stimulation are followed by 1 h of incubation before the assay detection (overnight incubation in the TANGO assay). In addition, it is worth noting that non-trivial modifications are introduced in the C-terminus of FSHR in these two assays, although this region is known to be critical for receptor phosphorylation by GRKs and β-arrestin interaction. The real-time kinetic analysis using BRET showed a time-dependent increase in β-arrestin 2 recruitment with a plateau reached after 20–30 min of stimulation consistent with previous BRET data on β-arrestin recruitment to other GPCRs (26, 27, 33, 34, 51, 54). The sustained BRET signals induced after 20–50 min of stimulation suggests that hFSHR and hLHR present a class B GPCR profile similarly to the prototypic vasopressin V2 receptor (41, 46). In addition, the BRET data on β-arrestin 2 recruitment were nicely correlated with the internalization data in terms of efficiency and to some extent kinetics (**Figure 7**; **Table 1**). This is consistent with the previously reported central role played by β-arrestins in the internalization of hFSHR and hLHR (55, 56) and fits well with the classical paradigm of GPCR trafficking (41, 42, 57, 58). However, our real-time BRET analysis on both receptors clearly showed receptor recycling and/or recruitment of new receptors at the plasma membrane as indicated by a recovery of BRET signals occurring after 10 min of stimulation and reaching a maximum

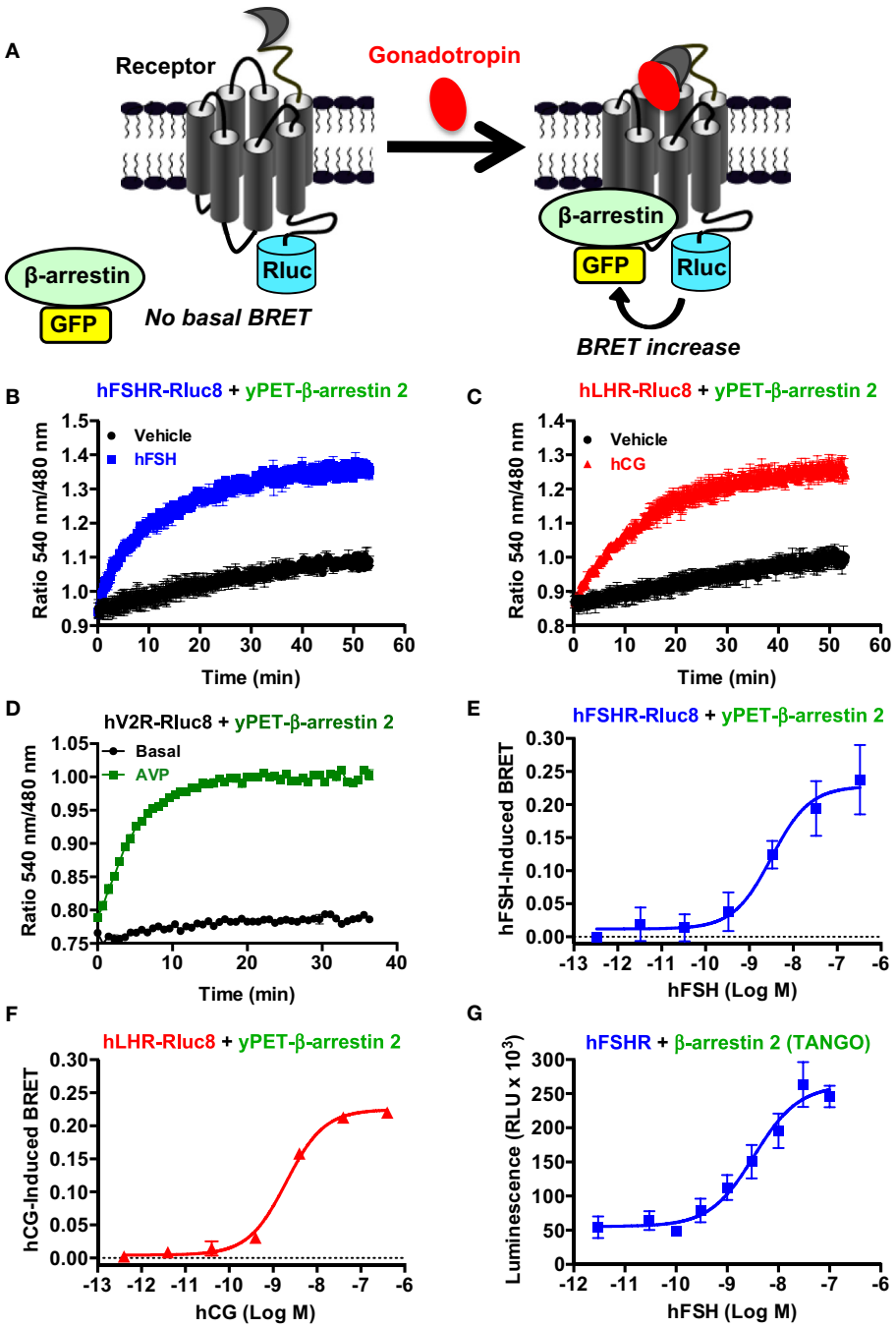

FIGURE 5 | β-arrestin 2 recruitment assessed by BRET. (A). Principle of the BRET-based β-arrestin assay. HEK 293 cells transiently co-expressing yPET-β-arrestin 2 with either hFSHR-Rluc8 **(B,E,G)**, hLHR-Rluc8 **(C,F)** or hV2R–Rluc8 **(D)** were used for BRET measurements in 96-well format using both real-time kinetics under basal (vehicle) and stimulated conditions in the presence of 10 nM of hormones **(B,C)** and endpoint signal recording after 30 min of stimulation with increasing hormone concentrations **(D–F)** as described in the Section "Materials and Methods." In parallel, hFSHR/β-arrestin 2 association was also assessed in dose-dependent way using TANGO assay in 384-well format **(G)**. Data are means ± SEM of three to four independent experiments performed in triplicate points.

higher than the basal level after 45–60 min. Such an observation was specific to hFSHR and hLHR since the internalization of hV2R was significantly delayed with no recycling of the receptor observed, as previously reported for this receptor (48–50). This difference with V2R suggests that the trafficking of hFSHR and hLHR is more complex than their simple classification into class A versus B GPCRs. In fact, the recovery phase observed with hFSHR and hLHR may be explained either by the recycling of the

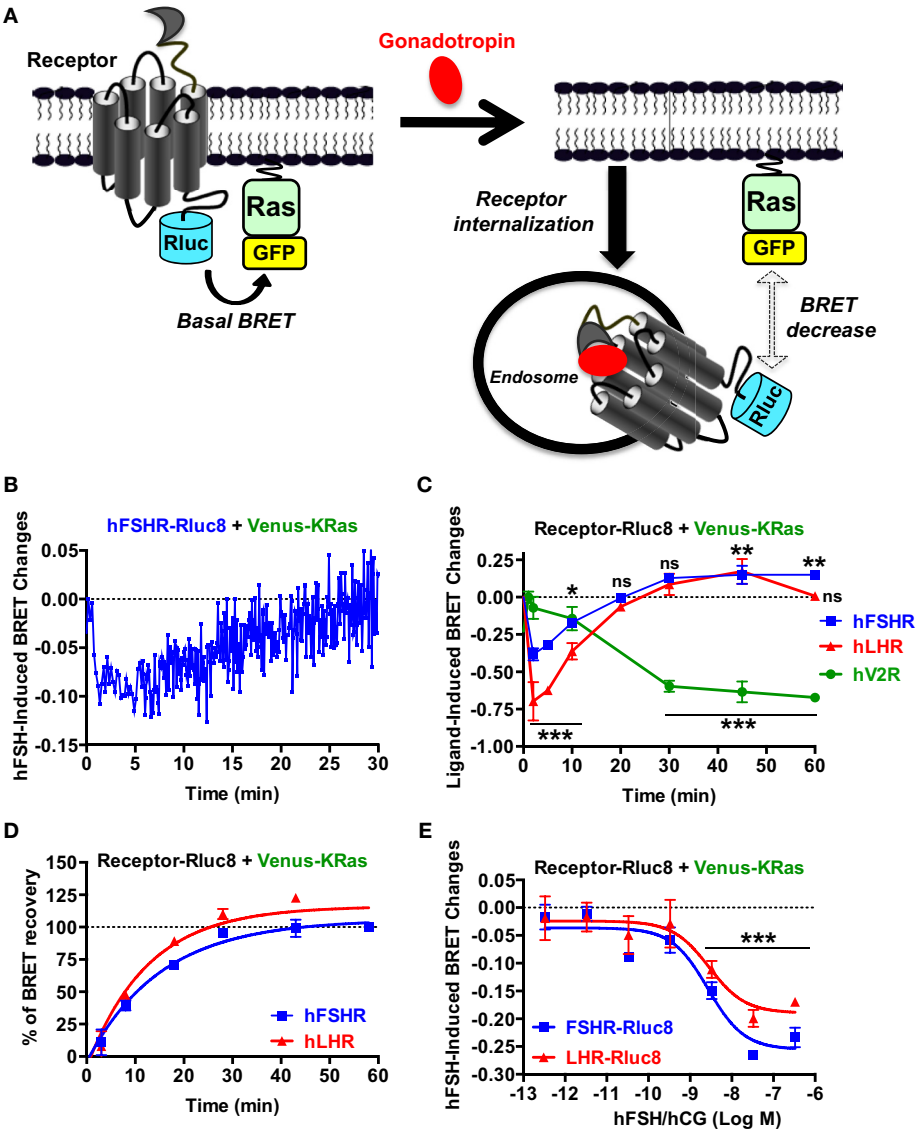

FIGURE 6 | Receptor internalization and recycling assessed by BRET. **(A)** Principle of the BRET-based receptor internalization assay. HEK 293 cells transiently co-expressing Venus-KRas with either hFSHR-Rluc8, hLHR-Rluc8, or hV2R–Rluc8 were used for BRET measurements using 96-well format as described the Section "Materials and Methods." Real-time kinetics **(B)** and dose–response analysis **(E)** after 2 min of stimulation with 10 nM **(B)** or increasing concentrations **(E)** of the hormones. In addition, time-course experiments were performed upon cell stimulation with 10 nM of the indicated agonists for 2, 5, 10, 20, 30, 45, and 60 min **(C)**. The BRET recovery phases for hFSHR and hLHR in **(C)** were also fitted using a non-linear regression (one phase kinetic equation) and by taking the signals after 2 and 60 min as 0 and 100% of recovery, respectively **(D)**. This allowed the calculation of $t_{1/2}$ values of receptor recycling indicated in **Table 1**. Data are means ± SEM of three independent experiments performed in triplicate points. $^{*}p < 0.05$, $^{**}p < 0.01$, $^{***}p < 0.001$, ns, not significant compared to unstimulated controls.

internalized receptors as previously shown for FSHR (44, 59) and LHR (60), or by the mobilization of a new intracellular pool of "spare receptors" or "receptor reserve" to the plasma membrane, or a combination of both processes. Beside, both FSHR and LHR have been reported to traffic through pre-early endosomes (60). This unusual trafficking may explain the fast internalization and recycling observed in our system.

To get a better picture of what happens with hFSH and hLHR in terms of activation, desensitization, and internalization, we normalized the dose-dependent responses of both receptors with regard to cAMP pathway, β-arrestin 2 recruitment, and receptor internalization assessed by different BRET assays reported in this study (**Figure 7**). For both hFSHR (**Figure 7A**) and hLHR (**Figure 7B**), we found a spectacular left-warded shift (about three logs) of cAMP curve ($EC_{50} \approx$ pM) as compared to β-arrestin 2 and internalization curves ($EC_{50} \approx$ nM), indicating the high efficiency of gonadotropins for this signaling pathway. In contrast, there was no difference between β-arrestin 2 recruitment and internalization

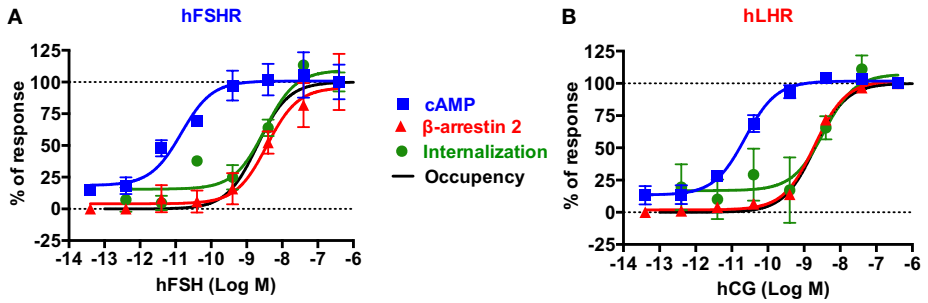

FIGURE 7 | Comparative analysis of the dose–response analysis on cAMP responses, β-arrestin 2 recruitment, and receptor internalization. For both hFSHR **(A)** and hLHR **(B)**, the individual dose–response data obtained in each BRET assay were normalized to the maximal signal taken as 100% of receptor-mediated responses. Moreover, receptor occupancy curves were incorporated to correlate the different specific responses with the percentage of occupied receptor. The occupancy was estimated using the following equation: % Occupancy = (Ligand)/(Ligand) + K_d, considering a K_d of 2 nM for both hFSH and hCG determined by radioligand binding assay on hFSHR expressed in HEK 293 cells (data not shown).

curves since both processes are tightly linked. Such a shift cannot be due to the fusion of the receptors with Rluc8 since both hFSHR-Rluc8 and hLHR-Rluc8 respond to gonadotropin stimulation with similar potencies as their respective unmodified receptors as shown by BRET (**Figures 1D,E**) and HTRF® (**Figures 1F,G**) assays. In addition, dose–response curves of receptor internalization using BRET with KRas were similar to that for β-arrestin 2 recruitment even though no yPET-β-arrestin overexpression was used in the internalization assay, ruling out the possibility that the shift observed for β-arrestin 2 recruitment could reflect a diminished functionality of the yPET-β-arrestin 2 (**Figures 5E** and **7**) or the modified variant in TANGO assay (**Figure 5G**).

Interestingly, the predicted receptor occupancy curves, using a K_d of 2 nM determined by radioligand binding assay on HEK 293 cells stably expressing hFSHR, indicated that <10% of the activated receptors is sufficient to promote maximal cAMP response whereas more than 90% of the receptors needed to be occupied to have full β-arrestin 2 recruitment as well as receptor internalization (**Figures 7A,B**). Noteworthy, our measurements of the rapid internalization phase displayed maximal response in the nanomolar range for both receptors, demonstrating that the full complement of receptor is accessible to hormone binding, even at early stimulation times. This observation rules out the scenario where only a limited fraction of receptors would be present at the plasma membrane at the time of stimulation. Together with the recycling data shown in **Figure 6**, our results are in accordance with the concept of "spare receptors," postulating that for high-efficacy hormones, a small population of receptors occupied is sufficient to fully promote the biological response (61–63), a paradigm, which has also been previously evoked for gonadotropin receptors (61, 64–66). The "spare receptors" concept predicates that there is a mechanism by which only small amount of gonadotropin receptors needs to be occupied to fully elicit cAMP-dependent function of the gonadotropin hormones. This is consistent with the well-established amplification of the intracellular cAMP signaling pathway and suggests a model where Gαs and/or adenylyl cyclase would be limiting yet accessible to all the occupied receptors in the cells. Alternatively, the existence of pre-assembled receptor-G protein complexes, as demonstrated for many GPCR-G protein pairs (27, 51, 67–69), may explain such an observation. Indeed, a limited amount of pre-assembled complexes could preferentially bind hormones by virtue of its well-established affinity increase for the ligand within the ternary complex (70). In contrast, β-arrestin recruitment and receptor internalization processes are remarkably proportional to receptor occupancy, suggesting that neither mechanism is amplified but rather that they depend on a 1:1 stoichiometric interaction with the receptors. Moreover, the differences in hormone potencies and receptor efficacies between cAMP and β-arrestin 2 recruitment/internalization pathways may explain the balance between receptor activation and receptor desensitization but also the balance between G protein-dependent and β-arrestin-dependent signaling pathways. Therefore, further investigation will be required to better dissect these aspects of FSHR and LHR trafficking and their putative link with the G protein- and β-arrestin-dependent downstream signaling in the gonads in physiological and pathophysiological settings. From the technological point of view, our study illustrates the advantage of applying BRET and FRET approaches to study the signaling and trafficking of FSHR and LHR in real-time and live cells. Of course, these approaches are based on transient expression of fusion proteins of the receptors and their different signaling and regulatory partners. Therefore, it will be important in the future, to apply other methods in order to confirm our observations in cells or native tissues expressing unmodified receptors and regulatory proteins at endogenous levels. Despite these potential shortcomings, the assays presented here may nonetheless have considerable potential for pharmacological profiling of gonadotropin receptors.

Acknowledgments

This work was funded by ARTE2, MODUPHAC, "ARD 2020 Biomédicament" grants from Région Centre. MAA is funded by LE STUDIUM® Loire Valley Institute for Advanced Studies and AgreenSkills Plus. FL is recipient of a doctoral fellowship from Région Centre. The authors thank Dr. A. Hanyaloglu from Imperial College (London) for kindly providing the receptor–Rluc8 fusion constructs. Special thanks to INRA and CNRS for their support.

References

1. Simoni M, Gromoll J, et al. The follicle-stimulating hormone receptor: biochemistry, molecular biology, physiology, and pathophysiology. *Endocr Rev* (1997) **18**(6):739–73. doi:10.1210/er.18.6.739
2. Ascoli M, Fanelli F, Segaloff DL. The lutropin/choriogonadotropin receptor, a 2002 perspective. *Endocr Rev* (2002) **23**(2):141–74. doi:10.1210/edrv.23.2.0462
3. Boutrel B, Kenny PJ, Specio SE, Martin-Fardon R, Markou A, Koob GF, et al. Role for hypocretin in mediating stress-induced reinstatement of cocaine-seeking behavior. *Proc Natl Acad Sci U S A* (2005) **102**(52):19168–73. doi:10.1073/pnas.0507480102
4. Jiang N, Saba NF, Chen ZG. Advances in targeting HER3 as an anticancer therapy. *Chemother Res Pract* (2012) **2012**:817304. doi:10.1155/2012/817304
5. Jiang X, Dias JA, He X. Structural biology of glycoprotein hormones and their receptors: insights to signaling. *Mol Cell Endocrinol* (2014) **382**(1):424–51. doi:10.1016/j.mce.2013.08.021
6. Arey BJ, Lopez FJ. Are circulating gonadotropin isoforms naturally occurring biased agonists? Basic and therapeutic implications. *Rev Endocr Metab Disord* (2011) **12**(4):275–88. doi:10.1007/s11154-011-9188-y
7. Gloaguen P, Crépieux P, Heitzler D, Poupon A, Reiter E. Mapping the follicle-stimulating hormone-induced signaling networks. *Frontiers in Endocrinology* (2011) **2**:45. doi:10.3389/fendo.2011.00045
8. Ulloa-Aguirre A, Crépieux P, Poupon A, Maurel MC, Reiter E. Novel pathways in gonadotropin receptor signaling and biased agonism. *Rev Endocr Metab Disord* (2011) **12**(4):259–74. doi:10.1007/s11154-011-9176-2
9. Landomiel F, Gallay N, Jégot G, Tranchant T, Durand G, Bourquard T, et al. Biased signalling in follicle stimulating hormone action. *Mol Cell Endocrinol* (2014) **382**(1):452–9. doi:10.1016/j.mce.2013.09.035
10. Kara E, Crépieux P, Gauthier C, Martinat N, Piketty V, Guillou F, et al. A phosphorylation cluster of five serine and threonine residues in the C-terminus of the follicle-stimulating hormone receptor is important for desensitization but not for beta-arrestin-mediated ERK activation. *Mol Endocrinol* (2006) **20**(11):3014–26. doi:10.1210/me.2006-0098
11. Wehbi V, Tranchant T, Durand G, Musnier A, Decourtye J, Piketty V, et al. Partially deglycosylated equine LH preferentially activates beta-arrestin-dependent signaling at the follicle-stimulating hormone receptor. *Mol Endocrinol* (2010) **24**(3):561–73. doi:10.1210/me.2009-0347
12. Tranchant T, Durand G, Gauthier C, Crépieux P, Ulloa-Aguirre A, Royère D, et al. Preferential beta-arrestin signalling at low receptor density revealed by functional characterization of the human FSH receptor A189 V mutation. *Mol Cell Endocrinol* (2011) **331**(1):109–18. doi:10.1016/j.mce.2010.08.016
13. Heitzler D, Durand G, Gallay N, Rizk A, Ahn S, Kim J, et al. Competing G protein-coupled receptor kinases balance G protein and beta-arrestin signaling. *Mol Syst Biol* (2012) **8**:590. doi:10.1038/msb.2012.22
14. Förster T. Intermolecular energy migration and fluorescence. *Annals of Physics* (1948) **437**(1–2):55–75.
15. Helms V. Fluorescence resonance energy transfer. In: W. VCH, editor. *Principles of Computational Cell Biology*. Weinheim: Wiley-Blackwell (2008). 202.
16. Pin JP, Ayoub MA, et al. Energy transfer technologies to monitor the dynamics and signaling properties of G – protein – coupled receptors in living cells. In: E. Pebay-Peyroula, editor. *Biophysical Analysis of Membrane Proteins – Investigating Structure and Function*. Weinheim, Wiley-VCH (2008). 311–34.
17. Boute N, Pernet K, Issad T. Monitoring the activation state of the insulin receptor using bioluminescence resonance energy transfer. *Mol Pharmacol* (2001) **60**(4):640–5.
18. Ayoub MA, See HB, Seeber RM, Armstrong SP, Pfleger KD. Profiling epidermal growth factor receptor and heregulin receptor 3 heteromerization using receptor tyrosine kinase heteromer investigation technology. *PLoS One* (2013) **8**(5):e64672. doi:10.1371/journal.pone.0064672
19. Pfleger KD, Eidne KA. Monitoring the formation of dynamic G-protein-coupled receptor-protein complexes in living cells. *Biochem J* (2005) **385**(Pt 3):625–37. doi:10.1042/BJ20041361
20. Lohse MJ, Nuber S, Hoffmann C. Fluorescence/bioluminescence resonance energy transfer techniques to study g-protein-coupled receptor activation and signaling. *Pharmacol Rev* (2012) **64**(2):299–336. doi:10.1124/pr.110.004309
21. Conn PM. Receptor-receptor interactions methods in cell biology. *P. M Conn Elsevier Science* (2013) **117**:538. doi:10.1016/B978-0-12-408143-7.10000-3
22. Hein P, Frank M, Hoffmann C, Lohse MJ, Bünemann M. Dynamics of receptor/G protein coupling in living cells. *EMBO J* (2005) **24**(23):4106–14. doi:10.1038/sj.emboj.7600870
23. Nguyen AW, Daugherty PS. Evolutionary optimization of fluorescent proteins for intracellular FRET. *Nat Biotechnol* (2005) **23**(3):355–60. doi:10.1038/nbt1066
24. Ayoub MA, Pfleger KD. Recent advances in bioluminescence resonance energy transfer technologies to study GPCR heteromerization. *Curr Opin Pharmacol* (2010) **10**(1):44–52. doi:10.1016/j.coph.2009.09.012
25. Cottet M, Faklaris O, Maurel D, Scholler P, Doumazane E, Trinquet E, et al. BRET and Time-resolved FRET strategy to study GPCR oligomerization: from cell lines toward native tissues. *Front Endocrinol (Lausanne)* (2012) **3**:92. doi:10.3389/fendo.2012.00092
26. Ayoub MA, Al-Senaidy A, Pin JP. Receptor-G protein interaction studied by bioluminescence resonance energy transfer: lessons from protease-activated receptor 1. *Front Endocrin* (2012) **3**:82. doi:10.3389/fendo.2012.00082
27. Ayoub MA, Maurel D, Binet V, Fink M, Prézeau L, Ansanay H, et al. Real-time analysis of agonist-induced activation of protease-activated receptor 1/Galphai1 protein complex measured by bioluminescence resonance energy transfer in living cells. *Mol Pharmacol* (2007) **71**(5):1329–40. doi:10.1124/mol.106.030304
28. Nørskov-Lauritsen L, Thomsen AR, Bräuner-Osborne H. G protein-coupled receptor signaling analysis using homogenous time-resolved Forster resonance energy transfer (HTRF(R)) technology. *Int J Mol Sci* (2014) **15**(2):2554–72. doi:10.3390/ijms15022554
29. Barnea G, Strapps W, Herrada G, Berman Y, Ong J, Kloss B, et al. The genetic design of signaling cascades to record receptor activation. *Proc Natl Acad Sci U S A* (2008) **105**(1):64–9. doi:10.1073/pnas.0710487105
30. Jiang LI, Collins J, Davis R, Lin KM, DeCamp D, Roach T, et al. Use of a cAMP BRET sensor to characterize a novel regulation of cAMP by the sphingosine 1-phosphate/G13 pathway. *J Biol Chem* (2007) **282**(14):10576–84. doi:10.1074/jbc.M701019200
31. DiPilato LM, Cheng X, Zhang J. Fluorescent indicators of cAMP and Epac activation reveal differential dynamics of cAMP signaling within discrete subcellular compartments. *Proc Natl Acad Sci U S A* (2004) **101**(47):16513–8. doi:10.1073/pnas.0405973101
32. Galés C, Van Durm JJ, Schaak S, Pontier S, Percherancier Y, Audet M, et al. Probing the activation-promoted structural rearrangements in preassembled receptor-G protein complexes. *Nat Struct Mol Biol* (2006) **13**:778–86. doi:10.1038/nsmb1134
33. Ayoub MA, Damian M, Gespach C, Ferrandis E, Lavergne O, De Wever O, et al. Inhibition of heterotrimeric G-protein signaling by a small molecule acting on galpha subunit. *J Biol Chem* (2009) **284**(42):29136–45. doi:10.1074/jbc.M109.042333
34. Ayoub MA, Zhang Y, Kelly RS, See HB, Johnstone EK, McCall EA, et al. Functional interaction between angiotensin II receptor type 1 and chemokine (C-C Motif) receptor 2 with implications for chronic kidney disease. *PLoS One* (2015) **10**(3):e0119803. doi:10.1371/journal.pone.0119803
35. Bellot M, Galandrin S, Boularan C, Matthies HJ, Despas F, Denis C, et al. Dual agonist occupancy of AT1-R-alpha2C-AR heterodimers results in atypical Gs-PKA signaling. *Nat Chem Biol* (2015) **11**(4):271–9. doi:10.1038/nchembio.1766
36. Damian M, Mary S, Maingot M, M'Kadmi C, Gagne D, Leyris JP, et al. Ghrelin receptor conformational dynamics regulate the transition from a preassembled to an active receptor: Gq complex. *Proc Natl Acad Sci U S A* (2015) **112**(5):1601–6. doi:10.1073/pnas.1414618112
37. Zhu X, Gilbert S, Birnbaumer M, Birnbaumer L. Dual signaling potential is common among Gs-coupled receptors and dependent on receptor density. *Mol Pharmacol* (1994) **46**(3):460–9.
38. Thomas RM, Nechamen CA, Mazurkiewicz JE, Ulloa-Aguirre A, Dias JA. The adapter protein APPL1 links FSH receptor to inositol 1,4,5-trisphosphate production and is implicated in intracellular Ca(2+) mobilization. *Endocrinology* (2011) **152**(4):1691–701. doi:10.1210/en.2010-1353
39. Gorokhovatsky AY, Marchenkov VV, Rudenko NV, Ivashina TV, Ksenzenko VN, Burkhardt N, et al. Fusion of *Aequorea victoria* GFP and aequorin provides their Ca(2+)-induced interaction that results in red shift of GFP absorption

and efficient bioluminescence energy transfer. *Biochem Biophys Res Commun* (2004) **320**(3):703–11. doi:10.1016/j.bbrc.2004.06.014
40. Naumann EA, Kampff AR, Prober DA, Schier AF, Engert F. Monitoring neural activity with bioluminescence during natural behavior. *Nat Neurosci* (2010) **13**(4):513–20. doi:10.1038/nn.2518
41. Luttrell LM, Lefkowitz RJ. The role of beta-arrestins in the termination and transduction of G-protein-coupled receptor signals. *J Cell Sci* (2002) **115**(Pt 3):455–65.
42. Lefkowitz RJ, Shenoy SK. Transduction of receptor signals by beta-arrestins. *Science* (2005) **308**(5721):512–7. doi:10.1126/science.1109237
43. Reiter E, Lefkowitz RJ. GRKs and beta-arrestins: roles in receptor silencing, trafficking and signaling. *Trends Endocrinol Metab* (2006) **17**(4):159–65. doi:10.1016/j.tem.2006.03.008
44. Kluetzman KS, Thomas RM, Nechamen CA, Dias JA. Decreased degradation of internalized follicle-stimulating hormone caused by mutation of aspartic acid 6.30(550) in a protein kinase-CK2 consensus sequence in the third intracellular loop of human follicle-stimulating hormone receptor. *Biol Reprod* (2011) **84**(6):1154–63. doi:10.1095/biolreprod.110.087965
45. Galet C, Ascoli M. Arrestin-3 is essential for the activation of Fyn by the luteinizing hormone receptor (LHR) in MA-10 cells. *Cell Signal* (2008) **20**(10):1822–9. doi:10.1016/j.cellsig.2008.06.005
46. Oakley RH, Laporte SA, Holt JA, Caron MG, Barak LS. Differential affinities of visual arrestin, beta arrestin1, and beta arrestin2 for G protein-coupled receptors delineate two major classes of receptors. *J Biol Chem* (2000) **275**(22):17201–10. doi:10.1074/jbc.M910348199
47. Lan TH, Kuravi S, Lambert NA. Internalization dissociates beta2-adrenergic receptors. *PLoS One* (2011) **6**(2):e17361. doi:10.1371/journal.pone.0017361
48. Robben JH, Knoers NV, Deen PM. Regulation of the vasopressin V2 receptor by vasopressin in polarized renal collecting duct cells. *Mol Biol Cell* (2004) **15**(12):5693–9. doi:10.1091/mbc.E04-04-0337
49. Terrillon S, Barberis C, Bouvier M. Heterodimerization of V1a and V2 vasopressin receptors determines the interaction with beta-arrestin and their trafficking patterns. *Proc Natl Acad Sci U S A* (2004) **101**(6):1548–53. doi:10.1073/pnas.0305322101
50. Bouley R, Lin HY, Raychowdhury MK, Marshansky V, Brown D, Ausiello DA. Downregulation of the vasopressin type 2 receptor after vasopressin-induced internalization: involvement of a lysosomal degradation pathway. *Am J Physiol Cell Physiol* (2005) **288**(6):C1390–401. doi:10.1152/ajpcell.00353.2004
51. Ayoub MA, Trinquet E, Pfleger KD, Pin JP. Differential association modes of the thrombin receptor PAR1 with Galphai1, Galpha12, and beta-arrestin 1. *FASEB J* (2010) **24**(9):3522–35. doi:10.1096/fj.10-154997
52. Guan Y, Zhang Y, Wu J, Qi Z, Yang G, Dou D, et al. Antihypertensive effects of selective prostaglandin E2 receptor subtype 1 targeting. *J Clin Invest* (2007) **117**(9):2496–505. doi:10.1172/JCI29838
53. Ulloa-Aguirre A, Reiter E, Bousfield G, Dias JA, Huhtaniemi I. Constitutive activity in gonadotropin receptors. *Adv Pharmacol* (2014) **70**:37–80. doi:10.1016/B978-0-12-417197-8.00002-X
54. Tenenbaum J, Ayoub MA, Perkovska S, Adra-Delenne AL, Mendre C, Ranchin B, et al. The constitutively active V2 receptor mutants conferring NSIAD are weakly sensitive to agonist and antagonist regulation. *PLoS One* (2009) **4**(12):e8383. doi:10.1371/journal.pone.0008383
55. Nakamura K, Lazari MF, Li S, Korgaonkar C, Ascoli M. Role of the rate of internalization of the agonist-receptor complex on the agonist-induced down-regulation of the lutropin/choriogonadotropin receptor. *Mol Endocrinol* (1999) **13**(8):1295–304. doi:10.1210/mend.13.8.0331
56. Bhaskaran RS, Min L, Krishnamurthy H, Ascoli M. Studies with chimeras of the gonadotropin receptors reveal the importance of third intracellular loop threonines on the formation of the receptor/nonvisual arrestin complex. *Biochemistry* (2003) **42**(47):13950–9. doi:10.1021/bi034907w
57. Ferguson SS, Downey WE III, Colapietro AM, Barak LS, Ménard L, Caron MG. Role of beta-arrestin in mediating agonist-promoted G protein-coupled receptor internalization. *Science* (1996) **271**(5247):363–6. doi:10.1126/science.271.5247.363
58. Shenoy SK, Lefkowitz RJ. beta-arrestin-mediated receptor trafficking and signal transduction. *Trends Pharmacol Sci* (2011) **32**(9):521–33. doi:10.1016/j.tips.2011.05.002
59. Krishnamurthy H, Kishi H, Shi M, Galet C, Bhaskaran RS, Hirakawa T, et al. Postendocytotic trafficking of the follicle-stimulating hormone (FSH)-FSH receptor complex. *Mol Endocrinol* (2003) **17**(11):2162–76. doi:10.1210/me.2003-0118
60. Jean-Alphonse F, Bowersox S, Chen S, Beard G, Puthenveedu MA, Hanyaloglu AC. Spatially restricted G protein-coupled receptor activity via divergent endocytic compartments. *J Biol Chem* (2014) **289**(7):3960–77. doi:10.1074/jbc.M113.526350
61. Catt KJ, Dufau ML. Spare gonadotrophin receptors in rat testis. *Nat New Biol* (1973) **244**(137):219–21. doi:10.1038/newbio244219a0
62. Marunaka Y, Niisato N, Miyazaki H. New concept of spare receptors and effectors. *J Membr Biol* (2005) **203**(1):31–9. doi:10.1007/s00232-004-0729-0
63. Charlton SJ. Agonist efficacy and receptor desensitization: from partial truths to a fuller picture. *Br J Pharmacol* (2009) **158**(1):165–8. doi:10.1111/j.1476-5381.2009.00352.x
64. Huhtaniemi IT, Clayton RN, Catt KJ. Gonadotropin binding and Leydig cell activation in the rat testis in vivo. *Endocrinology* (1982) **111**(3):982–7. doi:10.1210/endo-111-3-982
65. Uribe A, Zariñán T, Pérez-Solis MA, Gutiérrez-Sagal R, Jardón-Valadez E, Piñeiro A, et al. Functional and structural roles of conserved cysteine residues in the carboxyl-terminal domain of the follicle-stimulating hormone receptor in human embryonic kidney 293 cells. *Biol Reprod* (2008) **78**(5):869–82. doi:10.1095/biolreprod.107.063925
66. Rivero-Müller A, Chou YY, Ji I, Lajic S, Hanyaloglu AC, Jonas K, et al. Rescue of defective G protein-coupled receptor function in vivo by intermolecular cooperation. *Proc Natl Acad Sci U S A* (2010) **107**(5):2319–24. doi:10.1073/pnas.0906695106
67. Roka F, Brydon L, Waldhoer M, Strosberg AD, Freissmuth M, Jockers R, et al. Tight association of the human Mel(1a)-melatonin receptor and G(i): precoupling and constitutive activity. *Mol Pharmacol* (1999) **56**(5):1014–24.
68. Andressen KW, Norum JH, Levy FO, Krobert KA. Activation of adenylyl cyclase by endogenous G(s)-coupled receptors in human embryonic kidney 293 cells is attenuated by 5-HT(7) receptor expression. *Mol Pharmacol* (2006) **69**(1):207–15. doi:10.1124/mol.105.015396
69. Qin K, Sethi PR, Lambert NA. Abundance and stability of complexes containing inactive G protein-coupled receptors and G proteins. *FASEB J* (2008) **22**(8):2920–7. doi:10.1096/fj.08-105775
70. De Lean A, Stadel JM, Lefkowitz RJ. A ternary complex model explains the agonist-/specific binding properties of the adenylate cyclase-coupled beta-adrenergic receptor. *J Biol Chem* (1980) **255**(15):7108–17.

Conflict of Interest Statement: The authors declare that the research was conducted in the absence of any commercial or financial relationships that could be construed as a potential conflict of interest.

Advantages of publishing in Frontiers

OPEN ACCESS
Articles are free to read, for greatest visibility

COLLABORATIVE PEER-REVIEW
Designed to be rigorous – yet also collaborative, fair and constructive

FAST PUBLICATION
Average 85 days from submission to publication (across all journals)

COPYRIGHT TO AUTHORS
No limit to article distribution and re-use

TRANSPARENT
Editors and reviewers acknowledged by name on published articles

SUPPORT
By our Swiss-based editorial team

IMPACT METRICS
Advanced metrics track your article's impact

GLOBAL SPREAD
5'100'000+ monthly article views and downloads

LOOP RESEARCH NETWORK
Our network increases readership for your article

Frontiers
EPFL Innovation Park, Building I • 1015 Lausanne • Switzerland
Tel +41 21 510 17 00 • Fax +41 21 510 17 01 • info@frontiersin.org
www.frontiersin.org

Find us on